[redacted]

HANDBOOK FOR NUCLEAR WEAPONS EFFECTS
UNDER ARCTIC CONDITIONS. [redacted]

K-80-143(R)-SAN

30 April 1980

This work sponsored by the Defense Nuclear Agency
under: Subtask Code I25AAXHX633 and Work Unit 39
and by the Office of Naval Research Task NR089-145

[redacted]

KAMAN SCIENCES
CORPORATION
1500 Garden of the Gods Road
Colorado Springs, Colorado 80907

A KAMAN COMPANY

[redacted]

[redacted]

Classified By DC Form 254 for N00014-79-C-0532
dated 4 May 1979, [redacted]

COPY NO. 8 OF 46 COPIES, SERIES A

[redacted]

SECURITY C[redacted]PAGE (When Data E[redacted]

REPORT DOCUMENTATION PAGE	READ INSTRUCTIONS BEFORE COMPLETING FORM
1. REPORT NUMBER: K-80-143(R) — 2. GOVT ACCESSION NO. [redacted]	3. RECIPIENT'S CATALOG NUMBER
4. TITLE (and Subtitle): HANDBOOK FOR NUCLEAR WEAPONS EFFECTS UNDER ARCTIC CONDITIONS. [redacted]	5. TYPE OF REPORT & PERIOD COVERED: (9) Final Report, June 1979-April 1980
	6. PERFORMING ORG. REPORT NUMBER: (14) K-80-143(R)
7. AUTHOR(s): (10) J.R./Keith, W.E./Wallace (Underwater Systems, Inc)	8. CONTRACT OR GRANT NUMBER(s): (15) N00014-79-C-0532
9. PERFORMING ORGANIZATION NAME AND ADDRESS: Kaman Sciences Corporation, P.O. Box 7463, Colorado Springs, Colo 80933 (12) 377	10. PROGRAM ELEMENT, PROJECT, TASK AREA & WORK UNIT NUMBERS: DNA I25AAXHX632-39, ONR NR089-145 (17) X633
11. CONTROLLING OFFICE NAME AND ADDRESS: Defense Nuclear Agency, Washington, D.C. 20305 (16) I25AAXH	12. REPORT DATE: 30 April 1980
	13. NUMBER OF PAGES: 369
14. MONITORING AGENCY NAME & ADDRESS (if different from Controlling Office): Office of Naval Research, 800 North Quincy Street - Code 464, Arlington, VA 22217	15. SECURITY CLASS (of this report) [redacted]
	15a. DECLASSIFICATION DOWNGRADING [redacted]
16. DISTRIBUTION STATEMENT (of this Report)	
17. DISTRIBUTION STATEMENT (of the abstract entered in Block 20, if different from Report): Unlimited	
18. SUPPLEMENTARY NOTES: Research jointly sponsored by Defense Nuclear Agency and the Office of Naval Research under task numbers given above. Underwater Systems, Inc of Rockville, MD made major contributions to this effort under subcontract to Kaman Sciences Corp. USI was primarily responsible for preparation of sections 7, 8 & 9, and contributed to other sections.	
19. KEY WORDS (Continue on reverse side if necessary and identify by block number): Nuclear Weapons, Arctic, Underwater, Ice, Snow, Airshock, Watershock, Thermal Radiation, Nuclear Radiation, Fallout, Acoustic Effects, Reverberation, Water Waves	

20. ABSTRACT (Continue on reverse side if necessary and identify by block number)

[redacted] This report describes the changes to be expected in nuclear weapon effects in arctic conditions as compared with the temperate regions of the world. Previous research in this area has been reviewed and relevant information is presented. The emphasis was placed on low altitude and underwater bursts and effects. Inadequacies and uncertainties in current prediction techniques are given. → next page

DD FORM 1 JAN 73 1473 EDITION OF 1 NOV 65 IS OBSOLETE

[redacted] 389129

[redacted]

[redacted]

SECURITY CLASSIFICATION OF THIS PAGE(When Data Entered)

20. ABSTRACT

[redacted] The characteristics of the arctic region of importance in nuclear effect calculations are given. The effects considered include air blast, cratering, thermal radiation, nuclear radiation, EMP, HF communication degradation, water shock, water waves and acoustic effects.

[redacted]

QUALITY INSPECTED 2

Accession For	
NTIS GRA&I	☒
DTIC TAB	☐
Unannounced	☐
Justification	
By	
Distribution/	
Availability Codes	
Dist	Avail and/or Special
A-1	

[redacted]

SECURITY CLASSIFICATION OF THIS PAGE(When Data Entered)

[redacted]

TABLE OF CONTENTS

[redacted]

[redacted]

TABLE OF CONTENTS

[redacted]

[redacted]

TABLE OF CONTENTS

[redacted]

[redacted]

TABLE OF CONTENTS

[redacted]

[redacted]

TABLE OF CONTENTS

[redacted]

[redacted]

TABLE OF CONTENTS

[redacted]

[redacted]

LIST OF FIGURES

[redacted]

[redacted]

LIST OF FIGURES

[redacted]

[redacted]

LIST OF FIGURES

[redacted]

[redacted]

LIST OF FIGURES

[redacted]

Page xi was deleted

[redacted]

LIST OF FIGURES

[redacted]

[redacted]

LIST OF FIGURES

[redacted]

[redacted]

LIST OF TABLES

[redacted]

[redacted]

SECTION 1
INTRODUCTION

[redacted] There are several reasons why knowledge of nuclear weapon effects in the Arctic is important for United States security. A general reason for interest in security in the Arctic is the preservation of the freedom of the high seas and super-adjacent air spaces because of the importance of sea and air lanes to military operations. An important consideration is to provide security for Alaska including the energy and other economic resources. The area is an important strategic launch area for SLBM operations and for sea and land launched cruise missiles. The determination of the effect of the ice cover and other arctic environments on current ASW methods is very important.

1.1 [redacted] Objectives

[redacted] The intent of this handbook is to gather under one cover the sparse information available relating to nuclear weapons effects under arctic conditions which heretofore has existed primarily as technical reports on specialized subjects with typically very limited distributions. The handbook is intended to serve as a supplement to the other handbooks on nuclear effects such as Capabilities of Atomic Weapons (EM-1), Handbook of Underwater Nuclear Explosions, Nuclear Weapons Blast Phenomena, and Handbook of Explosion Generated Water Waves. Material contained in the above handbooks will not be repeated in this handbook except when needed for descriptive purposes.

[redacted]

[redacted]

[redacted] The emphasis is on low altitude and underwater effects. In particular, high altitude effects considering changes in the upper atmosphere and effects caused by the different high altitude energetic particle interactions with the polar magnetic field are not considered.

[redacted] A study entitled "Nuclear Weapons Effects in an Arctic Environment" performed by the Office of Special Weapons Development of The United States Continental Army Command at Ft. Bliss, Texas (OSWD, 1960) considered the changes to be expected in nuclear weapon effects in the Arctic. This study considered the nuclear effects over the land areas of the Arctic with respect to tactical army operations. This was a thorough and exhaustive study using the knowledge and techniques available at that time. The general conclusion was that, even though there were changes in the nuclear effects under arctic conditions, the changes were not large enough to cause any large changes in field methods of analysis of weapon effects. An excellent summary of the changes in weapon effects to be expected in the arctic and their possible effect on military land operations was included.

[redacted] Since the Ft. Bliss study, several HE test series have been performed in arctic conditions over frozen soils and ice and snow. These studies and their results are described in Section 2. In general, there are still large uncertainties in the blast effects in arctic conditions partially due to instrumentation differences among the various test series. Advances have been made in treating thermal radiation and nuclear radiation since the Ft. Bliss study and will be described in the appropriate sections.

[redacted]

[redacted]

[redacted] Submarine operation in the arctic has been considered in several studies such as "The Arctic Environment and Possible Implications for Submarine and Anti-Submarine Operations (U)" (Nakonechny, 1970). The current status of knowledge of the effects of the arctic environment on underwater shock, water waves and acoustics from nuclear bursts will be covered in the appropriate sections.

1.2 [redacted] Arctic Environmental Description

[redacted] In this subsection the Arctic environment is described with the emphasis being placed on the parameters of the environment that are significantly different than found in temperate regions and which can contribute to changes in predicted nuclear weapon effects.

1.2.1 [redacted] Atmospheric Parameters

[redacted] The model atmosphere developed for 75° North latitude (ESSA, 1966) will be used for defining the altitude profiles for Arctic pressure, temperature, and density. The paucity of rocket observations above this latitude preclude definition of 90° North standard atmospheres. The 75° North profiles extend only to an altitude of 30 km but are satisfactory for our purposes since we are interested primarily in low altitude nuclear weapon effects. The 45° North midlatitude spring/fall atmosphere is used as a standard reference atmosphere and is essentially the same as that used for most weapon effects studies in temperate latitudes (NASA, 1962). The molecular composition is assumed to be independent of latitude.

[redacted] In Figure 1-1 the temperature-altitude profile of the 75° North atmosphere is compared with the temperate model. The July 75° profile is seen to be very similar to the temperate model from 2 km to 10 km altitude. Below 2 km the July 75° model is somewhat cooler than the temperate model and above 10 km

[redacted]

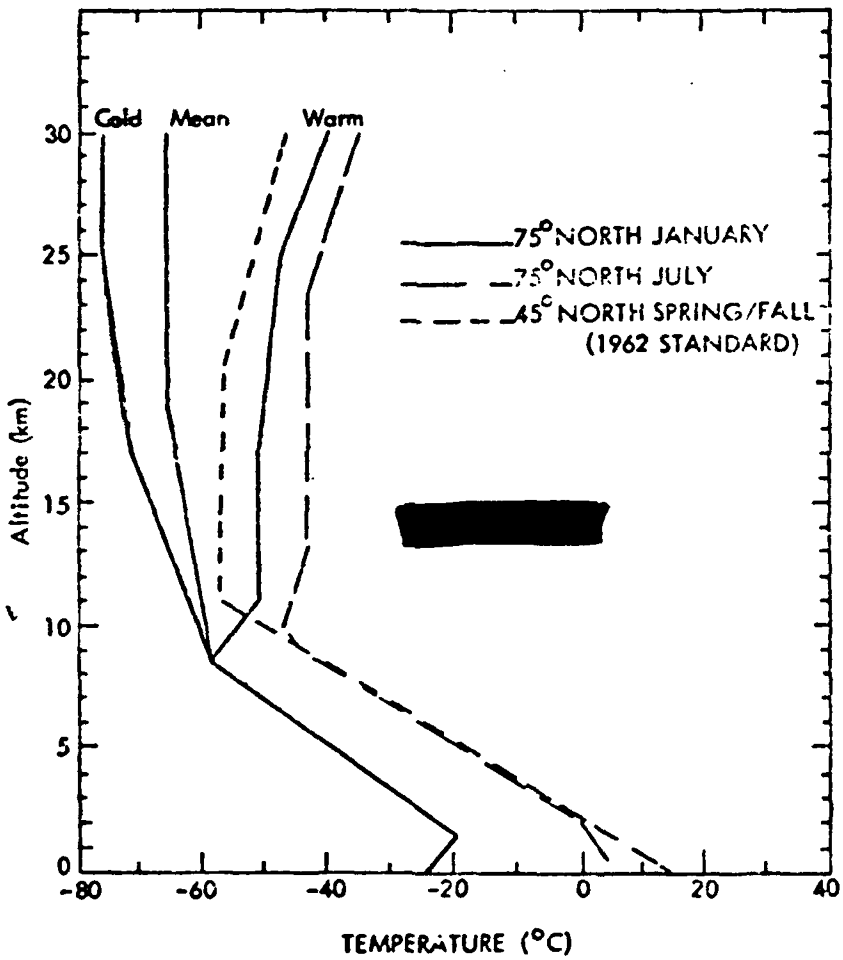

[redacted] FIGURE 1-1 COMPARISON OF 75° NORTH AND THE MIDLATITUDE TEMPERATURE PROFILES

[redacted]

[redacted] is somewhat warmer. The January 75° model has two different thermal regimes in the stratosphere with the relative probability of occurrence of the warm and cold regimes being dependent upon longitude. Extremely rapid warming from the cold to the warm regime can occur in the winter. The mean January 75° profile represents a reasonable average of the warm and cold profiles. The sea level temperature is seen to be about 40° C less than the temperate model. A temperature inversion below 1500 m is indicated. More detail on the occurrence of Arctic temperature inversions will be given in the next subsection.

[redacted] In Figure 1-2 the percentage departure of the 75° model pressures from standard are noted. The differences noted for the January 75° model of greater than 10% at 10 km could involve changes in the blast overpressure of the same order as will be discussed in Section 2.

[redacted] In Figure 1-3 the percentage departure of the 75° model density profiles from standard are shown. The about 16% higher density for the sea level January model can cause observable differences in radiation levels as discussed in Section 5.

[redacted] In Tables 1-1 through 1-4 the tables (ESSA, 1966) for the 75° N January mean, cold, and warm and July profiles are reproduced as a convenience to the reader. The geometric altitude is given by Z. The geopotential altitude is used in constructing the table and includes the variation of the gravitational constant. The other quantities and units are self explanatory.

[redacted] The absolute humidity is of some interest in thermal transmission calculations and is given in Table 1-5 (calculated from data in ESSA, 1966). The relative humidity is usually high near sea level in the Arctic but because of the cold temperatures the absolute humidity is low especially in the winter time.

[redacted]

[redacted]

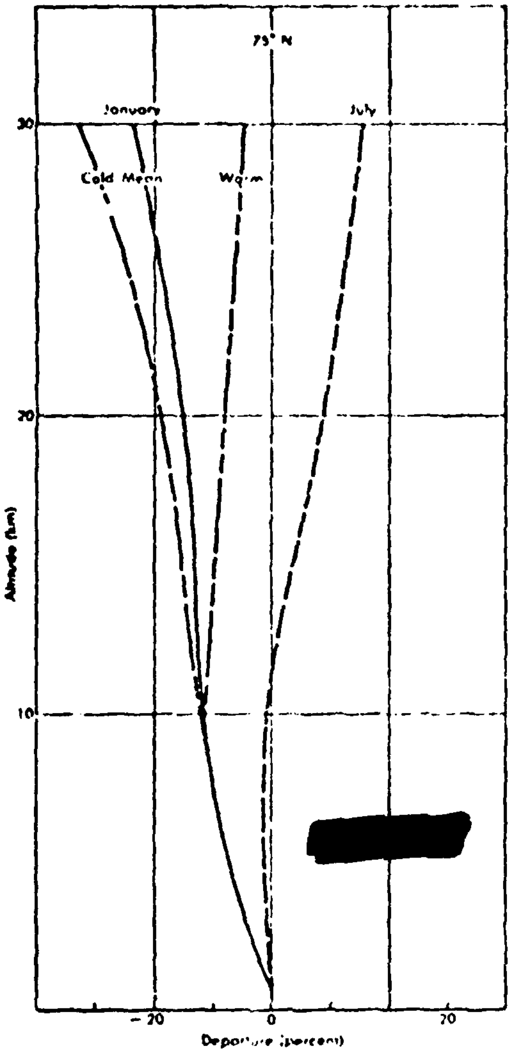

[redacted] **FIGURE 1-2.** Departures of 75° N Atmosphere pressures from Standard.

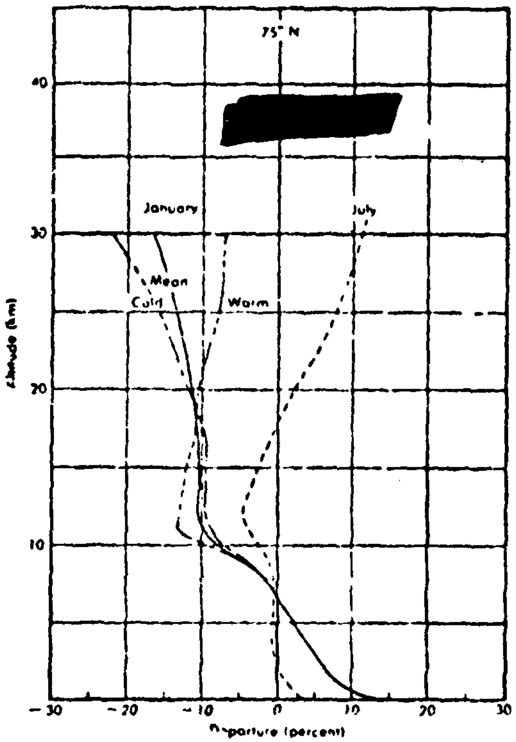

[redacted] FIGURE 1-3 Departures of 75° N Atmosphere densities from Standard

[redacted]

[redacted]

[redacted] TABLE 1-1. STANDARD ATMOSPHERE

75° N January

GEOMETRIC ALTITUDE, METRIC UNITS

Altitude Z, m	Altitude H, m'	Temperature T, °K	Temperature t, °C	Temperature $T - T_{std}$	Pressure P, mb	Pressure P/P_{std}	Density ρ, kg m^{-3}	Density ρ/ρ_{std}	Sound speed C_s, m sec^{-1}	Coefficient of viscosity μ, kg m^{-1} sec^{-1}	Thermal conductivity k, kcal m^{-1} sec^{-1} °K^{-1}
0	0	249.22	-23.93	-36.93	1.01350 + 3	1.000	1.417 + 0	1.157	316.5	1.595 − 5	5.307 − 6
250	251	249.97	-23.18	-36.55	[illegible] + 2	0.996	1.365	1.141	316.9	1.599	5.322
500	501	250.73	-22.42	-36.17	9.464	0.991	1.315	1.147	317.4	1.603	5.337
750	752	251.48	-21.67	-31.79	9.147	0.987	1.267	1.112	317.9	1.607	5.352
1000	1002	252.24	-20.91	-29.41	8.8	0.984	1.221	1.098	318.4	1.611	5.366
1250	1253	252.99	-20.16	-27.03	8.594	0.980	1.177	1.085	318.9	1.615	5.381
1500	1503	253.72	-19.43	-24.68	8.265	0.977	1.135	1.072	319.3	1.618	5.395
1750	1753	252.36	-20.81	-24.44	7.988	0.974	1.103	1.069	318.4	1.611	5.368
2000	2004	250.95	-22.20	-24.20	7.721	0.971	1.072	1.064	317.6	1.604	5.341
2250	2254	249.57	-23.58	-23.96	7.462	0.968	1.042	1.061	316.7	1.597	5.314
2500	2505	248.19	-24.96	-23.72	7.210 + 2	0.965	1.012 + 0	1.057	315.8	1.590 − 5	5.287 − 6
2750	2755	246.80	-26.35	-23.48	6.965	0.962	9.831 − 1	1.054	314.9	1.583	5.260
3000	3005	245.42	-27.73	-23.24	6.727	0.959	9.549	1.050	314.1	1.575	5.233
3250	3256	244.04	-29.11	-23.00	6.496	0.956	9.273	1.047	313.2	1.568	5.206
3500	3506	242.66	-30.49	-22.76	6.272	0.953	9.004	1.043	312.3	1.561	5.179
3750	3756	241.27	-31.88	-22.51	6.054	0.951	8.741	1.039	311.4	1.554	5.152
4000	4006	239.89	-33.26	-22.27	5.843	0.948	8.485	1.035	310.5	1.547	5.125
4250	4257	238.51	-34.64	-22.03	5.638	0.945	8.235	1.032	309.6	1.539	5.097
4500	4507	237.14	-36.01	-21.78	5.439	0.942	7.990	1.028	308.7	1.532	5.070
4750	4757	235.76	-37.39	-21.54	5.245	0.939	7.751	1.025	307.8	1.525	5.043
5000	5007	234.38	-38.77	-21.30	5.058 + 2	0.936	7.518 − 1	1.021	306.9	1.517 − 5	5.016 − 6
5250	5257	233.00	-40.15	-21.05	4.877	0.933	7.291	1.017	306.0	1.510	4.988
5500	5508	231.62	-41.53	-20.81	4.700	0.930	7.069	1.014	305.1	1.503	4.961
5750	5758	230.25	-42.90	-20.56	4.533	0.927	6.853	1.010	304.2	1.495	4.934
6000	6008	228.87	-44.28	-20.32	4.369	0.924	6.643	1.006	303.3	1.488	4.906
6250	6258	227.49	-45.66	-20.07	4.204	0.921	6.437	1.003	302.4	1.481	4.879
6500	6508	226.11	-47.04	-19.83	4.049	0.918	6.237	0.999	301.4	1.473	4.851
6750	6758	224.74	-48.41	-19.58	3.898	0.916	6.042	0.995	300.5	1.466	4.824
7000	7008	223.36	-49.79	-19.34	3.752	0.913	5.852	0.992	299.6	1.458	4.796
7250	7258	221.99	-51.16	-19.09	3.611	0.910	5.667	0.988	298.7	1.451	4.769
7500	7508	220.61	-52.54	-18.85	3.474 + 2	0.907	5.488 − 1	0.985	297.8	1.443 − 5	4.741 − 6
7750	7758	219.23	-53.92	-18.60	[redacted]	0.904	5.310	0.981	296.8	1.436	4.714
8000	8008	217.86	-55.29	-18.36	[redacted]	0.901	5.139	0.977	295.9	1.428	4.686
8250	8258	216.48	-56.67	-18.11	[redacted]	0.899	4.972	0.974	295.0	1.421	4.658
8500	8508	215.15	-58.00	-17.85	[redacted]	0.896	4.809	0.970	294.0	1.413	4.631
8750	8758	215.02	-58.13	-16.33	[redacted]	0.893	4.625	0.961	294.0	1.413	4.629
9000	9007	214.90	-58.25	-14.84	[redacted]	0.891	4.447	0.952	293.9	1.412	4.626
9250	9257	214.77	-58.38	-13.36	[redacted]	0.888	4.276	0.944	293.8	1.411	4.624
9500	9507	214.65	-58.50	-11.84	[redacted]	0.887	4.112	0.935	293.7	1.411	4.621
9750	9757	214.52	-58.63	-10.35	[redacted]	0.884	3.954	0.927	293.6	1.410	4.619
10000	10007	214.40	-58.75	-8.85	[redacted]	0.883	3.802 − 1	0.919	293.5	1.409 − 5	4.616 − 6
10250	10256	214.27	-58.88	-7.36	[redacted]	0.882	3.656	0.912	293.4	[illegible]	4.614
10500	10506	214.15	-59.00	-5.87	2.181	0.881	3.515	0.905	293.4	1.408	4.611
10750	10756	214.02	-59.13	-4.37	2.076	0.880	3.380	0.898	293.3	1.407	4.609
11000	11006	213.90	-59.25	-2.88	1.995	0.879	3.250	0.891	293.2	1.406	4.606
11500	11505	213.65	-59.50	-3.00	1.842	0.878	3.004	0.890	293.0	1.405	4.601
12000	12004	213.25	-59.90	-3.40	1.701	0.877	2.778	0.891	292.7	1.403	4.593
12500	12503	212.85	-60.30	-3.80	1.570	0.876	2.569	0.891	292.5	1.401	4.585
13000	13003	212.45	-60.70	-4.20	1.449	0.874	2.376	0.891	292.2	1.398	4.577
13500	13502	212.05	-61.10	-4.60	1.337	0.872	2.197	0.891	291.9	1.396	4.569
14000	14001	211.65	-61.50	-5.00	1.234 + 2	0.871	2.031 − 1	0.891	291.6	1.394 − 5	4.561 − 6
14500	14499	211.25	-61.90	-5.40	1.138	0.869	1.877	0.891	291.4	1.392	4.553
15000	14996	210.85	-62.30	-5.80	1.050	0.867	1.735	0.890	291.1	1.390	4.545
15500	15497	210.45	-62.70	-6.20	9.683 + 1	0.865	1.603	0.890	290.8	1.387	4.537
16000	15996	210.05	-63.10	-6.60	8.930	0.863	1.481	0.889	290.5	1.385	4.529
16500	16495	209.66	-63.49	-6.99	8.233	0.860	1.368	0.889	290.3	1.383	4.520
17000	16993	209.26	-63.89	-7.39	7.590	0.858	1.264	0.888	290.0	1.381	4.512
17500	17491	208.86	-64.29	-7.79	6.997	0.855	1.167	0.887	289.7	1.378	4.504
18000	17989	208.46	-64.69	-8.19	6.449	0.852	1.078	0.886	289.4	1.376	4.496
18500	18488	208.06	-65.09	-8.59	5.942	0.850	9.953 − 2	0.884	289.2	1.374	4.488
19000	18986	207.66	-65.49	-8.99	5.475 + 1	0.847	9.185 − 2	0.881	288.9	1.372 − 5	4.480 − 6
19500	19484	207.65	-65.50	-9.00	5.044	0.844	8.463	0.883	288.9	1.372	4.480
20000	19982	207.65	-65.50	-9.00	4.648	0.841	7.797	0.877	288.9	1.372	4.480
20500	20480	207.65	-65.50	-9.43	4.282	0.837	7.184	0.876	288.9	1.372	4.480
21000	20978	207.65	-65.50	-9.93	3.945	0.834	6.619	0.874	288.9	1.372	4.480
21500	21476	207.65	-65.50	-10.43	3.635	0.831	6.098	0.873	288.9	1.372	4.480
22000	21973	207.65	-65.50	-10.92	3.349	0.828	5.619	0.871	288.9	1.372	4.480
22500	22471	207.65	-65.50	-11.42	3.086	0.824	5.177	0.869	288.9	1.372	4.480
23000	22969	207.65	-65.50	-11.92	2.843	0.820	4.770	0.867	288.9	1.372	4.480
23500	23466	207.65	-65.50	-12.41	2.620	0.816	4.395	0.865	288.9	1.372	4.480
24000	23964	207.65	-65.50	-12.91	2.414 + 1	0.812	4.050 − 2	0.863	288.9	1.372 − 5	4.480 − 6
24500	24461	207.65	-65.50	-13.41	2.224	0.808	3.732	0.860	288.9	1.372	4.480
25000	24958	207.65	-65.50	-13.90	2.050	0.804	3.439	0.858	288.9	1.372	4.480
25500	25455	207.65	-65.50	-14.40	1.889	0.800	3.169	0.855	288.9	1.372	4.480
26000	25952	207.65	-65.50	-14.89	1.740	0.795	2.920	0.852	288.9	1.372	4.480
26500	26449	207.65	-65.50	-15.39	1.604	0.791	2.691	0.849	288.9	1.372	4.480
27000	26946	207.65	-65.50	-15.89	1.478	0.786	2.479	0.846	288.9	1.372	4.480
27500	27443	207.65	-65.50	-16.38	1.362	0.781	2.285	0.843	288.9	1.372	4.480
28000	27940	207.65	-65.50	-16.88	1.255	0.777	2.105	0.839	288.9	1.372	4.480
28500	28437	207.65	-65.50	-17.37	1.156	0.772	1.940	0.836	288.9	1.372	4.480
29000	28933	207.65	-65.50	-17.87	1.066 + 1	0.767	1.788 − 2	0.832	288.9	1.372 − 5	4.480 − 6
29500	29430	207.65	-65.50	-18.36	9.821 + 0	0.761	1.648	0.829	288.9	1.372	4.480
30000	29926	207.65	-65.50	-18.86	9.051	0.756	1.518	0.825	288.9	1.372	4.480

[redacted]

[redacted] PAGE IS BEST QUALITY PR[illegible] ABLE

[redacted] TABLE 1-2. STANDARD ATMOSPHERE [illegible]NISHED[illegible]

[illegible] N January [illegible]

GEOMETRIC ALTITUDE, METRIC UNITS

Altitude		Temperature			Pressure		Density		Sound speed	Coefficient of viscosity	Thermal conductivity
Z, m	H, m	T, °K	t, °C	$T - T_{std}$	P, mb	P/P_{std}	ρ, kg m⁻³	ρ/ρ_{std}	C_s, m sec⁻¹	μ, kg m⁻¹ sec⁻¹	k, kcal m⁻¹ sec⁻¹ °K⁻¹
0	0	249.[illegible]	-23.93	-38.93	1.01350 + 3	1.000	1.417 + 0	1.157	316.5	1.595 - 5	5.307 - 6
250	251	249.[illegible]	-23.10	-36.55	9.745 + 2	0.996	1.365	1.141	316.9	1.5[illegible]	5.322
500	501	250.[illegible]	-22.42	-34.17	9.464	0.991	1.315	1.127	317.4	1.603	5.337
750	752	251.[illegible]	-21.67	-31.79	9.147	0.987	1.267	1.112	317.9	1.607	5.352
1000	1002	252.[illegible]	-20.91	-29.41	8.841	0.984	1.221	1.098	318.4	1.611	5.366
1250	1253	252.[illegible]	-20.16	-27.03	8.547	0.980	1.177	1.085	318.9	1.615	5.381
1500	1503	253.[illegible]	-19.43	-24.68	8.263	0.977	1.135	1.072	319.3	1.618	5.395
1750	1753	252.[illegible]	-20.41	-24.44	7.988	0.974	1.103	1.064	318.4	1.611	5.368
2000	2004	250.[illegible]	-22.20	-24.20	7.721	0.971	1.072	1.064	317.6	1.604	5.341
2250	2254	249.[illegible]	-23.58	-23.96	7.462	0.968	1.042	1.061	316.7	1.597	5.314
2500	2505	248.[illegible]	-24.96	-23.72	7.210 + 2	0.965	1.012 + 0	1.057	315.8	1.590 - 5	5.287 - 6
2750	2755	246.[illegible]	-26.35	-23.48	6.965	0.962	9.831 - 1	1.054	314.9	1.583	5.260
3000	3005	245.[illegible]	-27.73	-23.24	6.727	0.959	9.549	1.050	314.1	1.575	5.233
3250	3256	244.[illegible]	-29.11	-23.00	6.496	0.956	9.273	1.047	313.2	1.568	5.206
3500	3506	242.[illegible]	-30.49	-22.76	6.272	0.953	9.004	1.043	312.3	1.561	5.179
3750	3756	241.28	-31.88	-22.51	6.054	0.951	8.741	1.039	311.4	1.554	5.152
4000	4006	239.[illegible]	-33.26	-22.27	5.843	0.948	8.485	1.035	310.[illegible]	1.547	5.125
4250	4257	238.[illegible]	-34.64	-22.03	5.638	0.945	8.234	1.032	309.6	1.539	5.097
[illegible]00	4507	237.[illegible]	-36.01	-21.78	5.439	0.942	7.990	1.028	308.7	1.532	5.070
[illegible]750	4757	235.[illegible]	-37.39	-21.54	5.245	0.939	7.751	1.025	307.8	1.525	5.043
5000	5007	234.[illegible]	-38.77	-21.30	5.058 + 2	0.936	7.518 - 1	1.021	306.9	1.517 - 5	5.016 - 6
5250	5257	233.[illegible]	-40.15	-21.05	4.877	0.933	7.291	1.017	306.0	1.510	4.988
5500	5508	231.[illegible]	-41.53	-20.81	4.700	0.930	7.069	1.014	305.1	1.503	4.961
5750	5758	230.25	-42.90	-20.56	4.530	0.927	6.853	1.010	304.2	1.495	4.934
6000	6008	228.[illegible]	-44.28	-20.32	4.364	0.924	6.643	1.006	303.3	1.488	4.906
6250	6258	227.[illegible]	-45.66	-20.07	4.204	0.921	6.437	1.003	302.4	1.481	4.879
6500	6508	226.[illegible]	-47.04	-19.83	4.048	0.918	6.237	0.999	301.4	1.473	4.851
6750	6758	224.[illegible]	-48.41	-19.58	3.898	0.916	6.042	0.995	300.5	1.466	4.824
7000	7008	223.[illegible]	-49.79	-19.34	3.752	0.913	5.852	0.992	299.6	1.458	4.796
7250	7258	221.[illegible]	-51.16	-19.09	3.611	0.910	5.667	0.988	298.7	1.451	4.769
7500	7508	220.[illegible]	-52.54	-18.85	3.474 [redacted]	0.907	5.486 - 1	0.985	297.8	1.443 - 5	4.741 - 6
7750	7758	219.25	-53.92	-18.60	3.342	0.904	5.310	0.981	296.8	1.435	4.714
8000	8008	217.[illegible]	-55.29	-18.36	3.214	0.901	5.139	0.977	295.9	1.428	4.686
8250	8258	216.[illegible]	-56.67	-18.11	3.090	0.899	4.972	0.974	295.0	1.421	4.658
8500	8508	215.[illegible]	-58.01	-17.83	2.970	0.896	4.809	0.970	294.0	1.413	4.631
8750	8758	214.[illegible]	-58.39	-16.59	2.854	0.893	4.650	0.962	293.8	1.411	4.6[illegible]
9000	9007	214.[illegible]	-58.76	-15.34	2.743	0.891	4.457	0.954	293.5	1.409	4.616
9250	9257	214.[illegible]	-59.13	-14.10	2.636	0.888	4.291	0.947	293.3	1.407	4.609
9500	9507	213.[illegible]	-59.51	-12.85	2.533	0.886	4.130	0.939	293.0	1.405	4.601
9750	9757	213.[illegible]	-59.88	-11.61	2.434	0.884	3.975	0.932	292.[illegible]	1.403	4.593
10000	10007	212.[illegible]	-60.26	-10.36	2.338 + 2	0.882	3.826 - 1	0.925	292.5	1.401 - 5	4.586 - 6
10250	10258	212.[illegible]	-60.63	-9.12	2.246	0.881	3.682	0.918	292.[illegible]	1.399	4.578
10500	10508	212.[illegible]	-61.01	-7.87	2.158	0.879	3.543	0.912	292.0	1.397	4.571
10750	10758	211.77	-61.38	-6.63	2.072	0.878	3.409	0.906	291.7	1.395	4.563
11000	11008	211.[illegible]	-61.76	-5.38	1.991	0.877	3.280	0.899	291.5	1.393	4.556
11500	11505	210.[illegible]	-62.51	-6.01	1.836	0.875	3.036	0.900	291.0	1.388	4.540
12000	12004	209.[illegible]	-63.26	-6.76	1.693	0.873	2.810	0.901	290.4	1.384	4.525
12500	12503	209.[illegible]	-64.00	-7.50	1.561	0.870	2.599	0.901	289.9	1.380	4.510
13000	13003	208.[illegible]	-64.75	-8.25	1.438	0.867	2.404	0.902	289.4	1.376	4.495
13500	13502	207.[illegible]	65.50	-9.00	1.325	0.864	2.223	0.902	288.9	1.372	4.4[illegible]
14000	14001	206.[illegible]	-66.25	-9.75	1.220 + 2	0.861	2.055 - 1	0.902	288.4	1.368 - 5	4.465 - 6
14500	14499	206.15	-67.00	-10.50	1.124	0.858	1.899	0.902	287.9	1.363	4.449
15000	14998	205.40	-67.75	-11.25	1.034	0.855	1.754	0.901	287.3	1.359	4.434
15500	15497	204.[illegible]	-68.49	-11.99	9.519 + 1	0.850	1.620	0.900	286.8	1.355	4.4[illegible]
16000	15996	203.[illegible]	-69.24	-12.74	8.758	0.846	1.496	0.899	286.3	1.351	4.404
16500	16494	203.[illegible]	-69.99	-13.49	8.055	0.841	1.381	0.897	285.7	1.346	4.388
17000	16993	202.48	-70.74	-14.24	7.406	0.837	1.275	0.896	285.2	1.342	4.373
17500	17491	201.[illegible]	-71.49	-14.99	6.807	0.832	1.176	0.894	284.7	1.338	4.358
18000	17989	201.3[illegible]	-71.79	-15.29	6.256	0.827	1.082	0.890	284.5	1.336	4.352
18500	18488	201.[illegible]	-72.09	-15.59	5.748	0.822	9.960 - 2	0.885	284.3	1.335	4.346
19000	18986	200.7[illegible]	-72.39	-15.89	5.281 + 1	0.817	9.165 - 2	0.881	284.0	1.333 - 5	4.339 - 6
19500	19484	200.[illegible]	-72.69	-16.19	4.852	0.811	8.432	0.877	283.8	1.331	4.333
20000	19982	200.16	-72.99	-16.49	4.457	0.806	7.757	0.872	283.6	1.329	4.327
20500	20480	199.8[illegible]	-73.29	-17.22	4.093	0.801	7.135	0.870	283.4	1.328	4.321
21000	20978	199.5[illegible]	-73.59	-18.02	3.759	0.795	6.562	0.867	283.2	1.326	4.315
21500	21476	199.2[illegible]	-73.88	-18.81	3.452	0.789	6.035	0.864	283.0	1.324	4.309
22[illegible]	21973	198.98	-74.18	-19.61	3.169	0.783	5.549	0.860	282.9	1.323	4.303
22500	22471	198.6[illegible]	-74.48	-20.40	2.910	0.777	5.102	0.857	282.6	1.321	4.297
23000	22969	198.37	-74.78	-21.20	2.671	0.770	4.690	0.853	282.3	1.319	4.291
23500	23466	198.07	-75.08	-21.99	2.451	0.764	4.312	0.849	282.1	1.318	4.285
24000	23964	197.77	-75.38	-22.79	2.250 + 1	0.757	3.963 - 2	0.844	281.9	1.316 - 5	4.278 - 6
24500	24461	197.47	-75.68	-23.58	2.064	0.750	3.642	0.840	281.7	1.314	4.272
25000	24958	197.18	-75.97	-24.38	1.894	0.743	3.348	0.835	281.5	1.312	4.266
25500	25455	197.15	-76.00	-24.90	1.738	0.736	3.071	0.829	281.5	1.312	4.266
26000	25952	197.15	-76.00	-25.39	1.594	0.729	2.817	0.822	281.5	1.312	4.266
26500	26449	197.15	-76.00	-25.89	1.463	0.721	2.585	0.816	281.5	1.312	4.266
27000	26946	197.15	-76.00	-26.39	1.342	0.714	2.371	0.809	281.5	1.312	4.266
27500	27443	197.15	-76.00	-26.88	1.231	0.706	2.176	0.803	281.5	1.312	4.266
28000	27940	197.15	-76.00	-27.38	1.130	0.699	1.996	0.796	281.5	1.312	4.266
28500	28437	197.15	-76.00	-27.87	1.037	0.692	1.832	0.789	281.5	1.312	4.266
29000	28933	197.15	-76.00	-28.37	9.511 + 0	0.684	1.681 - 2	0.782	281.5	1.312 - 5	4.266 - 6
29500	29430	197.15	-76.00	-28.86	8.727	0.677	1.542	0.776	281.5	1.312	4.266
30000	29926	197.15	-76.00	-29.36	8.006	0.669	1.415	0.769	281.5	1.312	4.266

[redacted]

[redacted] TABLE 1-3. STANDARD ATMOSPHERE

[illegible] N January [illegible]

GEOMETRIC ALTITUDE, METRIC UNITS

Altitude		Temperature			Pressure		Density		Sound speed	Coefficient of viscosity	Thermal conductivity
Z, m	H, m	T, °K	t, °C	$T - T_{std}$	P, mb	P/P_{std}	ρ, kg m⁻³	ρ/ρ_{std}	c_s, m/sec	μ, kg m⁻¹ sec⁻¹	k, kcal m⁻¹ sec⁻¹ (°K)⁻¹
0	0	249.22	-23.93	-38.93	1.01350 + 3	1.000	1.417 + 0	1.157	316.5	1.595 - 5	5.307 - 6
250	251	249.97	-23.18	-36.55	9.793 + 2	0.996	1.365	1.141	316.9	1.599	5.322
500	501	250.73	-22.42	-34.17	9.484	0.991	1.315	1.127	317.4	1.603	5.337
750	752	251.48	-21.67	-31.79	9.167	0.987	1.267	1.112	317.9	1.607	5.352
1000	1002	252.24	-20.91	-29.41	8.891	0.984	1.221	1.098	318.4	1.611	5.366
1250	1253	252.99	-20.16	-27.03	8.567	0.980	1.177	1.085	318.9	1.615	5.381
1500	1503	253.72	-19.43	-24.66	8.263	0.977	1.135	1.072	319.3	1.618	5.395
1750	1753	252.34	-20.81	-24.44	7.980	0.974	1.103	1.069	318.4	1.611	5.368
2000	2004	250.95	-22.20	-24.20	7.721	0.971	1.072	1.064	317.6	1.604	5.341
2250	2254	249.58	-23.58	-23.96	7.462	0.968	1.042	1.061	316.7	1.597	5.314
2500	2505	248.19	-24.96	-23.72	7.210 + 2	0.965	1.012 + 0	1.057	315.8	1.590 - 5	5.287 - 6
2750	2755	246.82	-26.33	-23.48	6.965	0.962	9.831 - 1	1.054	314.9	1.583	5.260
3000	3005	245.42	-27.73	-23.24	6.727	0.959	9.549	1.050	314.1	1.575	5.233
3250	3258	244.04	-29.11	-23.00	6.496	0.956	9.273	1.047	313.2	1.568	5.206
3500	3506	242.66	-30.49	-22.76	6.272	0.953	9.004	1.043	312.3	1.561	5.179
3750	3756	241.28	-31.88	-22.51	6.054	0.951	8.741	1.039	311.4	1.554	5.152
4000	4006	239.88	-33.26	-22.27	5.843	0.948	8.485	1.035	310.5	1.547	5.125
4250	4257	238.51	-34.64	-22.03	5.638	0.945	8.234	1.032	309.6	1.539	5.097
4500	4507	237.14	-36.01	-21.78	5.439	0.942	7.990	1.028	308.7	1.532	5.070
4750	4757	235.76	-37.39	-21.54	5.245	0.939	7.751	1.025	307.8	1.525	5.043
5000	5007	234.38	-38.77	-21.30	5.058 + 2	0.936	7.518 - 1	1.021	306.9	1.517 - 5	5.016 - 6
5250	5257	233.00	-40.15	-21.05	4.877	0.933	7.291	1.017	306.0	1.510	4.988
5500	5508	231.62	-41.53	-20.81	4.700	0.930	7.069	1.014	305.1	1.503	4.961
5750	5758	230.25	-42.90	-20.56	4.530	0.927	6.853	1.010	304.2	1.495	4.934
6000	6008	228.88	-44.28	-20.32	4.364	0.924	6.643	1.006	303.3	1.488	4.906
6250	6258	227.49	-45.66	-20.07	4.204	0.921	6.437	1.003	302.4	1.481	4.879
6500	6508	226.11	-47.04	-19.83	4.048	0.918	6.237	0.999	301.4	1.473	4.851
6750	6758	224.74	-48.41	-19.58	3.898	0.916	6.042	0.995	300.5	1.466	4.824
7000	7008	223.36	-49.79	-19.34	3.752	0.913	5.852	0.992	299.6	1.458	4.796
7250	7258	221.98	-51.16	-19.09	3.611	0.910	5.667	0.988	298.7	1.451	4.769
7500	7508	220.60	-52.55	-18.85	3.474 + 2	0.907	5.486 - 1	0.985	297.8	1.443 - 5	4.741 - 6
7750	7759	219.23	-53.92	-18.60	3.342	0.904	5.310	0.981	296.8	1.436	4.714
8000	8008	217.86	-55.29	-18.36	3.214	0.901	5.139	0.977	295.9	1.428	4.686
8250	8258	216.48	-56.67	-18.11	3.090	0.899	4.972	0.974	295.0	1.421	4.658
8500	8508	215.12	-58.03	-17.86	2.970	0.896	4.809	0.970	294.1	1.413	4.632
8750	8758	215.87	-57.28	-15.98	2.855	0.893	4.607	0.957	294.5	1.417	4.646
9000	9007	216.57	-56.58	-13.18	2.744	0.891	4.414	0.945	295.0	1.421	4.660
9250	9257	217.27	-55.88	-10.86	2.638	0.889	4.230	0.933	295.5	1.425	4.675
9500	9507	217.97	-55.18	-8.55	2.537	0.888	4.055	0.922	296.0	1.429	4.689
9750	9757	218.67	-54.48	-6.24	2.440	0.886	3.887	0.911	296.5	1.433	4.704
10000	10007	219.37	-53.78	-3.88	[redacted]	0.885	3.726 - 1	0.901	297.0	1.437 - 5	4.718 - 6
10250	10256	220.07	-53.08	-1.56	[redacted]	0.885	3.571	0.891	297.4	1.440	4.730
10500	10506	220.77	-52.38	0.76	[redacted]	0.885	3.426	0.882	297.9	1.444	4.744
10750	10756	221.47	-51.68	3.07	[redacted]	0.885	3.285	0.873	298.4	1.448	4.758
11000	11006	222.15	-51.00	5.38	[redacted]	0.886	3.152	0.866	298.8	1.452	4.772
11500	11505	222.15	-51.00	5.50	[redacted]	0.887	2.914	0.865	298.8	1.452	4.772
12000	12004	222.15	-51.00	5.50	[redacted]	0.889	2.704	0.867	298.8	1.452	4.772
12500	12503	222.15	-51.00	5.50	[redacted]	0.891	2.506	0.868	298.8	1.452	4.772
13000	13003	222.15	-51.00	5.50	[redacted]	0.892	2.317	0.870	298.8	1.452	4.772
13500	13502	222.15	-51.00	5.50	[redacted]	0.893	2.148	0.871	298.8	1.452	4.772
14000	14001	222.15	-51.00	5.50	[redacted]	0.895	1.989 - 1	0.873	298.8	1.452 - 5	4.772 - 6
14500	14499	222.15	-51.00	5.50	1.175	0.897	1.842	0.875	298.8	1.452	4.772
15000	14998	222.15	-51.00	5.50	1.088	0.898	1.706	0.876	298.8	1.452	4.772
15500	15497	222.15	-51.00	5.50	1.008	0.900	1.580	0.877	298.8	1.452	4.772
16000	15996	222.15	-51.00	5.50	9.332 + 1	0.902	1.461	0.879	298.8	1.452	4.772
16500	16495	222.15	-51.00	5.50	8.643	0.903	1.355	0.881	298.8	1.452	4.772
17000	16993	222.15	-51.00	5.50	8.006	0.905	1.255	0.882	298.8	1.452	4.772
17500	17491	222.40	-50.75	5.75	7.415	0.906	1.162	0.883	299.0	1.453	4.777
18000	17989	222.65	-50.50	6.00	6.869	0.908	1.075	0.884	299.1	1.454	4.782
18500	18488	222.89	-50.26	6.24	6.364	0.910	9.948 - 2	0.884	299.3	1.456	4.787
19000	18986	223.14	-50.01	6.49	5.896 + 1	0.912	9.205 - 2	0.885	299.5	1.457 - 5	4.792 - 6
19500	19484	223.39	-49.76	6.74	5.463	0.914	8.520	0.886	299.6	1.458	4.797
20000	19982	223.64	-49.51	6.99	5.063	0.916	7.887	0.887	299.8	1.460	4.802
20500	20480	223.89	-49.26	6.81	4.692	0.918	7.301	0.890	300.0	1.461	4.807
21000	20978	224.14	-49.01	6.56	4.349	0.920	6.760	0.893	300.1	1.462	4.812
21500	21476	224.39	-48.76	6.31	4.032	0.922	6.259	0.896	300.3	1.464	4.817
22000	21973	224.64	-48.51	6.06	3.738	0.924	5.796	0.899	300.5	1.465	4.822
22500	22471	224.89	-48.26	5.82	3.465	0.925	5.368	0.901	300.6	1.467	4.827
23000	22969	225.14	-48.01	5.57	3.213	0.927	4.972	0.904	300.8	1.468	4.832
23500	23466	225.38	-47.77	5.32	2.980	0.929	4.606	0.906	301.0	1.469	4.837
24000	23964	225.63	-47.52	5.07	2.763 + 1	0.930	4.267 - 2	0.909	301.1	1.471 - 5	4.842 - 6
24500	24461	225.88	-47.27	4.83	2.563	0.931	3.953	0.911	301.3	1.472	4.847
25000	24958	226.13	-47.02	4.58	2.377	0.933	3.663	0.914	301.5	1.473	4.852
25500	25455	226.83	-46.32	4.79	2.206	0.934	3.387	0.914	301.9	1.477	4.866
26000	25952	227.58	-45.57	5.04	2.047	0.935	3.133	0.915	302.4	1.481	4.881
26500	26449	228.32	-44.83	5.28	1.900	0.937	2.899	0.915	302.9	1.485	4.895
27000	26946	229.07	-44.08	5.53	1.764	0.938	2.683	0.916	303.4	1.489	4.910
27500	27443	229.82	-43.33	5.78	1.638	0.940	2.483	0.916	303.9	1.493	4.925
28000	27940	230.56	-42.59	6.03	1.522	0.942	2.299	0.917	304.4	1.497	4.940
28500	28437	231.31	-41.84	6.28	1.414	0.943	2.130	0.917	304.9	1.501	4.955
29000	28933	232.05	-41.10	6.53	1.314 + 1	0.945	1.973 - 2	0.918	305.4	1.505 - 5	4.970 - 6
29500	29430	232.80	-40.35	6.78	1.222	0.947	1.828	0.920	305.9	1.509	4.984
30000	29926	233.54	-39.61	7.03	1.136	0.949	1.694	0.920	306.4	1.513	4.999

[redacted]

[redacted]

[redacted] TABLE 1-4. STANDARD ATMOSPHERE

[illegible]

Altitude		Temperature			Pressure		Density		Speed of sound	Coefficient of viscosity	Kinematic viscosity
Z, m	H, m	T, °K	t, °C	T − T₀	P, mb	P/P₀	ρ	ρ/ρ₀	[illegible]	μ	ν
0	[illegible]	[illegible]	[illegible]	[illegible]	[illegible]	[illegible]	[illegible]	[illegible]	[illegible]	[illegible]	[illegible]
250	[illegible]	[illegible]	[illegible]	[illegible]	[illegible]	[illegible]	[illegible]	[illegible]	[illegible]	[illegible]	[illegible]
500	[illegible]	[illegible]	[illegible]	[illegible]	[illegible]	[illegible]	[illegible]	[illegible]	[illegible]	[illegible]	[illegible]
750	[illegible]	[illegible]	[illegible]	[illegible]	[illegible]	[illegible]	[illegible]	[illegible]	[illegible]	[illegible]	[illegible]
1000	[illegible]	[illegible]	[illegible]	[illegible]	[illegible]	[illegible]	[illegible]	[illegible]	[illegible]	[illegible]	[illegible]
1250	[illegible]	[illegible]	[illegible]	[illegible]	[illegible]	[illegible]	[illegible]	[illegible]	[illegible]	[illegible]	[illegible]
1500	[illegible]	[illegible]	[illegible]	[illegible]	[illegible]	[illegible]	[illegible]	[illegible]	[illegible]	[illegible]	[illegible]
1750	[illegible]	[illegible]	[illegible]	[illegible]	[illegible]	[illegible]	[illegible]	[illegible]	[illegible]	[illegible]	[illegible]
2000	[illegible]	[illegible]	[illegible]	[illegible]	[illegible]	[illegible]	[illegible]	[illegible]	[illegible]	[illegible]	[illegible]
[illegible]	[illegible]	[illegible]	[illegible]	[illegible]	[illegible]	[illegible]	[illegible]	[illegible]	[illegible]	[illegible]	[illegible]

[redacted]

[redacted] TABLE 1-5

WATER VAPOR CONCENTRATION IN THE ARCTIC

ALTITUDE (km)	JANUARY TEMPERATURE (°K)	JANUARY RELATIVE HUMIDITY (%)	JANUARY ABSOLUTE HUMIDITY (g/cm^3)	JULY TEMPERATURE (°K)	JULY RELATIVE HUMIDITY (%)	JULY ABSOLUTE HUMIDITY (g/cm^3) [redacted]
0	249	80	.46	278	85	5.6
1	252	65	.52	276	75	4.3
1.5	254	60	.56	274	-	-
2	251	60	.43	273	65	3.1
2.5	248	-	-	272	65	2.9
3	245	55	.22	268	-	-
4	240	50	.13	262	55	1.2
6	229	45	.05	249	45	.26
8	218	40	.01	236	35	.06
9.5	-		[redacted]	226	30	.02
10	-			227	20	.02

[redacted]

1.2.2 [redacted] Meteorological Conditions

[redacted] The above model atmospheres represent the average conditions to be expected in the Arctic. The probability of variation from these standard values is important especially near the surface where the land mass and ocean climate patterns should be considered.

[redacted] An extremely thorough presentation of the climates of the polar region is given by Orvig (1970). A large part of this section is extracted from that reference.

1.2.2.1 [redacted] Temperature

[redacted] The temperature of the air near the surface is dominated by the temperature of the ice surface and a thin layer of cold air covers the polar region. Warm air advection from the Atlantic or mixing of warmer upper air by strong winds can cause large temperature increases in the winter. The temperature of the ice surface over the ocean is determined by a balance of the radiative cooling of the surface and the heat conducted from the water. The minimum temperatures on the surface are typically -40°C or -50°C over thick ice. In overcast calm conditions a -25°C temperature will prevail. In Figure 1-4 the surface air temperature over the Arctic is shown. The influence of the open water in moderating the surface temperature is obvious.

[redacted] In the summer the temperature is held very close to the melting point over the ice pack as indicated in Figure 1-5. A warming is noted over open water areas and over land.

[redacted] A study (Salmela and Sissenwine, 1970) was conducted on the frequency of occurrence of low temperatures for use in specifying military requirements for low temperature operation. In Figures 1-6 through 1-9 show the estimated risk of experiencing

[redacted]

[redacted] Figure 1-4. MEAN AIR TEMPERATURE (°C), JANUARY

[redacted] FIGURE 1-5. MEAN AIR TEMPERATURE (°C), JULY

[redacted]

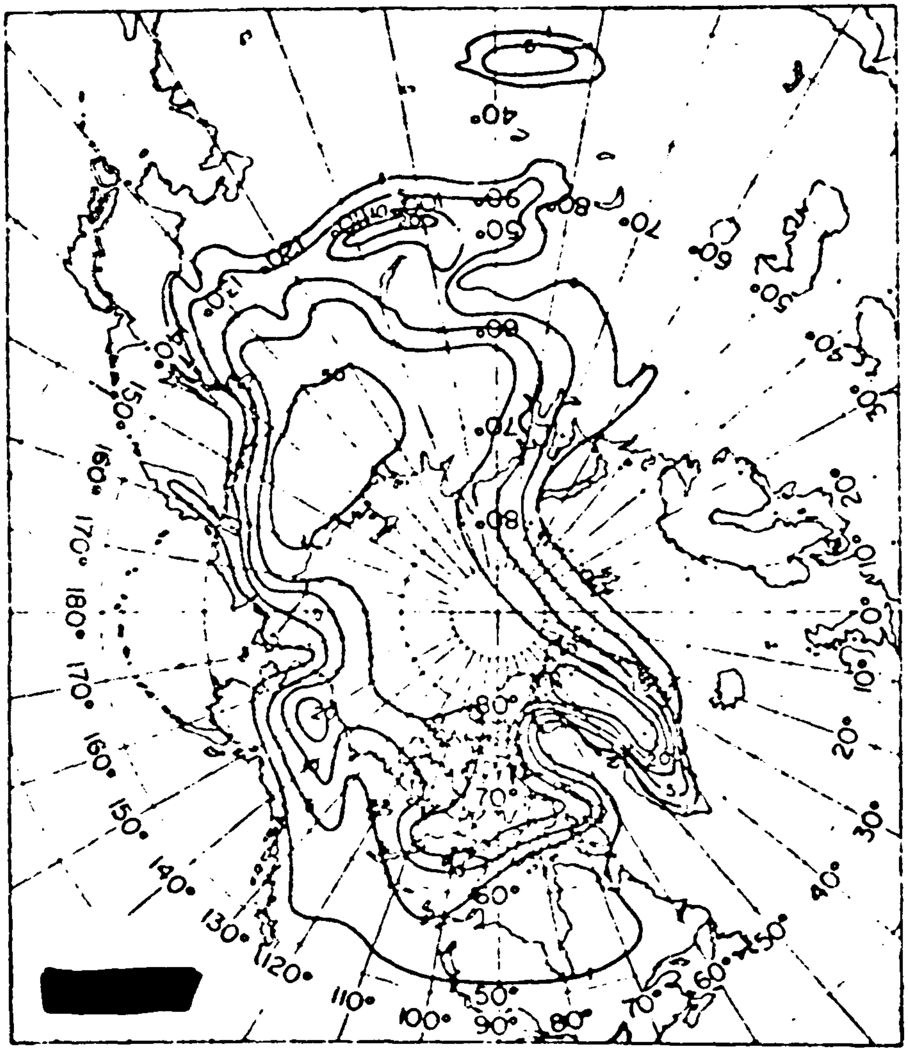

[redacted]

[redacted] Figure 1-6. Estimated Risk (Percent of Coldest Month) Temperature Below -40°F

[redacted]

[redacted]

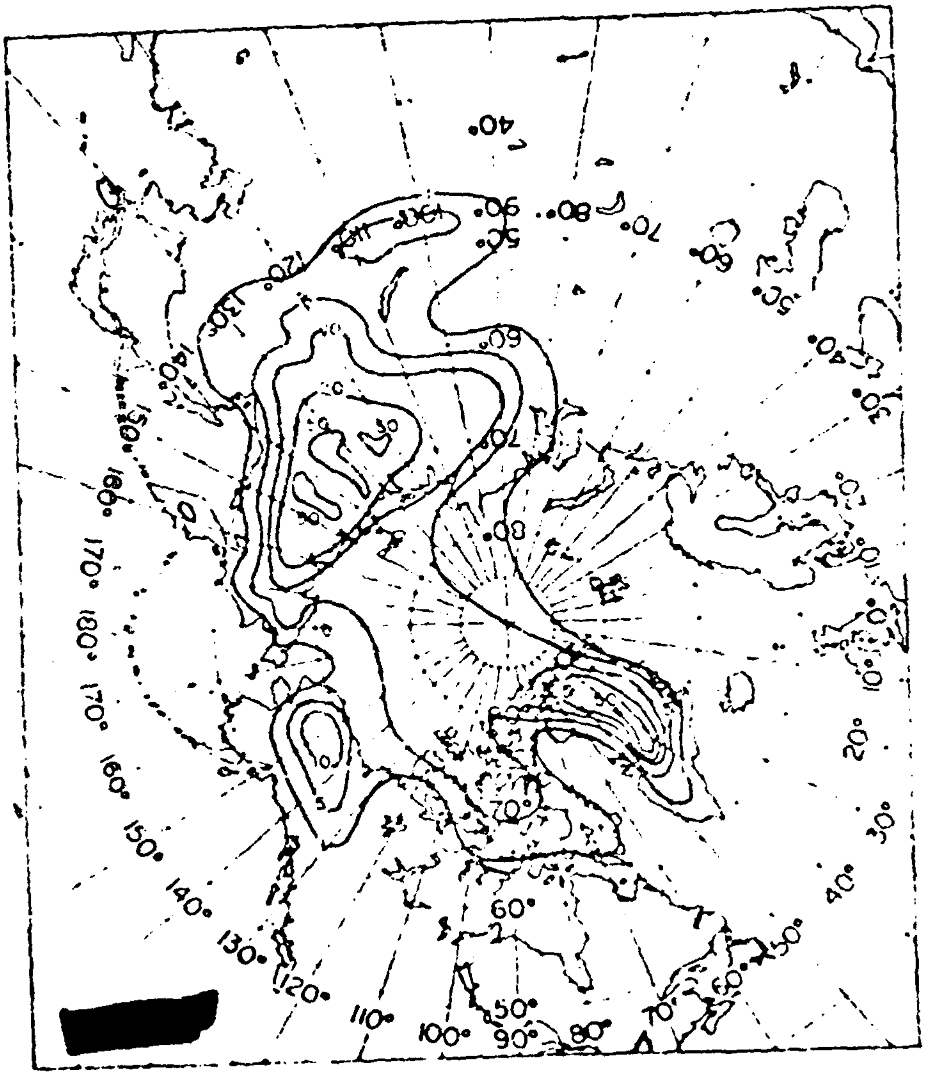

[redacted] Figure 1-? [illegible] (Percent of Coldest Month) Temperature [illegible]

[redacted]

[redacted]

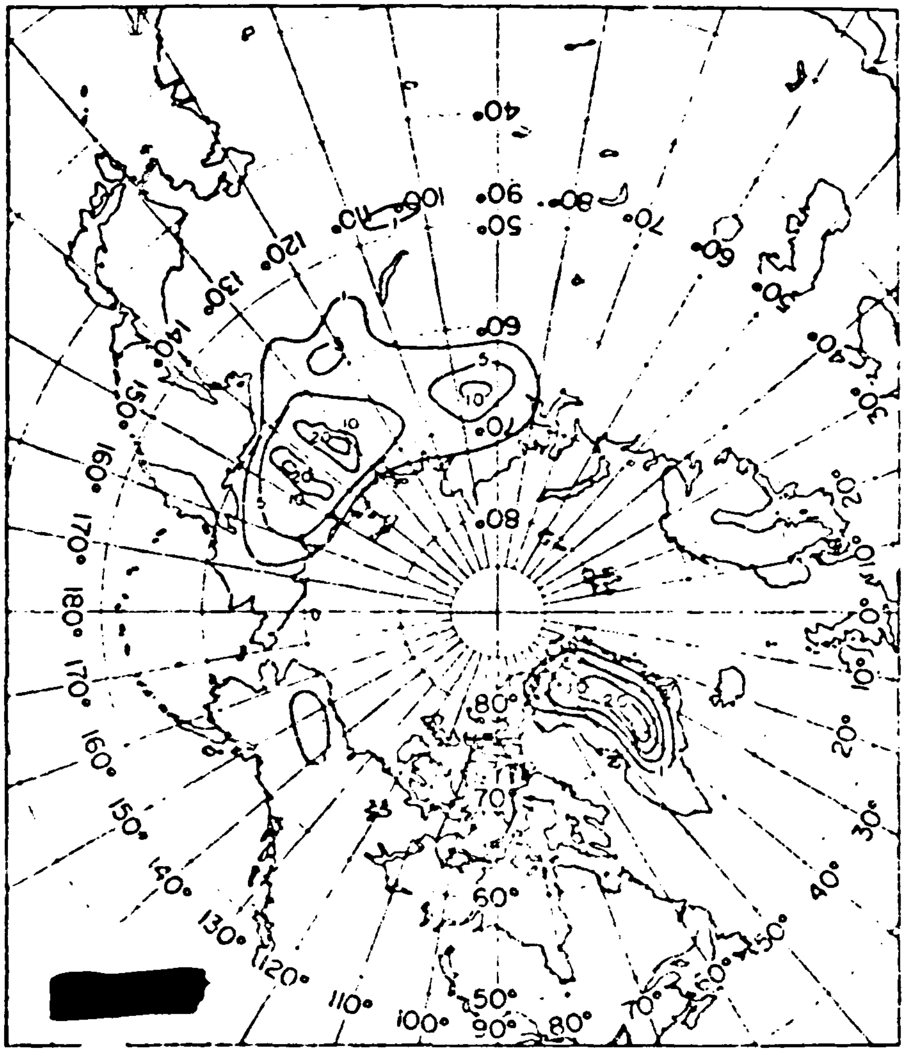

[redacted] Figure 8. Estimated Risk (Percent of Coldest Month) Temperature Below -60°F

[redacted]

[redacted]

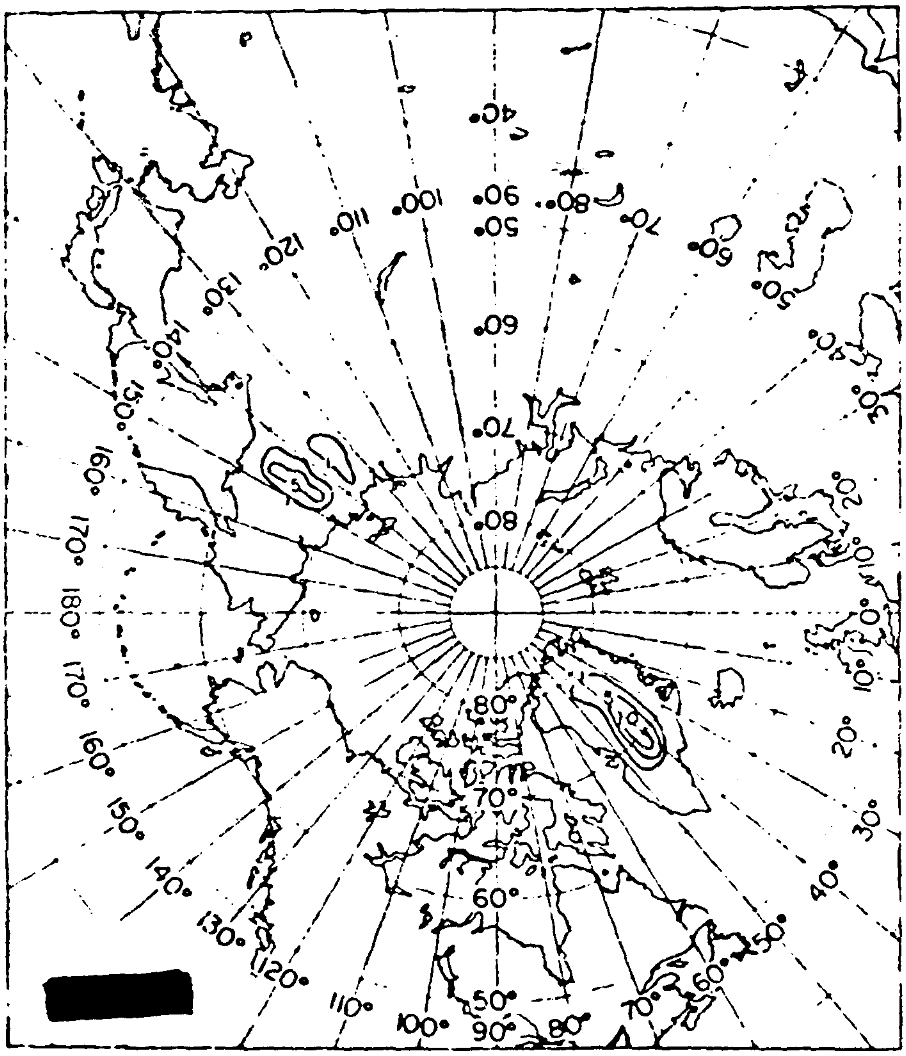

[redacted] Figure 1-8. Estimated Risk (Percent of Coldest Month) Temperature Below -70°F

[redacted]

[redacted] temperatures below -40°F (-40°C), -50°F (-45°C), -60°F (-51°C), and -70°F (-56.7°C) during the coldest month (usually January). As one expects the lowest temperatures occur in interior Greenland and in Siberia with extremes below -70°F possible. Temperatures below -60° are not expected over the ice cap and temperatures below -50°F will occur only about 5% of the time over a significant portion of the ice cap as shown in Figure 1-7. In the Barents and Greenland Sea Region there is less than 1% chance of experiencing temperatures below -40°F.

[redacted] Temperature inversions are very common in the Arctic as shown in Figure 1-10 (Orvig, 1970). The surface inversions can have very steep gradients (up to 1°C/m near the surface) and extend to 2 km altitude. When a combination of both types occurs the system may extend to 4 km with an intensity of 25°C. Variations in intensity and occurrence over the polar ocean are small but near the land areas pronounced differences can occur (Bilello, 1966).

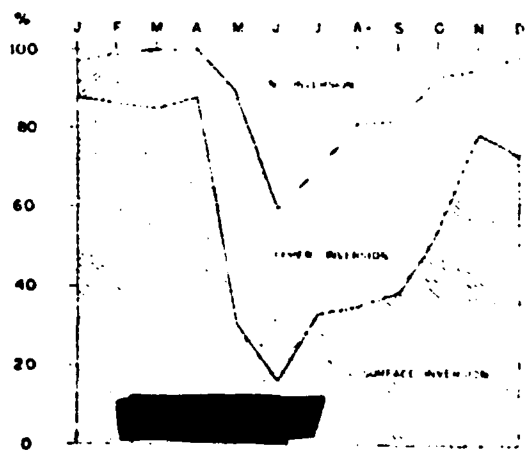

[redacted] FIGURE 1-10. FREQUENCY DISTRIBUTION OF INVERSION TYPES

[redacted]

1.2.2.2 [redacted] Surface Pressure and Wind

[redacted] The mean air pressure in January and July is shown in Figures 1-11 and 1-12 (from Orvig, 1970). There is a larger variability in January than July, but in general the variation from the 1013 mb value used in the standard 75° North atmosphere is less than that noted for the temperatures.

[redacted] The winds over the polar ice are usually representative of the pressure field. The wind speeds at the surface are usually not very high because the strong surface inversion isolates the surface from upper air movements. Table 1-6 (Orvig, 1970) summarizes the expected wind speed over the polar ocean. Near the coastal areas topography plays an important part in the wind patterns, and in areas near the polar cyclonic regions gale force winds can occur.

[redacted] TABLE 1-6

FREQUENCY DISTRIBUTION OF WIND SPEED OVER CENTRAL POLAR OCEAN (%)

Month	Wind speed (m sec): 0	1	2	3	4	5	6	7	8	9	10-14	15-19	≥20	>7
Jan	11	7	8	10	13	12	8	8	6	4	10	2	1	23
Feb	10	6	11	15	17	15	9	5	5	1	6	0	0	12
Mar	6	6	8	18	22	15	7	6	3	2	5	1	0	12
Apr	6	5	15	15	17	15	8	7	5	4	3	0	0	12
May	7	5	11	16	16	15	11	7	6	3	3	0	0	12
June	5	5	9	15	13	15	11	9	6	4	7	1	0	18
July	4	3	9	12	13	16	10	9	9	6	6	1	0	24
Aug	4	4	7	11	11	15	11	11	8	5	11	2	0	26
Sept	8	4	9	13	15	15	8	10	5	4	7	2	0	18
Oct	7	5	9	12	12	12	10	9	7	4	11	2	0	24
Nov	9	7	10	13	16	15	7	6	6	4	6	1	0	17
Dec	11	10	14	14	17	12	6	5	4	3	4	0	0	11

[redacted]

[redacted]

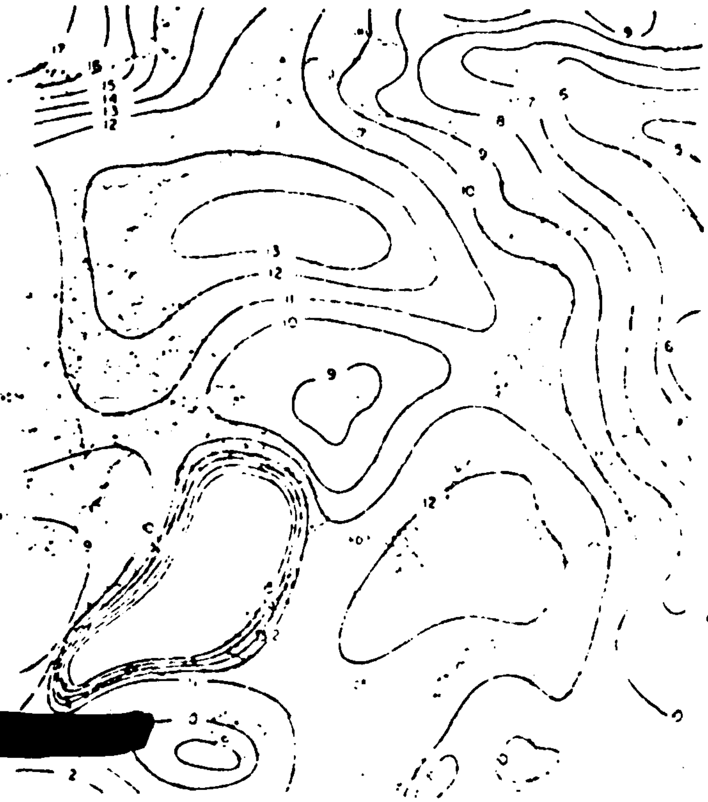

[redacted] FIGURE 1-11. MEAN AIR PRESSURE (mbar), JULY

[redacted] FIGURE 1-12. MEAN AIR PRESSURE (mbar), JANUARY

1.2.2.3 [redacted] Clouds

[redacted] Clouds are primarily important for their influence on thermal radiance from a nuclear weapon. If the source-to-receiver path intersects a cloud, very high absorption will occur but if the path is between snow cover and a low altitude cloud very large enhancements of thermal exposure can occur.

[redacted] The Arctic region especially over the polar ocean is characterized by a high probability of low, dense clouds during the summer months. The coastal areas show a large variability due to the perturbation of the continental regions. In Figures 1-13 and 1-14 the mean cloud coverage in January and July is shown (Orvig, 1970). Note that the probability of clouds in the Norwegian Barents Sea area is very large in January. A 40% probability of cloud cover exists over most of the polar ocean. In July the probability is over 80% north of the coastal regions and in the Norwegian-Barents Sea area.

1.2.2.4 [redacted] Precipitation and Fog

[redacted] The relative humidity over the Polar Ocean always remains near 100%. The saturation vapor pressure over ice is lower than over water. Thus, the humidity can be high enough to allow ice crystals to form even when water droplets are evaporating. Hoar frost formation can be expected much of the time during the winter.

[redacted] Persistent water fogs are experienced over the Polar Ocean with fog occurring over 100 days during the year. The probability of observing fog is 10% in June, 15% in July, 25% in August and 7% in September.

[redacted] Ice fog occurs when water vapor is added to cold air (-30°C) and is prevalant in the vicinity of human habitation where large sources of water vapor occur.

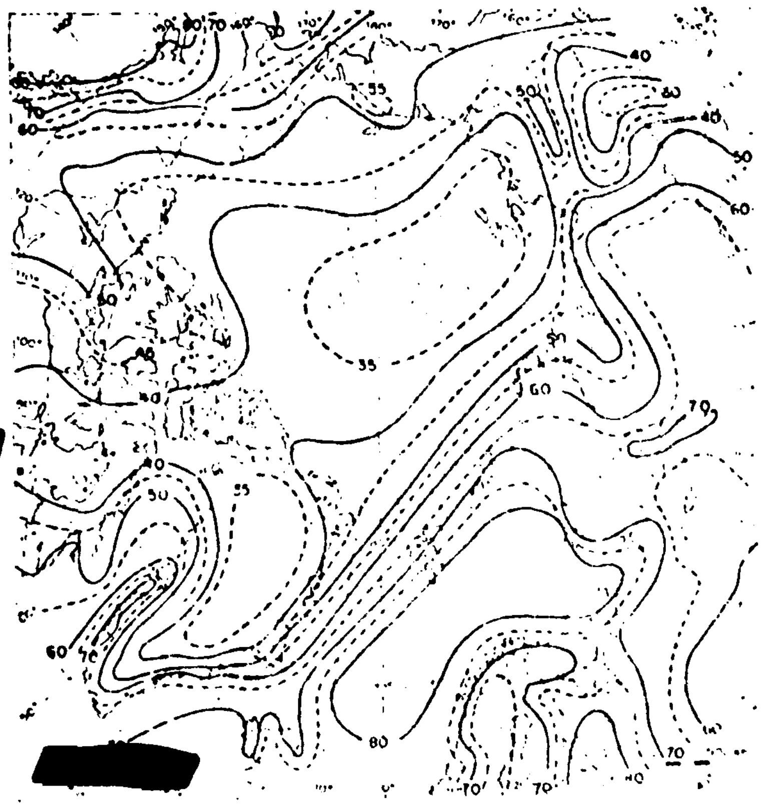

[redacted] FIGURE 1-13. MEAN CLOUD COVERAGE (%) IN JANUARY

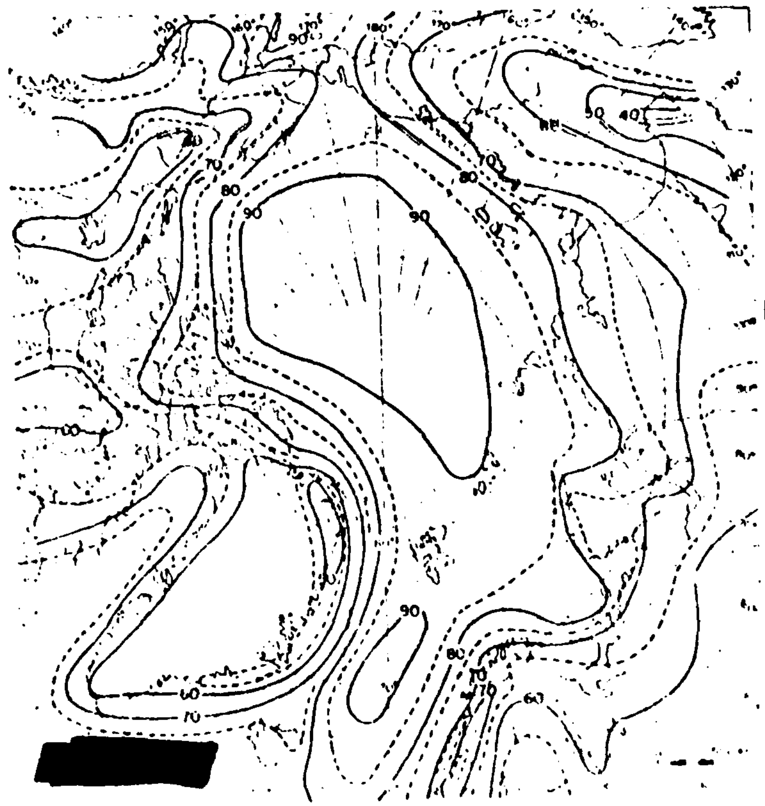

[redacted] FIGURE 1-14. MEAN CLOUD COVERAGE (%) IN JULY.

[redacted]

[redacted] Precipitation is very low over the polar region averaging about 135 mm water equivalent annually. In the southern regions the amount may reach 250 mm. Most of the snowfall occurs in the spring and the fall with the minimum occurring in the winter. Figure 1-15 shows (Orvig, 1970) the snow thickness and density observed in the Polar Ocean.

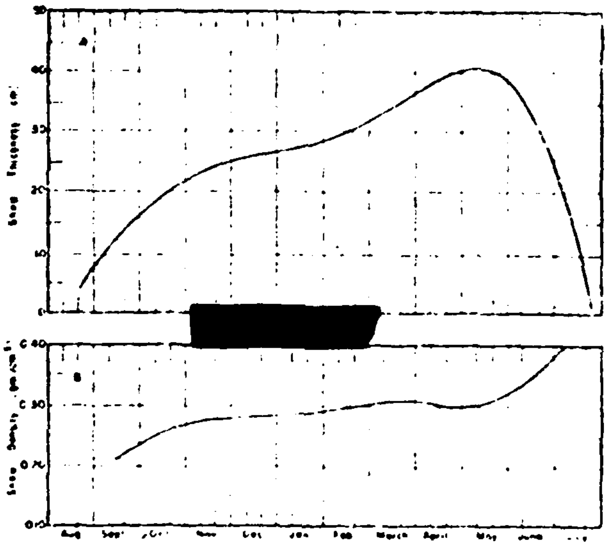

[redacted] FIGURE 1-15. AVERAGE OBSERVED SNOW THICKNESS AND SNOW DENSITY IN THE CENTRAL POLAR OCEAN.

1.2.2.5 [redacted] Visibility

[redacted] The visibility at the ground surface is a very important quantity in determining the thermal exposure expected from a nuclear weapon. The ground level concentration of aerosols is small compared to that in temperate regions except near inhabited areas. The ground level visibility is high over most of the Arctic unless precipitation is occurring, water or ice fog is

[redacted]

[redacted]

[redacted] present, or snow is blowing. All of these are characterized by low visibility. Thus, one expects that the variability in the visibility will be much larger in the Arctic than in most temperate regions.

[redacted] The visibility in the polar regions has been considered (Mitchell, 1956) with emphasis on the effects expected in aircraft operation, which is the usual reason for interest in visibilities. In addition to the low altitude clouds that are very likely especially during the summer, arctic haze is encountered a high percentage of the time that the weather is otherwise clear at altitudes up to 30 kft. The haze is characterized by a horizontal or slant visibility of 2-5 miles while the vertical visibility is unimpaired. The haze is not observable from ground level and is much less likely over land.

[redacted] The visibility in ice fog is very low, frequently less than 1/4 mile. Thus, when ice fog occurs in the winter it usually causes a deterioration of excellent visibility to very poor visibility (<1 mile). Ice fog is characteristic of an inhabited region. During the summer fogs over both the coastal regions and the polar ocean are present 10% - 30% of the time.

[redacted] Blowing snow is very common in the arctic because the snow is typically dry and composed of fine particles. Winds exceeding about 15 mph (7 m/sec) will (Mitchell, 1956) raise the snow to great enough heights to obscure buildings. In Table 1-6 the monthly frequency (%) of winds above 7 m/sec is indicated and is seen to be 11% to 26%. Of course, as indicated in Figure 1-15, during the summer fresh snow is unlikely and the snow cover would not be so susceptible to blowing.

[redacted]

[redacted]

[redacted] Model arctic atmospheres with the visibility as high as 200 km have been used (Wells et al, 1969) for thermal exposure calculations to correspond to clear air with a very small aerosol content. The weather conditions given above indicate that a significant fraction of the time the visibility may be <1 mile. Intermediate visibilities (10 - 30 km) are not as likely except over cities or industrial areas where significant sources of aerosol particles exist.

1.2.3 [redacted] Surface Properties

[redacted] The surface properties of interest are the material properties of the frozen ground, ice, and sea ice for consideration of the blast wave interactions and crater development, and the surface albedo for use in thermal exposure calculations.

[redacted] The arctic topography does not differ greatly from the temperate except for the surface changes caused by the colder temperatures. The mountains are high and rugged. The plains contain glacial characteristics, and shallow lakes are very common. There are essentially no forests in the true arctic. Extensive vegetation including small trees and grasses occur in many areas, and during the summer the tundra could be susceptible to surface fires. A large portion of the arctic land area is snow and ice covered the entire year with thicknesses of 100 feet or more common in Greenland.

[redacted] The surface albedos encountered in the arctic range from nearly 100% for fresh snow to a few percent for sea waters and vegetated areas. The general albedo patterns are indicated in Figure 1-16 (Orvig, 1970) in which the major seasonal and latitudinal variations of albedo determined from aircraft observations are shown as stereograms. Areas without daylight are

[redacted]

[redacted]

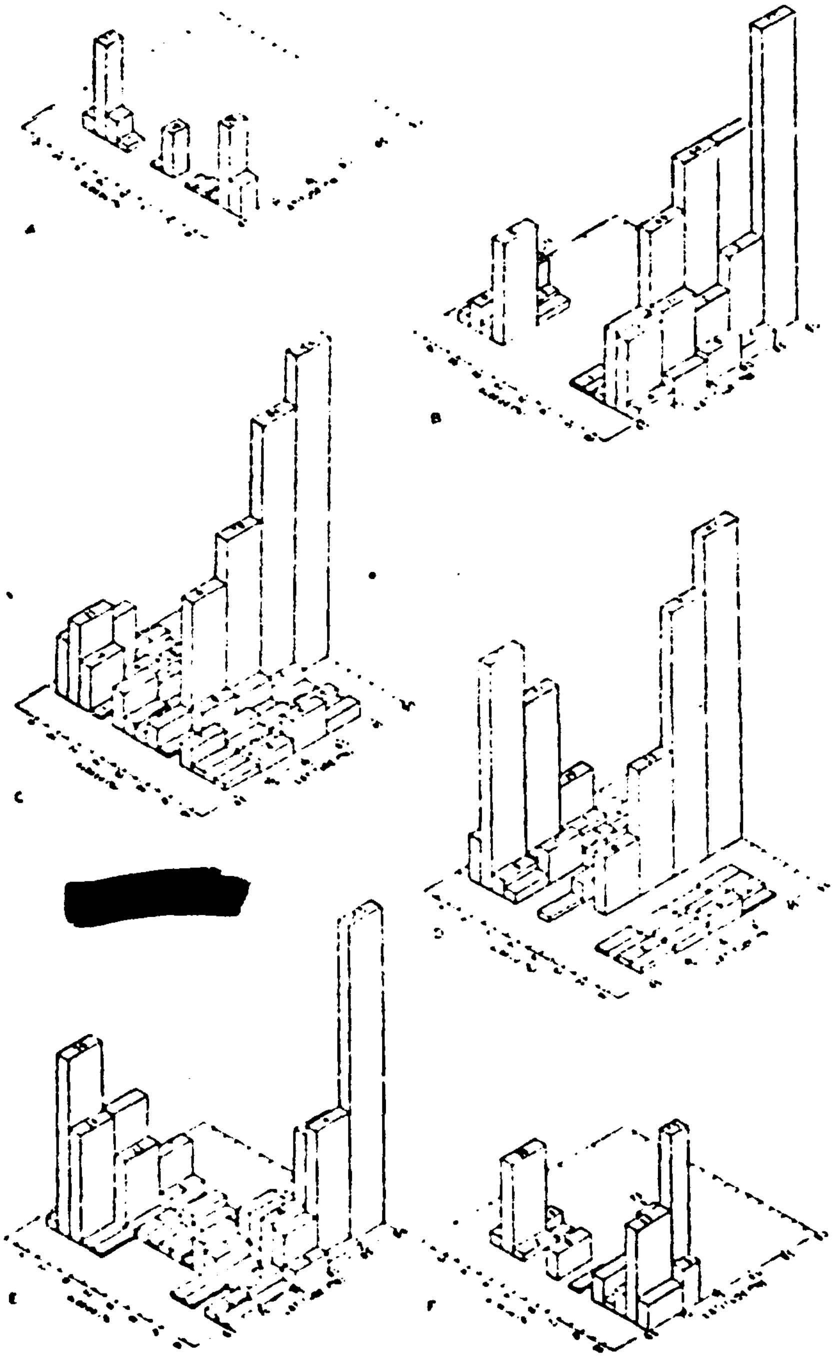

[redacted]

[redacted] Figure 1-16 Albedo stereograms. A. January; B April, C. June; D August; E September, F. November. (After LARSSON, 1963.)

[redacted]

[redacted]

[redacted] left blank but the latitudinal variation as shown for April would be expected during the winter months for the north latitudes. From January through May the incidence of high values from snow cover in combination with low values from forest or open water is expected with the albedo over the polar cap being uniformly large as shown for April.

[redacted] The June and August stereograms indicate the increase in low albedo values as the snow over land melts and open water appears. At high latitude the medium albedo represents an average over the value for ice and old snow of 60% and the value for melt puddles (20%) on the ice surface.

[redacted] By September the incidence of high albedos due to freshly fallen snow becomes obvious, and by November the winter pattern of a combination of low and high values has returned.

[redacted] Permafrost, which is a combination of soil and moisture continuously frozen, underlies a large fraction of the arctic depending upon local terrain, soil characteristics and snow cover. The equation of state parameters and material properties for ice and composite frozen soils have been determined (Anderson, 1968, and Chamberlain and Hoekstra, 1970) for use in hydrodynamic calculations relating to shock transmission and crater development in these materials. The Hugoniot data for two frozen soil types with different moisture content and for ice are shown in Figures 1-17, 1-18, and 1-19. Release curves are also given for two of the frozen soil configurations and for ice. The density of the various materials at -10°C is given in Table 1-7.

[redacted] In Table 1-8 several quantities of interest for considering linear coupling between ice, water and air are given.

[redacted]

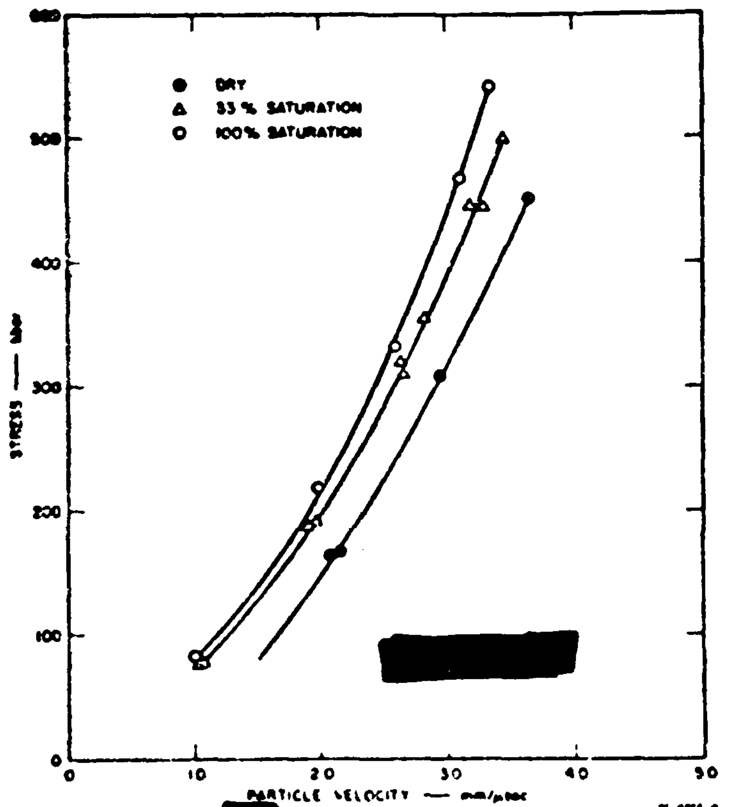

[redacted] FIGURE 1-17

HUGONIOT DATA FOR WEST LEBANON GLACIAL TILL (σ - u)

[redacted]

[redacted]

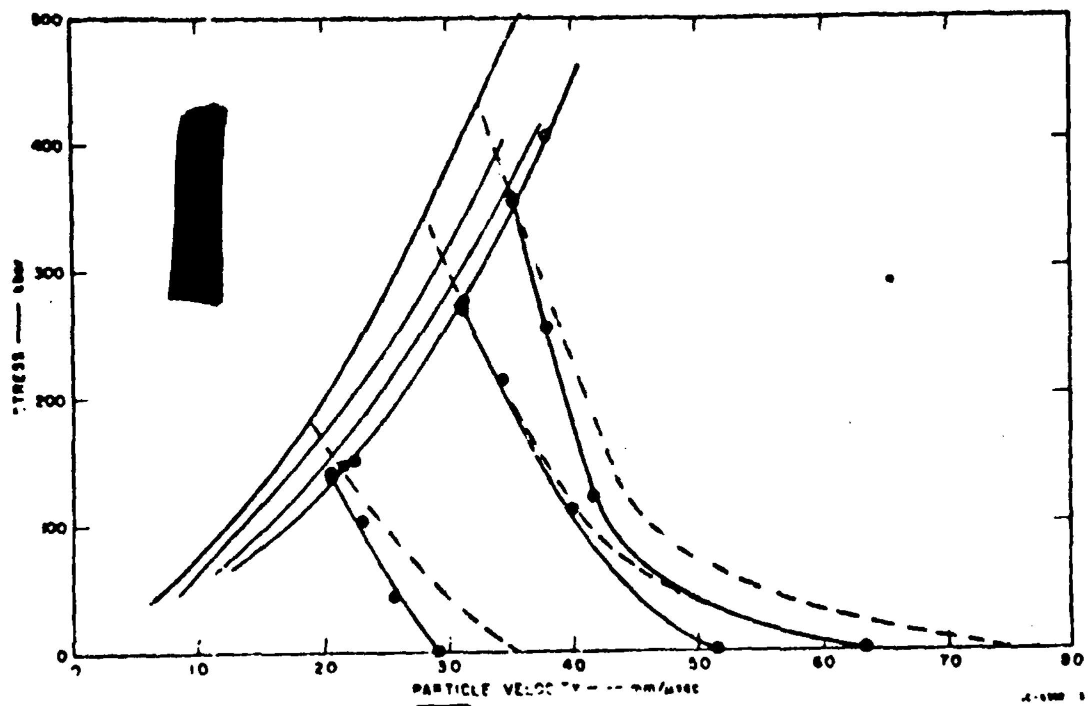

[redacted] FIGURE 1-18

HUGONIOT AND RELEASE CROSS CURVES FOR DRY OTTAWA BANDING SAND (σ - u)

[redacted]

[redacted]

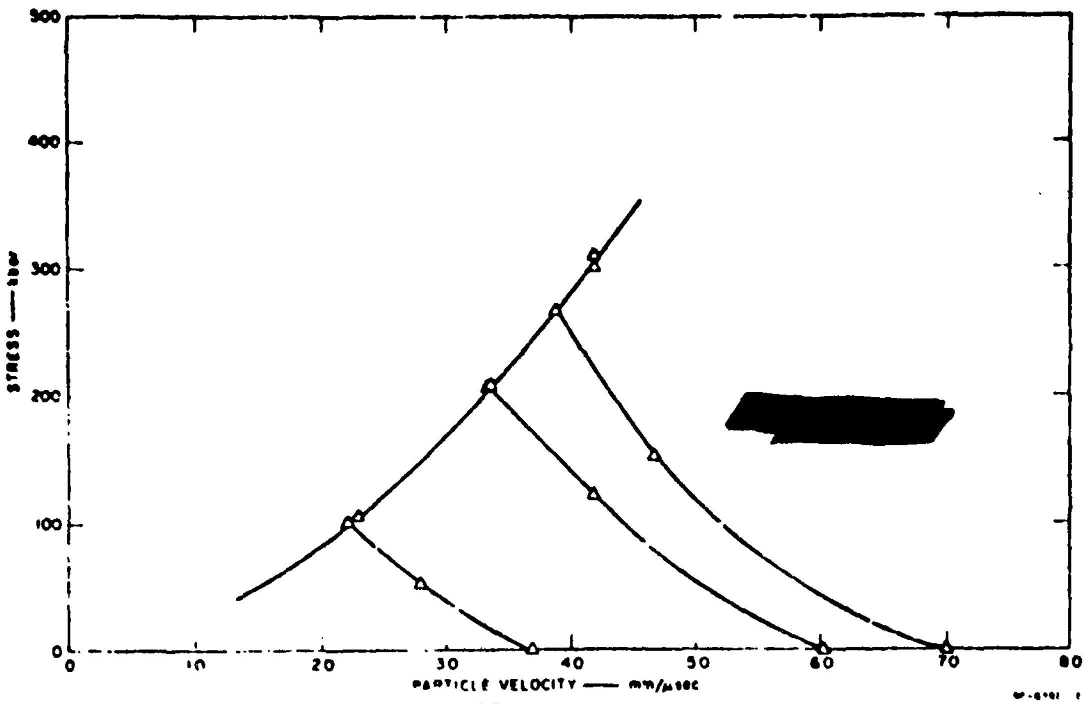

[redacted] FIGURE 1-19

HUGONIOT AND RELEASE CROSS CURVES FOR POLYCRYSTALLINE ICE

[redacted]

[redacted]

[redacted] TABLE 1-7

DENSITY OF FROZEN MATERIALS (g/cm^3)

[redacted]

Percent Water	Sand	Till	Ice
0	1.65	1.86	-
20	1.72	-	-
50	1.84	2.05	-
100	1.96	2.21	.917

[redacted] TABLE 1-8

ACOUSTIC PARAMETERS

[redacted]

	Temperature °C T	Density g/cm^3 ρ_o	Velocity m/sec c	Impedance mks rayl $\rho_o c$
Ice	-	.92	300	2.95×10^6
Water/fresh	20	.998	1481	1.48×10^6
Water/sea	13	1.026	1500	1.54×10^6
Air	0	1.293×10^{-3}	331.6	428
Air	20	1.21×10^{-3}	343	415

[redacted]

1.2.4 [redacted] Magnetic Field

[redacted] The location of the magnetic pole is near 75.5° north latitude and 100.5° west longitude. The main field can be represented to an accuracy of about 90 percent by a tilted dipole at the earth's center. The field is affected by regional anomalies covering thousands of square miles and small surface anomalies caused by localized magnetic ore deposits. Models of the geomagnetic field are available as a spherical harmonic expansion series fitted to the measured values of the field.

[redacted] In Figure 1-20 the geomagnetic field intensity (Valley, 1965) is shown. A region surrounding the magnetic pole and another region in Siberia have an intensity greater than .600 gauss. Over most of the polar region the intensity is greater than .550 gauss. Over the Barents-Norwegian Sea region the intensity is between .520 and .550 gauss. Over the northern portion of the United States the intensity is greater than .500 gauss. Thus, the intensity in the Arctic can be as much as 20% larger than values found in the U.S.

[redacted] The biggest difference between arctic and temperate regions is in the inclination of the magnetic field lines shown in Figure 1-21 (Valley, 1965). At the magnetic pole the lines are perpendicular to the surface with an inclination (dip) of 90°. Over much of the polar region the inclination is greater than 80°. The magnetic field intensity has a very small horizontal component as compared to temperate regions. The differences in the magnetic field result in changes in the EMP values on the surface from high altitude bursts as described in Section 6.

[redacted] The lateral extent of high altitude fireballs can be determined by the magnetic field because of the energy expended by charged material moving across the magnetic field lines. A burst over the north magnetic pole region where the field lines are diverging might be less constrained by the magnetic field

[redacted]

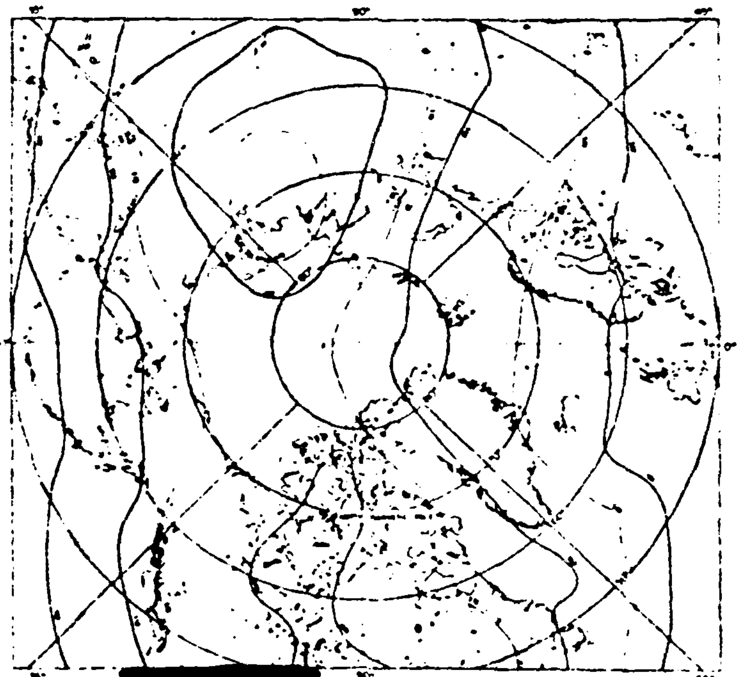

[redacted]

[redacted] FIGURE 1-20. THE TOTAL INTENSITY OF THE GEOMAGNETIC FIELD

[redacted]

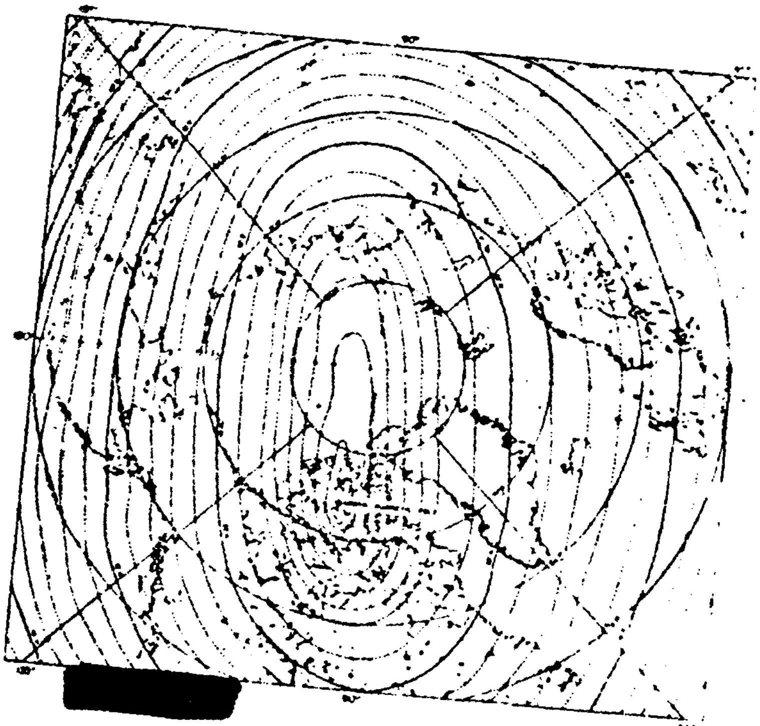

[redacted]

[redacted] FIGURE 1-21. THE INCLINATION (DIP) OF THE GEOMAGNETIC FIELD

[redacted]

[redacted]

[redacted] and spread over a larger volume. Likewise the beta particles being constrained to follow the field lines might be dispersed over a very large area at high altitudes. These effects might have implications for radar or communication blackout or for performance of high altitude optical or infrared sensors; but these effects are outside the field of interest for this handbook.

1.2.5 [redacted] Arctic Sea Ice

[redacted] Most of the ocean waters located north of 75°N latitude remain covered throughout the year by thick (~3 meters) perennial ice. Between roughly 60° and 70°N latitude lies the region known as the Marginal Ice Zone wherein both the geographical extent of the total ice cover and local areal ice concentrations exhibit strong seasonal dependencies. Within the Marginal Ice Zone many localities experience ice-free conditions at some time during the year.

1.2.5.1 [redacted] Extent and Thickness

[redacted] Figure 1-22 (Fairbridge, 1966) is a chart showing minimum and maximum extents of sea ice of concentrations of 0.5 or greater. It should be noted that the boundaries provided in the chart represent averages based on data collected over many years, and that during any given year ice extremes can vary considerably from those depicted.

[redacted] Table 1-9 indicates, for seven sub-areas of the Arctic Ocean, and for each season of the year, the percentage of the total ice cover falling in each of three categories; viz., (a) polar ice, which has an average winter thickness of about 3 meters, (b) thick winter ice, which varies between 0.3 and 2.4 meters in thickness and (c) new ice, which is generally less than 0.3 meter thick (Wittmann and Schule, 1967, and Anderson, 1971). It is emphasized that the percentages listed are percentages of the total ice cover and not the total ocean area which, depending

[redacted]

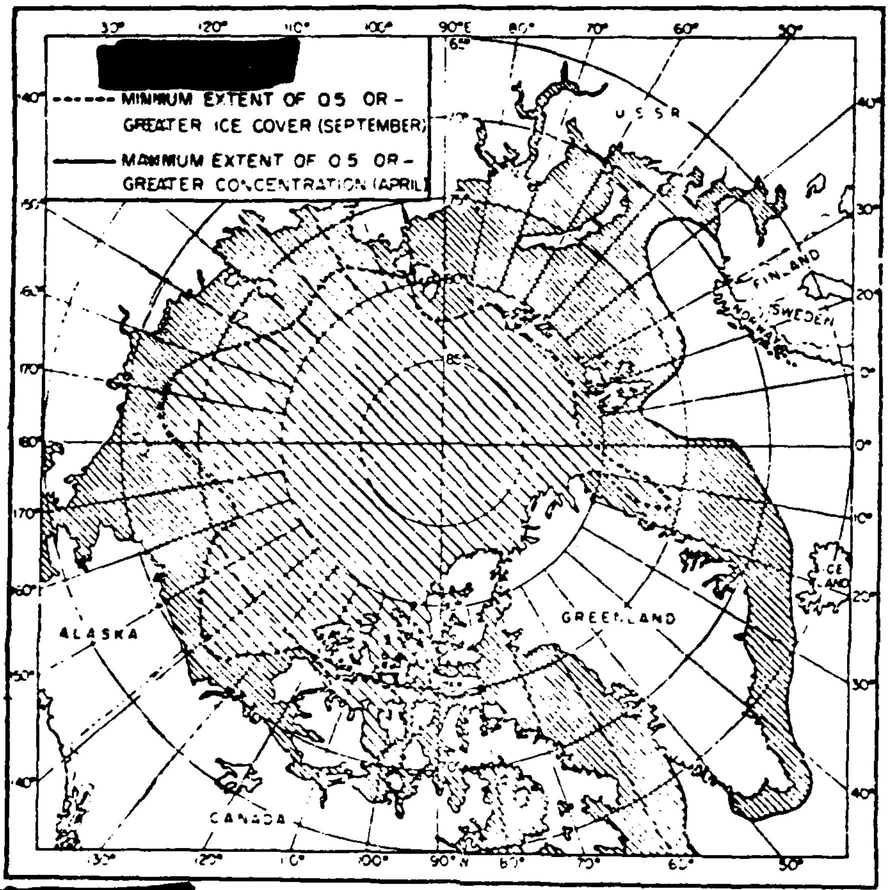

[redacted]igure 1-22. Yearly Extremes in Extent of Ice Concentrations of 0.5 or Higher. (Fairbridge, 1966) [redacted] Table 1-9. Relative Seasonal Percentages of Ice in Various Developmental Stages in Seven Sub-Areas of the Arctic Ocean. (Wittmann and Schule, 1967 and Anderson, 1971).

Period*	Polar Ice (Av. Winter Thickness ≃3 m)	Thick Winter (0.3 to 2.4 m)	New Ice (<0.3 m)	Number of Observations
Area: Eurasian Basin				
Jan-May	86%	10%	4%	158
June-July	93%	6%	1%	75
Aug-Oct	79%	12%	9%	126
Nov-Dec	91%	1%	8%	53
Area: Canadian Basin				
Jan-May	90%	7%	3%	287
June-July	91%	9%	trace	83
Aug-Oct	68%	17%	16%	197
Nov-Dec	80%	16%	4%	94
Area: Beaufort Sea				
Jan-May	65%	26%	9%	147
June-July	64%	32%	4%	44
Aug-Oct	40%	30%	30%	63
Nov-Dec	52%	24%	24%	36
Area: Lincoln Sea and N. Greenland				
Jan-May	71%	24%	6%	175
June-July	72%	26%	2%	41
Aug-Oct	59%	28%	13%	76
Nov-Dec	43%	32%	26%	40

*Winter, Jan-May; Spring, June-July; Summer, Aug-Oct; Autumn, Nov-Dec

[redacted]

Table 1-9 Cont'd.

Period*	Polar Ice (Av. Winter Thickness =3 m)	Thick Winter (0.3 to 2.4 m)	New Ice (<0.3 m)	Number of Observations
Area: Canadian Coastal Region				
Jan-May	86%	9%	5%	69
June-July	49%	48%	4%	76
Aug-Oct	64%	18%	19%	124
Nov-Dec	74%	23%	2%	35
Area: East Siberian Sea				
Jan-May	45%	43%	12%	40
June-July	--	--	--	---
Aug-Oct	36%	30%	34%	28
Nov-Dec	58%	28%	14%	12
Area: Northern Chukchi Sea				
Jan-May	53%	38%	9%	149
June-July	67%	31%	2%	26
Aug-Oct	42%	25%	38%	66
Nov-Dec	26%	50%	24%	36

*Winter, Jan-May; Spring, June-July, Summer, Aug-Oct; Autumn: Nov-Dec

[redacted]

[redacted]

[redacted]

[redacted] on the area and time of year, can contain considerable expanses of open water. Nowhere, except in the vicinity of coastlines, is the ice canopy ever continuous. In the two principal Arctic deeps, for example, about 15% of the total area is free of ice during the summer season. During winter from 5-8% of the region is composed of either open water (leads, polynyas) or thin ice (skylights).

[redacted] The ice over the polar ocean has a very complex structure. The pack ice reaches an equilibrium thickness after a 5-6 year period. The rate of accretion is dependent upon the thickness, and the freezing occurs primarily at the bottom with the melting in the summer occurring at the top. Thus, a particular ice crystal moves from the bottom to the top during this time period. In Table 1-10 the thickness of the ice in the polar ocean is given for various ages. In Table 1-11 the percentage of the area covered by ice of various ages is shown (Orvig, 1970).

(U) TABLE 1-10

THICKNESS OF ICE (cm) OF DIFFERENT AGES, CENTRAL POLAR OCEAN

AGE (YRS)	SEPT	OCT	NOV	DEC	JAN	FEB	MAR	APR	MAY	JUNE	JULY	AUG
1	0	34	67	102	135	168	203	236	270	258	245	233
2	220	230	240	250	260	270	280	290	300	288	275	263
3	250	259	268	276	287	296	304	312	230	308	295	283
4	270	277	284	291	297	304	311	318	325	313	300	288
5	275	282	289	296	302	309	316	323	330	318	305	293

[redacted]

[redacted]

[redacted]

[redacted] TABLE 1-11

AREA COVERED BY ICE OF VARIOUS AGES, CENTRAL POLAR OCEAN

ICE	AREA (%)
1 year old	11.6
2 year old	10.3
3 year old	9.1
4 year old	8.1
5 and more years	60.9 [redacted]

NOTE: The oldest ice is about 19 years old, 2% of the area is occupied by this oldest ice.

[redacted] Submarine determinations of ice thicknesses indicate that the presence of uniform ice cover is the exception rather than the rule. An average thickness obtained in August was 3.7 m. Large areas are covered by hummock ice which can be piled up 6-7 m above the surrounding ice over the polar ocean. The pile-up can reach 13 m near the coast and in shallow areas.

[redacted] About sixty ice islands have also been found in the Arctic with about 15 in the polar ocean and the remainder scattered in the Canadian Archipelago. The ice islands cover areas as large as 300 square miles, the average thickness of the ice is 200 feet and the surface may rise as much as 40 feet above the level of the surrounding ice pack. The surface of the ice islands is relatively uniform compared to the surrounding ridged and hummocked sea ice. Icebergs are not expected to be large enough or experienced frequently enough to be of importance. A nuclear burst occurring under an ice island could produce much different underwater effects than one under pack ice.

[redacted]

[redacted]

1.2.5.2 [redacted] Physical Properties

[redacted] As an introduction, it is appropriate to survey what is known about the strength of sea ice. Sea ice, as found in nature, is quite variable in its physical characteristics. On a macroscopic scale, Francois, 1977 has noted that the many pressure ridge keels always present in the ice pack are made up of large blocks of ice with individual voids between blocks. Voids between blocks in ridges formed from thick ice are larger than those between blocks formed from thinner ice. The voids permit water flow through the keel structure, which greatly impedes freezing of the internal voids. Francois concluded that consolidation into a homogeneous structure is very slow, and that the beam strength of ice in the pressure ridges is much less than would be predicted for ice of equivalent thickness that was homogeneous.

[redacted] Further evidence of the variability of sea ice is found in the seismic studies of Hunkins, 1960. He noted that air content in the form of bubbles, because of its variability, is an important factor in the density of sea ice, as is its liquid brine content. Furthermore, the way sea ice forms and grows causes it to be anisotropic in nature. Hunkins suggests that the shear modulus for stresses acting vertically is less than the shear modulus for stresses acting horizontally. This anisotropy was reflected in the different velocities found for propagation of longitudinal and transverse seismic waves.

[redacted] More detailed laboratory studies of the nature and properties of natural sea ice have been conducted by Assur, 1958 and Peyton, 1966. In sea ice, discrete volumes of entrapped brine are found within a matrix of pure ice. The brine is entrapped during the growth process because the growth rate of pure ice exceeds the downward convection rate of enriched brines at the growth face. Liquid brine exists within the sea ice

[redacted]

[redacted]

matrix at all temperatures and times. While it is possible to freeze all of the brine, with very few exceptions this does not occur in nature, (Peyton, 1966).

[redacted] Figure 1-23a (after Assur, 1958) identifies six well-defined regions in a temperature-salinity diagram for sea water and ice. Sea ice samples with temperature and salinity characteristics of different areas of the diagram have quite different physical characteristics. Seawater has a salinity of about $35^{\circ}/oo$ (read as 35 parts per thousand, or 35 per mil). It remains liquid at temperatures above and just a little below $0^{\circ}C$ (region A). At lower temperatures mushy ice begins to form that has no strength (region B).

[redacted] At extremely low temperatures (region F) the ice is a grayish white color and is hard and brittle. Its strength varies with its brine content, along the line marked F in Figure 1-23b, also after Assur. (The data presented by Assur represent tensile strengths of ice as measured by a standard ring tensile test, described in his paper. All strength values were adjusted to a common temperature of $-10^{\circ}C$ to remove any temperature effect). The horizontal dotted line in the figure is drawn at 14.2 kg/cm^2, which is comparable to the strength of fresh water ice, a little over 15 kg/cm^2. As can be seen, very cold sea ice is considerably stronger than fresh water ice.

[redacted] Ice at temperatures between -8.2 and $-22.9^{\circ}C$ (region E) is grayish-blue or greenish-gray in color and is considered by Assur to possess "normal" strength. Its strength varies with brine content along line E in Figure 1-23b, which is comparable to the strength of fresh water ice. At temperatures higher than $-8.2^{\circ}C$, in region D, the ice is dark and wet and is significantly weaker than normal, and weaker than fresh water ice. Its strength varies along line D. At temperatures and salinities characteristic of region C, the ice is so

[redacted]

[redacted]

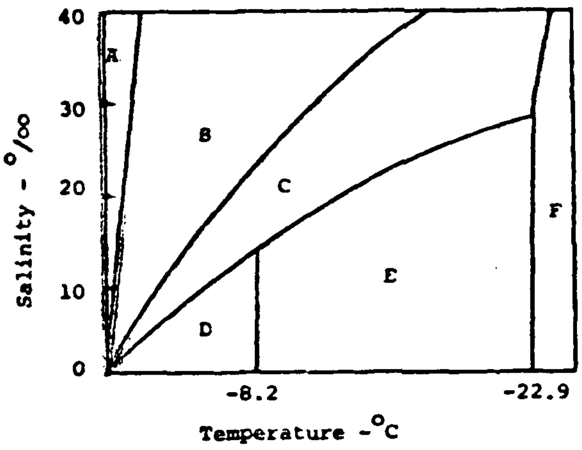

(a)

LEGEND

A - No ice
B - No strength, mush
C - Internal deterioration, "bleeding"
D - Weaker than normal, no solid salt reinforcement
t (temperature) > -8.2°C
E - Normal strength, precipitation of $Na_2SO_4 \cdot 10H_2O$ in brine pockets
-8.2°C > t > -22.9°C
F - Hard, brittle, precipitation of $NaCl \cdot 2H_2O$ in brine pockets
t < -22.9°C

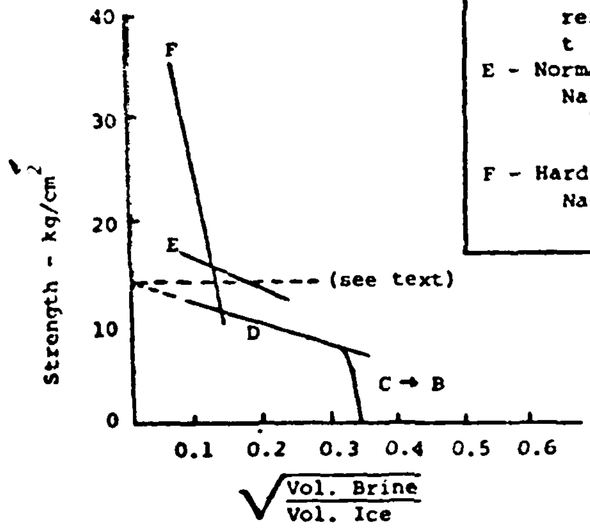

(b)

[redacted]

[redacted] Figure 1-23. Temperature, Salinity, and Strength Relationships for Sea Ice. (After Assur, 1958).

[redacted]

[redacted]

wet that it "bleeds." This is the region of rapid internal deterioration as the strength varies along the line marked C→B in the lower diagram.

[redacted] The regions of the upper diagram and the lines of the lower diagram in Figure 1-23 are determined by the temperatures at which various salts in the brine solution precipitate, providing what Assur calls solid salt reinforcement. In region D and along line D, all salts are in solution. It is line D projected to zero brine volume that develops the figure of 14.2 kg/cm^2 quoted above, what Assur calls the "basic strength" of sea ice. At a temperature of -8.2°C, sodium sulfate decahydrate begins to precipitate, providing the sudden increase in strength represented by line E vs line D. At -22.9°C, sodium chloride dihydrate precipitates, causing the increase in strength represented by line F. It has also been found that in perennial ice the strength varies along line E even though the temperature rises somewhat above -8.2°C. Assur attributes this to sodium sulfate remaining precipitated on the walls of the brine pockets rather than redissolving, the so-called hysteresis effect.

[redacted] Sea ice varies in salinity from 2°/oo to 20°/oo. The highest salinity is found in salt ice, produced by flooding and is only the initial salinity. Entrapped brine drains out of the pure ice matrix at warm temperatures, so there is a gradual reduction in salinity with time. The first formations of young sea ice are about 10°/oo. Normal one-season sea ice in the middle of winter averages about 5°/oo, while perennial sea ice is about 2°/oo. With this range of salinity, or brine content, to be expected, it is easy to see from the diagrams of Figure 1-23 why the strength of sea ice varies so widely, from almost no strength under some conditions, possibly 2/3 the strength of fresh water ice under others, a strength

[redacted]

[redacted]

comparable to fresh water ice under still other conditions, to two or three times the strength of fresh water ice for very cold perennial sea ice.

[redacted]

1.2.6 [redacted] Bathymetry and Bottom Properties

[redacted] A bathymetric chart of the Arctic Ocean is shown in Figure 1-26 (Fairbridge, 1966). As shown, the long, submarine Lomonosov Ridge divides the large central basin into two sub-basins. The sub-basin on the North American side of the ridge is known as the Hyperborean Basin, while that on the Eurasian side is called the Nansen Basin. The mean basin floor depth is about 4000 meters. Summit depths along the Lomonosov Ridge range from about 950 to 1650 meters.

[redacted] Approximately one-third of the total area of the floor of the Arctic Ocean is continental shelf. Shelf widths on the North American side are fairly typical of shelf regions in

Pages 1-46 and 1-47 were deleted

[redacted]

[redacted]

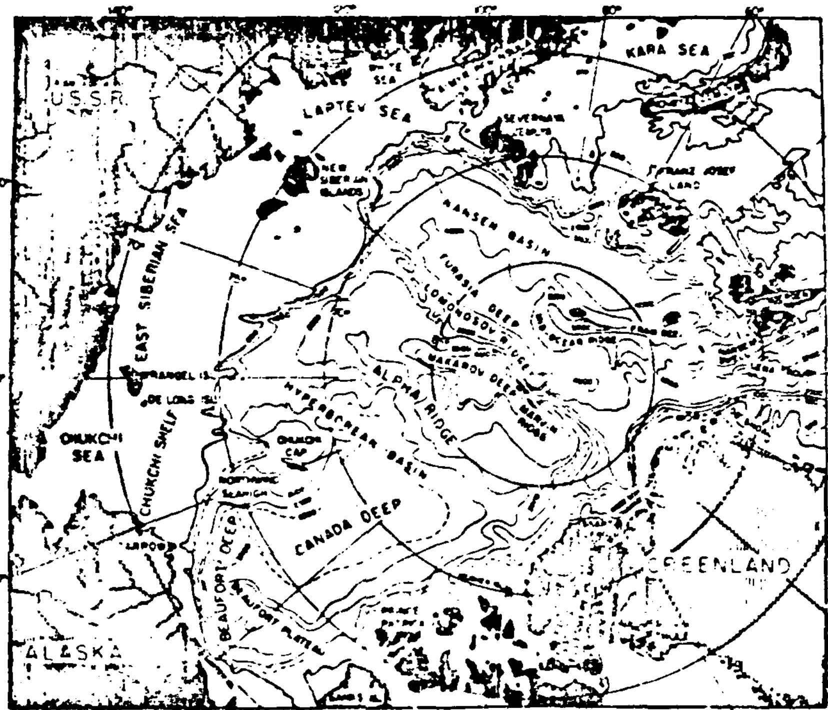

[redacted]

[redacted] Figure 1-26. Bathymetry of the Arctic Ocean. Depth Contours in Meters. (Fairbridge, 1966)

[redacted]

general, ranging from about 100 to 200 kilometers. By contrast, on the Eurasian side the shelf regions are quite extensive, ranging in width from 500 to 1700 kilometers.

[redacted] The bottom sediment of the Arctic Ocean is, with the exception of the Barents Sea region, predominantly mud, with isolated, small patches of mud-sand, sand and gravel. In the Barents Sea the sediment distribution pattern is uncharacteristically complex, comprising a very irregular patchwork of mud, sand, mud-sand, mud-sand-gravel, and gravel.

[redacted] The bathymetry of the Canadian Arctic Archipelago is shown in Figure 1-27 (Canadian Hydrographic Service, 1971). The channels of the archipelago, which connect the Arctic Ocean with Baffin Bay and Davis Strait, vary in width from 10 to 120 kilometers. Channel depths range from a few meters to more than 700 meters; the greatest depths occur in the Parry Channel System (McClure St., Viscount Melville Sd., Barrow St., Lancaster Sd.) and the Prince Gustaf Adolf Sea. In general, the shallower depths occur in the interior of the archipelago, well away from channel entrances and exists. Interior channel depths average about 100 meters. The amount of detailed information relating to bottom composition within the archipelago is sparse. Available data indicate a preponderance of mud and mud-sand sediments, a finding that is consistent with the hypothesis that the region is a partially-drowned land mass and that its channels correspond to a pre-Pleistocene river system.

1.2.7 [redacted] Water Properties

[redacted] Certain physical properties peculiar to the Arctic Ocean will be described. The information was found in various sources mentioned.

1.2.7.1 [redacted] Water Mass Characteristics and Sound Speed/Water Density Structures

[redacted] The most salient features of the sound speed and water density structures in the Arctic Ocean are determined by the presence of three rather distinct water masses. The uppermost of these, Arctic Surface Water, extends from the ocean

[redacted]

[redacted]

[redacted] Figure 1-27. Bathymetry of the Canadian Arctic Archipelago. Depth Contours in Meters. (Canadian Hydrographic Service, 1971).

[redacted]

surface to about 200 meters and is characterized by low salinities and temperatures at or near the freezing point. Salinities within the surface layer normally increase with increasing depth. Temperatures tend to increase below about 100 or 150 meters. Below the surface layer, and extending to a depth of about 900 meters, lies the highly saline water mass known as Atlantic Water. Atlantic Water is characterized by temperatures above $0^{\circ}C$. Salinities tend to increase down to about 400 meters, below which the water is nearly isohaline. That portion of the water column lying below the Atlantic Water layer is known as Bottom Water and is characterized by temperatures below $0^{\circ}C$ and uniform salinity.

[redacted] Normally, sound speeds in Arctic waters increase monotonically with depth from the surface to the bottom. Sound speed gradients tend to be relatively severe in the upper four or five hundred meters of the water column due to the generally increasing temperatures and salinities. At greater depths, where temperatures and salinities exhibit little depth dependence, typical pressure-effect gradients are observed. Significant temporal and spatial variability in the Arctic sound speed structure is confined to the top five or six hundred meters of the water column. At greater depths the structure is quite stable. A typical Arctic sound speed profile is shown in Figure 1-28 (Anderson, 1971).

[redacted] In ice-covered shallow waters (500 or 600 meters), sound speeds are somewhat variable but normally increase monotonically with depth. Shallow-water sound speed gradients are comparable to those encountered in the shallow region of the deep water column.

[redacted] The monotonic increase in sound speed with depth in the ice-covered waters of the Arctic results in the formation of an acoustic half channel, bounded by the ocean surface and

[redacted]

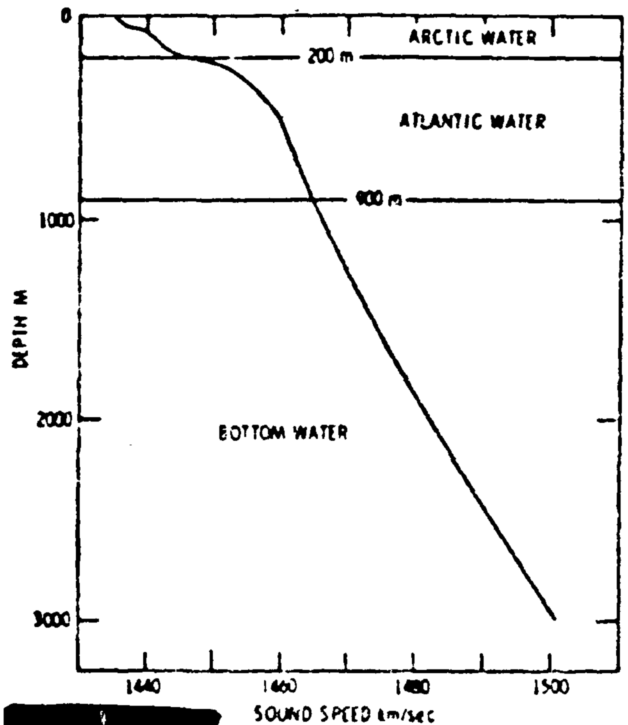

[redacted]

[redacted] Figure 1-28. Sound Speed Profile for the Canadian Basin. (Anderson, 1971)

[redacted]

bottom, within which long range acoustic propagation is effected primarily by repeated cycles of upward refraction to the surface followed by reflection back down into the water column. Acoustic energy losses incurred on interaction with the underside of the ice canopy are normally substantial, particularly at high frequencies, and impact significantly on both short- and long range propagation. A detailed treatment of Arctic hydroacoustics is presented in Section 9.

[redacted] In Arctic waters, water density (σ_t)* variations with depth are strongly controlled by the vertical salinity structure. In general, strong positive density gradients are observed in the upper few hundred meters of the water column. This region is known as the pycnocline. Below the pycnocline σ_t is practically invariant with depth. Figure 1-29 shows a density profile obtained in the Beaufort Sea in May 1968 by the Lamont-Doherty Geological Observatory of Columbia University (Hunkins, 1971).

[redacted] The pycnocline severely impedes the upward migration of heat and salt and hence effectively insulates the surface from the warmer water masses below.

1.2.7.2 [redacted] Currents

[redacted] The general pattern of Arctic water circulation is shown in Figure 1-30 (Fairbridge, 1966). The influx of water into the Arctic Ocean by precipitation, coastal runoff and currents through the Norwegian Sea and Bering Strait is balanced by the southerly outflow of water through the Greenland Sea and channels of the Canadian Arctic Archipelago. The Bering Strait and Norwegian Sea contribute 97% of the total water influx, with the latter contributing approximately 65% of

*σ_t = density at atmospheric pressure

[redacted]

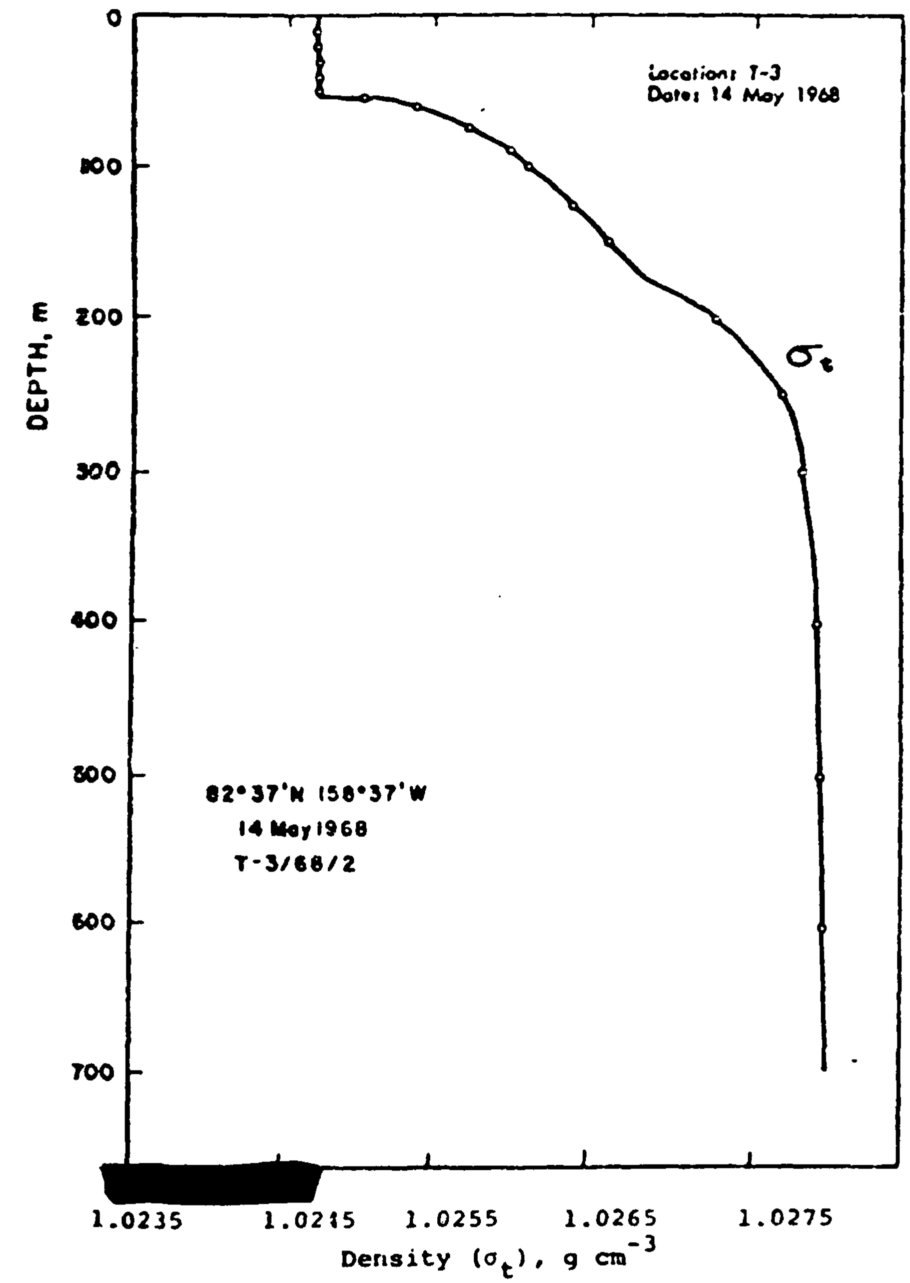

[redacted] Figure 1-29. Density (σ_t) Profile Obtained in the Beaufort Sea. (Hunkins, 1971)

[redacted]

[redacted]

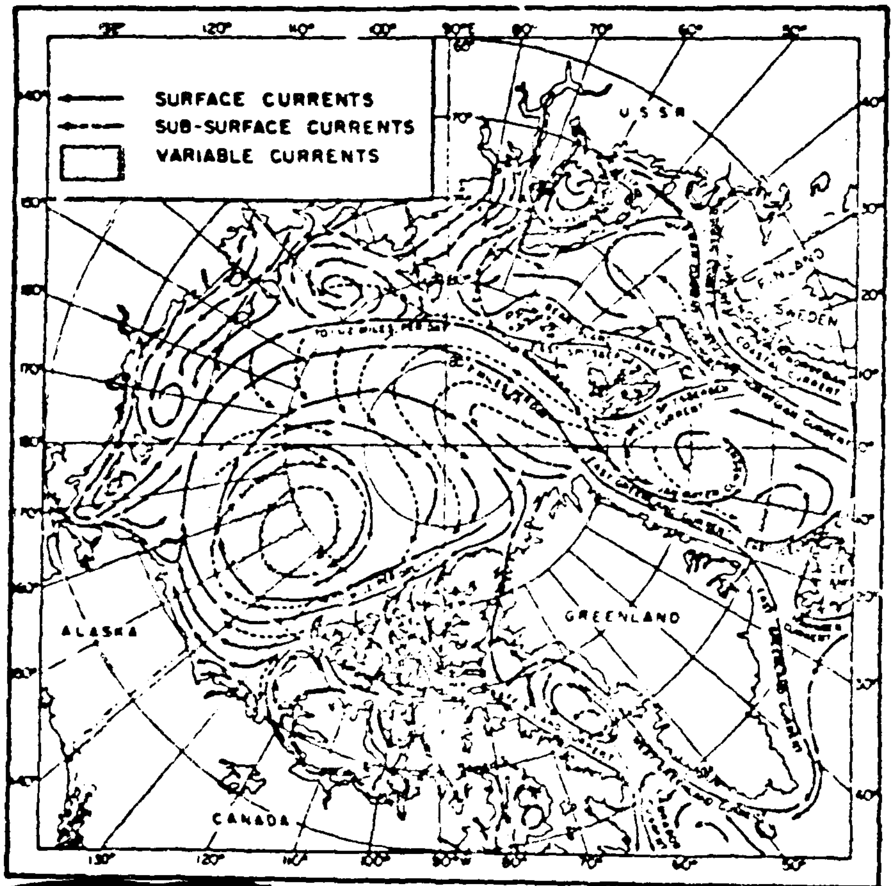

[redacted]

[redacted] Figure 1-30. Currents of the Arctic Ocean.
(Fairbridge, 1966)

[redacted]

[redacted]

the total. The discharge water into the Greenland Sea (East Greenland Current) accounts for nearly two-thirds of the total efflux.

[redacted] The circulation patterns of the Arctic result, principally, from water density differences, wind-induced effects and bathymetry. The surface currents over the deepest sections of the Arctic Ocean conform to a slow clockwise circulation. Current speeds on the North American side of the gyre are slow, averaging about 1.9 kilometers per day (0.04 kt). The flow on the Eurasian side, known as the Transpolar Drift Stream, is somewhat more intensive, attaining speeds on the order of 2.8 to 3.7 kilometers per day (0.06 to 0.08 kt). More complicated current patterns are noted adjacent to coastal areas where bathymetry changes play an important role. The center of the general anticyclonic flow is in the Beaufort Sea where variable currents can be expected.

[redacted] The extension of the Transpolar Drift Stream off the east coast of Greenland is known as the East Greenland Current. The East Greenland Current tends to intensify to the south; in the vicinity of Denmark Strait current speeds range from about 13.3 to 35.6 kilometers per day (0.3 to 0.8 kt).

[redacted] The general circulatory pattern of the Arctic subsurface waters differs somewhat from the surface pattern, particularly in the vicinity of the Greenland and Norwegian Seas. Water entering the Arctic Ocean from the Norwegian Sea sinks to depths between 180 and 460 meters in the channel between Spitzbergen and Greenland. This results in a relatively strong subsurface current of Atlantic Water moving initially counterclockwise (northeast) from Spitzbergen. This cyclonic flow pattern eventually joins the general pattern of the surface circulation in the vicinity of the Laptev Sea. Subsurface current speeds are, in general, comparable to but

[redacted]

[redacted]

[redacted] slower than surface flow rates. While little is known of Bottom Water flow directions and speeds, there is some evidence to support the contention that the entire mass of water below about 400 meters moves essentially as a unit with no significant shearing (Herman, 1974).

[redacted] 1.3 BIBLIOGRAPHY

Anderson, Gordon D., The Equation of State of Ice and Composite Frozen Materials, RR257, Cold Regions Research and Engineering Laboratory, Hanover, N. H., June 1968, UNCLASSIFIED, AD674248.

Anderson, John O., A Study of Factors Related to Arctic Underwater Acoustic Surveillance (U), TR71-01, Delco Electronics Division, General Motors Corporation, Santa Barbara, CA, January 1971, SECRET.

Assur, A., Composition of Sea Ice and Its Tensile Strength, Arctic Sea Ice, National Academy of Sciences - National Research Council, Washington, D. C., Publication 598, pp 106-138, December 1958, UNCLASSIFIED.

Bilello, Michael A., Survey of Arctic and Subarctic Temperature Inversions, Technical Report 161, Cold Regions Research and Engineering Laboratory, Hanover, NH, October 1966, UNCLASSIFIED, AD-645597.

Canadian Hydrographic Service, Arctic Islands, Chart 800 Ottowa, Ontario, 1971, UNCLASSIFIED.

Chamberlain, E. and Hoekstra, P., The Isothermal Compressibility of Frozen Soil and Ice to 30 Kilobars at -10°C, TR225, Cold Regions Research and Engineering Laboratory, Hanover, NH, June 1970, UNCLASSIFIED, AD-708867.

[redacted]

[redacted]

Defense Atomic Support Agency, Nuclear Weapons Blast Phenomena (U), DASA 1200, Defense Nuclear Agency, Washington, D. C., March 1971, SECRET RD.

Defense Nuclear Agency, Capabilities of Nuclear Weapons, Part I - Phenomenology, Part II - Damage Criteria (U), DNA EM-1, (Change 1), Dolan, P. J., Ed., Defense Nuclear Agency, Washington, D. C., July 1978, SECRET RD.

Defense Nuclear Agency, Handbook of Underwater Nuclear Explosions (U), Three volumes, each consisting of Parts 1 and 2, DNA 1240H, Defense Nuclear Agency, Washington, D. C., November 1961, SECRET RD.

Environmental Science Services Administration, U. S. Standard Atmosphere Supplements, National Aeronautics and Space Administration, Superintendent of Documents, U. S. Government Printing Office, Washington, D. C., 1966, UNCLASSIFIED.

Fairbridge, Rhodes W., Ed., The Encyclopedia of Oceanography, Encyclopedia of Earth Sciences Series, Volume 1, Reinhold Publishing Corporation, New York, 1966, UNCLASSIFIED.

Francois, Robert E., High Resolution Observations of Under-Ice Morphology, APL-UW 7712, Applied Physics Laboratory, University of Washington, 1013 N.E. 40th St., Seattle, WA 98105, 31 March 1977, UNCLASSIFIED.

Herman, Yvonne, Ed., Marine Geology and Oceanography of the Arctic Seas, Springer-Verlag New York, Inc., 1974, UNCLASSIFIED.

Hunkins, Kenneth, Seismic Studies of Sea Ice, J. Geophys. Res., Volume 65, No. 10, October 1960, Lamont Geological Observatory, Columbia University, Palisades, New York.

Hunkins, Kenneth L., Sound Scattering Layers in the Arctic Ocean, U. S. Navy Journal of Underwater Acoustics, Volume 21, No. 1, pp. 83-90, January 1971, CONFIDENTIAL (Hunkins' paper is unclassified).

[redacted]

[redacted]

Mitchell, J. M., Jr., Visual Range in the Polar Regions with Particular Reference to the Alaskan Arctic, From: Polar Atmosphere Symposium at Oslo, July 1956, Sutcliffe, R.C., Ed., Pergamon Press, Almsford, NY, 1958, UNCLASSIFIED.

Nakonechny, Basil V., The Arctic Environment and Possible Implications for Submarine and Anti-Submarine Operations (U), Report C-3382, Naval Ship Research and Development Center, Washington, D. C., June 1970, CONFIDENTIAL, AD-510234.

National Aeronautical and Space Administration, U. S. Standard Atmosphere, 1962, Superintendent of Documents, U. S. Government Printing Office, Washington, D. C., December 1962, UNCLASSIFIED.

Orvig, S., Ed., Climates of the Polar Regions, Volume 14 of World Survey of Climatology, American Elsevier Publishing Company, New York, NY, 1960, UNCLASSIFIED.

Office of Special Weapons Development, Nuclear Weapons Effects in an Arctic Environment, OSWD-59-2, United States Continental Army Command, Office of Special Weapons Development, Fort Bliss, TX, June 1960, UNCLASSIFIED, AD-344936.

Peyton, H. R., Sea Ice Strength, UAG R-182, Geophysical Institute, University of Alaska, College, Alaska, December 1966, UNCLASSIFIED, AD-653 883.

Salmela, H. A., and Sissenwine, N., Estimated Frequency of Cold Temperatures Over the Northern Hemisphere, AFCRL-70-0158, Air Force Cambridge Research Laboratories, Bedford, Mass., March 1970, UNCLASSIFIED.

Sater, J. E., Naval Surface Ship Arctic Missions (U); Volume III - Environment of the Arctic Ocean and the Rimland, SRC-70-TR-N3001, Systems Research Corporation, Washington, D. C., December 1970, Unclassified, AD-716 416.

[redacted]

[redacted]

U.S. Navy Hydrographic Office, Oceanographic Atlas of the North Atlantic Ocean; Part II - Arctic,, H. O. Publication No. 705, U. S. Navy Hydrographic Office, Washington, D. C., 1958 (Reprinted 1968), UNCLASSIFIED.

U. S. Naval Oceanographic Office, Oceanographic Atlas of the North Atlantic Ocean: Section III - Ice, Publication No. 700, U. S. Naval Oceanographic Office, Washington, D. C., 1968, UNCLASSIFIED.

Valley, S. L., Ed., Handbook of Geophysics and Space Environments, Air Force Cambridge Research Laboratories, Bedford, Mass., 1965.

VanDorn, W. B., LeMehaute, B., and Hwang, Li-San, Handbook of Explosion-Generated Water Waves, TC-130, Tetra Tech, Incorporated, Pasadena, CA, October 1968, UNCLASSIFIED, AD-845485.

Wells, M. B., Collins, D. G., and Marshall, J. D., Monte Carlo Calculations of the Transmission of Thermal Radiation from Nuclear Detonations in Model Atmospheres, RRA-T810, ECOM-00240-4, Radiation Research Associates, Inc., Fort Worth, TX, March 1969, UNCLASSIFIED.

Wittmann, Walter I. and Schule, John J., Comments on the Mass Budget of Arctic Pack Ice, IR 67-17, U. S. Naval Oceanographic Office, Washington, D. C., March 1967, UNCLASSIFIED.

[redacted]

[redacted]

SECTION 2

AIR BLAST

[redacted] Traditionally, the air blast parameter which has attracted the most interest is the maximum static overpressure. For the typical static overpressure vs time profile as measured by a pressure sensor, the maximum pressure occurs at the shock front, or almost coincident with the arrival of the wave at the sensor location. If one is concerned about damage or injury from air blast, one must, in addition to maximum static overpressure, be interested in the static overpressure impulse, the maximum dynamic overpressure, the dynamic overpressure impulse, and the time of arrival of the air blast shock front as a function of distance from the explosion.

2.1 [redacted] Arctic Environmental Differences

[redacted] The basic parameters of interest in determining the free field air blast values are the pressure and the sound velocity, which depends on the temperature and wind velocity. As shown in Section 1, the standard pressure for the Arctic is essentially the same as the midlatitude value. The temperature, however, is markedly colder during the winter months. The January standard 75° sea level temperature is given as -24°C and inspection of Figure 1-4 shows that the mean temperature is below this value for much of the Arctic. The extreme that can reasonably be expected is about -57°C. The effect of these decreased temperatures will be noted in Section 2.2.

[redacted] Temperature inversions are more probable, stronger, and more extensive in Arctic than in temperate climates. This can enhance the propagation of low overpressure values to long

[redacted]

[redacted]

[redacted] distances. Wind also affects the transmission of the low overpressure shock wave and causes an enhancement to low overpressure damage in the downwind direction.

[redacted] A major environmental difference in the Arctic is the high probability of snow or ice cover and frozen ground. Air blast over snow can be strongly affected as will be discussed in Section 2.3. The attenuation of the shock in snow can affect the coupling of the blast energy to the ground or structures. The presence of the ice layer over the sea can influence the air blast received from underwater bursts. Surface effects will be discussed in Section 2.4.

2.2 [redacted] Free Air Blast Prediction

[redacted] Free air blast predictions for nonstandard atmospheric conditions are generated as described in EM-1 (DNA, 1978) from the standard 1 kt curves by using Sachs scaling relationships. The effects of Arctic meteorological phenomena on predictions will be discussed.

2.2.1 [redacted] Sachs Scaling Techniques

[redacted] Two basic assumptions are inherent in the Sachs relations. First, it is assumed that the air blast wave propagates in a homogeneous atmosphere with the ambient conditions at the altitude of the observation point. Second, the total energy available for air blast is independent of altitude; that is, the energy partition is unchanged.

[redacted] The maximum static, maximum dynamic and total pressures are related by the expressions

$$P_2 = \left(\frac{P_{02}}{P_{01}}\right) P_1, \tag{2.1}$$

where the ranges are given by

$$R_2 = \left(\frac{P_{01}}{P_{02}}\right)^{1/3} \left(\frac{W_2}{W_1}\right)^{1/3} R_1, \tag{2.2}$$

[redacted]

[redacted]

[redacted] and the variables are defined as:

P is the appropriate maximum pressure,
P_0 is the ambient atmospheric pressure,
R is the distance from the explosion, and
W is the yield of nuclear explosion.

The subscripts 1 and 2 refer to conditions for the "reference" explosion (usually considered as 1-kt yield at standard sea level conditions) and the "problem" explosion, respectively.

[redacted] The time of arrival of shock front and the positive phase duration are given by

$$t_2 = \left(\frac{W_2}{W_1}\right)^{1/3} \left(\frac{P_{01}}{P_{02}}\right)^{1/3} \left(\frac{C_{01}}{C_{02}}\right) t_1, \tag{2.3}$$

where C_0 is the speed of sound in ambient atmosphere and the ranges are related by Equation 2.2.

[redacted] The total positive phase overpressure impulse and the dynamic pressure impulse are given by the expression

$$I_2 = \left(\frac{W_2}{W_1}\right)^{1/3} \left(\frac{P_{02}}{P_{01}}\right)^{2/3} \left(\frac{C_{01}}{C_{02}}\right) I_1, \tag{2.4}$$

where the variables are as previously defined and the ranges are related by Equation 2.2.

[redacted] In our application, the subscript 1 refers to the mid-latitude standard values and subscript 2 refers to the Arctic values of interest. The yield will be taken as 1 kt so we are interested in the changes that will occur when the 1 kt mid-latitude standard curves are scaled to 1 kt Arctic conditions.

[redacted]

[redacted]

[redacted] The pressures in the Arctic at sea level are virtually identical to those found in the midlatitudes. The variations from the standard values caused by meteorological perturbations is of the same order as for temperate climates. Thus, the pressure ratio P_{02}/P_{01} is essentially unity, and no differences are expected in the pressure radius curves in the Arctic.

[redacted] Note that the time and the impulse scaling relations also involve the ratio of the sound speed which is related to the temperature by the expression

$$\frac{C_{01}}{C_{02}} = \left(\frac{T_{01}}{T_{02}}\right)^{1/2}, \qquad (2.5)$$

where the temperatures must be degrees Kelvin. For the mean January Arctic temperature at sea level this ratio is 1.075, implying a 7.5% increase in the time and impulse values in the Arctic. For the extreme temperature case (-60°C) the increase is 15.5%.

[redacted] In Figure 2-1 the change in the shock front arrival time is noted for the extreme case. In Figure 2-2 the change in the impulse values for the extreme case is shown. Even these changes for the extreme case are of marginal interest since a 15% increase in the impulse would not in general cause any practical systems effects, and it would occur with only a small probability. The mean 7.5% increase which can be expected in the coldest months is within the basic uncertainties in the impulse predictions and the resulting damage effects.

[redacted]

[redacted]

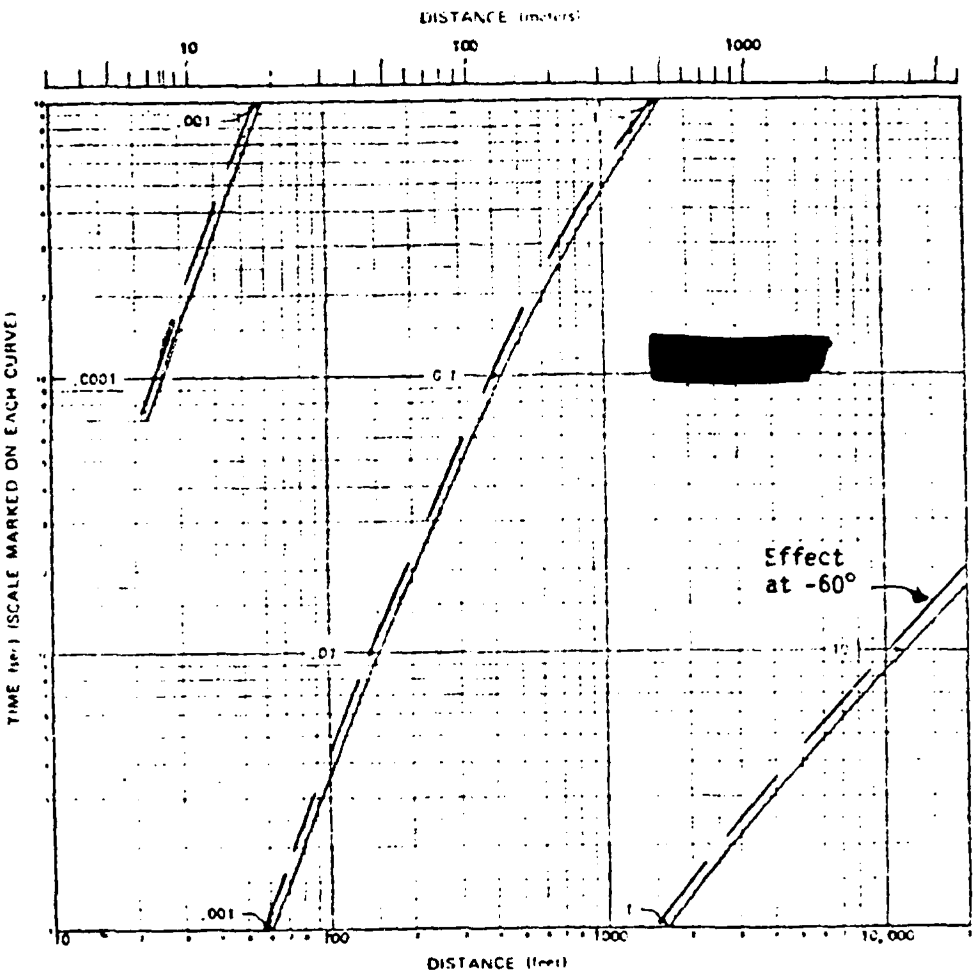

[redacted] Figure 2-1 Time of Arrival of the Shock Front from a 1 kt Free Air Burst in a Standard Sea Level Atmosphere [redacted]

[redacted]

[redacted]

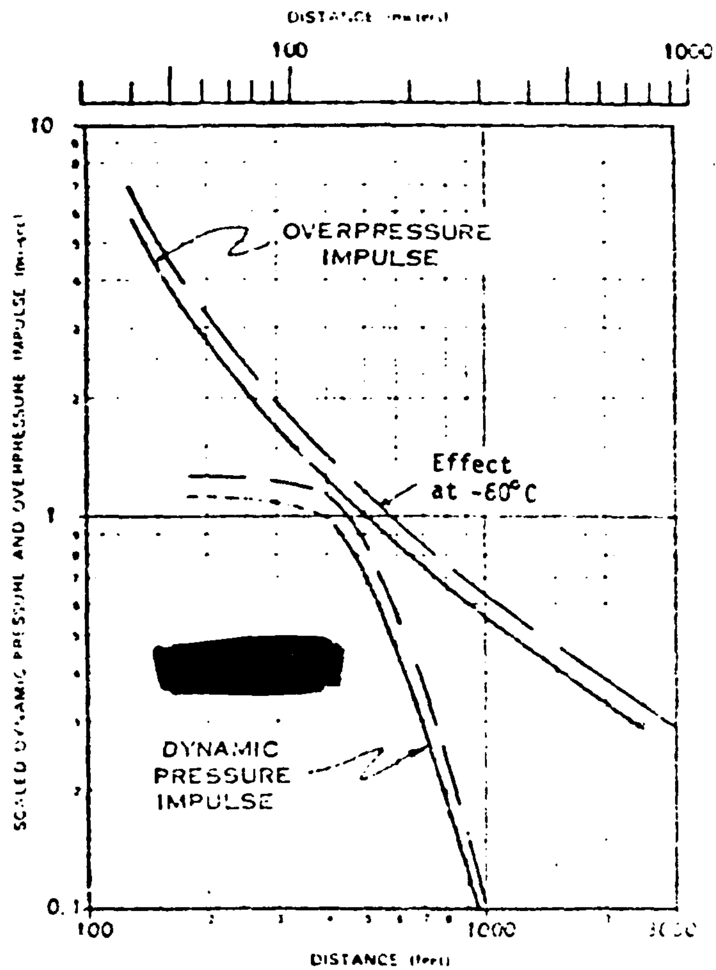

[redacted] Figure 2-2 Overpressure and Dynamic Pressure Impulse from [illegible] Free Air Burst in a Standard Sea Level Atmosphere [redacted]

[redacted]

[redacted]

[redacted] Inspection of Table 1-1 shows a small deviation of the Arctic pressures from the midlatitude values as a function of altitude. From equations 2.1 and 2.2 the coaltitude ranges to various overpressure values were calculated as a function of burst altitude for the Arctic and midlatitude pressure - altitude profiles. For all overpressure values considered between 1 and 1000 psi there were insignificant differences (<5%) in the Arctic and midlatitude coaltitude ranges.

[redacted] The conclusion is that no significant differences will be found in the free air blast values under Arctic conditions. Sachs scaling can be used to provide the free air values if precise time and impulse values are required.

[redacted] The reliability of Sachs scaling under Arctic conditions may be questionable. The Sachs relations can be derived rigorously from theoretical considerations. However, the 1 kt free air curve is based on a combination of theory, calculations and experimental data. For the low overpressure values there has always been some uncertainty. Scaling this curve to conditions far removed from the experimental data on which it is based must be treated cautiously.

[redacted] There is some evidence that Sachs scaling at depressed temperatures is valid. The technique has been used to correlate data in all of the high explosive (HE) tests that have been performed over snow and ice. In the Distant Plain events to be described in the next section, Sachs scaling was used to correlate summer and winter results and no inconsistencies were found.

[redacted] Modified Sachs scaling between altitudes using the atmospheric parameters at the target location has been used to correlate and predict blast values in inhomogeneous air with a high degree of success. Comparisons of computer code calculations in non-uniform air (Wells, 1971) with Sachs scaled blast parameters

[redacted]

[redacted] indicate that the technique can be used reliably for these cases. This would imply that modified Sachs scaling can be used for predicting the blast environment if a temperature inversion is present if the pressures are high enough to ignore refraction effects.

2.2.2 [redacted] The Effect of Temperature Inversion

[redacted] A temperature inversion causes a sound speed gradient to exist at low altitudes resulting in refractive effects and can, therefore, amplify the overpressure at the ground from a burst occurring below an inversion. Conversely, surface overpressures are reduced if the detonation is above the inversion. These refractive effects are important only for very low overpressures (<1 psi). The effects are serious enough in consideration of safety from HE tests, to restrict shots when inversions exist to inhibit long range damage to windows etc. This may be of interest militarily since in the very severe arctic winter losing building integrity due to window breakage is much more important than in temperate climates.

[redacted] The lapse rates of Arctic inversions are more severe than is typical of temperate areas, as described in Section 1. It is therefore likely that inversions will exert a more significant influence on blast phenomena in the Arctic than elsewhere. The increased incidence of inversions in Arctic areas will increase the probability of seeing these effects.

[redacted] Although corrections for inversions are small, the enhancement of low static overpressure at long ranges may somewhat increase the possibility of damage to blast-sensitive targets for bursts below the inversion. Later this year a report (Reed, 1980) of an extensive experimental study will be published detailing the effect of inversions and wind velocity on air blast. This study will supersede anything available at this time. Quantitative predictions should be delayed until the report is available.

[redacted]

2.2.3 [redacted] The Effect of Wind

[redacted] In addition to the temperature, the wind velocity causes a change in the relative sound speed and, therefore, on the blast parameters at very low overpressures. No direct effects would be expected at higher pressures. The effects of wind will be considered in a report to be published during 1980 (Reed, 1980).

[redacted] The dry snow of cold regions is easily lifted by turbulent winds to create a dense cloud that obscures vision and can become integrated with an air blast wave. Any wind of velocity over 15 miles per hour causes blowing snow if the temperature is well below the freezing point. As examples, periods during which blowing snow has reduced visibility to less than 1000 yards extend from 75 hours in one area to as long as 260 consecutive hours in another area. In sub-Arctic forests, such as grow in eastern Siberia, surface winds are impeded by the trees and blowing snow is less prevalent.

[redacted] The reduced visibility would have the most direct effect on the amount of thermal radiation from a nuclear weapon burst reaching the ground. This, in turn, would have an indirect effect upon the air blast phenomena; that is, the possibility of the formation of a precursor under these conditions would be very remote.

[redacted] A more significant aspect of the presence of dry snow is the fact that a blast wave could carry many snow particles as it propagates along the surface of the ground (or ice/water surfaces). This might lead to enhanced damage, which will be discussed in Section 2.5.

2.2.4 [redacted] The Effects of Precipitation, Fog and Clouds

[redacted] The effects of atmospheric moisture on blast propagation are not well known; however, theoretical studies agree qualitatively with the small amount of experimental data. As a strong blast wave propagates through air containing water droplets it

[redacted]

[redacted]

[redacted] vaporizes some or all of the water. Vaporization of the water absorbs energy that otherwise would be available for the blast wave to propagate through the air. As a result, the blast wave is attenuated more rapidly in air that contains water droplets than in air that does not.

[redacted] The effect of water droplets on peak overpressure may be calculated in terms of effective yield. This procedure is used to obtain lower calculated overpressures at some distance from the burst. Rain or fog has a negligible effect on the amount of available energy close to the nuclear source. The energy density within the fireball is orders of magnitude higher than the energy required to vaporize whatever water may be present, and the amount by which the suspended liquid increases effective air density, even under the extreme conditions within clouds producing severe thunderstorms, is not likely to exceed 2 percent.

[redacted] Figure 2-3 shows the effective yield for three yields and two conditions of moisture content. The water densities used in the calculations correspond roughly to precipitation rates of 0.1 (light rain) and 0.5 (heavy rain) inches per hour.

[redacted] The curves shown in Figure 2-3 are based on the assumption of uniform water content between the source and the target. In an actual rainstorm, this assumption is artificial, but without such an assumption the analysis of rain's effect would be unduly complex. Typically, water content is several times as high within a rain cloud as it is below the cloud. Actual water distribution patterns are complex, different for different rainstorms, and generally unpredictable.

[redacted]

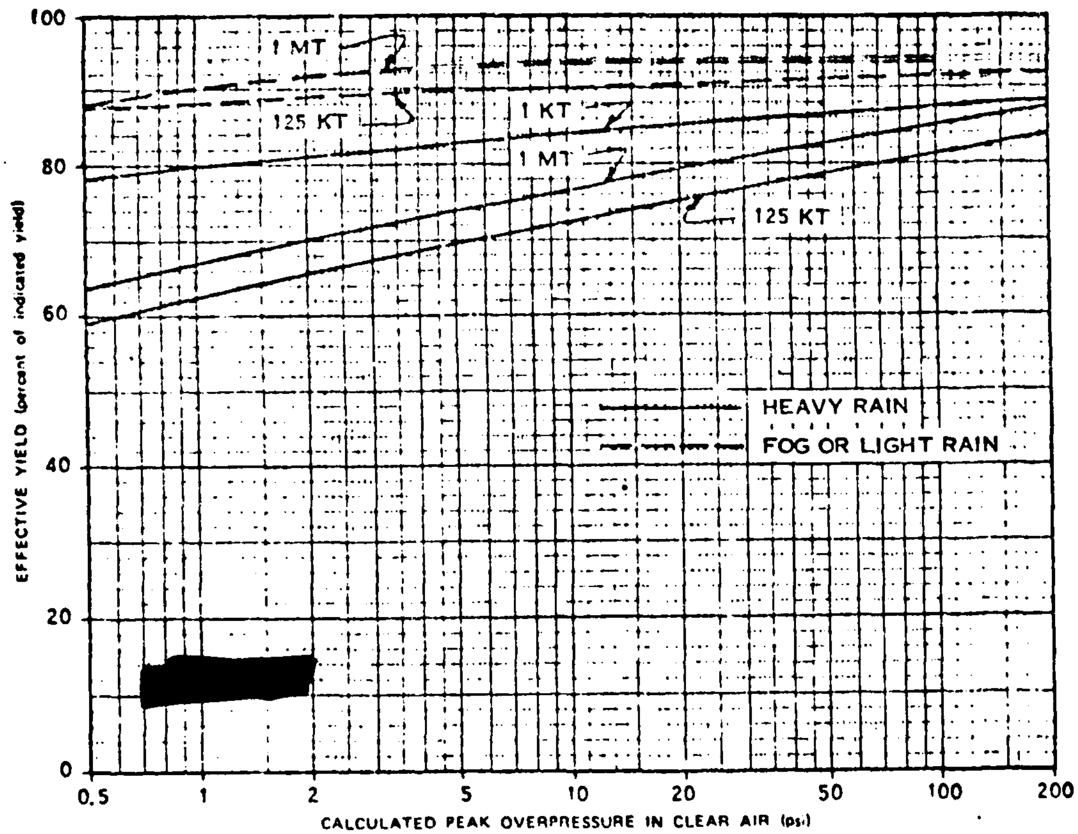

[redacted] FIGURE 2-3 REDUCTION OF PEAK OVERPRESSURE AT THE SURFACE BY RAIN OR FOG - NEAR-IDEAL SURFACE

[redacted]

[redacted] As stated in EM-1, rain or fog effects should be evaluated only when the optimization of blast against soft targets is important, and then only if the rain or fog extends throughout a volume that includes both the target and the burst. HOB curves for thermally near-ideal surface conditions should be used with Figure 2-3 since thermal energy is attenuated by rain or fog and precursor effects would not be expected above a wet surface.

[redacted] The effects of atmospheric moisture on other blast parameters, such as time of arrival, positive-phase duration, and dynamic pressure are not well known; however, theoretical considerations indicate that arrival times will remain essentially unchanged, positive-phase durations will be slightly reduced, and dynamic pressures will be slightly increased. Calculations of these other air blast parameters should be made in the normal manner, without applying any effective yield factors. Enhanced effects on dynamic overpressures are discussed in Section 2.3.6. Referring to Figure 2-3, and recalling that $(Y_{eff})^{1/3} = R_o/R_1$, one can derive some conclusions related to the applications to Arctic environments:

(1) For light rain or fog, the 125 KT and 1 MT curves indicate effective yields of 90% or above for the peak overpressures of interest. Since $(0.90)^{1/3} = 0.97$, it is evident that light rain or fog is not going to cause a significant perturbation to the ordinary air blast effects.

(2) For heavy rain and for peak overpressures in the 5-20 psi range, effective yields can be in the 70-80% range for the larger yields. Since $(0.7)^{1/3} = 0.89$, it is unlikely that, even for this extreme case, the deviations in blast effects from normal would be considered significant.

[redacted]

[redacted]

[redacted] No test data from nuclear bursts in snow are available to the U.S. A possible estimation of the general effect of snow can be made by an extension of the reasoning of the preceding paragraphs if we assume that the amount of water in heavy and light snows is similar to the amount of water in heavy and light rains. The snow particles would have to be first melted and then heated to evaporation with the resultant transfer of more of the blast energy. This could result in an increase in attenuation over that noted in Figure 2-3 since an additional energy of about 100 calories per gram of water would be required to melt the snow and evaporate it. The interaction may involve breakup of the snow flakes and water droplets for more efficient energy transfer. The force required to shatter the crystaline structure is probably larger, but the effect of this on the energy transfer is unknown. There is, however, no positive evidence that this reduction should be greatly different than that occasioned by temperate forms of precipitation at militarily significant ranges. It should be emphasized here that no valid numerical evaluation of this aspect of Arctic environment can be made without further experimentation.

[redacted] Since low dense clouds are very prevalent over the polar ice during the summer, the effect might be worth studying in more detail. A recent review and analytical consideration of this effect (Friedberg, 1976) points out that the attenuation in fogs and clouds is more severe because of the smaller water drops and more efficient transfer of energy to the water and subsequently larger attenuation of blast energy. No work in this area was referenced after the 1950s in the above report.

[redacted]

[redacted]

2.3 [redacted] Air Blast Over Frozen Surfaces

2.3.1 [redacted] Reflection Characteristics of Snow Layers

(U) When a shock front enters a layer of snow it is attenuated strongly. Drag forces on the snow crystals dissipate energy contained in the wind behind the shock front. The energy transmitted to the snow crystals is then consumed in compacting the snow layer.

[redacted] Reflection occurs at the top surface of a deep snow layer just as it does at a ground surface. Momentum is conserved in the interaction. A blast wave striking the earth transmits only a small fraction of its energy as ground shock; consequently, the earth's surface approximates an ideal reflector. A blast wave striking a snow surface is analogous to a ball bouncing from a heavy rug. The reflecting surface has a cushioning effect that makes it a poorer reflector.

[redacted] In the case of a thin layer of snow, the cushioning effect ceases when the pressure wave penetrates the snow layer, reflects from the ground surface, and propagates back to the snow surface. At this time, the snow layer is supported by an internal pressure as high as the pressure produced by the blast wave reflecting from the surface; the reflecting qualities of the snow layer then approach the near-ideal reflecting qualities of the underlying surface.

[redacted] Neither theoretical nor experimental data are available on the effects of thin snow layers on a blast wave, however, a rough calculation is enlightening. If a shock front in snow moves with a speed comparable to that of sound in air, a layer of snow one foot thick, struck by a normally incident blast wave, will absorb energy from the blast wave for about 2 milliseconds and will have the properties of a near-ideal reflecting surface after that time. This 2-millisecond interval is appreciably long only

[redacted]

[redacted]

[redacted] when compared with relatively short duration blast waves. For example, it might alter a 750 psi blast wave from a 1 kt source. The overpressure pulses of this blast wave have an effective triangular duration of about 20 milliseconds. At lower overpressures, the pulse becomes broader, and the snow layer would have less effect. For a given overpressure, larger yields than 1 kt also produce broader pulses. It should also be noted that, for a 1000-lb HE detonation, the triangular duration of about 20 msec occurs at a maximum overpressure of only 20 psi. For HE detonations of smaller charges, these durations would correspond to even lower peak overpressures. This discussion indicates the following:

- If a blast wave with a very short-duration pressure pulse strikes a thin layer of snow, the snow may alter the leading edge of the pressure pulse enough to reduce peak reflected overpressure. The short pressure vs time pulse corresponds to high overpressures from relatively low yield nuclear detonations and/or virtually all overpressures from small-charge HE detonations.

- For a situation where interest is in lower overpressures and yields greater than 1 kt a thin snow cover affects such a small portion of the overpressure pulse that peak reflected overpressure is essentially the same as for a near-ideal surface.

[redacted] Measurements of the properties of snow under dynamic loading have been made (Napadenskv, 1964) which indicate that relatively small amounts of energy will be absorbed by a snow layer because the snow is compacted to densities equivalent to ice by pressures in the 20 - 40 bar region. As one might expect,

[redacted]

[redacted]

[redacted] a very large variation in snow properties was found for different types of snow in different stages of compaction. The experiments were not taken to large pressure values so the integral of PdV cannot be obtained with any degree of accuracy. If the approximation 1/2 PΔV is used, which will overestimate the integral, then the energy loss due to this mechanism could be significant in reducing the effective blast yield for a 1 kt burst detonated over 1 m of snow, which is a reasonable upper limit for Arctic winter conditions.

[redacted] The U.S. has never detonated a nuclear weapon in the atmosphere in an Arctic environment. Therefore, all predictions related to the effects of an Arctic environment upon air blast parameters from nuclear explosions must be deduced either from theoretical calculations or from the results of experiments using HE sources. For many years, we have been interested in predicting the behavior of air blast phenomena from nuclear bursts in temperate environments; during that time, these deductive methods have proven effective, except for cases where thermal/air blast interactions are important, e.g. precursor wave formation and propagation. Experience and advancing developments in instrumentation techniques have revealed the utility of and the limitations on the data obtained from the small and large charge HE tests.

[redacted] Other than the inability of the HE charge tests to properly simulate the nuclear bursts' thermal/air blast interaction, the most important "sin of omission" in HE tests is insufficient band width of the instrumentation system used. Sometimes this is referred to as "inadequate frequency response of the transducer circuitry". In effect, this limited frequency response has a similar effect on the pressure vs time measure-

[redacted]

[redacted] ment as was described above for the snow layer case. That is, the gage electronic system would "chop off" the true peak overpressure and the recorded result would be in error. The magnitude of the error depends on the bandwidth of the circuit and the magnitude of the peak pressure.

[redacted] Recent HE experimental programs have emphasized these band width aspects; in particular the TRW 3-lb 9404 experiments (Carpenter and Brode, 1974) and the BRL (Dipole West) 1000-lb TNT tests (Reisler et al, 1975 and 1976) employed instrumentation band widths which were compatible with the sizes of the explosive charge. Unfortunately, the same was not the case for many HE experiments performed during the 1950's and 1960's.

[redacted] To explain this concept further, Table 2-1 is presented. The Table lists the instrumentation band widths normalized to Carpenter's experiment, which are required to be compatible with each size of explosive charge used for an HE test. It is obvious that as the charge sizes increase the band width requirement relaxes.

2.3.2 [redacted] Air Blast Over Shallow Snow

[redacted] An interesting pair of HE events was conducted as part of the DISTANT PLAIN test series (Reisler et al, 1967). These events were 20 ton TNT surface bursts with the same conditions except that Event 3 was a summer shot and Event 5 was a winter shot. The temperature for the summer shot was 110°F and for the winter shot was 33°F. The winter shot had a snow cover of about 4 inches over soil frozen to a depth of about 9".

[redacted]

[redacted] TABLE 2-1

"REQUIRED" BANDWIDTH VS. TNT CHARGE SIZE

	CHARGE SIZE (TNT)	REQUIRED BANDWIDTH *(NORMALIZED TO CARPENTER'S)
	1 lb.	800 kHz
Carpenter	8 lb.	400 kHz
	32 lb.	252 kHz
	256 lb.	126 kHz
Dipole West	1000 lb.	80 kHz
Suffield, etc	20 tons	23.4 kHz
	100 tons	13.7 kHz
	500 tons	8 kHz

[redacted]

*i.e., These are the bandwidths required so that the data system would be equivalent to Carpenter's system used for the 8-lb. experiments.

[redacted]

[redacted] The comparison of the overpressures obtained on the two shots is shown in Figure 2-4. Note that the data points agree closely except at the high overpressure values where the experimenters drew the pressure curve for the winter event below the curve for the summer event. There is obviously some scatter in the data points, and there are only four gage positions in the high pressure region. The interesting fact is that the pressure-time records for these high pressure positions indicate a very narrow pulse of the order of shock traversal time through the shallow snow while the time width for the shock at the lower pressures is significantly longer than the snow shock transit time. This may be only an interesting coincidence. Additional experiments or calculations could resolve the question.

[redacted] The dynamic pressure and impulse measurements indicated good agreement between the two events. In this case there was no increase in dynamic pressure due to entrainment of snow by the blast wave.

2.3.3 [redacted] Air Blast Over Deep Snow

[redacted] Denver Research Institute (DRI) (Wisotski, 1966) and U.S. Army Waterways Experiment Station (WES) (Ingram, 1960 and 1962, Joachim, 1964 and 1967) performed HE tests which are most applicable to our Arctic environment situation. The DRI tests employed 1-lb and 8-lb size charges, while WES used 32-lb and 256-lb charges, primarily. In both cases, the band width of the instrumentation was in the region of 0-20 kHz, too limited with respect to the size of the sources used. Fortunately, most of these measurements were confined to the lower overpressures (less than 20 psi) where the limited band width would have less effect on the accuracy of the measurements. However, because it is difficult to determine the magnitude of the errors due to the

[redacted]

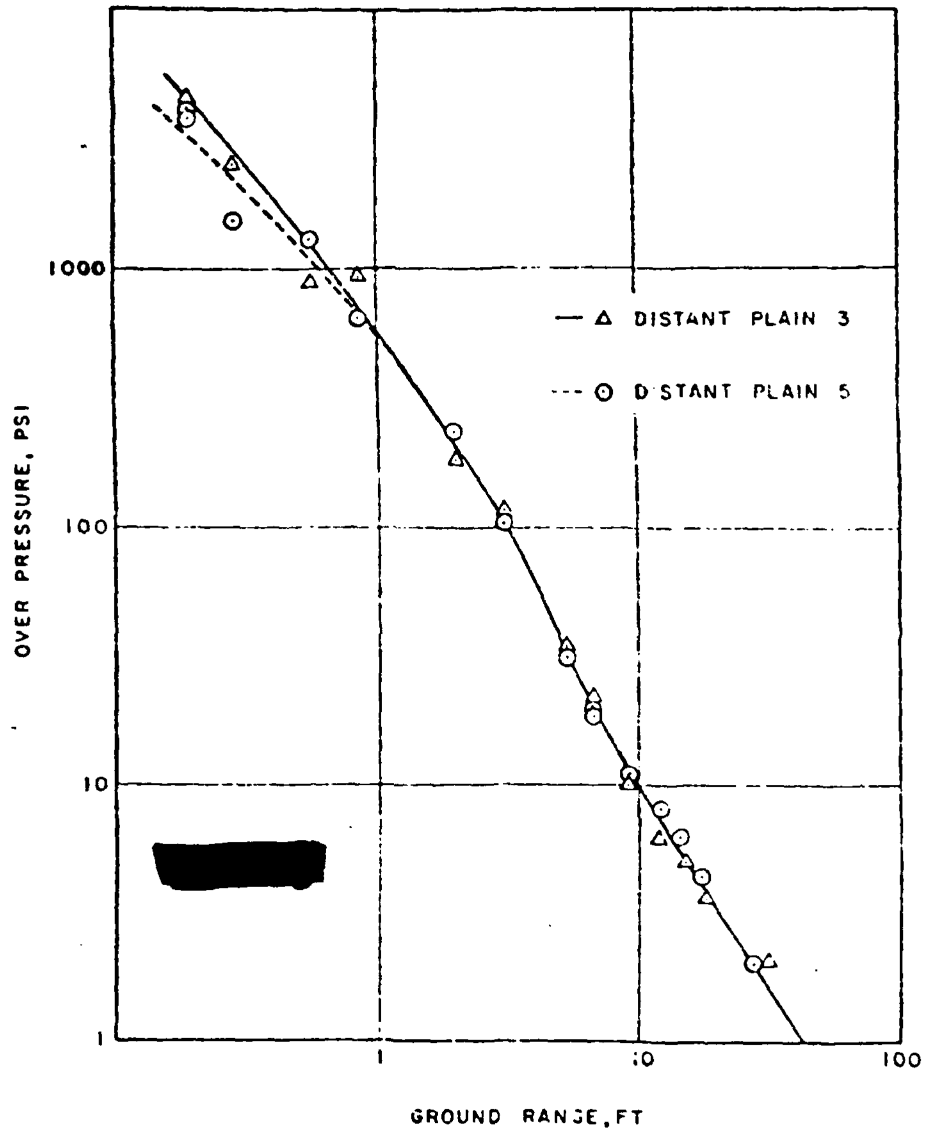

[redacted] FIGURE 2-4. Measured overpressure for Events 3 and 5 (Reisler, et al, 1967)

[redacted]

[redacted] limited band width, one must be very cautious when attempts are made to compare data collected by one agency with similar data collected by another group using different instrumentation. Thus, the most valid conclusions come from the DRI bare ground vs snow-covered ground air blast data; more tentative conclusions are derived from the WES data taken in the Arctic compared with data taken over bare ground by BRL at Suffield, Canada.

[redacted] Of course, we must not forget that all of these conclusions are based upon HE test data; therefore, the implied assumption is that the thermal radiation from the nuclear burst fireball affects the air blast parameters similarly in both temperate and Arctic environments--an assumption which requires much more thorough investigation.

[redacted] DRI performed a series of small-charge HE tests over bare ground and over snow-covered ground using the same gage arrays and electronic instrumentation on each test. These data comprise the most complete set of results available on the effects of a deep snow layer on air blast parameters. Although the charges used were only 1-lb and 8-lbs, since the same instrumentation was used for all tests, the lack of sufficient band width is probably not serious as far as the overall comparisons are concerned.

[redacted] The effect of snow and bare ground surfaces on Mach-region peak static overpressures is summarized in Figures 2-5 through 2-8. Note that the plotted data are "as read" and they correspond to an average ambient atmospheric pressure of 510 mm Hg (9.86 psi). The results shown in Figure 2-5 are typical; the data indicate that the peak static overpressures for the snow-covered surface are depressed from those measured over bare ground. For the Hc = 1/2 ft case, the two curves are very close to parallel,

[redacted]

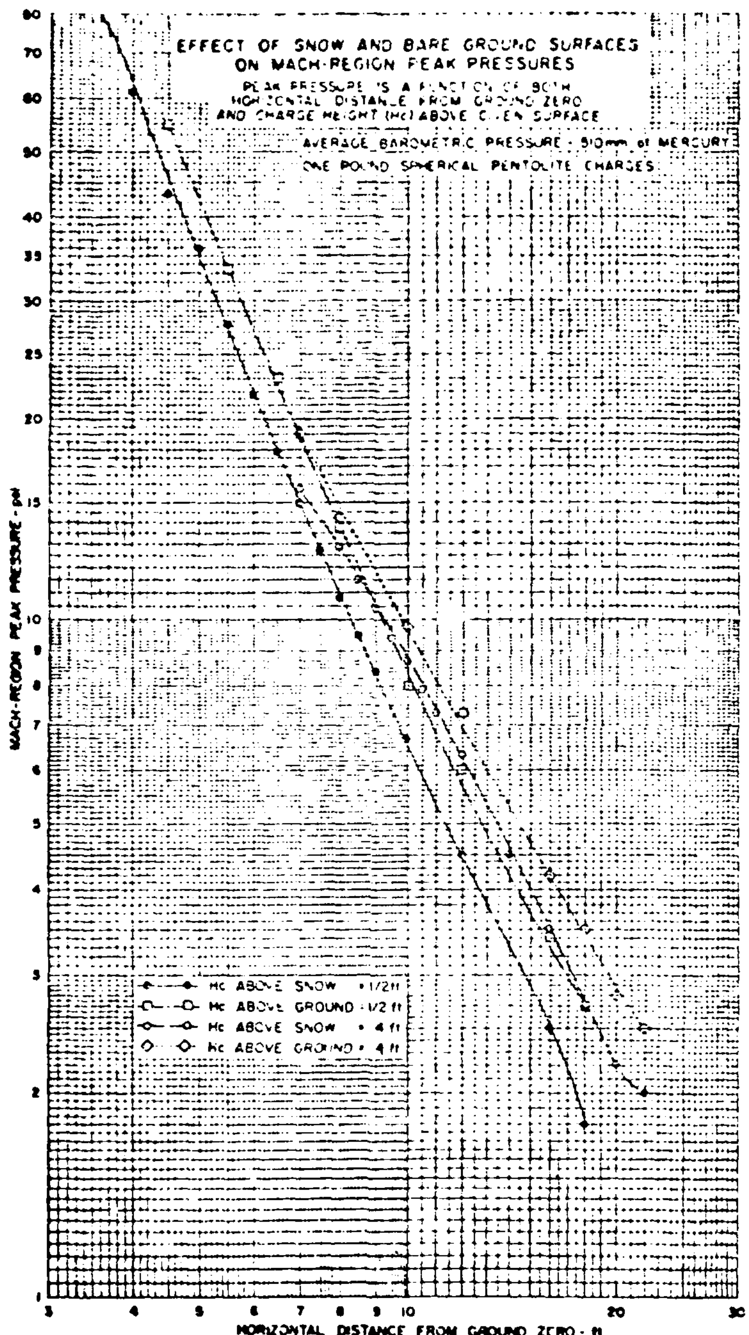

[redacted]

[redacted] FIGURE 2-5. (Wisotski and Snyer, 1966)

[redacted]

[redacted]

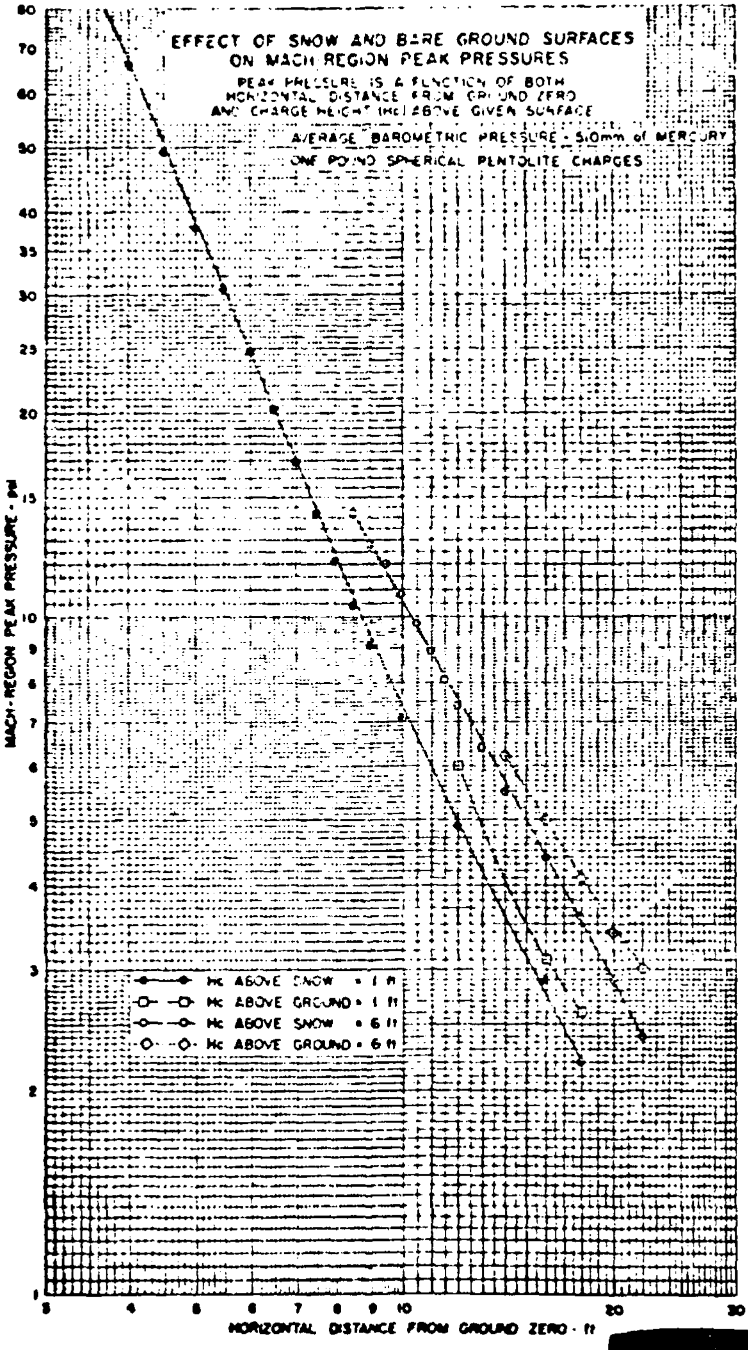

[redacted]

[redacted] FIGURE 2-6. (Wisotski and Snyer, 1966)

[redacted]

[redacted]

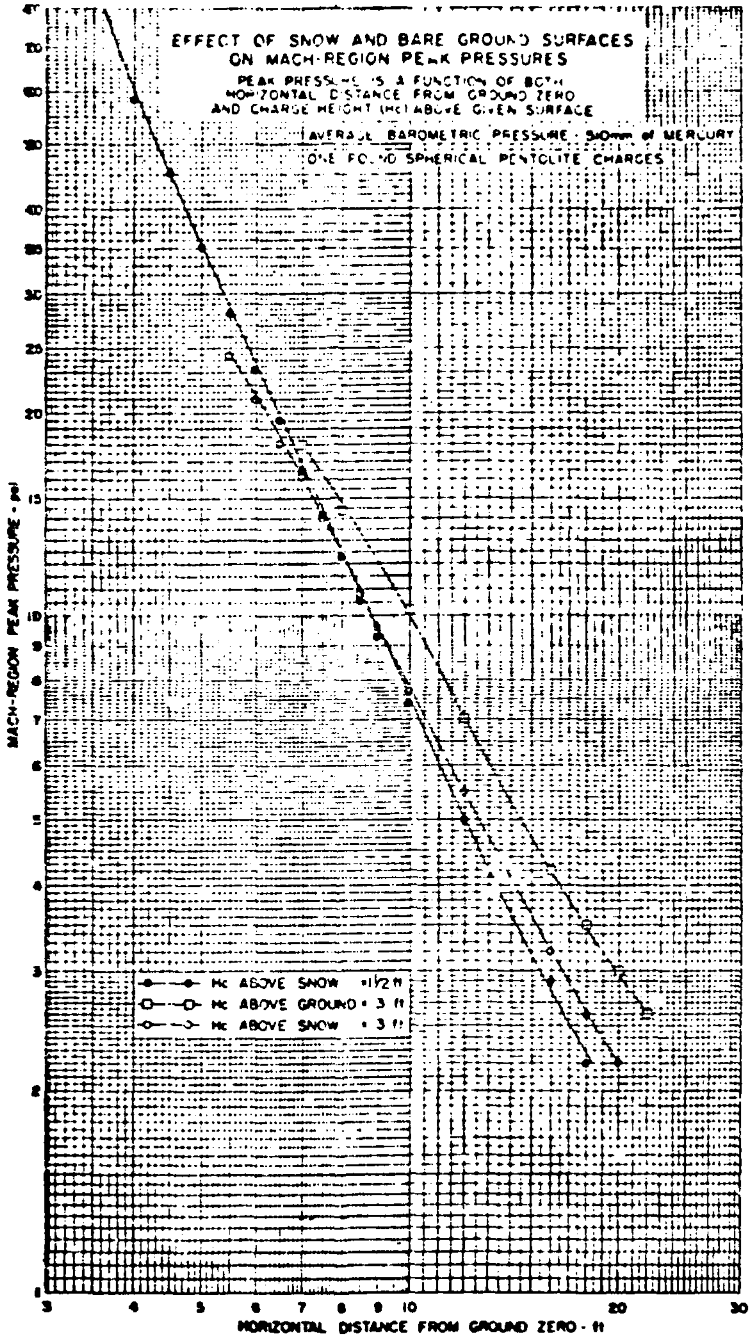

[redacted] FIGURE 2-7. (Wisotski and Snyer, 1966)

[redacted]

[redacted]

[redacted]

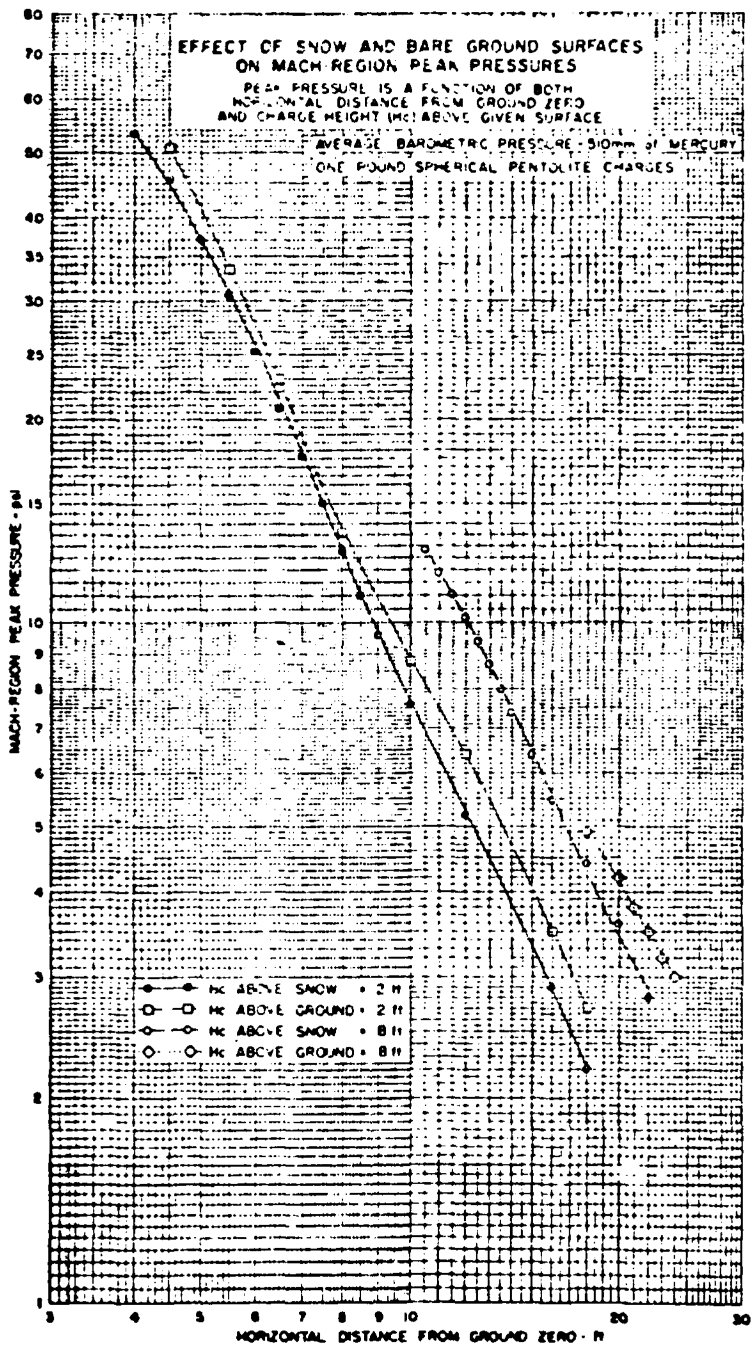

[redacted]

[redacted]IGURE 2-8. (Wisotski and Snyer, 1966)

[redacted]

[redacted] so the decrease in pressure over snow is independent of pressure magnitude. For Hc = 4 ft, there is some variation with pressure level indicated; particularly at the higher overpressures where the above-snow curve appears to "turn over" slightly. This latter behavior is noted also on Figures 2-7 and 2-8 at the higher overpressures. Also, the figures indicate that the peak overpressures for the low burst height (Hc = 1/2 ft) are depressed the most by the snow cover.

[redacted] The effect of snow-covered and bare ground on static overpressure impulse is shown on Figures 2-9 through 2-12 for the various burst heights. In general, the comparisons indicate that the snow layer tends to suppress the total impulse; however, the scatter in the data is quite severe, and it is difficult to detect a consistent amount of suppression due to the different surfaces. Looking at Figure 2-12, it is evident that the variations between the snow-covered and bare ground values are reduced as the burst height is increased.

[redacted] The reflection coefficients from snow, bare ground and concrete are plotted vs scaled charge height in Figure 2-13. Qualitatively, the results are as expected; one would expect that the least amount of energy of the explosive would be transferred to the concrete surface and that the most would be absorbed by the snow. Because we are comparing data (concrete) taken on another test, using instrumentation with an unknown bandwidth, we must be cautious in using the values shown for prediction purposes.

[redacted] The effect of snow-covered and bare ground on the path of the Mach triple point is shown in Figure 2-14. In general, the triple point rises faster over bare ground than over the snow cover. Data from tests having burst heights higher than

[redacted]

[redacted]

EFFECT OF SNOW AND BARE GROUND SURFACES ON IMPULSE VALUES

IMPULSE AS A FUNCTION OF BOTH
HORIZONTAL DISTANCE FROM GROUND ZERO
AND CHARGE HEIGHT (Hc) ABOVE GIVEN SURFACE

AVERAGE BAROMETRIC PRESSURE - 510mm of MERCURY
ONE POUND SPHERICAL PENTOLITE CHARGES

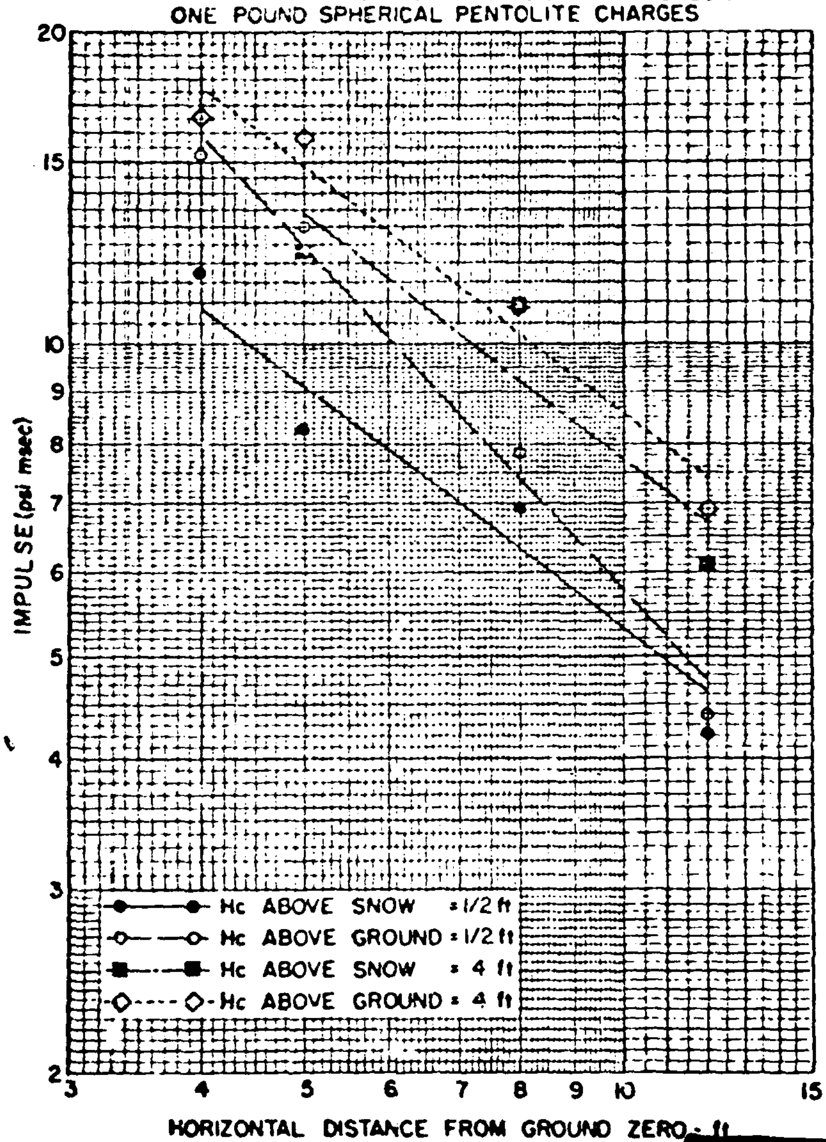

[redacted]

[redacted]IGURE 2-9. (Wisotski and Snyer, 1966)

[redacted]

[redacted]

EFFECT OF SNOW AND BARE GROUND SURFACES ON IMPULSE VALUES

IMPULSE AS A FUNCTION OF BOTH HORIZONTAL DISTANCE FROM GROUND ZERO AND CHARGE HEIGHT (Hc) ABOVE GIVEN SURFACE

AVERAGE BAROMETRIC PRESSURE - 510mm of MERCURY
ONE POUND SPHERICAL PENTOLITE CHARGES

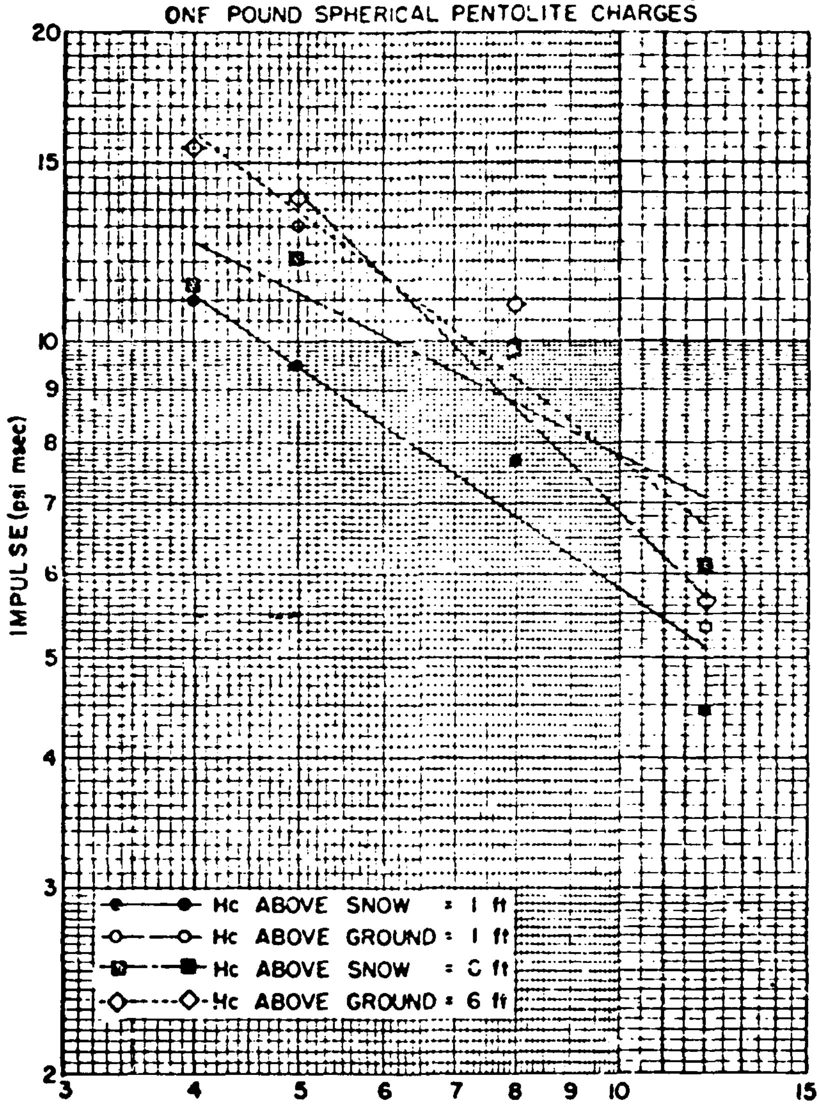

HORIZONTAL DISTANCE FROM GROUND ZERO - ft [redacted]

[redacted] FIGURE 2-10. (Wisotski and Snyer, 1966)

[redacted]

[redacted]

EFFECT OF SNOW AND BARE GROUND SURFACES ON IMPULSE VALUES

IMPULSE AS A FUNCTION OF BOTH HORIZONTAL DISTANCE FROM GROUND ZERO AND CHARGE HEIGHT (Hc) ABOVE GIVEN SURFACE

AVERAGE BAROMETRIC PRESSURE - 510mm of MERCURY
ONE POUND SPHERICAL PENTOLITE CHARGES

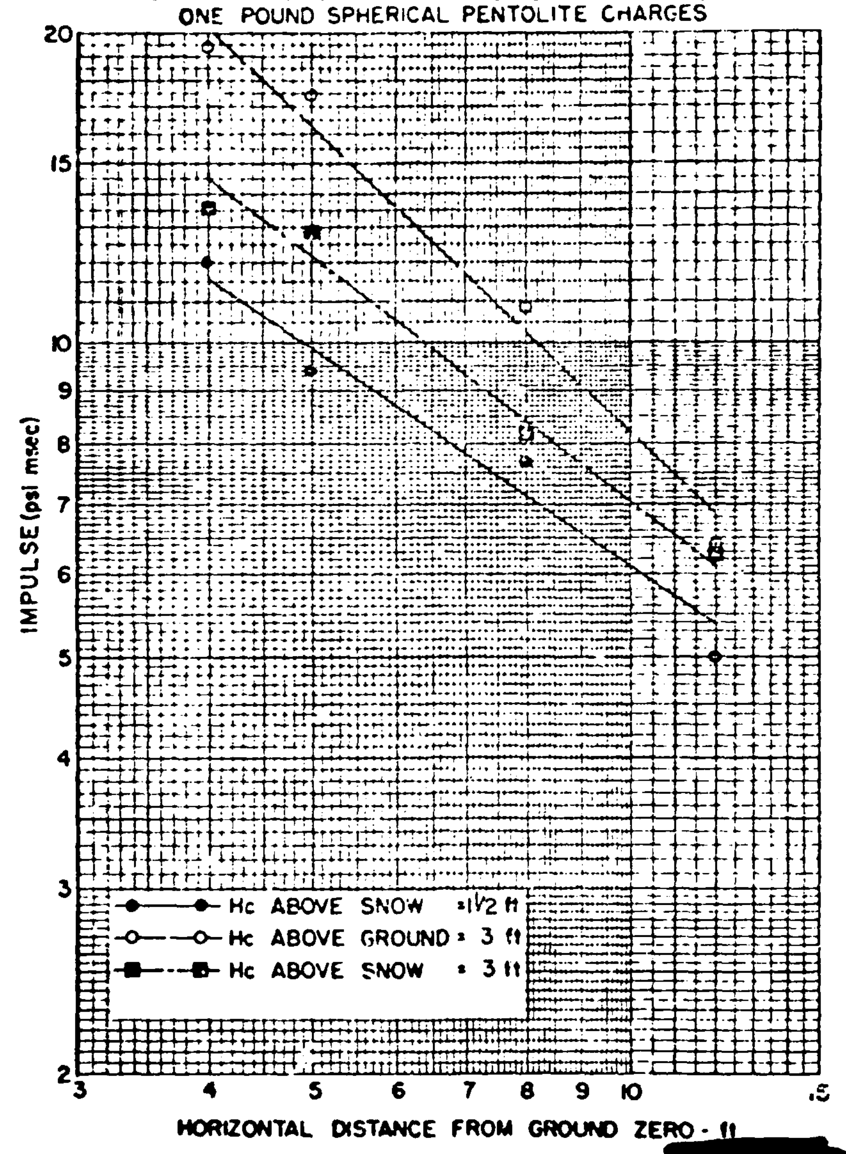

[redacted]

[redacted] FIGURE 2-11. (Wisotski and Snyer, 1966)

[redacted]

[redacted]

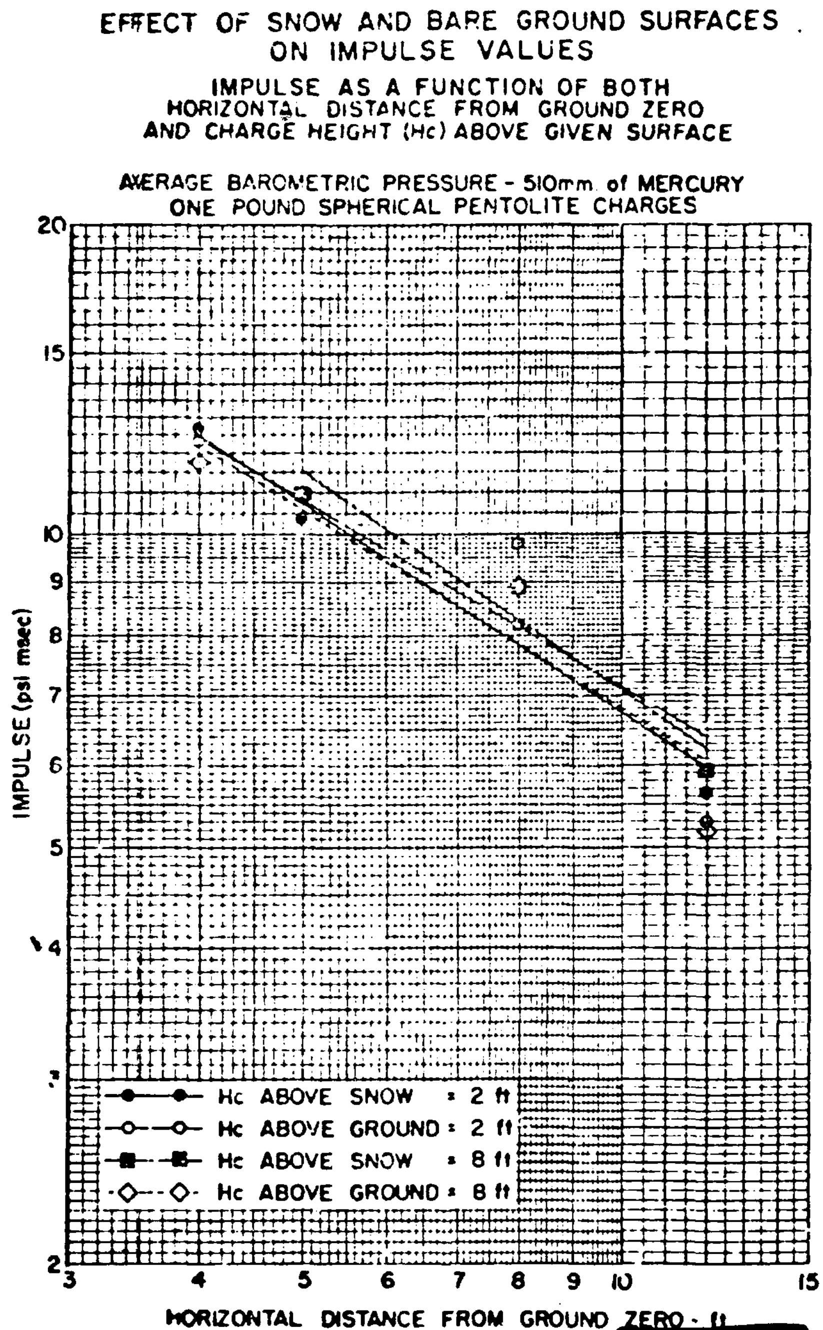

[redacted]

[redacted] FIGURE 2-12. (Wisotski and Snyer, 1966)

[redacted]

[redacted]

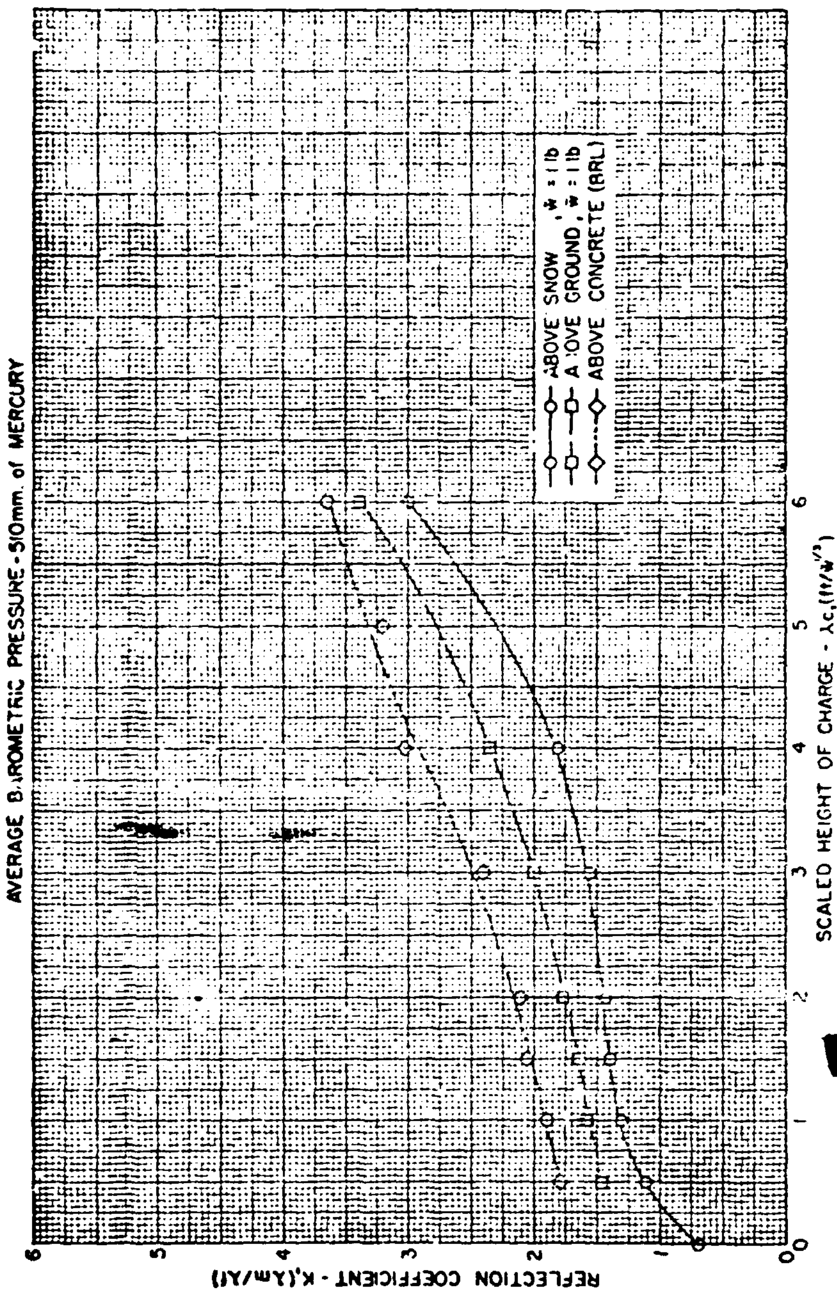

[redacted]

EFFECT OF SNOW AND BARE GROUND SURFACES ON REFLECTION COEFFICIENT

[redacted] FIGURE 2-13. (Wisotski and Snyer, 1966)

[redacted]

[redacted]

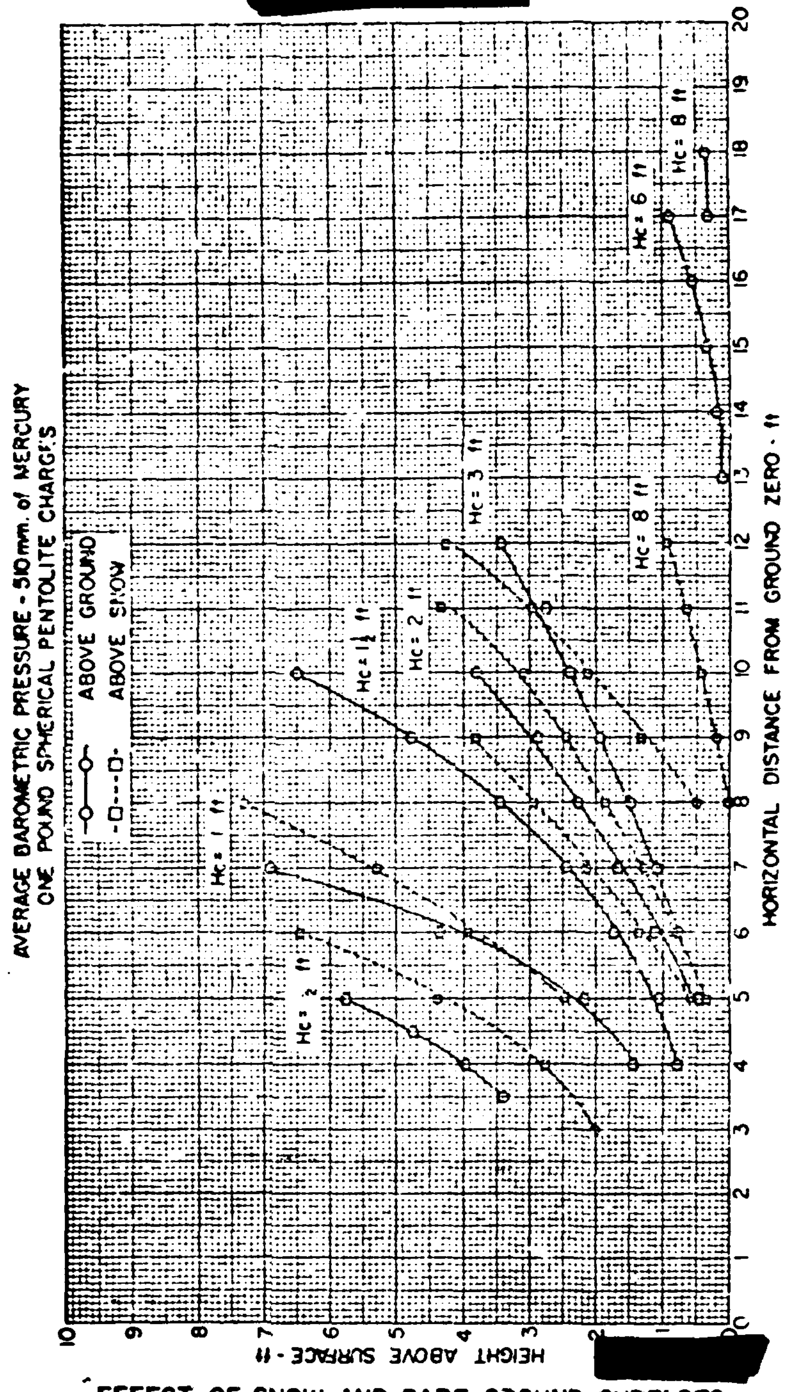

[redacted]

EFFECT OF SNOW AND BARE GROUND SURFACES ON PATH OF THE TRIPLE-POINT

[redacted] FIGURE 2-14. (Wisotski and Snyer, 1966)

[redacted]

[redacted]

[redacted] 2 ft are not definitive and may not follow this trend. Data on the ground range at which the triple point forms are incomplete; so, no comparison is possible for the snow-covered and bare ground tests.

[redacted] Finally, the DRI data are plotted on a height-of-burst (HOB) chart shown in Figure 2-15. The above-snow curves are supported with more data, and it is possible to be fairly confident as to the form of these curves. The bare-ground data are less extensive, but it is again evident that the snow reduces the distance at which a particular peak overpressure is observed. The magnitude of the distance reduction appears to increase as the overpressure level decreases. There is strong evidence of the over snow contours "pulling in" for the surface burst case (HOB = 0); this is consistent with the fact that a surface detonation over snow loses a large portion of its explosive energy to the snow which is close to the explosion.

[redacted] The Greenland HE series involved a large number of tests from about 1958 to the middle of the 1960s. A large number of WES and Cold Regions Research and Engineering Laboratory (CRREL) reports which were referred to previously were written to describe the results of the various tests. Included were tests over and under the deep snow on the Greenland ice cap, and over and under ice. Shock transmission through snow and ice were measured as well as a large number of cratering shots in snow and ice. A report never widely distributed summarizes these results (Smith, undated).

[redacted] The HOB related shots were primarily 32 and 256 pound charges with scaled heights of burst to 12 ft/lb$^{1/3}$. The instrumentation band width was too narrow to adequately resolve

[redacted]

[redacted]

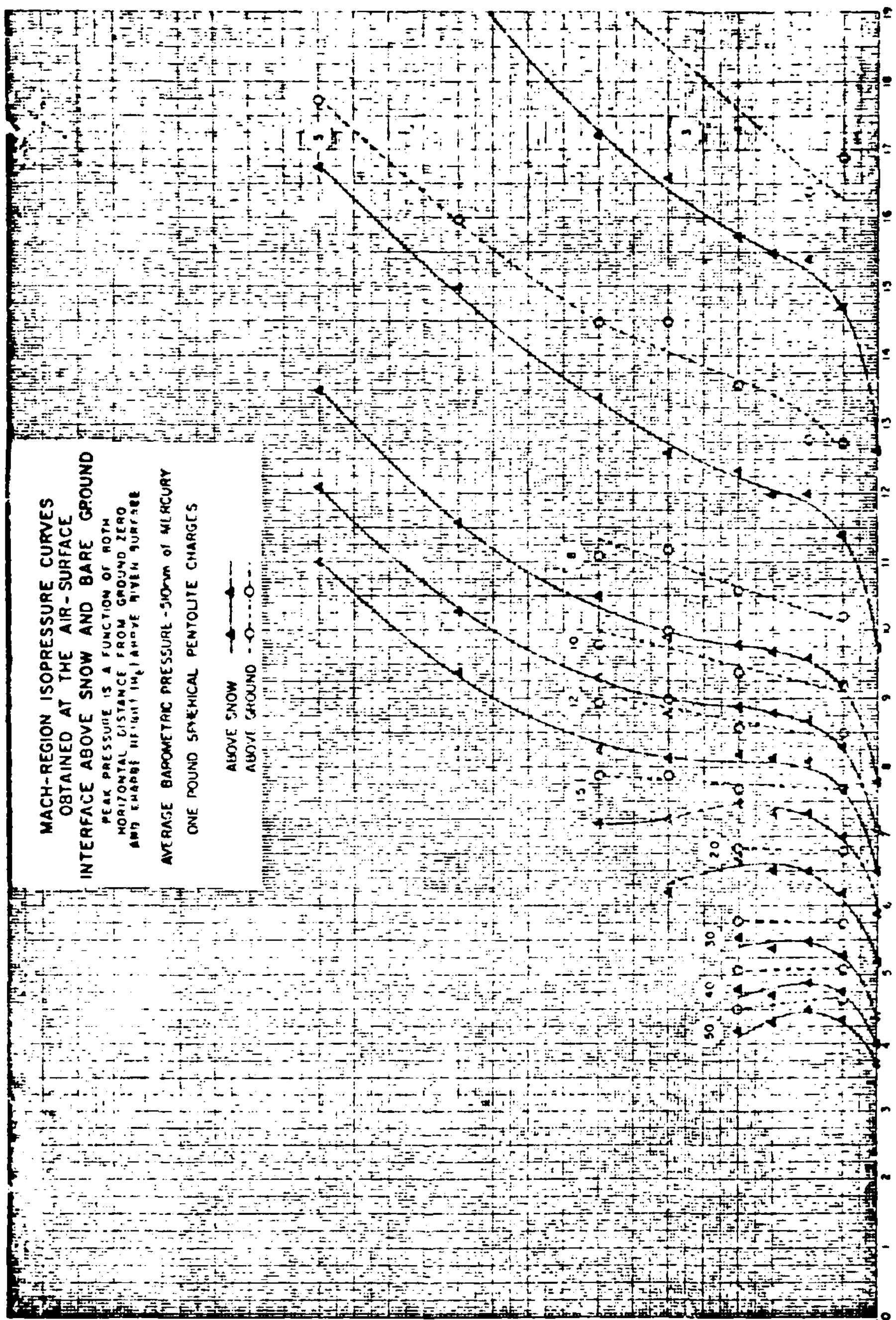

[redacted]

[redacted] FIGURE 2-15. (Wisotski and Snyer, 1966)

[redacted]

[redacted]

[redacted] the narrow pulses; so, as is the case with the DRI experiments, one must be very careful in comparing the WES data with other data. In this case, however, no comparison measurements were made over ground with the same instrumentation; so the comparisons are more uncertain than with the DRI measurements.

2.3.4 [redacted] Overpressure Contours from HOB Tests

[redacted] For the military planner, the air blast height-of-burst (HOB) charts are the most useful for prediction purposes. Since the Arctic environment data we have for air blast is from HE tests, we shall emphasize the HE HOB charts; also, maximum overpressure is the principal parameter we shall consider.

[redacted] A series of high explosive (HE) blast tests was conducted jointly by the U.S. Army Ballistic Research Laboratories (BRL) and the Canadian Defense Research Establishment Suffield (DRES) during the fall of 1969. These tests, held at the Watching Hill test range at DRES in Alberta, Canada, were known as the 1969 Height-of-Burst Series (Reisler et al, 1976 and 1969). Later, during the summer of 1975, another series of HOB tests was conducted by BRL as a part of the three-year DIPOLE WEST series (Reisler, 1975).

[redacted] Some of the results from these HOB tests are plotted in Figures 2-16 through 2-18, showing the peak overpressure contours for various overpressure values (Reisler, to be published). These data correspond to air blast wave propagation over bare ground under "near-ideal" conditions, which implies that there are no significant thermal effects.

[redacted] Looking at these figures, the plotted data and the solid-line contours correspond to the BRL tests referred to above. Additional curves are shown to correspond to data collected by other agencies on their tests using various HE

[redacted]

[redacted]

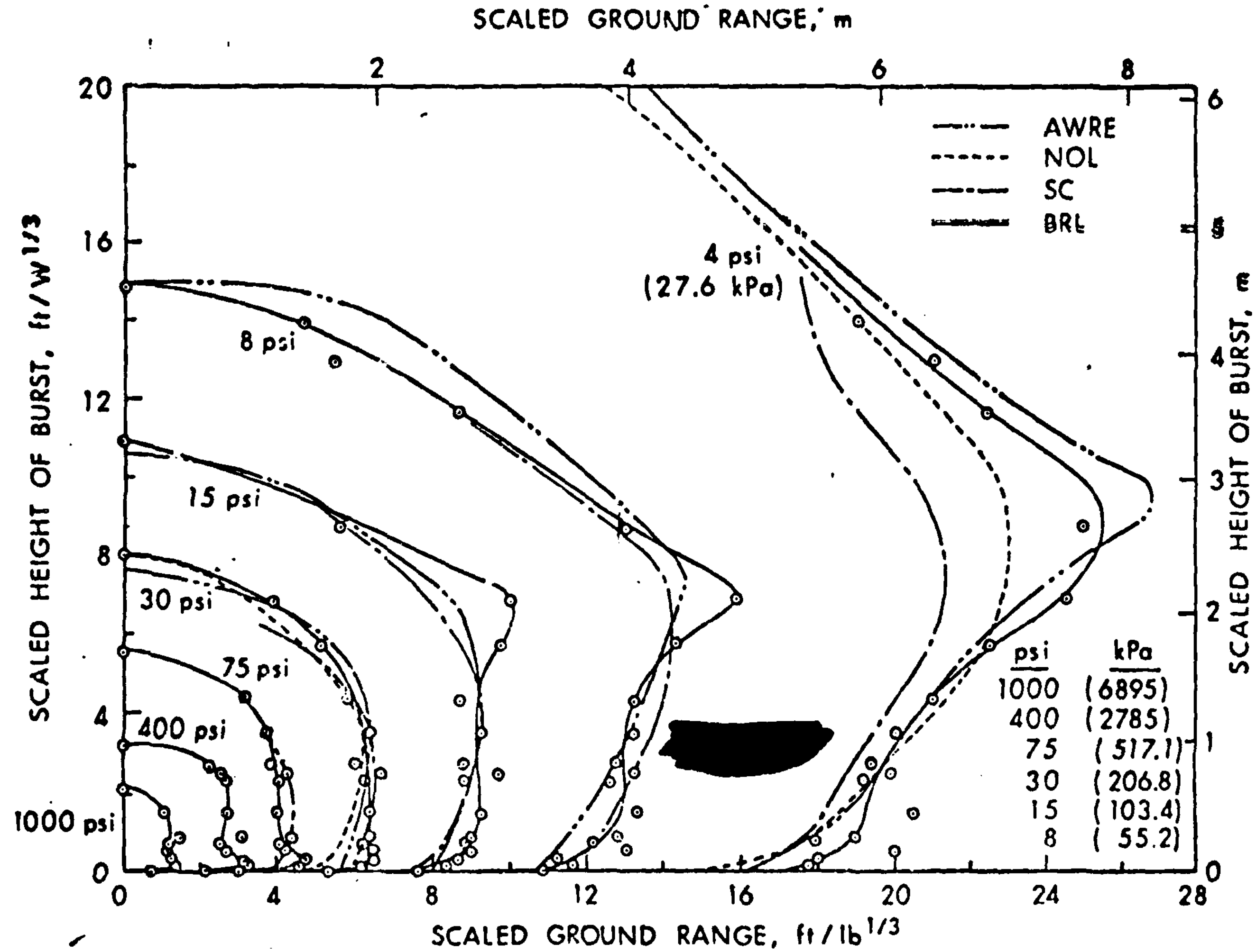

[redacted]IGURE 2-16. OVERPRESSURE HOB CURVES, 1000 - 4 PSI
(Reisler, to be published)

[redacted]

[redacted]

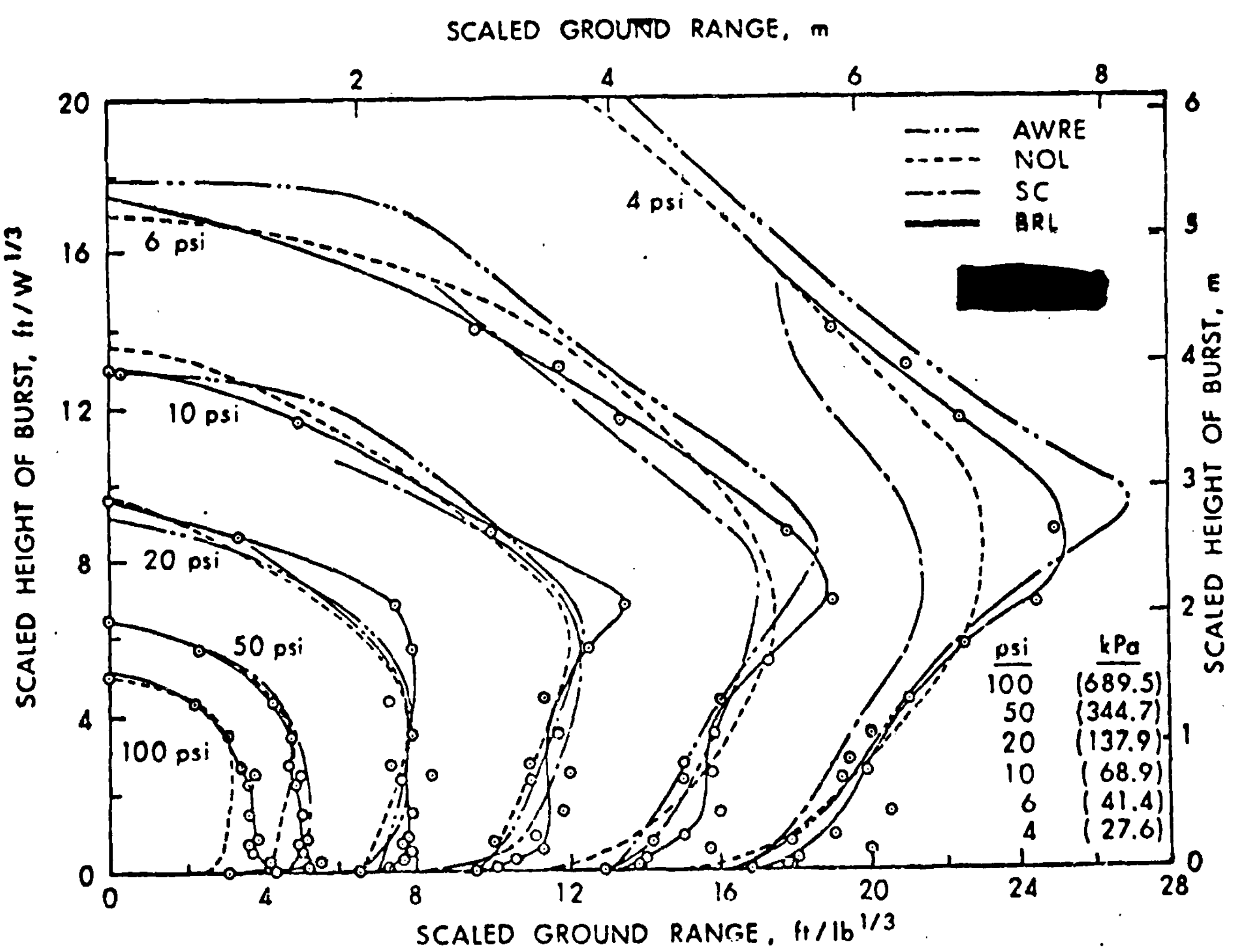

[redacted] FIGURE 2-17. OVERPRESSURE HOB CURVES, 100 - 4 PSI
(Riesler, to be published)

[redacted]

[redacted]

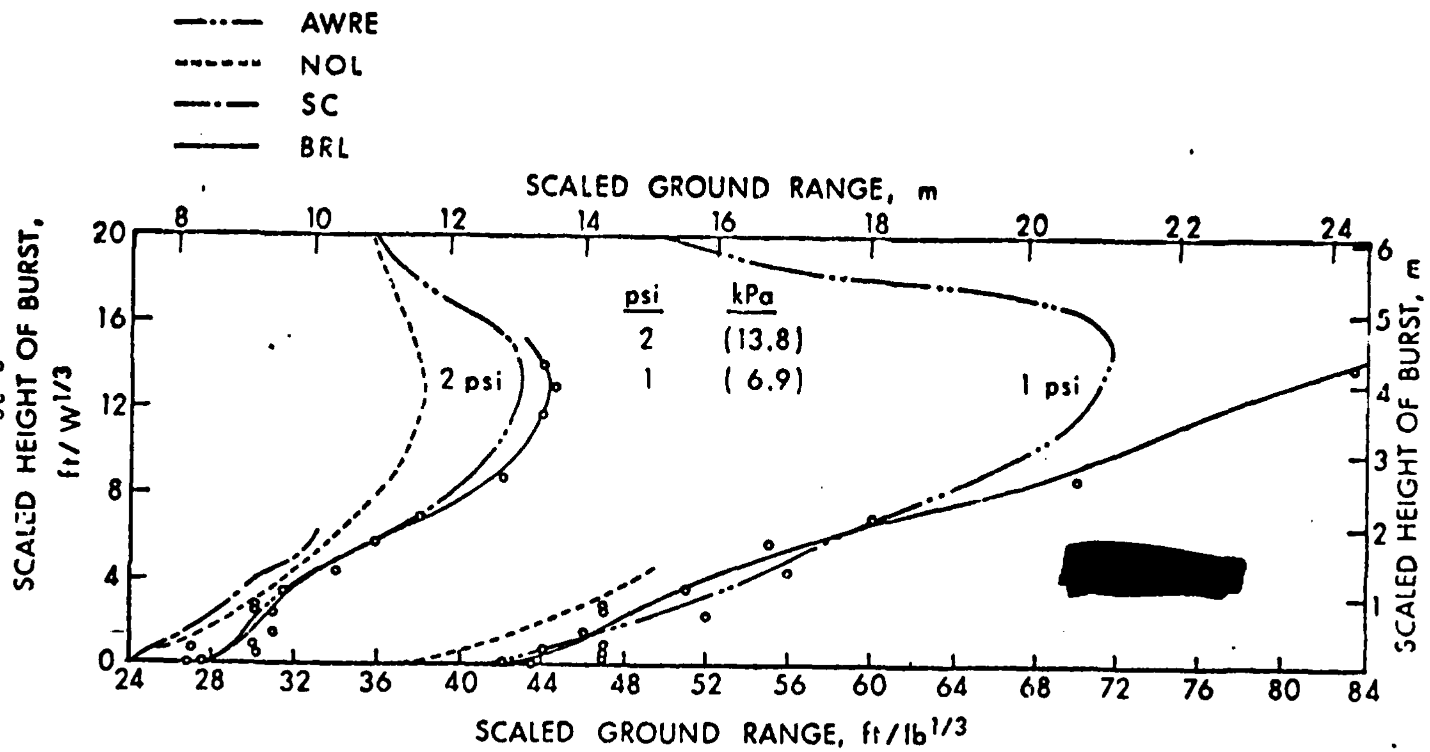

[redacted] FIGURE 2-18. OVERPRESSURE HOB CURVES, 2 and 1 PSI
(Reisler, to be published)

[redacted]

[redacted] charge sizes; tests were performed by Sandia Corporation (SC) (Vortman & Shreve, 1976), the Naval Ordnance Laboratory (NOL) (Hartman and Kalanski, 1952), and the Atomic Weapons Research Establishment (AWRE), United Kingdon (UK) (Worsfold, 1957 and 1963). The BRL contours indicate that there is some data scatter around the actual contour lines; as is usually the case, the data scatter is more pronounced for the lower overpressure contours. It is also significant to note that HOB data from other agency tests do not always agree with the BRL curves. In fact, for overpressures of 10 psi and lower, the deviations are significant. For comparison purposes, we shall use the BRL contours, but we should remember that an error band of ± 10% is estimated for the data.

[redacted] The data plotted on Figures 2-16 through 2-18 are "as read", and although they are scaled to 1 lb TNT, they are not scaled to sea level conditions. The atmospheric pressure at the test site varied from about 13.38 to 13.87 psi. The pressure scaling factor (S_p) for this test series varies from about 1.060 to 1.098. This means that the correction to sea level conditions would be between 6% and 10% for the data shown.

[redacted] Data from both the WES and DRI HE studies have been combined in Figures 2-19 and 2-20 to show how the data over snow compare with the BRL bare-ground HE data. It should be noted that the small-charge data have been Sachs-scaled to BRL average pressure P_o = 13.63 psi. As was discussed in some detail in Section 2.3.3, such data comparisons can be misleading, if taken too literally. This is because the WES and DRI data were obtained by using instruments with inadequate frequency response. Therefore, it is likely that a portion of the obvious displacements of the over-snow overpressure contours

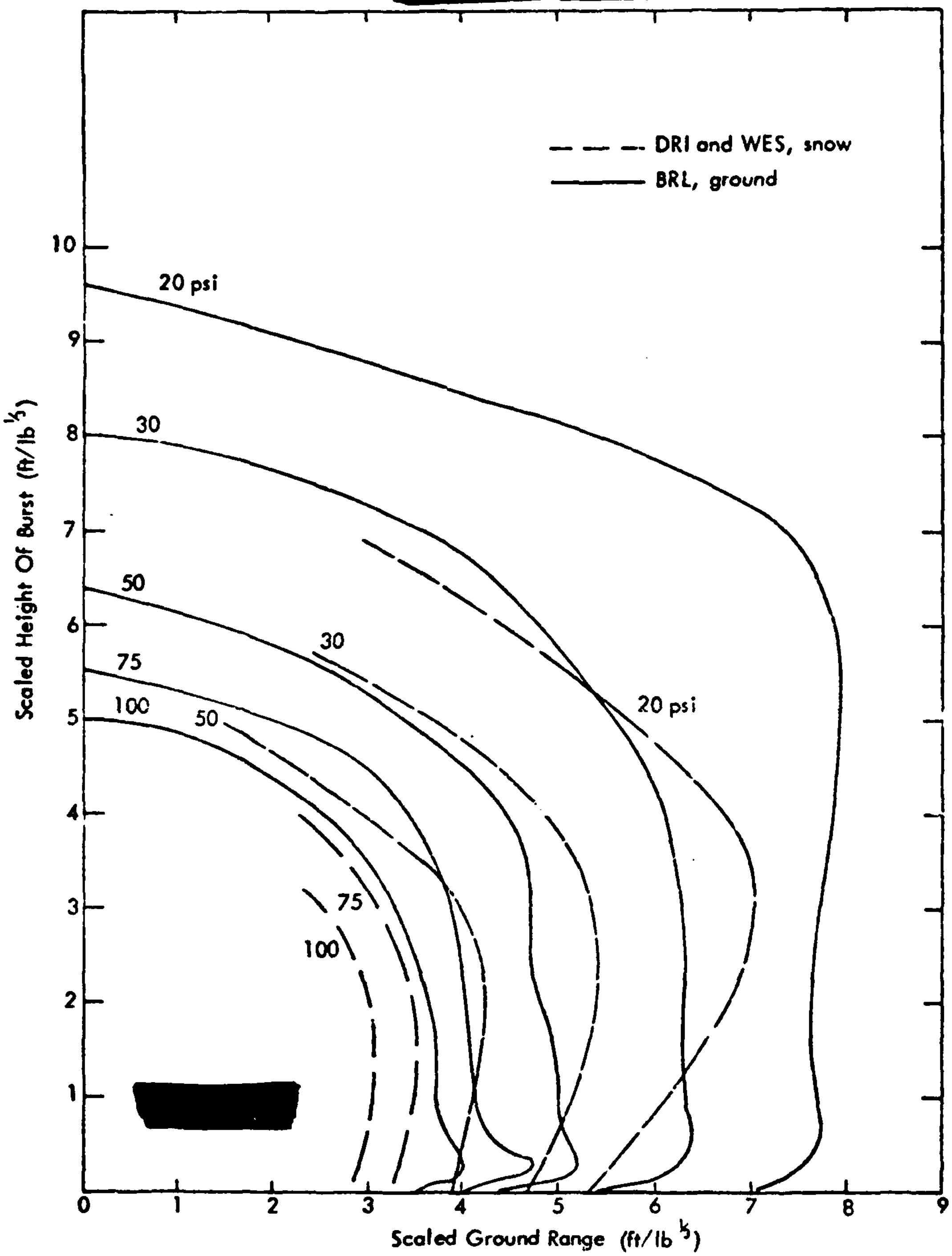

[redacted] FIGURE 2-19. COMPARISON OF OVERPRESSURE HOB CURVES - HIGH PRESSURE

[redacted]

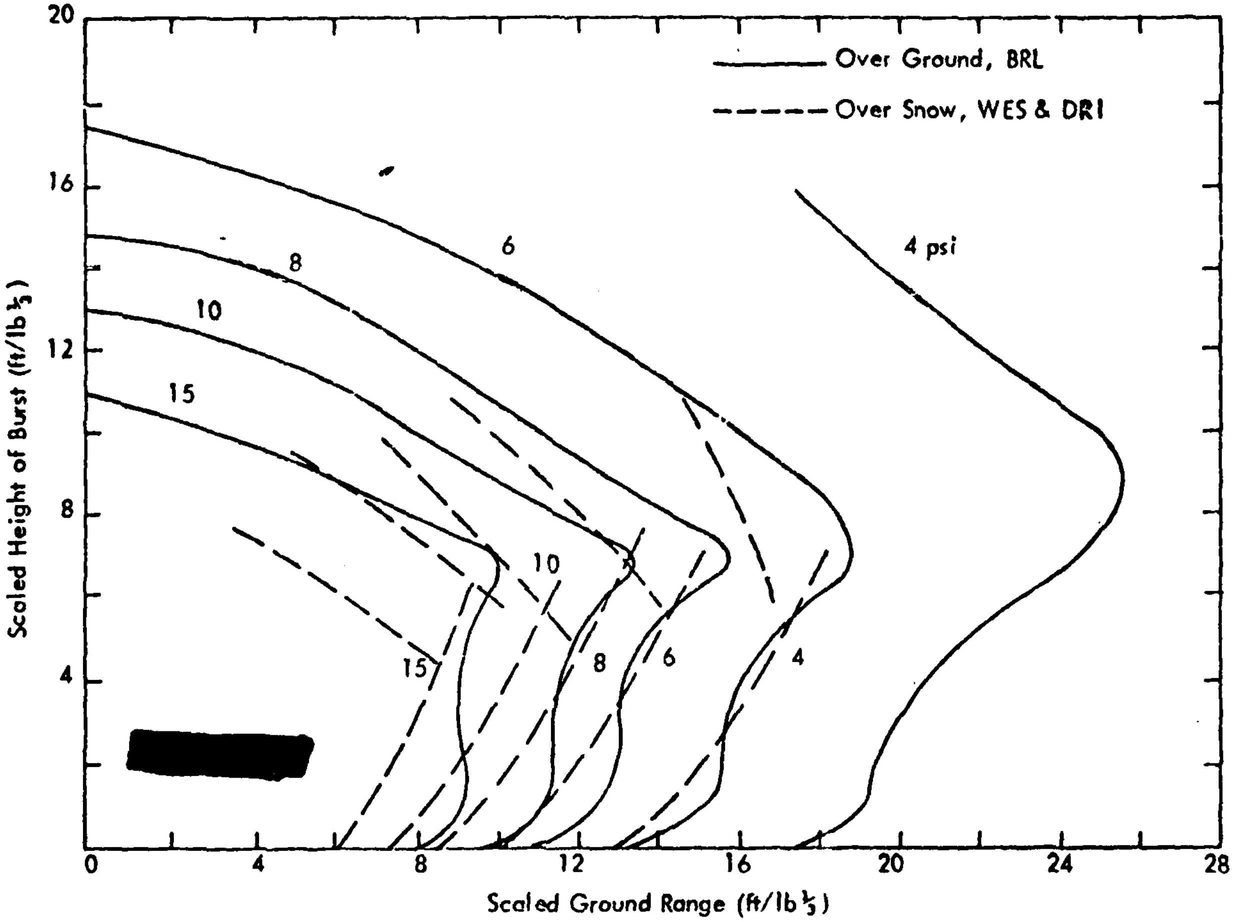

[redacted] FIGURE 2-20. COMPARISON OF OVERPRESSURE HOB CURVES - LOW PRESSURE

[redacted]

[redacted]

[redacted] from the bare ground contours is due to the limited bandwidths, and it is difficult to determine what portion of each displacement is "real". The conclusion is that there is an effect, shown qualitatively in Figures 2-19 and 2-20; however, to attempt to quantify that effect based on the data available, will probably lead to larger effects than actually exist.

2.3.5 [redacted] Yield Scaling of Snow Depth Effects

[redacted] The minimum snow depth on the various DRI HOB measurements over snow was about 6"/lb$^{1/3}$. If this snow depth is scaled to nuclear yields by the $W^{1/3}$ relation, then these HOB curves for a 1 kt would correspond to snow depths of at least sixty feet, which is much deeper than snow encountered in the Arctic except for the snow/ice depths found in the highly glaciated areas.

[redacted] The DISTANT PLAIN winter event snow depth of 4" is equivalent to a depth of about one foot when scaled for a kt. The typical snow depth can range up to 60 cm to 1 m near the end of the winter season over much of the Arctic region. Thus, we are left in a quandary. The HOB curves over deep snow show a marked drawing-in of the curves for surface bursts over deep snow with no dependence on snow depth, while the surface burst over shallow snow showed no effect or at most a questionable effect at high overpressures.

[redacted] There is no real reason to expect a priori that the standard $W^{1/3}$ scaling should be used when considering surface interaction effects due to the snow which is far from an ideal reflecting surface. For an ideal reflecting surface with no energy loss at the surface or for near-ideal situations where only minor effects are expected then the $W^{1/3}$ relation can be justified.

[redacted]

[redacted]

[redacted] Measurements of the response of snow to loading (Napadensky, 1964) indicate an elastic response at overpressures below 10 to 30 atmospheres depending on the snow type, then a crushing region where a large volume decrease occurs with small increases in pressure, then a region with relatively small volume decrease as the pressure increases to 150 atmospheres or so until the density of ice is approached. Thus, for pressures below the yield threshold no permanent deformation of the surface would result.

[redacted] The snow surface does not act like a rigid boundary even in this elastic region. In Figure 2-21 (Ingram, 1962) the magnitude of the reflected shock measured over a snow surface is compared with the theoretical value over a rigid surface for normally incident shock waves. The values of the incident shock are considerably less than the yield strength of snow. Note that the measured shock pressure is about 70% of the theoretical value and the difference seems to be increasing at the higher overpressures. No data were given for non-normal incident shock waves. These measurements were taken in Greenland with 100 foot snow depths; so extrapolation to shallow snow cases is uncertain. The DRI experiments involved snow depths as small as $6''/lb^{1/3}$. The reduction of the pressure over snow as compared to bare ground was about 11% averaged over all ground ranges and burst heights. The DRI bare ground values were less than the rigid surface values as indicated by Figure 2-13, where the reflection coefficient for ground is less than for concrete. No calculations are available to indicate the depth of snow required to induce these effects as a function of yield and specifically to indicate the magnitude of the effect expected for the nuclear case.

[redacted]

[redacted]

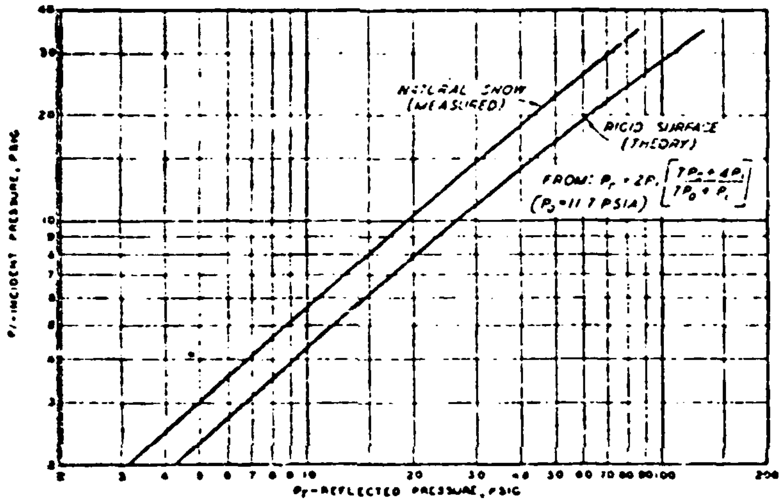

[redacted]

[redacted] FIGURE 2-21. REFLECTED VERSUS INCIDENT PRESSURE FOR NORMAL INCIDENCE (INGRAM, 1962).

[redacted]

[redacted] For incident pressures above the yield limit, PV work is done by the crushing process and energy is removed from available blast energy. Porzel (1962) gives $Q = 1/2(P-P_o)(V_o-V)$ as an estimate of the energy absorbed by an ideal absorber which will overestimate the energy absorbed. If we use P_o as 150 psi or about 10 atmospheres and (V_o-V) of 2 for compressing snow of density of about .3 g/cm^2 then we get the following estimate of the energy absorbed by a snow layer. The energy loss as a function of range is given by the expression

$$\Delta E = \int_{R_o}^{R} \frac{\Delta E}{\Delta m}\, dm = 2\pi D \int_{R_c}^{R} \frac{\Delta E}{\Delta m}\, r\, dr$$

$$\cong 1.04\times10^{2} D \int_{R_o}^{R} (P-P_o) r\, dr \qquad (2.6)$$

the integral can be evaluated from the 1 kt standard pressure radius curve. If the fractional energy loss is considered and if yields other than 1 kt are allowed we have

$$\frac{\Delta E}{W} = \frac{D}{W^{1/3}} \times \left\{1.04\times10^{-10} \int_{R_o/W^{1/3}}^{R/W^{1/3}} \Delta P \frac{r}{W^{1/3}} \frac{dr}{W^{1/3}}\right\} \qquad (2.7)$$

where D represents the snow loading in g/cm^2 and the ranges are in cm. The integral has been evaluated from R_o corresponding to the charge radius, and the expression in the braces is shown in Figure 2-22. Beyond the range corresponding to 150 psi the integral is zero; the value of the braces is essentially 7×10^{-4}.

[redacted]

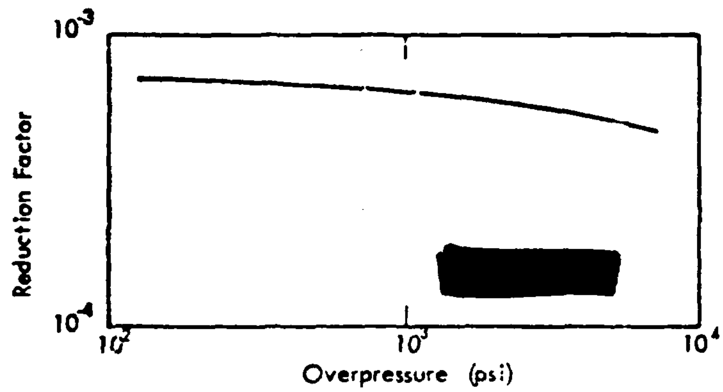

[redacted] FIGURE 2-22 ENERGY REDUCTION FACTOR DUE TO SNOW LAYER

[redacted] Thus, one might expect if the above assumptions are correct that the reduction in yield for overpressures below about 150 is given by

$$\frac{\Delta E}{W} = \frac{D}{W^{1/3}} \times 7\text{x}10^{-4} \ .$$

The ranges to these overpressure values might be given by scaling by the expression

$$R'(P) = (W - \Delta E)^{1/3} \, R_{1\ kt}(P) \tag{2.8}$$

rather than $R(P) = W^{1/3} \, R_{1\ kt}(P)$ (2.9)

so that $R'/R = (1 - \frac{\Delta E}{W})^{1/3}$. (2.10)

[redacted] Consider the HE charges over deep snow. The snow depth was at least 6" scaled to 1 pound charge. Therefore $D \cong 4.6$ g/cm^2 and $\Delta E/W \sim .4$. Therefore, $R'/R \sim (1 - .4)^{1/3} = .84$

[redacted]

[redacted] or a reduction in range of about 20%, which is of the order of the changes noted in the experiments. In practice one might expect that the ranges would be depressed more for stations closer to the ground and less at the higher altitudes, whereas the above estimate is an average reduction assuming that the blast wave is developing symmetrically from the burst point. Details of the interaction at the surface such as the effect of angle of incidence of the shock wave have been ignored.

[redacted] Recall that the experiment showed no effect of snow depth for snow depths considerably larger than the 6" scaled minimum. Making the same calculations for the 20 ton HE shot with a maximum snow depth of 4" or about 3 g/cm^2 gives $\Delta E/W \sim 7.7\times10^{-3}$ or essentially no reduction in yield and no reduction in the pressure-radius relations, confirming the experimental results.

[redacted] Note that the above relation does involve a $W^{1/3}$ scaling of snow depth. Extrapolating to the nuclear 1 kt case and a snow depth of 1 m or a loading of 30 g/cm^2 we obtain $\Delta E/W = .021$ or a negligible effect. The effect would be even smaller for larger nuclear yields. The above general agreement may, of course, be fortuitous and a thorough theoretical investigation of the subject considering the air shock interaction with the nonideal surface should be made.

2.3.6 [redacted] hermal Effects and Precursors

[redacted] Observations on the low-altitude nuclear weapons tests over bare ground show that at a thermal exposure level of 10-30 cal/cm^2 a popcorning effect occurs where particles of the soil are forcibly ejected into the air. This apparently occurs due to the very rapid heating and vaporization of the water entrained in the sand (or other) crystals in the soil.

[redacted]

[redacted] The ejected particles are heated and form a very efficient mechanism for heating the layer of air for a few feet above the surface. A similar effect occurs when rapid heating of organic materials takes place on the surface. The natural convective heat transfer will also be very high and will assist in heating the air layer. These types of effects are certainly strong enough to lead to the formation of a precursor wave.

[redacted] The precursor is characterized by a highly turbulent flow behind the wave front. Dense dust clouds raised by this turbulence tend to follow the shock front as it propagates outward.

[redacted] No empirical evidence is available to indicate the effect of the thermal and shock environment from a nuclear burst over snow. The following assumptions have been made in determining the effect of the thermal pulse on snow. First the energy is assumed to be deposited in the top centimeter of the snow layer. This thickness is arbitrary and the thermal energy is undoubtedly transmitted deeper than this in new light snow and to shallower depths for old packed snow. The actual depth is not critical; however, the point is that very high temperatures that would be obtained by assuming the energy to be deposited in a very thin surface layer are not realistic. Secondly, it is assumed that any melted snow is not heated above the melting point because of the very high conductivity of the slush that will result from surface melting. This means that the energy contained in the thermal pulse will result in melting the maximum depth of snow possible instead of raising the temperature of the melted snow. Of course, if the snow melts completely, the temperature of the surface may begin to increase above 0°C.

[redacted]

[redacted]

[redacted] The characteristics of snow cover a wide range. The reflectivity can vary from .5 to .9, depending upon the condition of the surface so that the absorptivity may vary from .5 to .1. Fresh snow, then, will require about .9 cal/cm^2 deposited to reach the temperature of 0°C and another 8.1 cal/cm^2 to melt each centimeter layer for a total of 9 cal/cm^2 for each centimeter of snow depth. Since only about .1 of the energy is absorbed, an incident exposure of about 90 cal/cm^2 will be required for each centimeter of depth. Assuming packed dirty surface conditions, the required exposure is about the same since the density and the absorptivity can increase about a factor of 5 each.

[redacted] The above estimates indicate that about 2700 cal/cm^2 would be needed to completely melt one foot of snow. No mechanism is available to transfer the energy to the air. This is far above the 30 cal/cm^2 of thermal energy that typically will produce popcorning and other surface effects which serve to transfer energy to the air layer. The conclusion from this discussion is that under most arctic environments, conditions will not be favorable for the formation of a precursor blast wave; that is, the thermal/air-blast interaction effects will be minimal. This conclusion may be substantiated by experimental measurements being performed presently in solar furnaces (Knasel, 1980).

2.3.7 [redacted] Influence of Snow and Water on Dynamic Pressures

[redacted] The air blast dynamic pressure is defined by the relation $1/2\ \delta\ V^2$, where δ is the density of the air behind the shock front and V is the particle velocity of the air. Experiment has shown that blast waves which are "loaded" with dust, e.g., precursor waves, can produce higher-than-expected damage to drag-sensitive targets.

[redacted]

[redacted]

[redacted] The explanation is that the dust picked up by the blast is accelerated to near shock-front velocities, and the increased average density of the air/dust combination results in enhanced pressures.

[redacted] It is expected that the same would be true to some extent for the Arctic environment; however, in this case the blast wave would be loaded with ice crystals and/or water particles. The net effect would be similar to the dust case with density and dynamic pressures increased. In order to determine the magnitude of these increases under various conditions, thorough investigation is needed; some data are available from blast waves propagating over water. Other useful information could be obtained from computer code results.

2.4 [redacted] Air Blast from Underwater Bursts

[redacted] The air shock resulting from an underwater burst has been measured on a few underwater nuclear bursts and several series of small charge conventional explosives tests.

2.4.1 [redacted] Comparison of HE and Nuclear Tests

[redacted] Chapter 7 of DASA 1200 gives analytical techniques for computing the air shock expected from underwater bursts for several DOB, which take into account the available empirical evidence. Prediction curves are given to show the expected air shock for a 1 kt nuclear burst for a wide range of DOB.

[redacted] A series of 5 ton HE tests were made (Pittman, 1970) to determine the air blast from underwater bursts and to correlate with the sparse nuclear data available. Very good correlation with the Baker and Umbrella nuclear data was obtained by using the water column or plume velocity as the scaling parameter for shallow bursts. No correlation of the air blast effects with cavitation closure was possible.

[redacted]

[redacted]

[redacted] NOL has a program to compute the airblast from underwater bursts by using two-dimensional hydrodynamic techniques, but results have not been released for publication (Lorenz, 1980). No calculations including the effects of an ice cover have been made or are planned.

2.4.2 [redacted] Effect of Ice Cover

[redacted] No experiments have been done to determine the effect of an ice cover on the air blast from a nuclear weapon. Consideration of the air blast production mechanisms described in DASA 1200 lead one to expect, if anything, a decrease in the air shock if an ice cover were present. It does not appear that an increase in the air blast due to an ice cover could occur for equivalent DOB as compared with an underwater burst.

[redacted] Contribution to air blast arise from three different mechanisms, the relative importance of which depends upon the DOB. The initial air pulse results from the transmission of the water shock across the interface, another contribution arises from the spray dome, and the third from the plume.

[redacted] The direct transmission of the water shock into the air is the dominant mechanism only for depths below about 700 $W^{1/4}$ feet where the spray dome and plume effects are minimal. In this region the water pressures are low enough that acoustic theory can be used to provide an estimate of the coupling at the interface. DASA 1200 explains several techniques of varying complexity to describe the energy transfer across the interface and propagation into the air. The expected air shocks are very weak ($\leq$ 1 psi).

[redacted] Replacement of a layer of water with ice at the surface would result in a decrease in the coupling efficiency because of the introduction of a second interface where mis-

[redacted]

[redacted]

[redacted] matching and energy loss can occur. Using the values of the ice, water, and air acoustic characteristics given in Section 1.2, we can estimate the size of the effect as follows:

[redacted] The overpressure in the air is given by the expression

$$\frac{\Delta P_a}{\Delta P_w} = \frac{2\ P_a\ C_a \cos\ \phi_w}{P_a\ C_a \cos\ \phi_w + P_w\ C_u \cos\ \phi_a} \qquad (2.11)$$

where a and w subscripts refer to air and water values of the parameters, P is the density, C is the sound speed and ϕ is the angle from the normal to the wave front. The angles are related by Snell's law:

$$\frac{\sin\ \phi_a}{\sin\ \phi_w} = \frac{C_a}{C_w}\ . \qquad (2.12)$$

For simplicity consider normal incidence, then substitute values for parameters and we have $\Delta P_a/\Delta P_w = 5.6 \times 10^{-4}$ which indicates the reason why such small air blast occurs with deep bursts.

[redacted] If we have an ice layer between the water and air then we have

$$\frac{\Delta P_a}{\Delta P_w} \cong \frac{\Delta P_a}{\Delta P_i}\,\frac{\Delta P_i}{\Delta P_w} \cong \frac{2x428}{2.95x10^6} \times \frac{2*2.95x10^6}{1.54x10^6+2.95x10^6} = 3.8x10^{-4}. \qquad (2.13)$$

Therefore the effect of the ice layer is to reduce the air blast pressure by about 1/3.

[redacted] The spray dome results when the water shock pressure is strong enough when it reaches the surface that the resultant tension in the water from the combination of the reflected tensile wave and the incident compression wave exceeds the tensile strength of water. This results in cavitation and the separation of a layer of water from the surface with some imparted upward momentum. The spray dome then produces an air shock which can be predicted by the techniques noted in DASA 1200.

[redacted]

[redacted]

[redacted] Introduction of an ice layer for an equivalent layer of water on the surface would obviously cause changes in spray dome development. The pressure pulse transferred to the ice and reflecting as a tensile pulse at the upper ice surface could lead to ejection of a layer of ice whenever the tensile strength of ice is exceeded. Since the tensile strength of ice is much larger than that of water, this will occur only for much larger values of water shock pressures than are needed for spray dome development. This probably will imply a smaller value of air shock than produced from the spray dome. If the tensile strength of the ice is not exceeded, no air shock from this type of mechanism would be expected.

[redacted] The plume or water column is the dominant air blast mechanism when the DOB is less than about $75W^{1/3}$ ft. The plume is treated as a supersonic body moving through the air, and the air shock is computed as described in DASA 1200 by standard hydrodynamic considerations of the bow shock from a blunt body. At the depths where this mechanism is important the water shock pressures are so large ($>10^4$ psi) that a considerable thickness of ice would be shattered. If the entire thickness were shattered, the effect of the ice on plume development would probably be similar to an increased DOB equivalent to the ice thickness. If the ice layer were not completely shattered, then some of the energy of the plume would be expended in breaking up the ice layer and the air blast would be expected to be less.

[redacted] In the above considerations, the effect of the ice cover, if any, would reduce the magnitude of the air blast. It is not expected that more detailed calculations involving hydrodynamic considerations would change these qualitative conclusions. Detailed calculations would be necessary to determine safe escape ranges for aircraft delivering for instance an ice penetrating ASW nuclear burst.

[redacted]

[redacted]

2.5 [redacted] Energy Coupling to the Surface from a Low Altitude Burst

[redacted] The coupling of energy into the surface from a low altitude burst is obviously very intimately connected to the cratering problem which is considered in Section 3 and also is related to the air blast HOB curves which are considered in Section 2.3.

2.5.1 [redacted] Ground Coupling Effects

[redacted] Two cases are of interest involving a snow-ice-ground configuration. In the first the burst occurs above the snow layer so that the shock must traverse the snow layer to reach the underlying ground or structure. In the other case a burst occurs below the snow layer as might happen with an impact fuze which is not actuated by the less dense snow layer. In the first case the snow layer will act as an attenuating medium and will reduce the energy transferred to the underlying medium. In the second case a tamping action might occur and an increase in energy coupled into the underlying material may occur.

[redacted] Both the WES and DRI HE test series included shots in snow with an attempt to measure shock wave parameters in the snow as well as the movement of the snow (acceleration, velocity and displacement). A common problem of these measurements was a very large scatter in the data as evidenced in Figure 2-23 (Wisotski, 1966) and Figure 2-24 which shows the bounds for the data points for shock measurements in ice and snow (Ingram, 1960). The long dashed lines in Figure 2-23 are the limit lines for the snow data from Figure 2-24. The two sets of data are seen to be in essential agreement and suffer from the same order of uncertainty. The source of the data uncertainties include possible quenching of the charge by the snow surrounding the charge and the difficulty of getting good coupling between snow and the gages since snow is a mixture of air and suspended ice crystals.

[redacted]

[redacted]

PEAK PRESSURE AS A FUNCTION OF BOTH HORIZONTAL DISTANCE FROM GROUND ZERO AND CHARGE DEPTH IN SNOW LAYER

MEASUREMENTS TAKEN AT MID-DEPTH OF SNOW LAYER

AVERAGE BAROMETRIC PRESSURE - 510mm of MERCURY
ONE POUND SPHERICAL PENTOLITE CHARGES

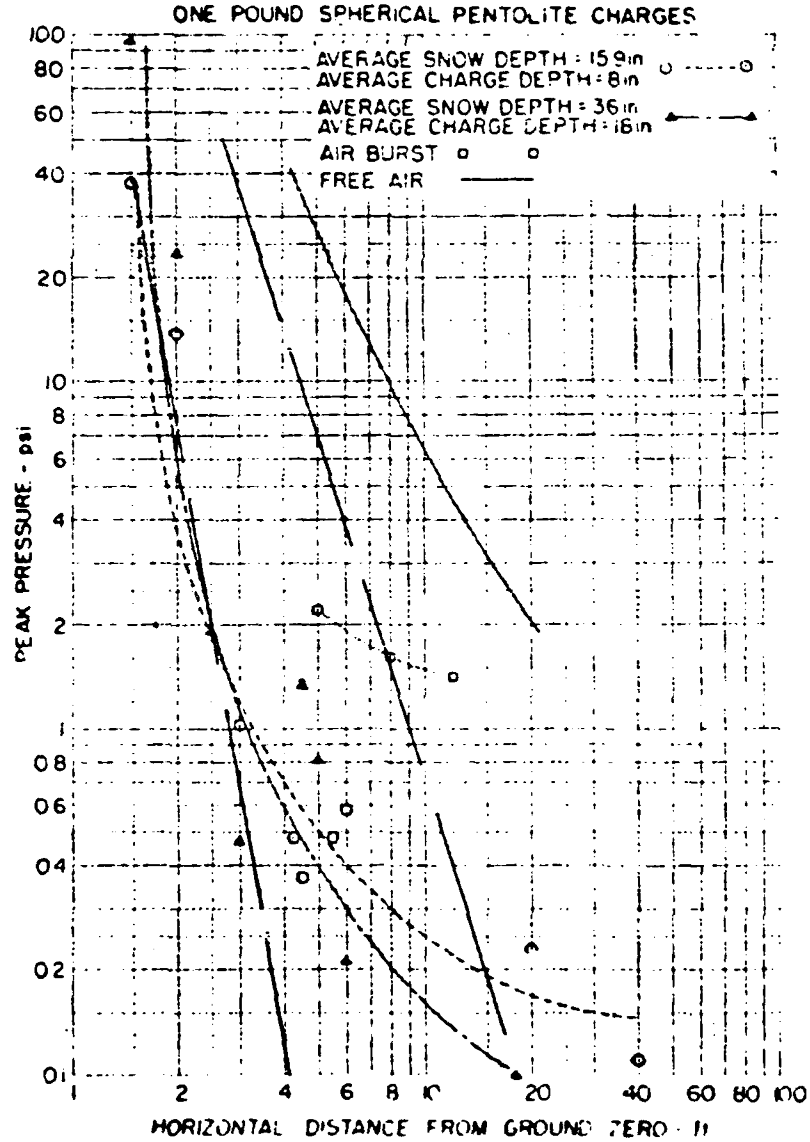

[redacted] FIGURE 2-23 [redacted]

2-55

[redacted]

[redacted]

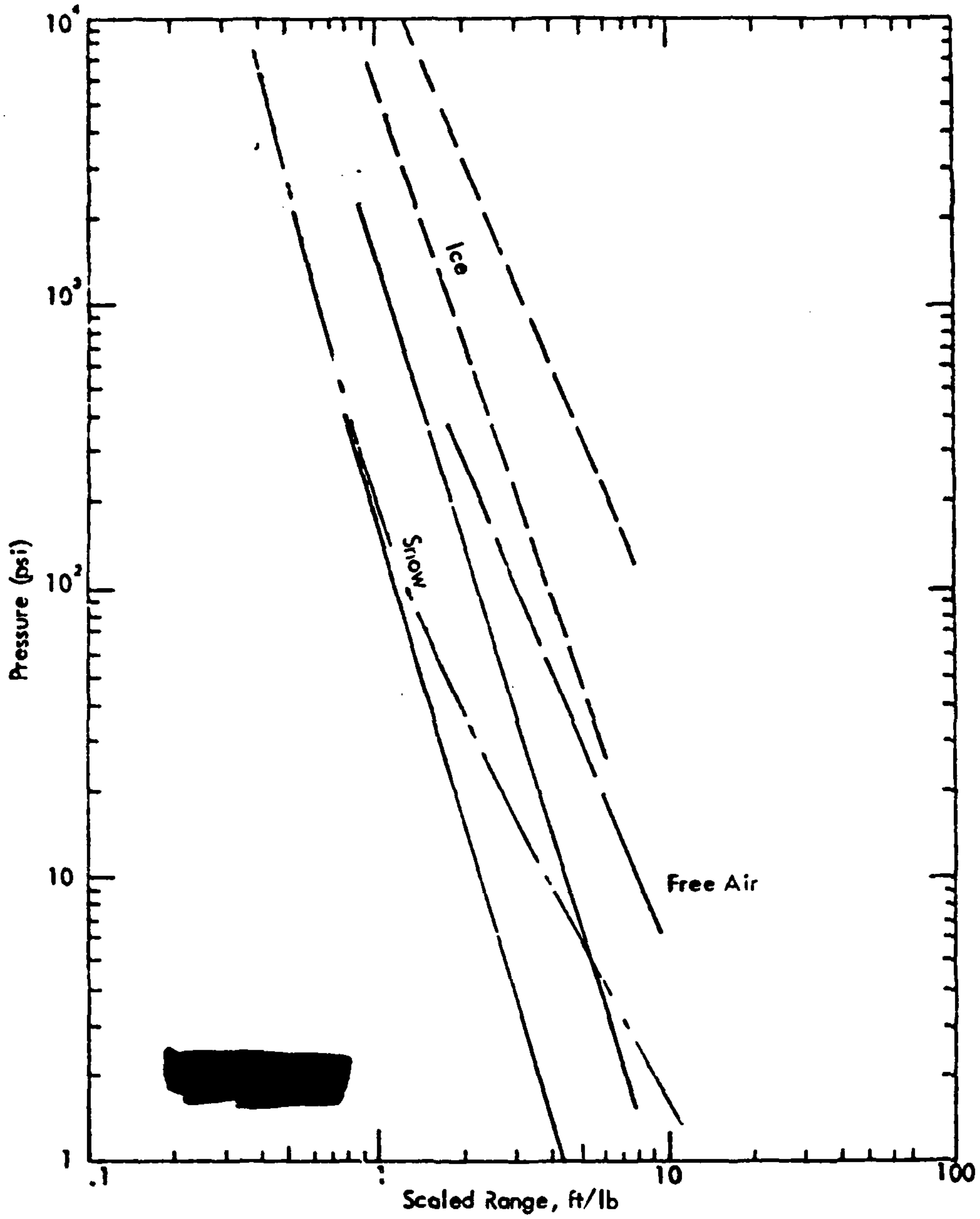

[redacted] FIGURE 2-24

PRESSURE IN ICE AND SNOW FROM HE EXPLOSION

[redacted]

[redacted]

[redacted] The slope of the snow curve is much steeper than that of air showing that more attenuation of shock energy is taking place. A decay of pressure as $R^{-3.8}$ has been suggested (Smith, undated) as being a reasonable fit of the snow shock measurements. The DRI measurements at pressures less than 1 psi show a marked reduction of the slope, but the curves drawn to represent the data are very subjective.

[redacted] Note that for pressures well under the yield limit there is appreciable attenuation of blast energy. Calculations of the attenuation of blast energy by precipitation referred to in Section 2.2.4 considered energy transferred to water droplets and resulting in vaporization of the suspended water for overpressures as low as 13 psi. The cutoff pressure was assumed to be a function of water droplet size but independent of water concentration. However, the highest concentration considered was about 5% by weight. Scaling of these results to a snow density of .3 g/cm^3 results in attenuations much larger than noted in Figures 2-23 and 2-24. Friedberg considered evaporation of the water requiring about 700 cal/g. It is possible that the shocks in snow involve melting of the snow, which would require about 80 cal/g and which might occur at lower overpressures since smaller temperature rises are involved. Then, however, one should ask why the shock in ice shows no indication of attenuation. If the energies involved are large enough to involve phase change effects then an attenuation in ice shocks would be expected.

[redacted] If we assume attenuation is due to energy lost in crushing the snow, then the effect can be estimated by using the same general procedure as in Section 2.3.4. The energy lost up to a range R is given by

$$\Delta E = \int_{R_o}^{R} \frac{\Delta t}{\Delta m}\, dm = 4\pi\rho \int_{R_o}^{R} \frac{\Delta E}{\Delta m}\, r^2 dr = 2.073\times10^{-2}\rho \int_{R_o}^{R} \Delta P r^2 dr. \quad (2.14)$$

[redacted]

[redacted]

[redacted] For a particular yield W (kt) we have

$$\frac{\Delta E}{W} = 2.073\times 10^{-2}\ \rho \int_{R_o/W^{1/3}}^{R/W^{1/3}} \Delta P(r/W^{1/3})^2\ d(r/W^{1/3}) \qquad (2.15)$$

where ΔP is the overpressure minus the yield strength. If the above expression is evaluated for a 1 pound charge, then the dash-dot line in Figure 2-24 is obtained. The shock falls progressively lower than the free air curve until the assumed yield strength of 140 psi or about 10 atmospheres is reached then parallels the free air curve. This is of course only a very crude estimate of the effect, but again it is interesting that it is in the range expected.

[redacted] In the nuclear case we do not have a burst in a large amount of snow, but are interested in the attenuation of the blast wave crossing a depth of snow of order of a meter or less in thickness. The above calculation shows that the energy losses in a spherical case scales as $W^{1/3}$. This would imply distances about 126 times larger for 1 kt than for the 1 pound HE charges and would indicate that the snow depths normally encountered in the Arctic would have essentially no effect on the coupling.

[redacted]

[redacted]

[redacted] This is to be expected if the shock energy density is considered. A one thousand psi shock wave has an areal energy density of about 5×10^4 cal/cm^2. The energy loss per gram of snow is $1.65 \times 10^{-3}\ \Delta p$ or 1.65 cal/g for 1000 psi. Since the snow loading is of order 30 g/cm^2 at most, the energy loss is insignificant. Of course we are assuming that no PV work is done for pressures below the yield strength so the attenuation to low pressure blast waves would be zero. This does not agree with the experiments which do show attenuation as compared with the air curve. The stress-strain curves of Napadensky may not be accurate at low overpressures and there may be no well defined yield point as he measured. Unconsolidated snow would be expected to have a very low yield strength. At the present time a quantitative measure of the protection of the snow layer is not possible but the effect is expected to be small for typical Arctic snow depths for nuclear yields.

[redacted] The possible tamping action of snow if a burst is detonated below the snow layer has been considered by Science, Systems & Software (Allen, et al, 1975). In Figure 2-25 the results are shown for a snow depth of 6 g/cm^2. At 6 μsec there is about a 15% enhancement of energy coupled to the ground and the energy in the air is somewhat less for the snow case as would be expected. The calculations were not carried out to later times but the difference might well disappear by later times. However, note that the snow loading is considerably less than the 30 g/cm^2 that can be present in the Arctic. A larger coupling efficiency might be found at lower yields. In practice, the snow layer above the burst would be perturbed which would tend to reduce the tamping effect. A sample calculation with deeper snow should be made to later times to determine the magnitude of this effect even though a large effect is not expected.

Page 2-60 was deleted

[redacted]

[redacted]

2.5.2 [redacted] Water Coupling Effects

[redacted] The coupling of energy from a low altitude or surface burst has been considered experimentally as well as theoretically. However, there is not a large amount of data in this area and certainly none that considers the complications due to an ice layer. For low altitude bursts where the coupling of the air blast into the water is of interest, one would expect the presence of the ice cover to decrease the shock transmitted into the water because there are two surfaces with impedance missmatches instead of only one.

[redacted] For near surface bursts where there is interaction of the weapon outputs with the surface, the situation is much more complicated. There were several nuclear weapon tests involving very small heights of burst over sea water in the Pacific. However, the weapons were mounted on barges in the tests. The area covered by the barge was large enough to have a strong effect on the coupling to the sea water. For this reason, any underwater shock measurements in these tests would probably be different than for a burst directly over the water.

[redacted] Systems, Science and Software has performed a series of calculations to determine the early time coupling of energy from a 1 MT burst to various surfaces. The coupling of energy to sea water was compared to that with NTS Tuff (Allen, et al 1974). At very early times the energy in the sea water is about 50% higher than that in Tuff. The calculations did not continue to late times to consider the underwater shock formation and growth. The increase in coupling was due to the lower opacity of sea water as compared to soil. The presence of salts in sea water does affect the opacity. The salinity of sea ice is less than sea water but is highly variable depending on the ice history. Because of the vast energy available and the high temperatures that are reached, one would

[redacted]

[redacted]

[redacted] expect the ice calculations to be very similar to the water calcultions. Radiation-hydrodynamic calculations of the subseqent shock development would be necessary to determine the effectiveness of this method of coupling energy into the water pressure pulse as compared to an underwater burst.

[redacted] The presence of snow cover on the ice canopy could affect the coupling of energy to the ice then into the water as discussed in Section 2.5.1. The magnitude of the tamping action versus snow depth and yield is unknown. This effect could have implications in ASW. If a technique for locating Soviet submarines under the ice is developed, then the necessity of using an ice penetration weapon must be addressed. In this case the coupling efficiency for the various ice surface configurations will be of great interest.

[redacted]

Page 2-63 was deleted

[redacted]

[redacted]

[redacted] There is much uncertainty connected with the underwater shock from near surface nuclear bursts even if the ice cover is not present. A large dependence on the details of the surface configuration may exist even for the late time air and water shocks. In the past there has been little incentive for work in this area. Increased Soviet use of patrols and the current nonavailability of ASW techniques for the polar area may result in an interest in these problems. In order to develop effective airborne tactical nuclear ASW techniques it will be necessary to consider the surface effects on underwater shock.

2.6 [redacted] Air Blast Target Damage Effects

[redacted] The two most important environmental effects on targets or target response in the Arctic are the snow cover on targets and the temperature of the materials used to build the targets. A possible effect is an increase in dynamic pressure due to snow loading of the shock wave.

2.6.1 [redacted] Snow Cover on Targets

[redacted] It is a fact of life in the Arctic that target structures, even those built above ground, will be covered with a layer of snow and/or ice. In fact, most structures designed for arctic use are built to take the most advantage of this cover layer. Snow cover over surface or buried structures affords protection to the structures because it attenuates the air blast load transmitted to the structure. Air-blast-induced accelerations in a snow layer from detonations above the surface attenuate rapidly with depth. Peak vertical downward accelerations at 2 feet below the snow surface are 3 or 4 times greater than those at 5 feet. Much of the air blast energy is absorbed in compacting the snow layer.

[redacted] For structures and equipment above ground, the most effective snow cover protection is afforded by a snow berm over the top of the structure. This berm eliminates any corners

[redacted]

[redacted]

[redacted] or vertical walls and presents a smooth aerodynamic surface to the air blast wave; this has the advantage of preventing large reflected pressure loading of the structure. Also, as the snow berm becomes somewhat compacted, it can contribute to the overall structural strength of the target.

[redacted] For underground (or undersnow) structures and equipment, the snow cover, in addition to providing attenuation of the shock loading, again contributes to the structural strength. This strength contribution can be traced to the "bridging" effect of the snow arch over the buried structure. In a sense, this snow arch acts as an additional structural member when a load is applied.

[redacted] The protection afforded by the snow cover is, of course, a functi... of the geometry of the snow cover in relation to the construction of the target in question and is dependent on the properties (density, moisture/ice content, etc.) of the snow cover vs depth. Therefore, it is not possible to present useful generalized predictions of the effectiveness of snow cover protection; each case must be considered individually.

[redacted] During the Greenland HE test series, the resistance of snow arches was considered (Smith). A summary of the results obtained is shown in Figure 2-27. As one would expect, the damage level depends primarily on the ratio of arch span to the crown thickness. A strong word of caution is necessary because these were HE tests, and the width of the pressure pulse is much less than would be experienced from nuclear tests at the same overpressure levels. No calculations have been made predicting the magnitude of this effect.

[redacted]

[redacted]

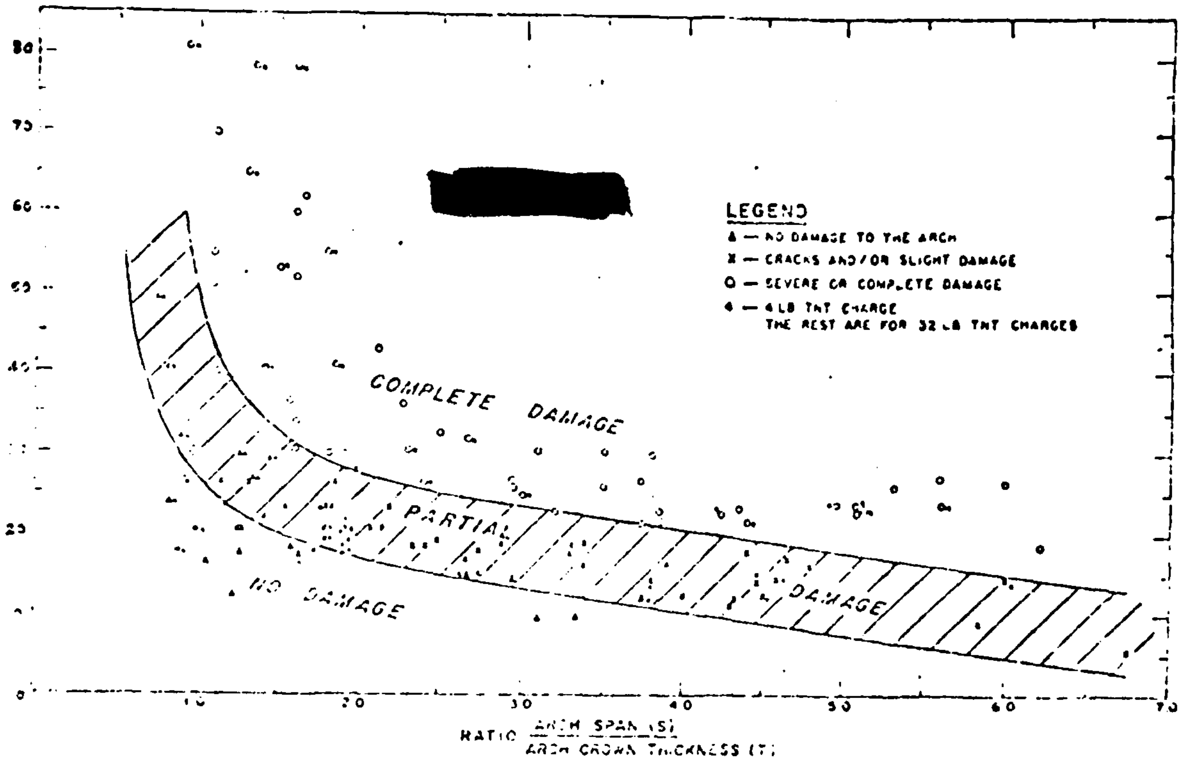

[redacted] Figure 2-27. Summary of data for damage to model snow arches. Real arches withstood considerably higher overpressures than the model arches. (From Szostak and Benert, ref. 11) (Smith, undated)

[redacted]

[redacted]

2.6.2 [redacted] Effect of Target Temperature

[redacted] Those structural materials which are used on targets essentially the same in Arctic climates as they are elsewhere may react to cold in such a manner as to alter their vulnerability to nuclear effects. Specifically, metals, rubber, plastics, ceramics, and fabrics will undergo changes in their strength, elasticity, impact resistance, and other related characteristics. These changes will increase the susceptibility of the material to damage. Steel is an important material for military targets. The mechanical properties of steel vary with temperature in a non-uniform fashion. However, the most important effect of low temperatures on steel is to reduce its ductility. This property change can cause brittle fracture to occur in structures exposed to relatively small static loads. A significant reduction in impact resistance will also accompany a loss in ductility.

[redacted] During the series of HE tests conducted by WES on the Greenland ice cap, some military equipment was inadvertently exposed to air blast loading. However, during those tests, no measure of the loads and/or response of these targets was obtained. Thus, without any definitive data on the subject, we could only speculate on the quantitative effect of the reduced temperatures of the target materials with regard to damage criteria. This is a technical area which requires more thorough investigation.

2.6.3 [redacted] Enhanced Dynamic Pressure

[redacted] It has been speculated that air blast dynamic pressures in the Arctic would be "loaded" with ice crystals and/or particles for many situations of military interest. These waves impinging upon drag-sensitive targets could impose enhanced forces, which would result in more severe damage than one would predict for the unloaded waves.

[redacted]

[redacted]

[redacted] Virtually no pertinent data are available pertaining to this effect; before one could attempt to quantify the effect, a great deal of effort would be required to collect data and perform computer code calculations to check the data consistency.

2.7 [redacted] Conclusions and Recommendations

[redacted] In the previous sections the current status of knowledge of air blast and surface effects predictions under arctic conditions were considered including the free air blast parameters, precursor effects near the surface, the effects of precipitation, clouds and inversion layers, changes in the height-of-burst curves over shallow and deep snow, and surface coupling considerations including the attenuation or possible tamping effect of a snow layer and the effect of the snow/ice canopy on shock transmission accross the air-water interface. The uncertainties in the various subjects can be corrected by a recommended research program.

2.7.1 [redacted] Conclusions

[redacted] The cold temperatures in the Arctic cause a slight increase in the time of arrival, time duration and impulse expected from a free air burst. If one were considering the effect of attacking a specific impulse sensitive target in the coldest area of Siberia, the change might be worth including. The overpressure-radius and dynamic pressure-radius relations are unchanged since the atmospheric pressure and the variations in the Arctic are essentially the same as in temperate climates. In conclusion, the free air prediction values given in EM-1 are adequate for Arctic free air values, and scaling to arctic pressure and temperate values is not necessary.

[redacted] The attenuation of blast wave energy by precipitation, fogs, and clouds is considered in EM-1 and has been treated in later studies. The amount of precipitation and the precipitation rates in the Arctic are in general less than in most

[redacted]

[redacted]

[redacted] temperate areas. The fact that the precipitation will likely be snow will not increase the magnitude of the effect. Light rain and fogs reduce the effective blast yield of at most 10% even for large yields at overpressures as low as 1 psi. For most studies the attenuation could be ignored since it is very difficult to have accurate knowledge of precipitation patterns and rates.

[redacted] If a burst occurs below a temperature inversion refractive effects can cause a focusing action and increase the extent of blast effects along the ground for very small overpressures (<1 psi). If the burst occurs above the inversion layer, the opposite effect is noted. The high probability of strong inversion layers in the Arctic would lead to an enhancement of these effects noted in temperate climates. Since the effects are only noted at very small overpressures, the military effects of inversions could be important only for low overpressure targets. Inversion effects should definitely be considered in determining fail-safe ranges for HE testing. An experimental program concerning the effect of temperature inversions and wind on blast has recently been completed and a definitive report on this subject will be published during 1980. Calculations have been proposed to determine whether temperature inversion effects can occur for overpressure values as high as 1 psi.

[redacted] In EM-1 the recommendation is made to treat frozen ground, snow, and ice as thermally ideal surfaces and, therefore, not to expect any classical precursor effects as discussed in EM-1. This is a result of the very large amounts of energy required to produce water vapor and heat up a layer of air near the ground and the fact that these surfaces will

[redacted]

[redacted] usually have a large albedo implying absorption of a small fraction of the incident thermal energy. Experimental confirmation of this fact is expected in the very near future. Frozen soil, ice and snow samples will be exposed in the French solar furnace to determine their response to thermal loading and their capability of transferring heat to the near surface air layer.

[redacted] Even though snow is expected to be a thermally ideal surface, because of the strong attenuation in snow, significant reduction of air blast over snow has been measured for bursts over deep snow. Reductions in ranges of 25 - 40% to the overpressures less than 100 psi were noted in these experiments. Scaling the snow depths to nuclear yields would result in depths of about 50 ft/kt$^{1/3}$. Depths this deep would only be found in Greenland or other highly glaciated areas. However, the validity of scaling the snow depths with yield in this manner is very questionable. No theoretical work has been done in this area to determine exactly what interaction is occurring in the snow layer and to determine the proper scaling method.

[redacted] Comparisons have been made of the air blast from 20 ton surface shots over bare ground and with a snow depth of 4", which scales to 1.25 ft/kt$^{1/3}$. No change was noted in dynamic pressures on impulse. A possible reduction was noted in the overpressure over 600 psi over the snow. This difference was not explainable and could be due to data uncertainties.

[redacted] Thus, we have two sets of data, one with scaled snow depths of 50 ft/kt$^{1/3}$ where large differences were noted in the overpressure contours, and another with a scaled snow depth of 1.25 ft/kt$^{1/3}$ where no change was noted for a surface burst.

[redacted]

[redacted] The typical arctic snow depth will usually be less than 3' which is in the shallow scaled regime. However, there is no assurance that this type of scaling is valid.

[redacted] The presence of deep snow can affect the coupling of blast energy in two ways. In the first, if a low altitude air burst is used to attack a hardened structure either above or below the ground covered by a layer of snow, then one would expect a decrease in the blast energy coupled to the structure and a decrease in the damage. Large numbers of measurements of shock in snow from HE shots have been made. The scatter in the data range over an order of magnitude. The experimental uncertainties are large and involve an effect on the HE burning due to the snow and the difficulty of getting a good match between the snow and the measuring instruments. There have been experiments performed to measure the basic shock properties of snow and the data again show a very wide scatter depending on the state of the snow. No calculations of the attentuation to be expected from snow layers have been located. Theoretical predictions have been made that snow shock values are very similar to NTS Tuff. At the present time, no predictions on the attenuation properties can be made.

[redacted] In the second case, if a weapon were detonated below a snow layer (for example by having an impact fuze that does not actuate in snow) the tamping action of the snow because of the larger opacity as compared with air could result in a larger coupling of energy into the ground. Likewise, if a weapon were detonated on the surface of the snow, the decrease in opacity as compared to ground might result in a larger transfer of energy into the snow and ultimately into the ground than for a ground surface burst. A single calculation of the tamping effect showed

[redacted]

[redacted]

[redacted] about a 15% increase in the (6 μsec) ground coupling for a 1 MT burst under 6 g/cm^2 of snow. Considering that a typical Arctic case involves about 5 times this amount of snow, one might experience a significant increase in the ground coupling. However, until calculations are extended to later times, no predictions of the magnitude of the effect are possible.

[redacted] Both of these snow effects could have implications for attacking targets in northern USSR. In the first case, the snow may tend to decouple the air blast energy from the target and lead to less damage and attack effectiveness than expected. In the second case, the snow may enhance the damage and attack effectiveness. The second case may have implications in ASW also. Currently, one desires a burst at a sufficient DOB so that little energy is dissipated above the water surface to maximize the submarine damage range. This would require an ice penetrating weapon in the Arctic. However, because of the snow and/or ice tamping effect, it may be possible to fuze the weapon to go off under the surface of the snow or ice and enhance the coupling of energy to the water so that an under water burst may not be required.

2.7.2 [redacted] Recommendations

[redacted] Significant uncertainties which may be important for systems in the Arctic were found to exist in the following areas:

- The effects of precipitation, fogs, clouds and temperature inversions on the air blast
- HOB curves over snow for nuclear yields
- Effects of snow cover in altering the coupling of energy to the surface versus HOB/DOB
- Air blast from underwater bursts through an ice canopy.

[redacted]

[redacted]

[redacted] Note that all of the above items involve shock propagation through and interaction with lossy materials consisting of air mixed with quantities of water in various states (vapor, liquid or solid). No recent hydrodynamic calculations were found considering these materials. Resolution of uncertainties in all of the above areas could be obtained by a three part research program.

Preliminary Analytical and 1-Dimensional Hydrodynamic Calculations

[redacted] During this phase equation of state information should be collected on snow, ice and frozen ground materials. Analytical calculations using the developed theories of shock propagation through lossy materials should be made to determine the attenuation of shocks through these materials and to provide confirmation of hydrodynamic runs. A series of 1-d hydrodynamic calculations should be made addressing the attenuation of shocks in air-water mixtures and snow, the coupling of shocks from air to the ground and structures through various snow depths, and to compare the response of frozen grounds with rocks. These calculations might provide resolution of some of the uncertainties in the above areas and would provide guidance in setting up multidimensional hydrodynamics runs.

[redacted] Specifically the effects of precipitation, fog and clouds in causing attenuation to the air shock could be determined and compared with current calculations and predictions. The runs showing the coupling of air shock through various snow depths into the ground and structural materials will show the degree of protection provided by snow cover. These calculations should be done for various incident shock strengths to show the effect on both very hard targets such as silos (1000 - 2000 psi) as well as softer structures (<100 psi). The

[redacted]

[redacted]

[redacted] shock angle should be varied to see what effect this has on the coupling and air interaction process. This will provide guidance in the effect of the snow layer on the air blast and effects expected in HOB studies.

Two-dimensional Hydrodynamic Calculations

[redacted] The results of the phase 1 calculations would be used to determine what 2-d hydrodynamic runs are necessary to resolve the remaining uncertainties.

[redacted] A series of runs may be necessary to produce HOB curves over snow. The effect of the snow depth on the air blast may be yield dependent and it may be necessary to generate curves for more than one snow depth.

[redacted] Calculations of the shock transmitted to hard targets covered by a snow layer from a low altitude air burst may be necessary depending upon the results of the 1-d coupling and attenuation calculations.

[redacted] The tamping effect of a snow layer should be determined by repeating the calculations of S^3 for depths of snow representative of Arctic conditions. If a coupling significantly greater than 15% is noted at the early times, then the calculations should be carried to later times to determine the increase in the ground shock.

[redacted] The tamping effect for smaller yields representative of ASW weapons should be determined in a snow-ice-water geometry to determine if ice penetrating weapons would be required in attacking submarines beneath the ice.

[redacted]

[redacted]

[redacted] Depending on the results of the phase 1 calculations 2-d calculations of the air blast from underwater bursts with an ice canopy may be warranted. If ice under strong shocks loses its integrity then these calculations will not be necessary, and the ice can be treated as an increased equivalent water layer for air blast predictions.

Experimental Program

[redacted] During phases 1 and 2 of the program requirements for experiments to define the basic physical properties of snow, ice, and frozen ground can be determined. Information in this area exists, but in the ten years since these experiments were performed better techniques have been developed.

[redacted] Depending on the results of the computer calculations a series of HE tests in an Arctic environment may be warranted. The subjects of interest would be effect of depth of snow on air blast measurements at the surface and above the surface, effect of inversions, correlation if any between yield and depth of snow, effect of ice canopy on water and air shock from underwater bursts and coupling of airshock through the snow to the ground for a burst above the ground. Such a series should include static overpressure and dynamic pressure versus time measurements and have an instrumentation system with an adequate band width to resolve the narrow pulse widths.

[redacted]

[redacted]

[redacted].8 Bibliography

Allen, R. T., Bailey, L. E., and Schneyer, G. P., Energy Coupling for Near Surface Nuclear Explosions, DNA 3400F, Systems, Science, and Software, LaJolla, CA, November 1974, SECRET RD CNWDI.

Allen, R. T. and Baker, J. C., Energy Coupling with Sea Water, DNA 3550F, Systems, Science and Software, LaJolla, CA, 11 October 1974, SECRET RD.

Allen, R. T., et al, Energy Coupling for Near Surface Nuclear Bursts (U), DNA 3564F, Systems, Science and Software, LaJolla, CA, 2 April 1975, SECRET RD.

Carpenter, J. and Brode, H. L., Height of Burst Blast at High Overpressure, Paper, Fourth International Symposium, The Military Applications of Blast Simulation, September 1974, R & D Associates, Marina del Rey, California, UNCLASSIFIED.

Defense Atomic Support Agency, Nuclear Weapons Blast Phenomena (U), DASA 1200, Defense Nuclear Agency, Washington, D.C. 1 March 1971, SECRET RD.

Defense Nuclear Agency, Capabilities of Nuclear Weapons (U), DNA EM-1, Defense Nuclear Agency, Washington, D. C., 1 July 1972 (change 1, 1 July 1978), SECRET RD.

Friedberg, R., Weather Effects on Blast, NWEF-1138, Naval Weapons Evaluation Facility, Albuquerque, NM, July 1976, UNCLASSIFIED, AD-B012752L.

Hartman, G. K. and Kalanski, P. Z. The Optimum Height-of-Burst for High Explosives, NAVORD Report 2451, July 1952, Naval Ordnance Laboratory, White Oak, Maryland.

[redacted]

[redacted]

Ingram, L. F., Blast Effects on a Snow Tunnel, Camp Century, Greenland, WES MP 2-378, U. S. Army Engineer Waterways Experiment Station, Vicksburg, MS, February 1960, UNCLASSIFIED.

Ingram, L. F., Air Blast in an Arctic Environment, WES TR 2-597, U. S. Army Engineer Waterways Experiment Station, Vicksburg, MS, February 1962, UNCLASSIFIED, AD-274722L.

Joachim, C. E., Structures in an Arctic Environment, Airblast and Subsurface Shock of High Explosive Tests, U. S. Army Engineer Waterways Experiment Station, Vicksburg, MS, October 1964, UNCLASSIFIED, AD-450624.

Joachim, C. E., Shock Transmission Through Ice and Snow, WES TR 1-794, Report 3, U. S. Army Engineer Waterways Experiment Station, Vicksburg, MS, September 1967, UNCLASSIFIED, AD-659774.

Knasel, M., private communication, results expected in mid 1980.

Lorenz, R. A., private communication, February 1980.

Napadensky, H., Dynamic Response of Snow to High Rates of Loading, CRREL RR-119, Cold Regions Research and Engineering Laboratory, Hanover, NH, 1964, UNCLASSIFIED, AD-600075.

Pittman, J., Airblast from Underwater Explosions; Mono Lake, NOLTR 70-212, United States Naval Ordnance Laboratory, White Oak, MD, 12 November 1970, UNCLASSIFIED.

Porzel, F. B., Cratering in Snow, Technical Note Number 62-35, Institute for Defense Analyses, July 1962, UNCLASSIFIED AD347266.

Reed, J., private communication, report to be published during 1980.

[redacted]

[redacted]

Reisler, R. E., Giglio-Tos, L., Teel, G. D., and LeFevre, D. P., Air Blast Parameters from Summer and Winter 20-Ton TNT Explosions, Operation Distant Plain, Events 3 and 5, BRL MR 1894, Ballistic Research Laboratories, Aberdeen Proving Ground, MD, November 1967, UNCLASSIFIED, AD-830308.

Reisler, R. E., et al, Air Blast Measurements from the Detonation of Large Spherical TNT Charges Resting on the Surface (Operation DISTANT PLAIN, Events 6A and 6), BRL Memo Report No. 1955, USA Ballistic Research Laboratories, Aberdeen Proving Ground, Maryland 21005, January 1969.

Reisler, R. E., et al, Air Blast Data From Height-of-Burst Studies in Canada, Volume II - 1975 Dipole West Series (HOB 45.4 to 144.5 Feet), BRL Report No. RM 1990, USA Ballistic Research Laboratory, Aberdeen Proving Ground, Maryland 21005.

Reisler, R. E., Pettit, B. A., and Kennedy, L. W., Air Blast Data from Height-of-Burst Studies in Canada, Volume I HOB 5.4 to 71.9 Feet, BRL Report No. 1950, USA Ballistic Research Laboratory, Aberdeen Proving Ground, Maryland 21005, December 1976 (AD #B016344L).

Reisler, R. E., HE Height-of-Burst Blast at Moderate to Low Overpressures, USA Ballistic Research Laboratory, Aberdeen Proving Ground, Maryland 21005 (to be published).

Smith, J. L., Effects of Frozen Surfaces on Air Blast Phenomena, Cold Regions Research and Engineering Laboratory, Hanover, NH, undated, UNCLASSIFIED.

Vortman, L. J., and Shreve, J. C., The Effects of Height of Explosion on Blast Parameters, Sandia Corporation Report SC-3858 (TR), June 1976, Sandia Laboratories, Albuquerque, New Mexico.

[redacted]

[redacted]

Wells, P. B., et al, Air Blast from Special Weapons in Homogeneous and Non-Homogeneous Atmospheres (U), DNA 2751P, Kaman Sciences Corporation, Colorado Springs, CO, 30 April 1971, SECRET RD CNWDI.

Wisotski, John and Snyer, W. H., A Study of the Effects of Snow Cover on High Explosive Blast Parameters, DU-DRI-2303, Denver University, Denver Research Institute, Denver, CO, March 1966, UNCLASSIFIED.

[redacted]

[redacted]

THIS PAGE IS INTENTIONALLY LEFT BLANK.

[redacted]

[redacted]

SECTION 3
CRATERING PHENOMENA

[redacted] The mechanisms producing a crater for near surface, surface or subsurface bursts are closely allied to the air blast and surface effects considered in Section 2. There have been no nuclear tests by the U.S. in cold climates; so the U.S. has no experimental data base for nuclear cratering phenomena in the Arctic. As discussed in EM-1 the data base for nuclear craters consists entirely of large yield bursts in the Pacific and small yield bursts in Nevada. Thus, cratering from nuclear bursts is a very uncertain subject at best. Adding the complexity of Arctic conditions increases the uncertainty.

3.1 [redacted] Arctic Environmental Differences

[redacted] The difference of importance in cratering is the large probability of occurrence of snow, ice and frozen ground in the Arctic. In heavily glaciated areas the snow/ice thickness will be deep enough that the entire crater forms in these materials. Most of the area, however, will have only 1 m or less of snow or ice over frozen ground; so a layered geometry must be considered in the cratering predictions. For large yields the scaled depths of snow or ice are negligible, and as will be shown later, the crater in the ground will be little affected by the snow layer.

[redacted] The ice canopy may influence the underwater crater development. The existence of underwater permafrost may be important. Adequate experimental data are not available in these cases.

[redacted]

3.2 [redacted] Cratering Mechanisms in Arctic Media

[redacted] In the Arctic environment, it is obvious that the medium in which the explosion crater is created can take many different forms. Some of the forms are bare ground (frozen and/or underlain with permafrost), frozen ground covered with snow and/or ice, thick ice layers over water, and shallow bodies of water. In the latter case, the crater could form in the solid medium under the water.

[redacted] Figure 3-1 is a schematic illustration of a crater formed by a surface burst, showing descriptive nomenclature. Since crater size varies primarily with charge yield, depth of burst (DOB), and the cratered medium, it is desirable that tests be conducted with as many different charge geometries and in as many different media as possible. This also involves the development of suitable scaling relations by which results of small-scale tests can be used to predict the results to be obtained with much larger yields. Thus far, attempts to correlate theory with empirically developed exponents, or scaling laws, have met with only limited success.

[redacted] Figure 3-2 shows some ideal crater cross sections from nuclear bursts, illustrating the effect of HOB and DOB on crater volumes. If a nuclear or HE burst is sufficiently high above the ground surface, only a shallow compressional crater is formed and no ejecta produced. As the height of burst decreases, the crater volume increases and an increasing fraction of the crater is due to excavation and ejection of material from the crater region.

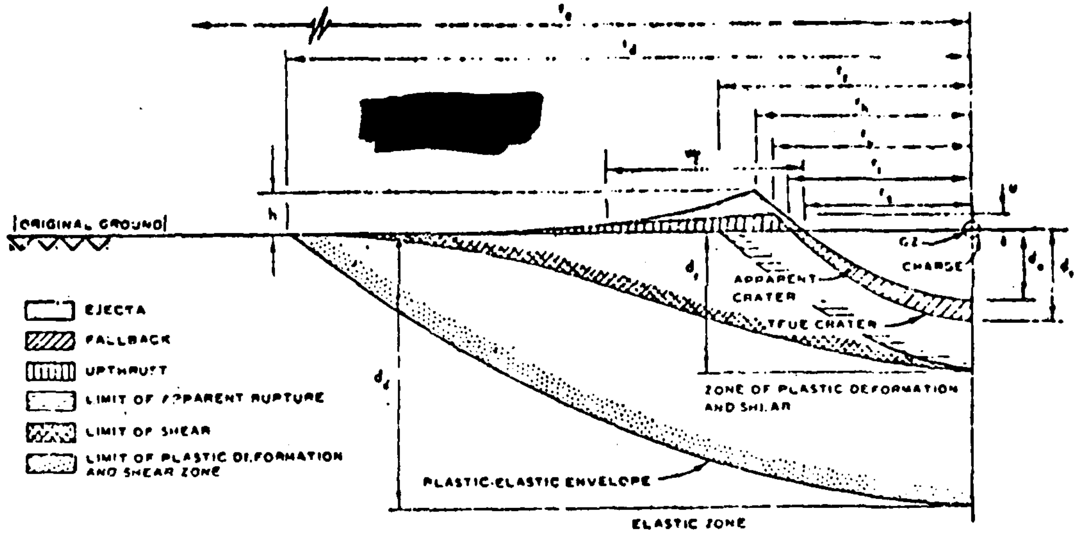

[redacted]igure 3-1 Typical half-crater profile and nomenclature for surface burst. Profiles and dimensions are symmetrical about the centerline.

[redacted]

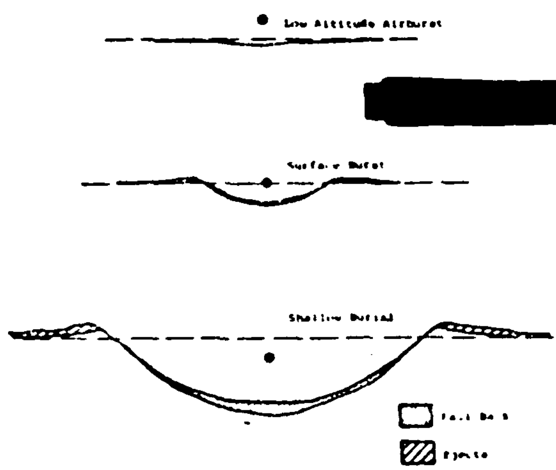

[redacted] FIGURE 3-2. EFFECT OF DEPTH OF NUCLEAR BURST ON CRATER SIZE AND SHAPE

[redacted]

[redacted]

[redacted] The large difference in energy density (ratio of explosive yield to explosive mass) between high explosive and nuclear devices can cause substantial differences in cratering efficiency (the ratio of volume of crater to explosive yield) and in the relative importance of various cratering mechanisms between the two types of sources.

[redacted] The material properties of the medium in the crater region influence the crater volume primarily through their compressibility and shear strength under dynamic loading conditions. Water content plays a large role in determining shear strength, especially in soils. The largest crater volumes are found in wet soils and the smallest crater volumes are found in rock. Jointing is an important factor in determining the crater size in rock geologies. Geologic layering is a rough indicator of material properties with depth and must be considered when predicting crater volumes. Frozen ground or ground interspersed with ice lenses and/or permafrost will behave like rock as far as crater formation is concerned.

[redacted] The failure process in snow differs from that in glacial ice, frozen ground, rock, and certain types of soil. Characteristic features of this failure (referred to here as "viscous-damping failure") are: 1) damping of the disturbance during the rise to peak pressure, and 2) substantial recovery of stored potential energy during unloading. Due to the unique physical properties of snow, craters formed by explosions in snow will be unusual in appearance and size compared with craters formed in other media. Snow is a composite material that consists of a relatively incompressible crystalline solid (ice) and a compressible gas (air).

[redacted]

[redacted] The air is found in the interconnecting voids in the ice matrix and comprises up to 70% of the volume of snow near the surface of the ice cap. Other properties of snow of importance in cratering are low melting and vaporizing temperatures.

[redacted] Immediately after detonation, as the hot gas bubble begins to form a cavity by vaporization, the surrounding snow is compacted radially, and the air in the voids is compressed. Cavity walls are fractured and an ice skin is formed by fusion. During this loading of the snow, a significant amount of the explosive energy is expended in compacting and deforming the snow without destroying cohesion. Some snow is dissociated and thrown out as ejecta.

[redacted] Much of the energy used to compress the air during loading is recovered during unloading (after the pressure wave has passed), which results in fracturing and deforming the snow. The primary cavity then exhibits a reversal in the direction of displacement (implosion) as the snow attempts to regain its original location. This part of the mechanism is referred to as pseudo-elastic rebound. Simultaneously, the compacted snow zone and the ice skin are fractured.

[redacted] A sensitively balanced transition condition appears to exist at critical depth. The balance determines under what conditions fractures during the rise of pressure and the outward expansion of the gas bubble predominate over fractures formed as a result of implosion. Implosion is closely followed by a vortex within the snow and scouring action as the gas bubble emerges from the rising column defined by the vortex. This scouring largely determines the final shape of the apparent crater.

[redacted]

[redacted] At a charge depth less than that at which maximum scouring occurs, more of the energy of the explosion is expended in the atmosphere and less is available to the snow. An apparent crater is formed in the air blast range and the secondary zone of the fragmentation range. Refer to Figure 3-1. The volume of the apparent crater per pound of explosive charge is maximum at the transition limit between the two ranges, where scouring is a maximum. Dimensions of the apparent crater are neither predictable with accuracy by conventional cube root scaling nor usable as a basis for predicting undersnow damage because 1) it is difficult to determine the proportion of the explosive energy partitioned to loading the snow, and 2) the apparent crater in snow occurs subsequently to loading and is the result of the scouring action of the vented gas bubble.

3.3 [redacted] High Explosive Cratering Experiments

[redacted] There have been many HE cratering experiments performed in the Arctic or sub-Arctic. The surface materials include snow, ice and frozen ground of various types. Many of the experiments have been designed to determine the optimum depth of burst of various HE types and charge sizes for producing the largest crater for mining and excavating. In Figure 3-3 (Bauer et al, 1973) representative cratering efficiencies are given as a function of depth of burst for several arctic materials. For purposes of nuclear cratering emphasis on shallow or surface bursts would be of more interest.

[redacted] The large differences in the lower and upper limits for frozen materials noted in Figure 3-3 are typical in cratering experiments due to variations in local geology and material properties. The cratering efficiency of HE charges increases with increasing water content. As discussed in EM-1 this has also been noted in unfrozen ground materials.

[redacted]

[redacted]

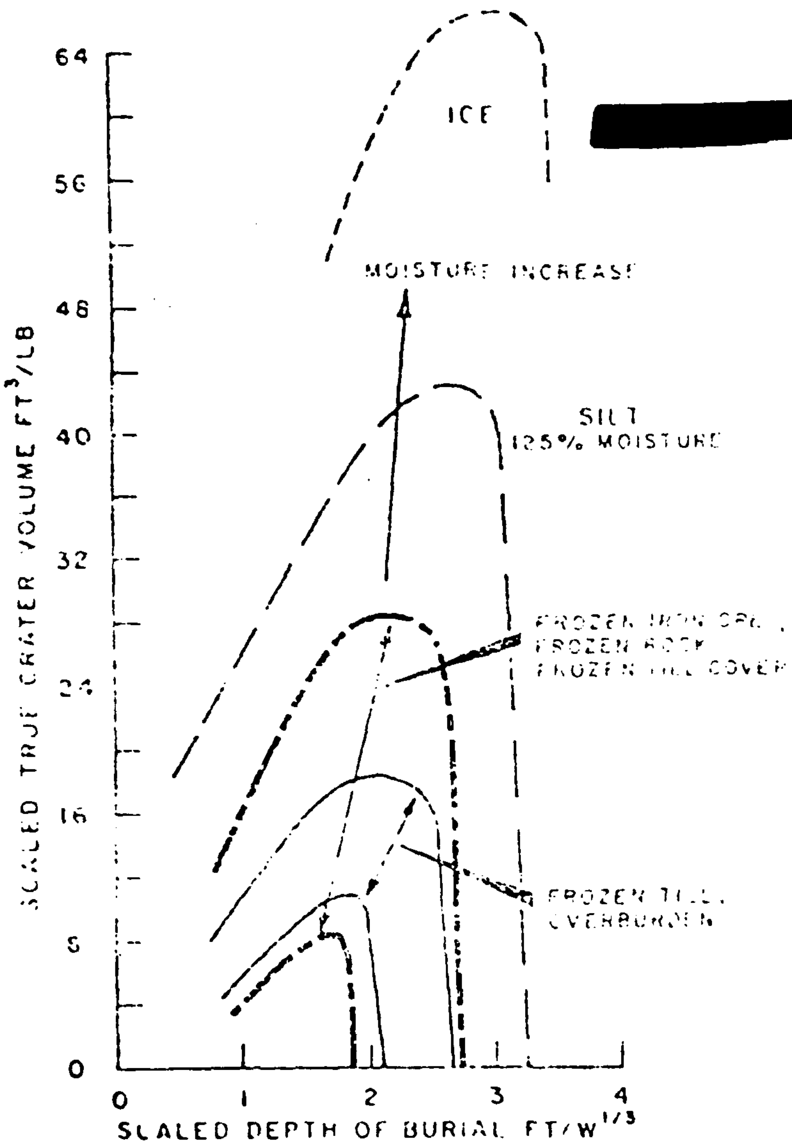

[redacted] FIGURE 3-3. SCALED CRATER VOLUME VS SCALED DEPTH OF BURST FOR VARIOUS FROZEN MATERIALS AND EXPLOSIVE COMBINATIONS.

[redacted]

[redacted]

[redacted] In conjunction with the WES and CRREL air blast experiments in Greenland, extensive measurements (Livingston, 1970 and 1968) were made of craters in deep snow and ice. The depths were such that the entire crater was in the snow or ice. Shallow and even above ground burst heights were used in addition to depths of burst extending below the optimum depth of burst.

[redacted] In Figure 3-4 the efficiencies of HE cratering in ice and snow as a function of the scaled DOB are compared. The very wide bounds shown in the figure result from several different types of explosives and several charge sizes. Thus, the scatter is due to material properties and differences in efficiencies of explosives as well as possibly to inapplicability of cube-root scaling of the charge weight. Note that at optimum depth of burst the snow crater will be about 3 times as large as a crater in ice. The optimum depth of burst in ice is somewhat deeper. For a surface burst the snow crater is about twice as large as an ice crater. No data were provided for near surface air bursts over ice.

[redacted] In Figure 3-5 the scaled radius of snow and ice craters are compared as a function of scaled depth of burst. The radius of the snow crater is much larger than ice especially at the deeper depths. For a surface burst the radius for snow is about 50% larger than for ice. In Figure 3-6 the scaled crater depths in snow and ice are compared. The differences for deeper depth of burst are not as large as for the radii but for a surface burst the crater depth in snow is about twice that in ice.

[redacted] Surface bursts are very important militarily; so the Greenland surface burst experiments have been analyzed as a function of charge weight (Conway and Meyer, 1970). The apparent crater depths and radii are summarized in Figure 3-7; also included on these figures are data from Sager (1960 and 1961). Figure 3-8 shows the apparent crater volume as a function of charge weight. Other cratering data from surface events in snow are virtually non-existent.

[redacted]

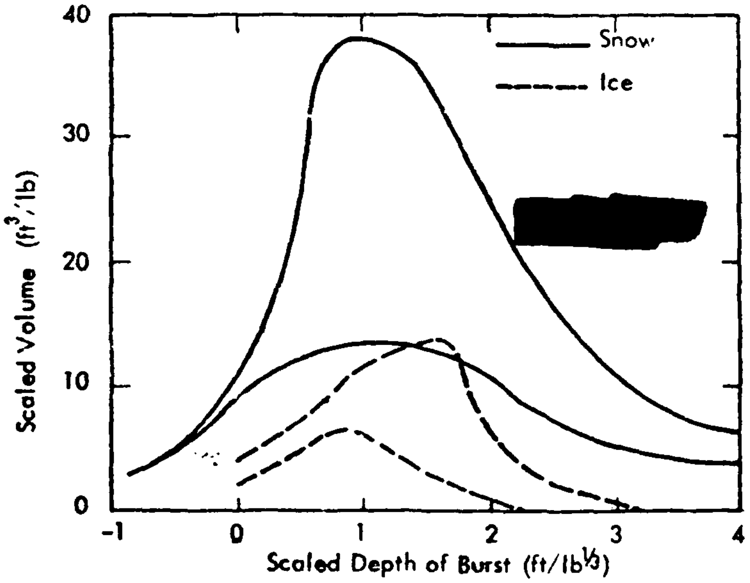

[redacted] FIGURE 3-4 HIGH EXPLOSIVE CRATER VOLUME IN SNOW AND ICE

[redacted]

[redacted]

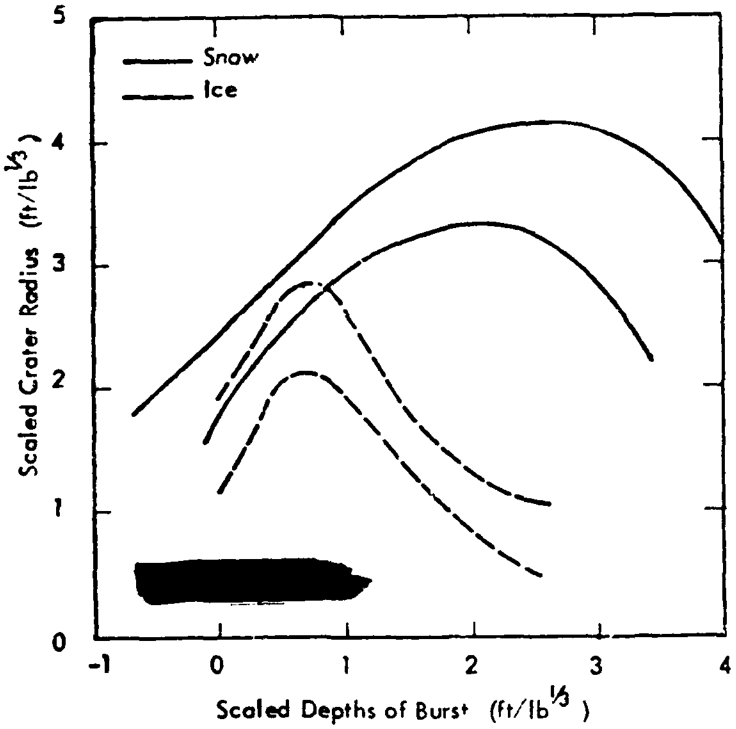

[redacted] FIGURE 3.5 HIGH EXPLOSIVE CRATER RADII IN SNOW AND ICE

[redacted]

[redacted]

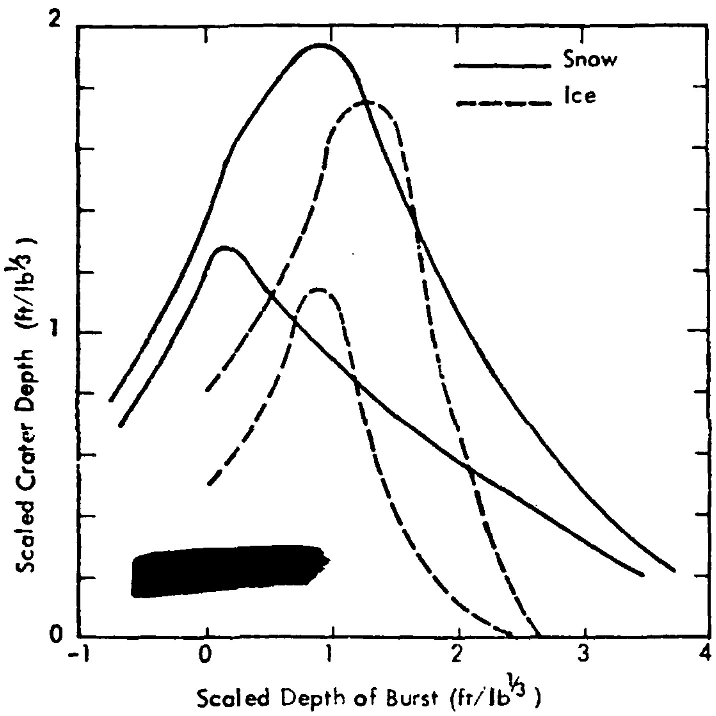

[redacted] FIGURE 3-6 HIGH EXPLOSIVE CRATER DEPTHS IN SNOW AND ICE

[redacted]

[redacted]

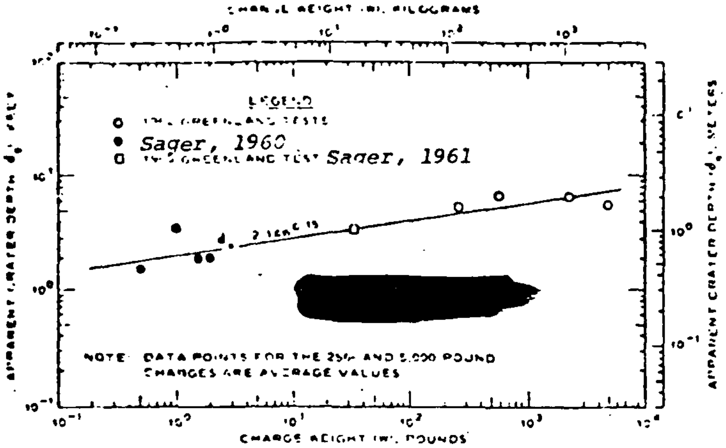

a. APPARENT CRATER DEPTH (d_a) VERSUS CHARGE WEIGHT (W)

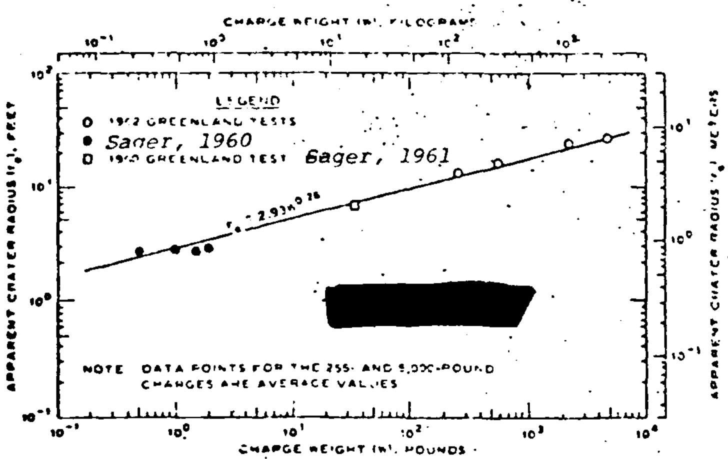

b. APPARENT CRATER RADIUS (r_a) VERSUS CHARGE WEIGHT (W)

[redacted]gure 3-7 Apparent crater dimensions as functions of charge weight.

[redacted]

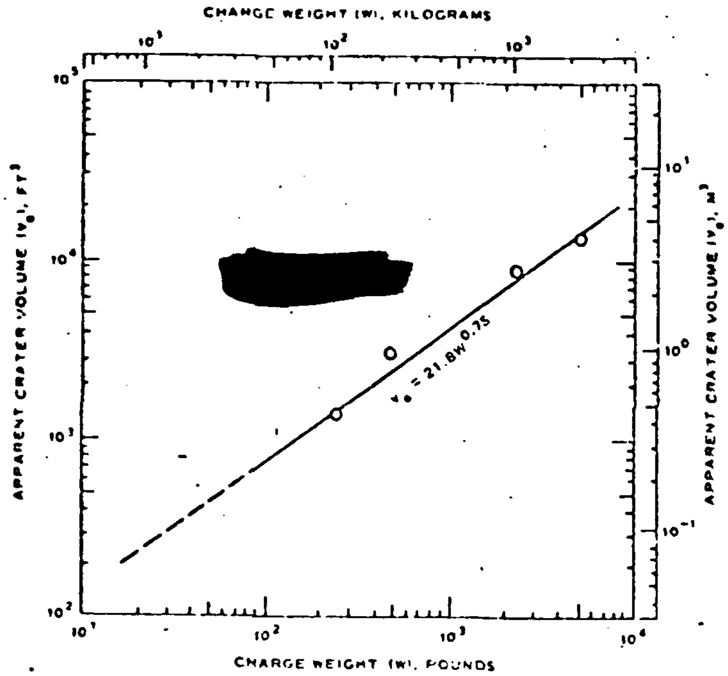

[redacted] Figure 3–8 Apparent crater volume as a function of charge weight.

[redacted]

[redacted] Figure 3-9 shows the variation of apparent crater radius with charge weight for surface bursts in snow as compared with craters from surface TNT events in clay, sand, basalt and shale. Similarly, Figure 3-10 presents a comparison of apparent crater depths versus charge weights. These figures show that craters in snow tend to be larger than craters in other media for the same charge yield.

[redacted] This increased size appears to be due to the greater amount of material vaporized and compacted during the explosion. Although no ejecta measurements were made, examination of the crater lip profiles indicates that the contribution (to volume) of the ejection mechanism in snow craters is correspondingly less than in craters in other media. Craters in snow have a characteristic wide shallow appearance. The magnitude of the pseudo-elastic rebound in snow is greater directly under the charge than in the material pushed laterally outward because of the greater lateral confinement of the material under the charge.

3.3.1 [redacted] Scaling Considerations

[redacted] Equations for scaling crater dimensions in snow within a range of yields of 0.5 to 5,000 lbs, as determined by the use of the method of least squares, are presented in Figures 3-7 and 3-8. These equations show a significant departure from the common cube-root scaling. For the apparent crater radius, a slightly smaller scaling exponent of 0.26 is indicated. The scaling exponent for apparent crater depth, 0.15, is considerably smaller than that normally applied to craters in soil. These unusual scaling exponents are probably best explained by the mechanism of pseudo-elastic rebound in snow. A correspondingly low scaling exponent of 0.75 is evident (Figure 3-8) for the apparent crater volume. It should be noted that these empirical

[redacted]

[redacted]

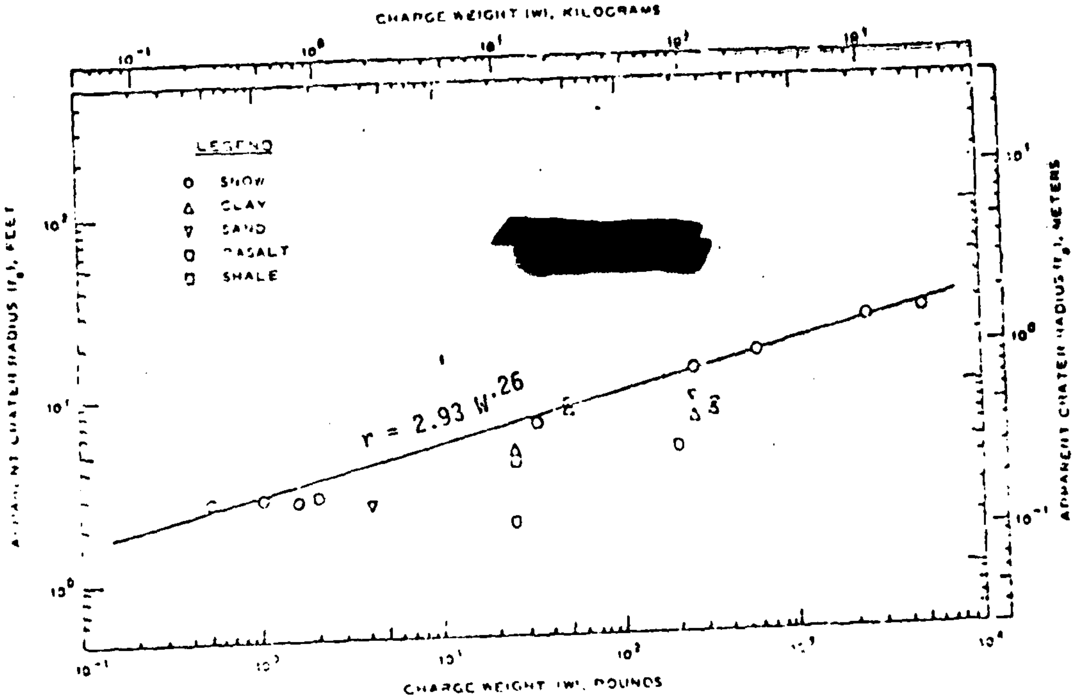

[redacted]

FIGURE 3-9. COMPARISON OF APPARENT CRATER RADIUS VERSUS CHARGE WEIGHT FOR SURFACE-BURST CRATERS IN VARIOUS MATERIALS

[redacted]

[redacted]

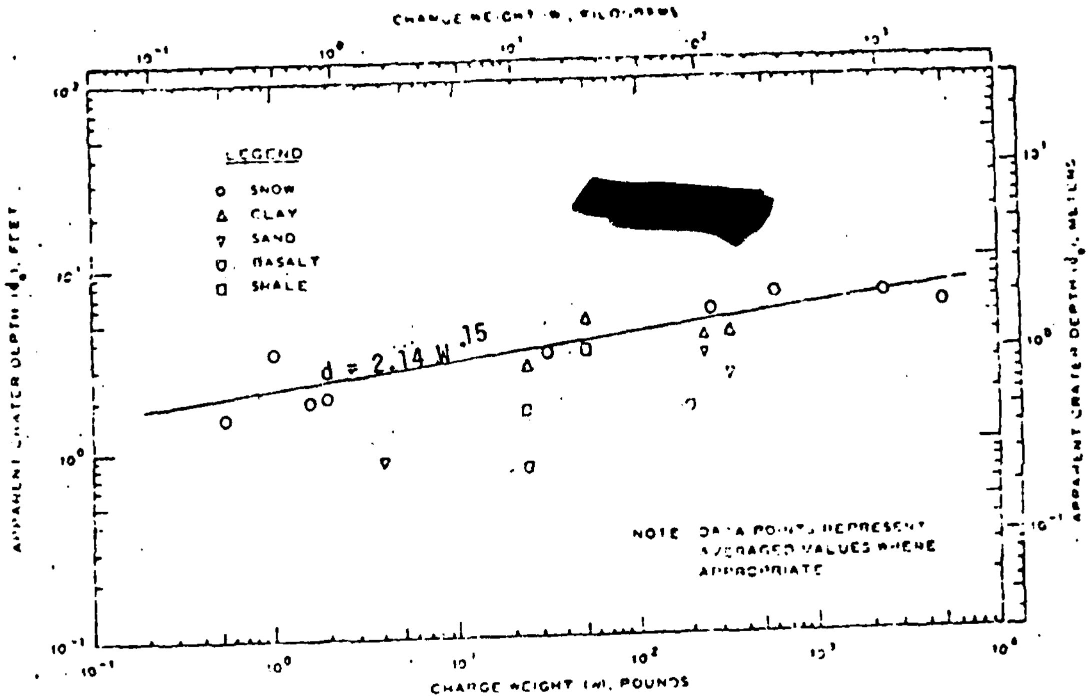

[redacted]

FIGURE 3-10. COMPARISON OF APPARENT CRATER DEPTH VERSUS CHARGE WEIGHT FOR SURFACE-BURST CRATERS IN VARIOUS MATERIALS.

[redacted]

[redacted] scaling components are based on a limited amount of data and should be considered as approximations. The use of these exponents to scale HE data to nuclear explosions would be questionable because of the magnitudes of the NE yields and the differences in thermal energy release, which appears to influence crater formation in snow significantly.

[redacted] Even though the scaling rules for the snow radius and depth are very uncertain when extended to nuclear yields, it is instructive to compare these results with the wet soil EM-1 predictions. Using the relations in Figures 3-9 and 3-10 a crater from a 1 kT surface burst over snow would have a radius of 127 ft and a depth of 19 ft. Using the relations given in the revised cratering section of EM-1, a crater from a 1 kT burst in wet soil would have a radius of 101 ft and a depth of 42 ft. Thus, a wide shallow crater is predicted by the HE snow data when scaled to nuclear yields.

[redacted] Snow efficiency varies from about 7×10^{3} to 3×10^{4} ft^{3} per ton, being equivalent to wet sand or muck. Ice varies from 4×10^{3} to 8×10^{3} ft^{3} per ton. Frozen soils range from 3×10^{3} to 6×10^{3} ft^{3} per ton. The highest efficiencies are found in frozen silts which are equivalent to wet soft rock, and the lower efficiencies are for frozen aggregates which are equivalent to hard rocks. As is normal for cratering measurements, a wide range of values is noted. It is suggested that for want of a better method these efficiencies be used in conjunction with the prediction methods in EM-1.

[redacted]

[redacted] The effect of the increased thermal yield of nuclear bursts as compared with HE is unknown. For typical soil materials small yield nuclear devices (<1 kt) are assumed to be about 1/7 as efficient as HE and large yield devices ($\geq$1 kt) are assumed to be 1/20 as efficient as HE charges. Thus, a 1 kt nuclear burst would produce a crater volume of about 3×10^5 to 1.5×10^6 ft^3 per kt. A kt of energy is capable of melting about 1.5×10^6 ft^3 of snow (ρ = .3 g/cm^2, melting energy about 80 cal/g) and vaporizing about 1.7×10^5 ft^3 of snow (vaporizing energy about 700 cal/g). If a fraction of this energy were available to increase the cratering efficiency for nuclear bursts, then the efficiencies obtained using the current prediction methods may be too low by as much as a factor of two.

3.3.2 [redacted] Layered Geometry Considerations

[redacted] Consider the 19 ft. crater depth found for a 1 kT burst in snow. This is much deeper than typical snow depths except in highly glaciated areas. Thus, the cratering data considered above must be modified to include the effects of the shallow snow. HE experiments considering a layered geometry of dry soil over wet soil have been represented by the expression

$$(V-V_L)/(V_U-V_L) = 1 - \exp(-5.4\ d/V^{1/3})$$

where

- d = depth to base material (water table or cemented layer)
- V = apparent crater volume in the layered geology
- V_U = apparent crater volume in the surface material when $d = \infty$
- V_L = apparent crater volume in the base material when $d = 0$.

In Figure 3-11 the data for a sand over a cemented soil layer is shown. The upper curve will represent a case with a definite boundary between the surface and base layer such as would occur for snow over frozen ground. The dashed line is the equation given above.

[redacted]

[redacted]

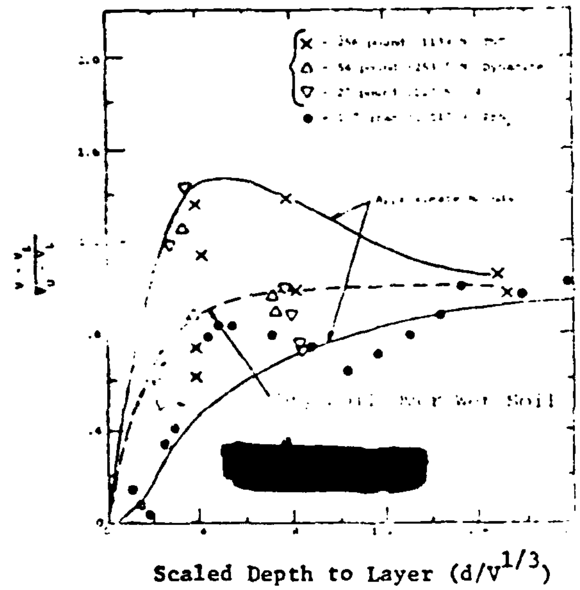

[redacted] FIGURE 3-11. CRATERING DATA: SAND OVER A CEMENTED LAYER

[redacted]

[redacted]

[redacted] In using the technique given above an iterative process is necessary since the volume appears on both sides of the equation (or on both axes in Figure 3-11). The volumes V_U and V_L are obtained by using the HE efficiencies along with the proper nuclear yield and efficiency ratio factor. When this is done for the typical Arctic case of 1 m of snow over frozen ground then the following observations can be made. For 1 kt $V_U = 1x10^6$ ft^3 and V_L could be as low as $2x10^4$ ft^3. The value of V would be about $2.5x10^5$ ft. The scaled snow depth is only about .05. In this case the volume of the crater in the base material would not be altered appreciably by the thin snow layer. For larger nuclear yields this depth of snow would be insignificant.

[redacted] The calculations for the layered geometry are very uncertain, and we are applying the results of layered geometry cases far outside the original configuration.

3.4 [redacted] Underwater Cratering

[redacted] Underwater cratering is discussed as a major topic in Chapter 2 of DNA EM-1 and in Chapter 8 of the Underwater Hand-book. However, existing manuals do not discuss any effects that may be caused by conditions peculiar to cold-weather regions, nor do there appear to have been any experimental investigations into this matter. The discussion that follows must therefore be regarded as conjectural. The factors that might cause variations under Arctic conditions from what is predicted under temperate conditions are differences in bottom composition, if any, and the presence of ice.

[redacted] Reference to Table 2-12 in Problem 2-36 of DNA EM-1, wherein soil correction factors are given for various bottom materials, reveals that the range of bottom materials covered encompasses the range of materials expected to be found in any

[redacted]

[redacted] of the world's oceans, including the Arctic. It is known, however, that subsea permafrost exists in several of the seas of the Arctic, the Laptev, Kara, E. Siberian, Chukchi and Beaufort Seas for example (Lewellen, 1973, 1974, 1977). The extent of the subsea permafrost is not known, and there is a limited amount of information as to its characteristics (Chamberlain et al., 1978). Of particular importance is whether the permafrost in a given area is bonded, with ice in the interstices, or unbonded, saturated with brines that have a depressed freezing point. The soil correction factors may well be different for the two states, and different from that applicable to the basic material forming the permafrost.

[redacted] Underwater cratering from an underwater detonation occurs when the first expanding bubble interacts with the bottom. The presence of an ice cover would affect the early time history of this bubble only if the bubble interacts with the ice layer as well as with the bottom, and then only to the extent that the energy required to vaporize ice differs from that required to vaporize seawater. Depending upon whether the ice is old ice of low salinity, or more recently-formed ice of higher salinity, the latent heat of fusion may vary from less than 40 cal/g to the 80 cal/g of ice of zero salinity at -1°C (Neuman and Pierson, 1966). The energy used to vaporize ice is thus some 6-12% more than would be used to vaporize an equivalent amount of seawater at 0°C.

[redacted] In analogous fashion, for a surface burst or low air burst over water to create an underwater crater, the expanding fireball must vaporize the water layer beneath and interact with the bottom. Again, the presence of ice cover may require 6-12% more energy for vaporization than if no ice were present. Except in extremely shallow water, the volume of ice to be vaporized, even in the case of a relatively thick solid ice pack, would be

[redacted]

[redacted] a small percentage of the water to be vaporized. The decrease in energy available for cratering would therefore be expected to be extremely small in most cases.

[redacted] It is concluded that, except where the bottom is subsea permafrost, the methods of predicting underwater crater dimensions given in Problem 2-36 of DNA EM-1 are valid under Arctic conditions, regardless of the amount of ice present. The uncertainties in crater dimensions given are of the order of plus 150-160% to minus 50-60%. These are large enough to encompass any additional uncertainty due to ice cover. In very shallow water, if the crater lip height were such that it extended above the water or ice (unwashed crater), or to just below the water surface, the scouring action of broken ice caused by its wave-induced motion would be expected to hasten the erosion of the crater lip. If the bottom is composed of subsea permafrost, the proper soil correction factor to use is not currently known.

3.5 [redacted] Conclusions and Recommendations

[redacted] The following conclusions are drawn from the rather scant information applicable to arctic cratering and recommendations of research necessary to reduce the uncertainties are given.

3.5.1 Conclusions

[redacted] Equations for scaling crater dimensions in snow within a range of yields of 0.5 to 5000 lbs TNT show a significant departure from the customary cube-root scaling. For apparent crater radius, the scaling exponent 0.26 is indicated, which is close to fourth-root scaling. The scaling exponent for apparent crater depth is 0.15, which is considerably smaller than that usually applied to craters in soil. A correspondingly low scaling exponent of 0.75 is derived for apparent crater volume.

[redacted] It should be noted that these empirical scaling exponents are based upon a limited amount of data and should be considered as approximations. The use of these exponents to scale up to nuclear explosion craters would be questionable because

[redacted]

[redacted]

[redacted] magnitudes of the nuclear burst yields and the profound differences in thermal energy release, which appears to influence crater formation in snow significantly. When comparisons of apparent crater radii for TNT tests in snow are made with craters from TNT tests in clay, sand, basalt, and shale, the comparisons show that craters in snow tend to be larger than craters in other media for the same charge size. This increased size appears to be due to the greater amount of material vaporized and compacted during the explosion and to a scouring action.

[redacted] Although no ejecta measurements were made in the WES tests, examination of the crater lip profiles indicate that the contribution of the ejection mechanism (to volume) in snow craters is correspondingly less than in craters in other media. Craters in snow have a characteristic wide, shallow appearance. The magnitude of the pseudo-elastic rebound in snow is larger directly under the charge than in the snow pushed laterally outward, because of the greater lateral confinement of the snow directly under the charge.

[redacted] Craters in frozen soil or permafrost have similar appearance and dimensions to craters formed in hard rock. It is speculated that the mechanisms for the formation of these craters are similar to those in other soils.

[redacted] Since all of the available cratering data obtained under Arctic environmental conditions have been collected from HE charge tests, the main questions which remain when one uses these data to predict craters from nuclear weapon bursts are:

1. Does the enhanced thermal radiation associated with the nuclear burst have a profound effect on the partition of the total energy going into the snow and/or ice cap?

[redacted]

[redacted]

[redacted] 2. Further, does this enhanced thermal radiation significantly alter the mechanisms of crater formation which are associated with the crater formed in snow by the relatively small HE charges?

[redacted] In areas where subsea permafrost is not present, the methods of EM-1 are adequate for predicting crater dimensions, using the soil factor appropriate to the bottom composition. Other arctic environmental factors are not expected to have a significant effect on underwater cratering.

3.5.2 [redacted] Recommendations

[redacted] To establish whether or not it is valid to scale HE-charge crater data to the nuclear burst cases, computer code calculations should be performed for the different charge output characteristics and sizes. The results of the HE-charge calculations can be checked against test data to verify the accuracy of the code(s).

[redacted] Should a large-charge HE test (100-ton TNT or more) be implemented in the Arctic, the crater and ejecta measurements should be obtained. Early-time photography of the crater formation should be obtained also. Additional crater dimension data from small-charge HE explosions should be collected on a "test of opportunity" basis, but a test series performed specifically to obtain crater data is not recommended.

[redacted] The recommended series of calculations, experiments and field tests described in Section 2.7.2 should be planned such that the above questions will be answered.

[redacted] A research program to narrow the uncertainties in underwater cratering should take a dual approach - to support the collection of data to delineate the areas of bonded and unbonded permafrost, and to determine the appropriate soil

[redacted]

[redacted] correction factor to use for each type. Whether seismic methods can be used to delineate the two types of permafrost areas or whether a program of subsea coring is required should be investigated by experts in the field. The determination of soil correction factor should be accomplished by analytic means if possible, but laboratory or field testing might be required. This question should be studied by experts in the area before embarking on a program of field testing.

[redacted] 3.6 Bibliography

Bauer, A., Calder, P. N., MacLachlan, R. R., and Halupka, M., Cratering and Ditching with Explosives in Frozen Soils, DREV R-699-73, Queens University, Kingston, Ontario, for Defense Research Establishment, Valcartier, Quebec, July 1973, UNCLASSIFIED, AD-913283.

Conway, J. A. and Myer, J. W., Cratering in Greenland Icecap Snow, WES MP N-70-6, U. S. Army Engineer Waterways Experiment Station, Vicksburg, MS, July 1970, UNCLASSIFIED, AD-711861.

Chamberlain, Edwin J., Sellmann, P. V., Blouin, S. E., Hopkins, D. M., and Lewellen, R. I., Engineering Properties of Subsea Permafrost in the Prudhoe Bay Region of the Beaufort Sea, Report of the Third International Conference on Permafrost, pp. 629-635, National Research Council of Canada, 1978.

Defense Nuclear Agency, Capabilities of Nuclear Weapons (U), DNA EM-1, Defense Nuclear Agency Effects Manual Number 1, Headquarters, Defense Nuclear Agency, Washington, D. C., 1 July 1972 (Change 1, 1 July 1978), SECRET RESTRICTED DATA.

Defense Nuclear Agency Handbook of Underwater Nuclear Explosions (U), DNA 1240 H, Defense Nuclear Agency, Washington, D. C., November 1971, SECRET RESTRICTED DATA.

[redacted]

Lewellen, Robert I., The Occurrence and Characteristics of Nearshore Permafrost, Northern Alaska, in Permafrost: The North American Contribution to the Second International Conference, pp. 131-136, National Academy of Sciences, Washington, D. C., 1973.

Lewellen, Robert I. Offshore Permafrost of Beaufort Sea, Alaska, in The Coast and Shelf of the Beaufort Sea, J. C. Reed and J. E. Sater (ed.), pp. 417-426, The Arctic Institute of North America, 3426 N. Washington Blvd., Arlington, VA 22201, 1974.

Lewellen, Robert I., Subsea Permafrost Research Techniques, Geoscience and Man, Vol. XVIII, pp. 29-34, December 30, 1977.

Livingston, C. W., Explosions in Ice, Technical Report 75, USA SIPRE, now Cold Regions Research and Engineering Laboratory, Hanover, NH, December 1960, UNCLASSIFIED.

Livingston, C. W., Explosions in Snow, Technical Report No. 86, Cold Regions Research and Engineering Laboratory, Hanover, NH, 1968, UNCLASSIFIED.

Neuman, Gerhard and Pierson, Willard J. Jr., Principles of Physical Oceanography, Prentice-Hall, Inc., Englewood Cliffs, NJ, 1966.

Sager, R. A. et al, Cratering from HE Charges: Compendium of Crater Data, Tech. Report No. 2-547, May 1960, U. S. Army Engineer Waterways Experiment Station, CE, Vicksburg, Miss.

Sager, R. A., Cratering Data from 1960 Greenland Test Series of HE Charges in Snow, Feb. 1961 (unpublished), U. S. Army Engineer Waterways Experiment Station, CE, Vicksburg, Miss.

[redacted]

[redacted]

THIS PAGE IS INTENTIONALLY LEFT BLANK

[redacted]

[redacted]

SECTION 4
THERMAL RADIATION

[redacted] About a third of the yield of a nuclear weapon detonated at low altitudes in the atmosphere is emitted as infrared, visible and ultraviolet radiation with a pulse width depending on the yield and altitude typically lasting for a few seconds for a megaton weapon. This thermal energy can be transmitted to large ranges in the atmosphere and is usually readily absorbed in a thin surface layer on most target material causing large surface temperature increases which can cause damage to the targets. The types of damage usually of concern result from fires that start due to ignition of combustible materials and from burns to personnel but also can involve thermo-mechanical loading due to very large fluences incident on hardened facilities such as radars.

4.1 [redacted] Arctic Environmental Differences

[redacted] A large variability is expected in the effects of thermal radiation in an arctic environment because extreme variations in clouds, atmospheric moisture, visibility, precipitation, and the earth's surface occur more commonly in the arctic region than elsewhere in the world. These variations create conditions that can as much as double significant thermal effects or reduce them by even larger factors. The following briefly described effects will be discussed further in subsequent sections of the handbook.

4.1.1 [redacted] Visibility

[redacted] Surface visibility in arctic and subarctic climates during clear seasons is often exceptionally good because of the low humidity coincident with cold temperatures and the absence of dust in the air. The northern and coastal regions during the warmer months are subjected to extensive sea fog and low cloud-

[redacted]

[redacted]
iness. Falling or blowing snow can reduce the visible range to less than a mile during stormy periods. These extremes of atmospheric conditions require examination of their effects on transmission of thermal energy.

4.1.2 [redacted] Fog

[redacted] Arctic fog and precipitation generally reduce the range of thermal phenomena. At the very low temperatures of the arctic winter the atmosphere is capable of holding very little mosture. Such low temperatures as a rule are accompanied by minimal surface wind, and these conditions together are favorable to the formation of fog. Ice-fog crystals consist of many spherical particles and some hexagonal plates and columns of 2μ to 30μ diameter formed at about -40°C in high concentration that reduces visibility significantly. In addition ice fog can cause extinction of the infrared beam of an infrared guidance system.

4.1.3 [redacted] Albedo Surfaces

[redacted] Ground surfaces covered by snow and ice have a much higher albedo than bare ground in temperate climates. The transmission of thermal radiation is considerably enhanced by the presence of these high albedo surfaces. Layers of cloud, smoke, or haze are other common albedo surfaces.

4.1.4 [redacted] Cloud Cover

[redacted] The low dense cloud cover characteristic of arctic areas can result in significant enhancement of thermal environment for targets at low altitudes from a low altitude burst. A high albedo ground surface is very likely in the arctic. The combination of a high albedo ground surface and a low cloud cover results in a definite channeling of thermal energy and a marked increase in thermal fluences.

[redacted]

4.1.5 [redacted] Humidity

[redacted] Even though t'e relative humidity is generally high in the arctic especially over the ocean areas because of the low temperatures, the absolute concentration of water vapor is much lower than in temperate areas. This results in less absorption of thermal radiation in the important infrared water vapor absorption bands and tends to increase the thermal transmission.

4.1.6 [redacted] Low Temperatures

[redacted] The low temperatures in themselves do not result in changes in the thermal transmission except for their influence in producing ice fogs, ice/snow surfaces, etc.

[redacted] Materials used for clothing and supplies in arctic climates do not possess the same vulnerability to thermal effects as materials used in less severe temperatures. Furthermore, cold temperatures reduce somewhat the vulnerability of most materials to thermal effects.

[redacted] Besides a reduction in flammability with reduction in temperature, combustible material is less susceptible to thermal damage when protected by snow and frost covering. Characteristic low humidity of the arctic air will somewhat mitigate the reduction of combustibility. In some of the tundra, expanses of coarse vegetation growing on a thick peaty layer might be subject to surface fires started by nuclear detonations.

4.2 [redacted] Transmission Effects

[redacted] The quantity and effectiveness of thermal radiation that reaches a target is dependent on a large number of parameters whose variability in an arctic environment is sufficiently great to produce a significant change in thermal radiation transmission. The parameters to be considered here may be grouped

[redacted]

[redacted] into two general categories; first, those parameters which determine the manner in which thermal radiation is scattered and absorbed and in the atmosphere are discussed here, and secondly, those that determine the manner and extent of its reflection will be considered in Section 4.3.

[redacted] The thermal irradiance, H, received at a distance R from a nuclear burst is given by the expression

$$H = \frac{PT}{4\pi R^2} \cos \lambda, \tag{4.1}$$

where P is the total power radiated by the burst as a function of time, $\cos \lambda = 1$ if the receiver area is normal to the burst, and T is the transmission factor. T is used here in a very general sense and includes such effects as atmospheric attenuation, surface albedo effects (ground, water, or clouds), and source asymmetries.

[redacted] The radiant exposure, Q, during time from zero to t is then defined to be

$$Q_t = \int_0^t H\, dt, \tag{4.2}$$

where in general P, T and R may depend upon time. If we assume that the transmission T and the radius R to a unit area facing the burst are constant, then

$$Q = \frac{fWT}{4\ R^2} \tag{4.3}$$

where W is the yield of the weapon in calories and f is the thermal partition or efficiency, and fW = E is the thermal

[redacted]

[redacted] yield. Even though both T and R are seldom truly independent of time, sufficient accuracy may often be obtained by using the values corresponding to the time of peak radiated power. Often it is assumed that defining T = 1 will give the worst case environment. This assumption is usually good unless the conditions include source asymmetries and albedo from clouds and ground surfaces.

[redacted] In order to determine the amount of thermal energy actually transmitted to the receiver, allowance must be made for the attenuation of the radiation by the atmosphere. This attenuation is mainly of two forms - absorption and scattering. There are no strong absorption processes for the visible wavelengths but strong absorption bands exist in the ultraviolet and infrared. Scattering occurs with radiations of all wavelengths. The state of the atmosphere in the visible region can be represented by what is known as daylight visibility.

4.2.1 [redacted] Arctic Visibility

[redacted] There are several highly variable climatological characteristics that could significantly change the absorption and scattering of thermal radiation in the arctic and subartic atmosphere. As indicated although the arctic and subarctic regions are generally areas of comparatively low absolute humidity and little industrial dust, characterized by good visibility; the northern and coastal regions are seasonally subjected to extensive sea fog and low clouds, and falling or blowing snow can reduce visibility to less than one mile for extended periods in some areas.

[redacted] There is no single correct value of the attenuation coefficient μ for any given set of atmospheric conditions. The value of μ is a function of both the nature and distribution of the scattering and absorbing particles, and also of the wave

[redacted]

[redacted] length of the radiation involved. There is no simple average value of μ because the spectral distribution of the radiation will change with the distance "R" involved. In spite of the variable nature of μ, an assumption is often made that reasonable average values of μ can be determined in terms of visibility. This is not too unreasonable an assumption since that portion of the spectral distribution of radiated energy which penetrates any considerable distance in the atmosphere is concentrated mostly in the visible and near visible wave lengths. The conventional visibility as given in weather forecasts is generally the distance at which the transmission is reduced to 5.5%, i.e., $T = e^{-V\mu} = .055$.

[redacted] It is convenient to calculate the visibility on the basis of the above approximation to illustrate the dependence of atmospheric transmission and attenuation on visual properties of the atmosphere. There is wide discrepancy among values assumed for the distance called visibility and in relating that parameter to the optical properties of the atmosphere one should be aware of its very approximate and necessarily subjective nature. In most technical literature on atmospheric transmission the term meteorological range is defined as that distance where the transmission is 2%, i.e., $T = e^{-m\mu} = .02$. Unfortunately some authors use the terms visibility and meteorological range interchangeably.

[redacted] The international code for correlating the condition of the atmosphere with visibility is given in Table 4-1. In temperate climates one may see variations in the visibility from the highest to lowest visibilities depending upon the concentration of aerosol particles from pollution sources. In most areas of the arctic the background level of pollutants at the surface is low leading to very high visibilities. However, the occurrence of certain weather conditions such as blowing snow, ice fog, etc. result in very low visibilities of one mile or less.

[redacted]

[redacted] TABLE 4-1 INTERNATIONAL VISIBILITY CODE

Code Number	Description	Visibility From	Visibility To
0	Dense Fog	----	50 m (55 yds)
1	Thick Fog	50 m	200 m (220 yds)
2	Moderate Fog	200 m	500 m (550 yds)
3	Light Fog	500 m	1 km (0.6 mi)
4	Thin Fog	1½ km	2 km (1.2 mi)
5	Haze	2 km	4 km (2.5 mi)
6 [redacted]	Light Haze	4 km	10 km (6 mi)
7	Clear	10 km	20 km (12 mi)
8	Very Clear	20 km	50 km (30 mi)
9	Exceptionally Clear	50 km	280 km (170 mi)

(Glasstone, 1977)

[redacted] When one is considering the transmission for a broad spectrum as results from a nuclear weapon, the relation between the visibility and transmission is not as straightforward as indicated above. Scattering and buildup effects occur which result in a non-exponential falloff of the transmission. The various interaction cross sections vary as a function of wavelength so that integration of results across the broad wavelength must be considered. Extensive discussion of all aspects of this problem are presented in the DNA Thermal Sourcebook (Keith, 1973) and EM-1 (DNA, 1978) which is currently under revision.

[redacted] Figure 4-1 (Keith and Sachs 1977) shows predicted transmission as it varies with visibility of one to 30 miles. In the figure the variation of transmission with the ground level visibility is noted as a function of ground range for a large yield weapon

[redacted]

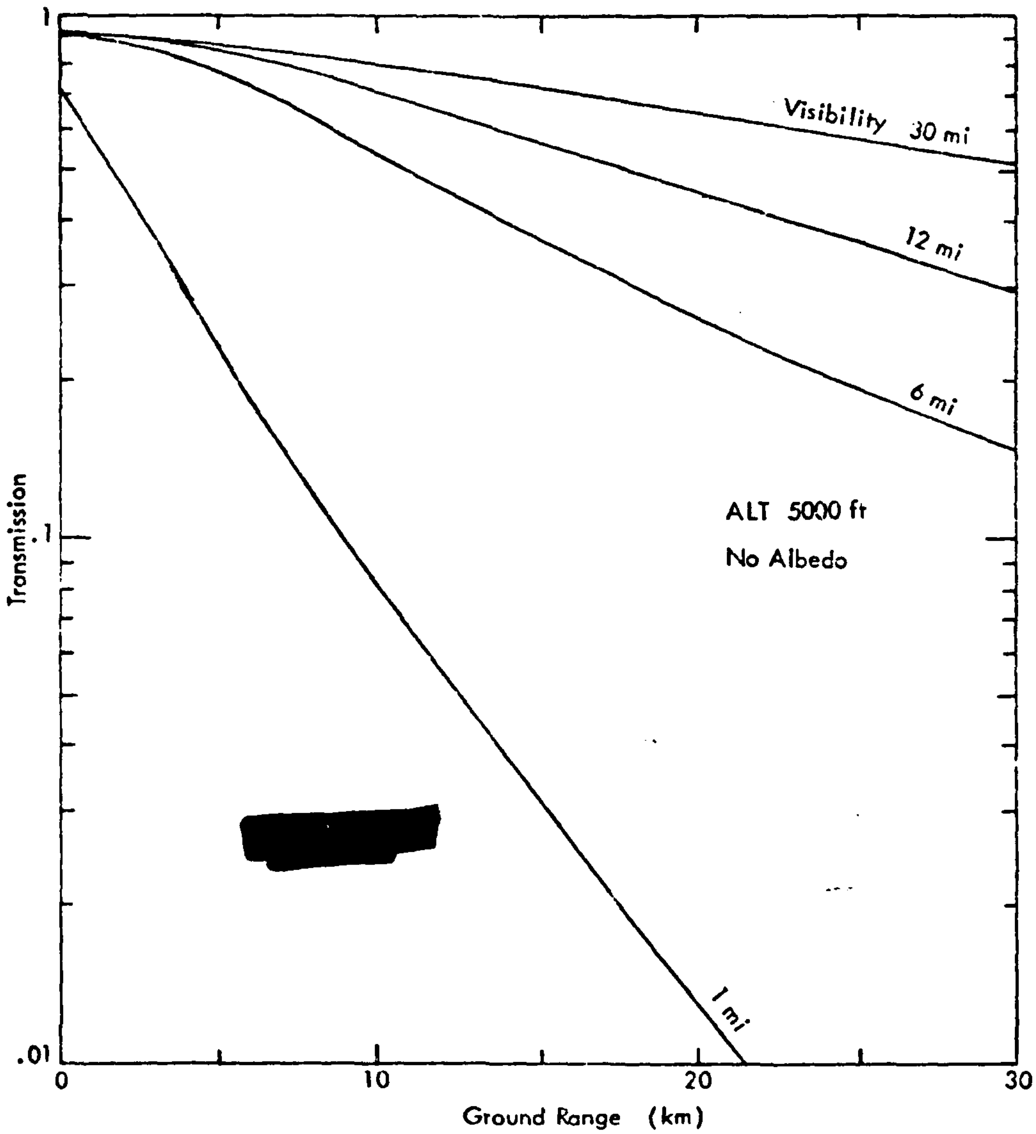

[redacted] FIGURE 4-1 VARIATION OF TRANSMISSION WITH VISIBILITY

[redacted]

[redacted] detonated at 5000 ft above the ground. The atmospheric profiles for every quantity except the aerosol concentration are unchanged for the various calculations. The aerosol concentration at ground level is adjusted to give the desired visibility; then a constant exponential lapse rate is defined between ground level and 5 km. The aerosol concentration profile, as in most atmospheric models, is assumed to be unchanged above 5 km altitude regardless of the visibility at the surface. This implies that essentially none of the particulate contaminants are carried above 5 km altitude.

[redacted] The calculated transmission increases as expected with increasing visibility. These curves represent a burst at 5000 ft with no albedo surfaces present. The representative arctic humidity is 1 g/m^3, and the spectrum corresponds to a high-yield burst. At a range of 10 km the transmission for 30-mile visibility is about 50% higher than that for 6 miles and 10 times that for visibility of 1 mile. At a range of 30 km the transmission for 30-mile visibility is about 3.5 times that for 6-mile visibility, and transmission for 1-mile visibility is practically negligible.

[redacted] The transmission curves given above refer to a ground level absolute humidity of 1 g/m^3. As shown in Table 1-5 the absolute humidities of the standard atmospheres are .46 in January and 5.6 in July. The effect of the humidity for a particular visibility is very small in the visible region of the spectrum but can strongly affect the portion of the weapon energy emitted in the infrared. The clear visibility curves from reported results correspond to a water vapor concentration that is considerably in excess of that normal for an arctic winter.

[redacted]

[redacted] In Figure 4-2 the effect of changing the absolute humidity at ground level is shown. All quantities except the water vapor concentration are held constant. The ground level concentration is set equal to the desired value and an exponential lapse rate is defined between ground level and 5 km. The profile above 5 km is assumed to remain the same for the various humidities. As expected the effect is not as large as noted with changing the visibility. A surface burst where the entire path is along the ground should show the maximum effect. The overall slope of these curves is determined by the visibility, which here is 30 miles, and the relative placement shows the effect of the water vapor. For the higher concentrations the water vapor absorbs strongly within the first km of the path until the infrared energy is depleted; then the transmission versus range is determined by the visibility. Note that increasing the concentration beyond 5 g/m^3 has a relatively small effect.

[redacted] The large yield bursts have a relatively larger fraction of the yield in the infrared region where humidity effects are important, therefore, these results represent a reasonable upper limit to the effect of humidity on the transmission. The differences shown are not of importance considering the uncertainties in the other meteorological parameters.

4.2.2 [redacted] Ice Fog

[redacted] Some of the effects of ice fog on infrared transmission in Alaska have been reported (Kumai and Russel, 1969). Besides reducing visibility significantly, ice fog can cause attenuation of the infrared beam in an infrared guidance system. The optical properties of fog depend on the number concentration and size distribution of the particles, which can vary significantly during different meteorological conditions. Ice-fog crystals appear as initial stages in the formation of snow crystals at about -40°F. At the very low temperatures often occurring during

[redacted]

[redacted]

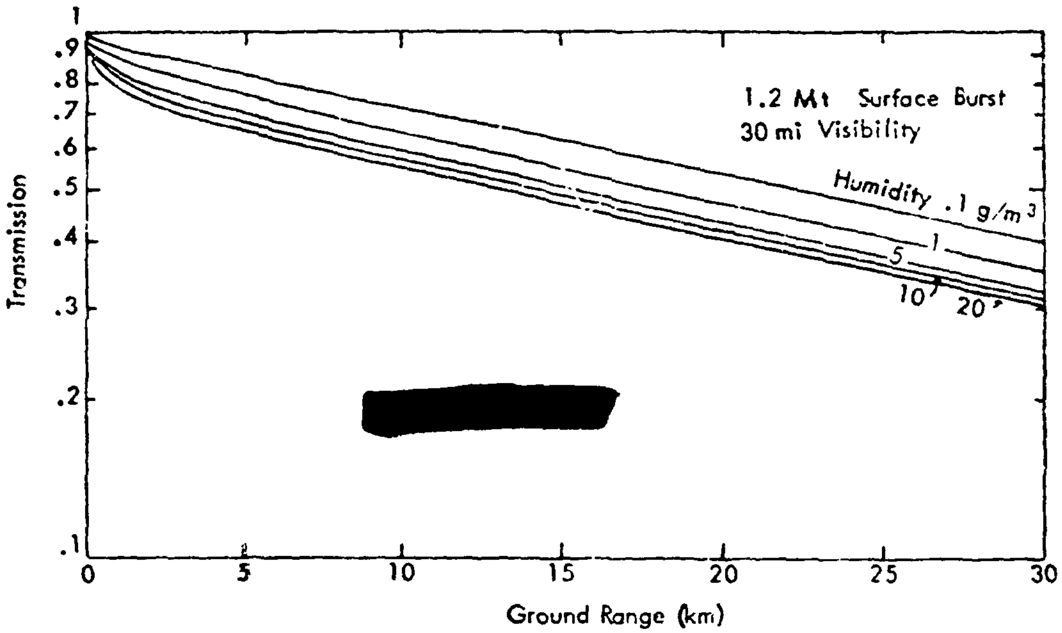

[redacted] FIGURE 4-2 VARIATION OF TRANSMISSION WITH HUMIDITY FOR A SURFACE BURST.

[redacted]

[redacted]

[redacted]

[redacted] the polar winter, the atmosphere can hold very little moisture and surface wind is almost invariably calm. Since conditions are frequently conducive to formation of ice fog from any source of water vapor, the frequency of ice fog has increased with human activity in the arctic.

[redacted] Table 4-2 from the report summarizes the important physical properties of the ice fog at -39°C and -41°C. The ice-fog distribution at -39°C is shown in Figure 4-3. The number of particles and the mass of fog per unit volume are shown as a function of particle diameter.

[redacted] TABLE 4-2

PHYSICAL PROPERTIES OF ICE FOG AT FAIRBANKS, ALASKA

Observations	N ($no./cm^3$)	r_{mode} (μ)	r_{min} (μ)	r_{max} (μ)	Δr (μ)	Air temp (°C)	L.W.C. (g/m^3)
No. 1(Fig 4-3)	140	3.0	1.5	12.0	0.5	-39	0.08
No. 2	90	1.5	1.5	12.0	0.5	-41	0.02

UNCLASSIFIED

N = total concentration

r_{mode} = mode radius = radius corresponding to the maximum number of ice-fog crystals

r_{min} = minimum radius

r_{max} = maximum radius

Δr = radius interval containing n(r) crystals, where $N = \sum_r n(r)$

L.W.C. = liquid water content

[redacted]

[redacted]

[redacted]

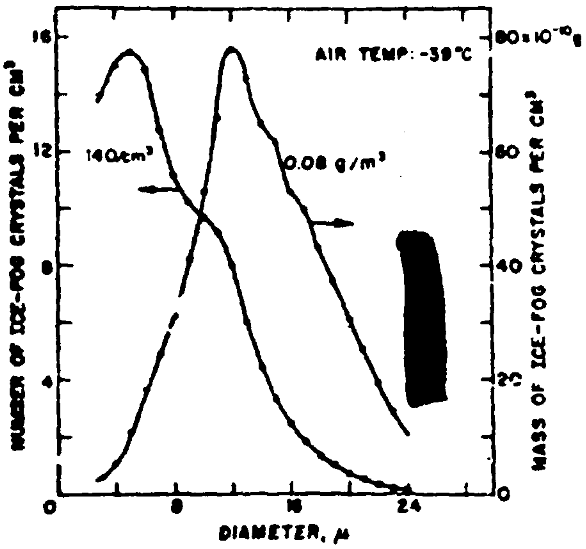

[redacted] Figure 4-3. Size and mass distribution of ice-fog crystals formed at -39°C ambient temperature.

[redacted] Computer calculations of the attenuation and backscattering of radiation by ice fog alone showed them to be within the same order of magnitude as those for water fog of equivalent fog concentrations and observed wavelengths. The optical constants used in the calculations were considered to be known much less exactly for ice than for water. Calculations made for the distribution in Figure 4-3 were presented and are reproduced as Table 4-3 (Kumai and Russell, 1969).

[redacted] These calculations were done for narrow wavelength intervals in the infrared and do show detailed differences at specific wavelengths due to the different scattering characteristics of the ice crystals and water droplets with equivalent amounts of water involved. The same size distributions were assumed for these calculations which may not be a realistic assumption since the size distribution of the ice fog is considerably different from other types of fog.

[redacted]

[redacted]

[redacted] TABLE 4-3

INFRARED ATTENUATION COEFFICIENTS (m^{-1})

Concentration no./cm^3	Water Content g/m^3	2.2	2.7	4.5	5.75	9.7	10.9
				Wavelength, Microns			
			Ice-Fog				
70	.039	.01153	.01212	.01321	.01304	.00513	.00679
140	.077	.02306	.02424	.02642	.02608	.01026	.01359
280	.15	.04611	.04848	.05283	.05216	.02052	.02717
420	.23	.06917	.07272	.07925	.07824	.03078	.04076
			Water-Fog				
70	.039	.01153	.01217	.01314	.01282	.00784	.00546
140	.077	.02305	.02434	.02628	.02564	.01568	.01091
280	.15	.04611	.04868	.05256	.05127	.03137	.02182
420	.23	.06916	.07303	.07885	.07691	.04705	.03273

[redacted]

[redacted] Another paper on visual range in polar regions (Mitchell, 1958) also states that the visual range in ice fog is characteristically very low, frequently less than a quarter of a mile. The total particulate water content of ice fog is comparable to that of other fogs, as shown in Figure 4-4, but the average ice-fog particle is smaller. Thus the ice-fog contains more particles and favors greater optical scattering. Because ice fog is often a man-made phenomenon, it is a particular problem at arctic military installations.

[redacted] The details of the transmission of thermal energy in the atmosphere depend upon the aerosol particle distribution as well as the concentrations. The scattering phase functions determine the details of the thermal transport including the angular distributions and transmission factors. The

[redacted]

[redacted]

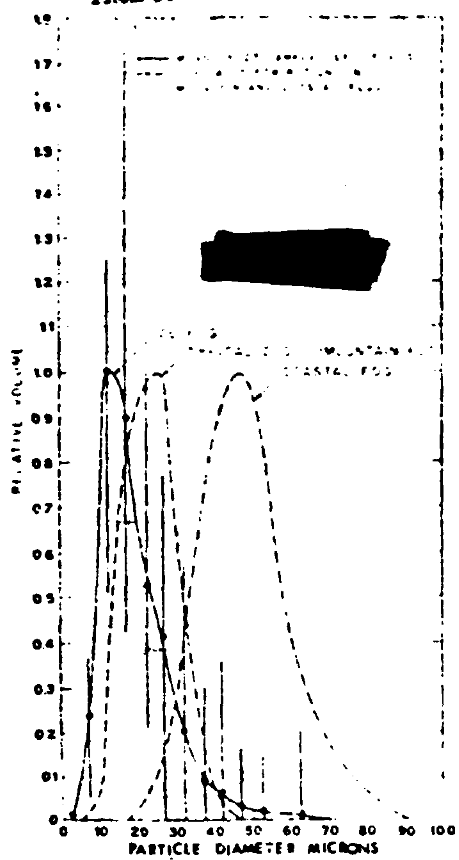

[redacted] Figure 4-4. Comparison of typical particle volume distributions for ice fogs and water fogs (Mitchell, 1956).

[redacted]

phase functions depend upon the particle properties and size distribution. No calculations of the Mie scattering functions have been made for distributions peculiar to the arctic region. All transmission curves in this section were prepared by using available phase functions derived to represent the aerosol distributions found in temperate polluted areas.

[redacted]

[redacted]

4.3 [redacted] Albedo Surface Effects

[redacted] The nature of the clouds and the condition of the surface in the vicinity of a nuclear detonation can considerably alter the amount and direction of thermal radiation reaching a target. Although there is great geographical and seasonal variability throughout the world in these parameters, more extreme variations occur in arctic and subarctic areas. The number of variables involved and the range of possible variations in these parameters make a comprehensive consideration of the reflection or albedo problems very complex.

[redacted] In terms of thermal radiation, surfaces or atmospheric anomalies which reflect radiation are known as albedo surfaces. Surface albedos range from 0 to 1, where the value 1 indicates a perfect reflector. Typical albedo surfaces are the ground plane, especially when covered by snow, ice or water, a cloud layer, and a smoke or haze layer. Dense clouds may have albedos as high as 0.9.

[redacted] Even if albedo surfaces are not present, all sides of an object will receive radiation even though the side facing the fireball will usually receive the dominant exposure. A portion of the radiation traveling upward is lost to space with relatively little being scattered downward unless clouds are present above a burst. If a cloud layer is present a large portion of the incident radiation will be diffusely reflected from the surface with a small fraction being diffusely transmitted. A typical ground surface also reflects the radiation diffusely with the albedo varying from near zero to near unity for snow or ice surfaces. Some materials such as water or ice may also have a fairly large specular reflection. The thermal exposure for targets bounded by clouds and a high albedo ground surface can be several times the vacuum exposure value.

[redacted]

[redacted]

[redacted] Seasonal aspects of the albedo of arctic surfaces north of 65° N latitude have been examined (Larsson and Orvig, 1962) from data in the literature. At high latitudes seasonal variations in albedo are largely determined by the presence or absence of snow cover. In the tundra zone the contrast is greatest. In forested tundra albedo from snow cover beneath the trees is approximately twice as great as from the ground vegetation except in a close-crown forest where snow is caught on the surface for a relatively short time. Different types of ice reflect differently, and although open water and low cloud cover usually are found coincidentally, little information is available on the albedo of open water containing ice. Albedo stereograms in Figure 1-16 represent the seasonal and latitudinal changes in arctic surface albedo.

4.3.1 [redacted] Experimental Results

[redacted] A series of arctic transmission measurements were made by the United States Army Electronics Command, Fort Monmouth, New Jersey (Cantor and Petriw, 1964) in Greenland under various weather conditions with particular emphasis given to the albedo effects of the ground surface and cloud layers.

[redacted] Under many atmospheric and surface conditions, the indirect radiation effects can equal or exceed the direct radiation. A 2π detector is used to simulate a flat plate receiver so that the full indirect as well as the direct transmission can be measured.

[redacted] Such a receiver, near ground level, was employed with a 6500°K point light source about 400 feet above the surface, under generally hazy atmospheres on the New Jersey shore from October 1960 to February 1961. These tests indicated sharp increases of radiation under relatively high surface albedos. The maximum surface albedos, however, are readily obtainable in the arctic or antarctic regions. This led to studying trans-

[redacted]

[redacted] mission effects of an energy source located between two high albedo surfaces, a snow-covered surface and an extensive cloud cover at Camp Century, Greenland.

[redacted] Cantor and Petriw give a very complete description of the experiments of thermal transmission made at Camp Century, Greenland in March, October, and November 1962, where measurements were made on the Greenland icecap to try to maximize the effect of albedo. The terrain was essentially flat and had an albedo of almost unity extending for about 100 miles in all directions.

[redacted] The light source was a xenon flash tube surrounded by a 10"-diameter opal-covered sphere about 100 feet above the surface. The blackbody temperature of the source was about 6500°K. Photomultiplier tubes were used as 2π detectors with no variation in the field of view possible. Occulters were used to block the direct irradiance. Measurements were made at ranges of 0.13, 0.5, 1., 4.5, 7.6, and 10.3 miles whenever conditions permitted.

[redacted] Their report gives a detailed explanation of the weather conditions, experimental configuration, and data obtained each night measurements were made. Plots of the total and scattered transmittance for each night and many of the signal variations as a function of time are also given. Very large, short-term variations of up to 160% were noted in the intensity in time intervals of less than 30 seconds. These largest variations occurred in periods of high visibility and steep temperature inversions with smaller variations occurring for smaller temperature inversions.

[redacted] Figure 4-5 is derived from the summary graph from the report and gives the transmission as a function of range. The labels refer to the visibility in miles followed by the altitude of the cloud layer in feet. Several interesting effects can be

[redacted]

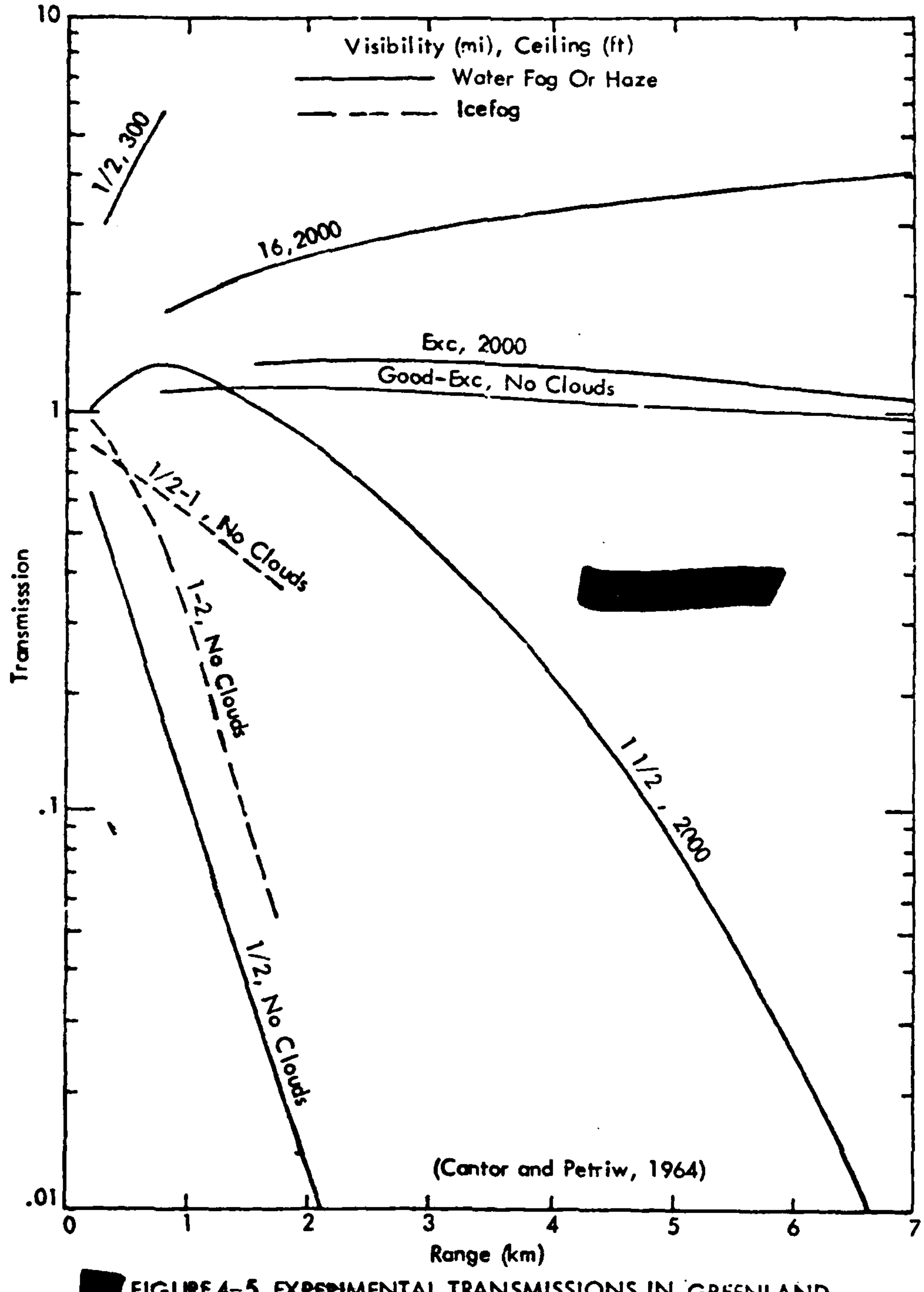

[redacted] FIGURE 4-5 EXPERIMENTAL TRANSMISSIONS IN GREENLAND

[redacted]

[redacted]

[redacted] seen [redacted] comparing the transmissions for the different atmospheric conditions. First note that the case referred to as good to excellent visibility with no clouds shows essentially no transmission variation with range over the fairly short range of the experiment. The addition of a cloud layer at 2000 feet did introduce an increase due to the ducting effect but the change is of the order of only 25%. A much larger increase is noted for the case with 2000 ft cloud layers and a lesser visibility of 16 miles. This general type of behavior is noted in Monte Carlo calculations of this effect as will be discussed in the next subsection, but the calculated effects are much less extreme. Note that for a visibility of 1 1/2 miles and clouds at 2000 ft there is an initial increase in the transmission above unity followed by a decrease in the transmission.

[redacted] For the 1/2 mile visibility case with no clouds a rapidly decreasing transmission is shown. For a cloud layer at 300 feet and 1/2 mile visibility the transmission increases to over 5 at a range of about 1 km beyond which no measurements were made. One would then expect a precipitious drop with increasing range.

[redacted] The dashed curves refer to cases in which the visibility reduction was due to ice fog rather than water fog. There is an indication that for the same visibility the transmission may be higher for ice fog indicating larger scattering contributions and differences in the scattering phase functions.

[redacted] The experimental uncertainty is fairly large; so quantitative measures of the effects should not be derived from these experiments. The measurements do not extend to long ranges as are necessary for nuclear weapon thermal prediction methods. The general trend of the results does agree with results of Monte Carlo calculations of thermal transmission including the effects of albedo surfaces.

[redacted]

[redacted]

4.3.2 [redacted] Monte Carlo Calculations

[redacted] This section will summarize work at RRA (Wells, Collins, Marshall, 1969; Wells, Collins, Cunningham, 1966) begun in the mid 1960's and the further work at KSC (Keith, 1973) in developing Monte Carlo codes describing the thermal radiation transport model atmospheres. Given a complete specification of the atmospheric parameters a calculation of the transmission with these codes will probably be the most accurate that can be obtained theoretically.

[redacted] Monte Carlo calculations (Wells, Collins, Marshall, 1969) have been made of the transmission for a 6000°K blackbody source at 1 km altitude for the model atmospheres representing meteorological conditions for an arctic case and three mid-latitude cases - summer, winter, and a winter inversion. Calculations were run with and without a ground albedo factor. Table 4-4 lists some parameters used in the four atmospheres compared on the graph. The only difference in the summer and winter midlatitude case is in the absolute humidity. The winter case with the inversion added the very low visibility region of aerosols below 2 km. The arctic case was chosen to provide exceptionally high visibility and zero humidity, which as noted previously will increase the transmission by a relatively small factor. A snow-covered surface with cloud distribution was also assumed.

[redacted] In Figure 4-6 the results of their calculations for a target on the ground surface are summarized and replotted. The differences between the summer and winter midlatitude clear visibility cases are relatively small as expected. The exceptionally clear visibility assumed for the arctic case gives a much larger transmission factor. The winter inversion case for a haze visibility of 2.2 km or 1.4 miles results in significant attenuation even at fairly small ranges. The effect of changing the ground albedo from 0 to .9 is seen to result in a significant

[redacted]

[redacted]

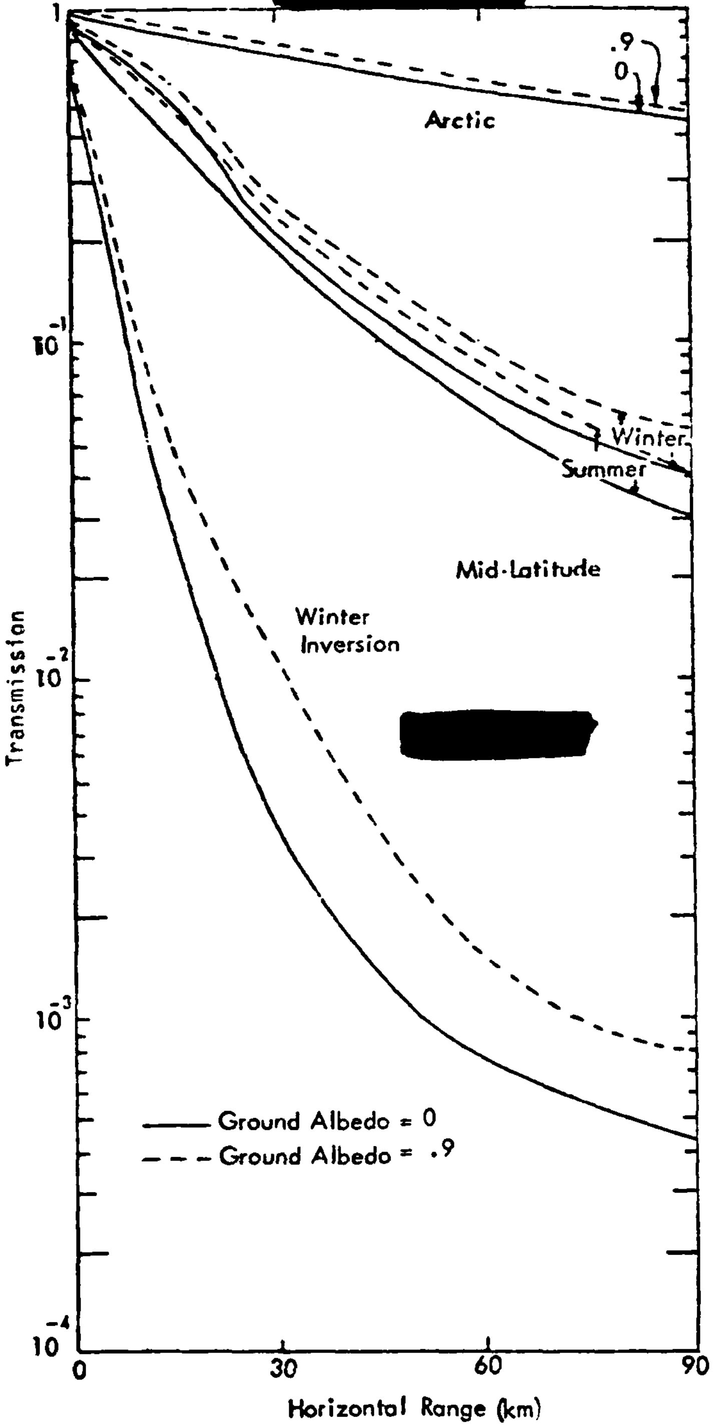

[redacted] FIGURE 4-6. TRANSMISSION IN MODEL ATMOSPHERES (from Wells, 1969)

[redacted]

[redacted]

[redacted] TABLE 4-4

METEOROLOGICAL CONDITIONS
USED FOR MODEL ATMOSPHERES

[redacted]

Atmospheric Model	Ground Level Absolute Humidity (g/m³)	Ground Level Visibility (km)	Aerosol Size Distribution
Summer Midlatitude	12	18	$N(r) \propto r^{-4}$
Winter Midlatitude	3	18	$N(r) \propto r^{-4}$
Winter Midlatitude (Inversion Profile to 2 km altitude)	3	2.2	$N(r) \propto r^{-3}$ to 2 km altitude $N(r) \propto r^{-4}$ above 2 km altitude
Arctic	0	148 (Exceptionally clear)	$N(r) \propto r^{-4}$

* r - radius of aerosol particles

N(r) = aerosol concentration as a function of r

[redacted] buildup of the transmission for the midlatitude cases considered. The effect is only about 5% for the arctic case so that the effect of one high albedo surface for exceptionally high visibilities is not large. For targets above the surface a larger effect is noted.

[redacted] In a recent study (Kaman Sciences, 1978) calculations with Monte Carlo computer codes were done including the effect of introducing albedo surfaces. In Figure 4-7 the effects of various combinations of albedo surfaces are compared. The burst conditions

[redacted]

[redacted]

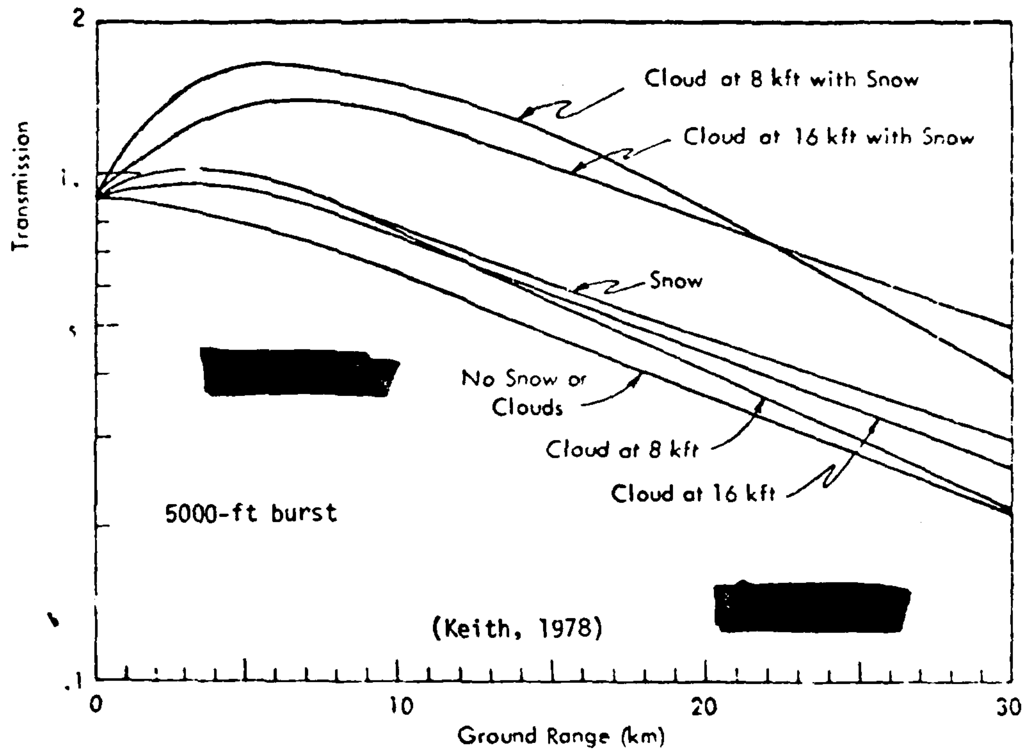

[redacted] Figure 4-7. VARIATION OF TRANSMISSION WITH ALBEDO SURFACES AT 12-MILE VISIBILITY.

[redacted]

[redacted] the same as in the transmission figures in Section 4.2 for varying visibilities and humidities. The ground level visibility is 12 miles and the absolute humidity is 10 g/m^3. The addition of a single albedo surface, either snow covered ground or a cloud layer, causes a modest increase in the transmission of about 20% to 30%. The transmission with only snow cover is seen to be somewhat higher than with only cloud cover. The effect of a cloud layer at 8 kft becomes less with increasing range, and for ranges greater than 30 km a reduction in transmission will occur. The effect of a 16 kft cloud layer is similar except the increase and decrease occur over a longer range. The combined effect of snow cover and a cloud layer can be quite large as noted by the two upper curves on the figure. An increase of up to a factor of about 2.5 is possible. The effect is larger at the small ranges for the lower cloud layer. At much larger ranges than shown on the figure a reduction in transmission will result. In Figure 4-8 similar curves are given for a visibility of 30 miles. The same general trends relative to the curve with no albedo surfaces are obtained with the albedo effect being somewhat larger with the higher visibility. The presence of the albedo surfaces causes a large effect in the transmission factors but since the effect depends upon the cloud height, it must be quantified for specific cases of interest.

[redacted] The effect of two albedo surfaces on the transmission is seen to be very large. The calculations of RRA were done with too large a visibility to represent realistic Arctic conditions and the KSC calculations were done with a visibility lower than can be expected in the Arctic. Neither set of calculations was done with aerosol scattering functions representing aerosol concentrations appropriate for arctic conditions.

[redacted]

[redacted]

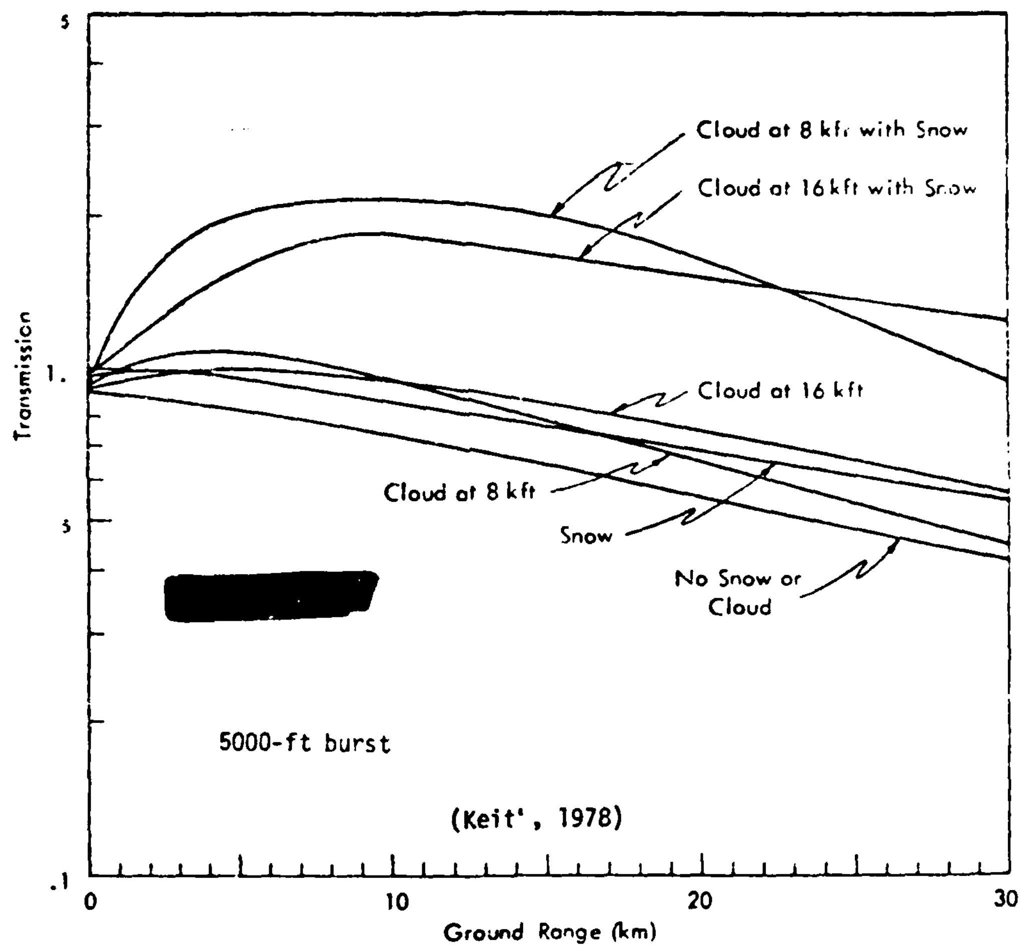

[redacted] FIGURE 4-8. VARIATION OF TRANSMISSION WITH ALBEDO SURFACES AT 30-MILE VISIBILITY

[redacted]

[redacted]

4.4 [redacted] Example Thermal Exposures

[redacted] Figure 4-9 gives curves of radiant exposure from 1 to 1000 cal/cm^2 versus ground range from the point beneath a high-yield burst at 5000 feet altitude. For a very clear atmosphere (30 mi visibility) the exposure is 10 calories per square centimeter at a range of about 15 miles. This same damaging exposure is seen to occur approximately half as far from the burst in a thin fog with visibility of a mile. The upper curve shows the exposure for a visibility of 30 miles with snow cover and a cloud layer bottom at 8 kft altitude. The 10 cal/cm^2 exposure occurs at a ground range of about 22 km which is about 50% larger than for the 30 mile visibility case with no albedo surfaces and a factor of three larger than for the 1 mile visibility case.

[redacted] A recent study (Keith, 1979) considered the thermal environment for a selection of Soviet cities considering the wide variation of meteorological conditions that may result in this area. Representative and extreme days were defined which happen to be of some interest for considering the thermal environment in the arctic. The results are shown in Figure 4-10. The extreme low day refers to a .3 mile visibility with no cloud cover and medium ground albedo which corresponds roughly to a heavy ice fog with no cloud. The extreme high day refers to a 50 mile visibility with a 16 kft complete cloud cover and a medium ground albedo which corresponds roughly to a clear winter arctic day with no fog or haze. For these extreme cases the range corresponding to 10 cal/cm^2 varies from about 25 km to 4 km which is a somewhat larger spread than noted in Figure 4-9 and is much larger than typical for temperate climates.

[redacted]

[redacted]

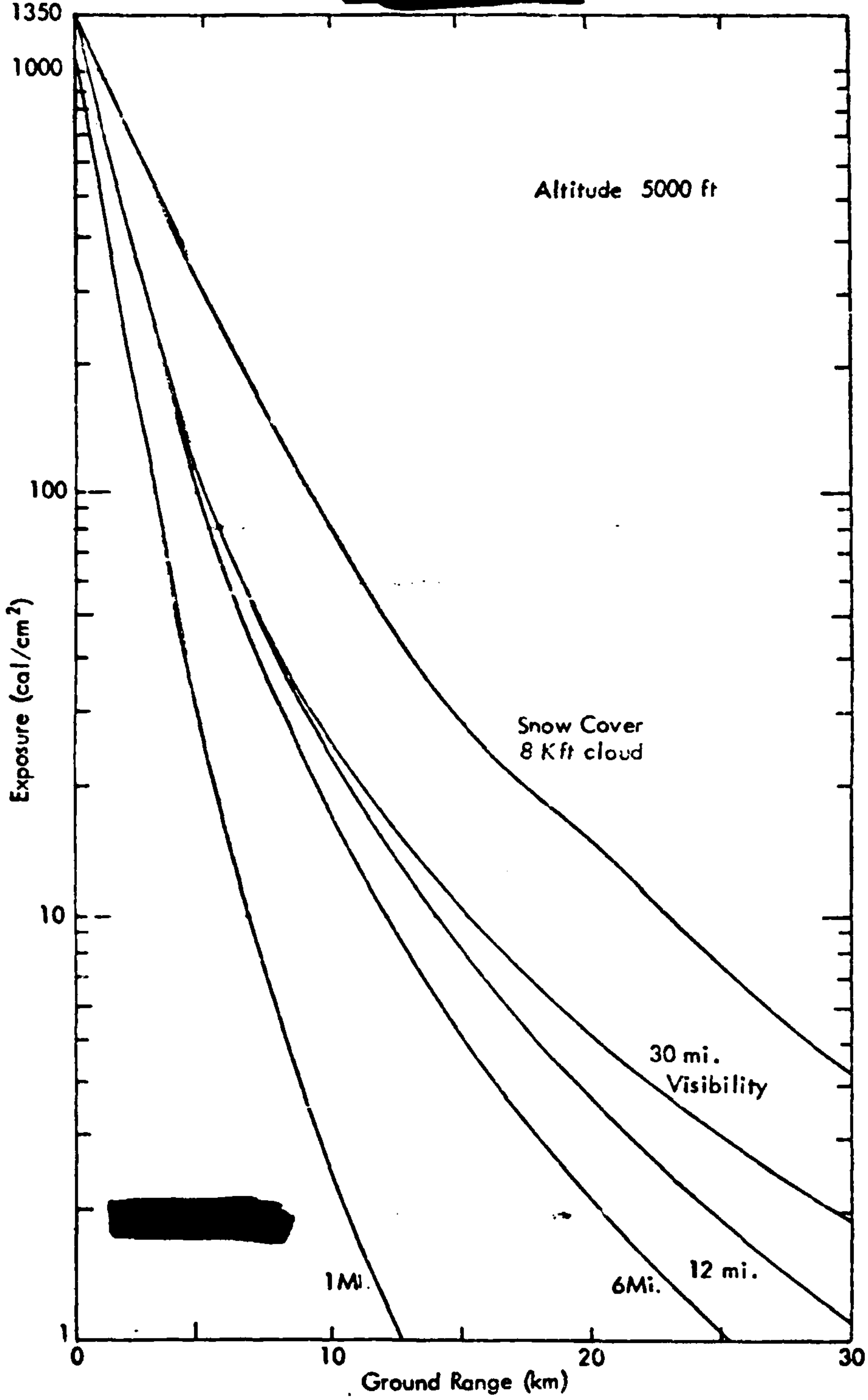

[redacted]

[redacted] FIGURE 4-9 PREDICTED EXPOSURE VS GROUND RANGE AT SAMPLE VISIBILITIES

[redacted] Page 4-29 was deleted

[redacted]

[redacted] All of the examples given previously refer to the thermal exposure received by a target on the ground surface. An important consideration is the thermal exposure on aircraft in the vicinity of the nuclear burst both for consideration of a safe escape range for a delivery aircraft as well as determining the thermal damage potential for attacks on Soviet airbases in the Arctic. No calculations are available for the specific Arctic cases of interest but the transmission results presented in Figure 4-11 shows the type of effect that will be experienced. The transmission is given as a function of horizontal range and altitude from a burst at an altitude of 1 km. The solid lines give the exposure contours for a case with a cloud bottom at an altitude of 6 km and with a medium ground albedo corresponding to desert sand. The transmission for the Arctic albedo case would be somewhat larger. The dashed lines refer to the same burst conditions without albedo surfaces.

[redacted] The ratio of the solid to dashed contour values at the same point in space give an indication of the buildup introduced by the albedo surfaces. Note that the dashed contours are all less than unity and tend to decrease with increasing range and decreasing altitude in a regular pattern. The introduction of the albedo surfaces leads to a much more complicated spatial dependence for the transmission because of the complicated interaction occurring between the attenuation and scattering properties of the atmosphere and the diffuse scattering of the two albedo surfaces.

[redacted] Vulnerability levels of about 100 cal/cm^2 are realistic for aircraft which in previous figures would occur at a range of about 7 km near the ground for the albedo case. Ratios of 1.8

[redacted]

[redacted]

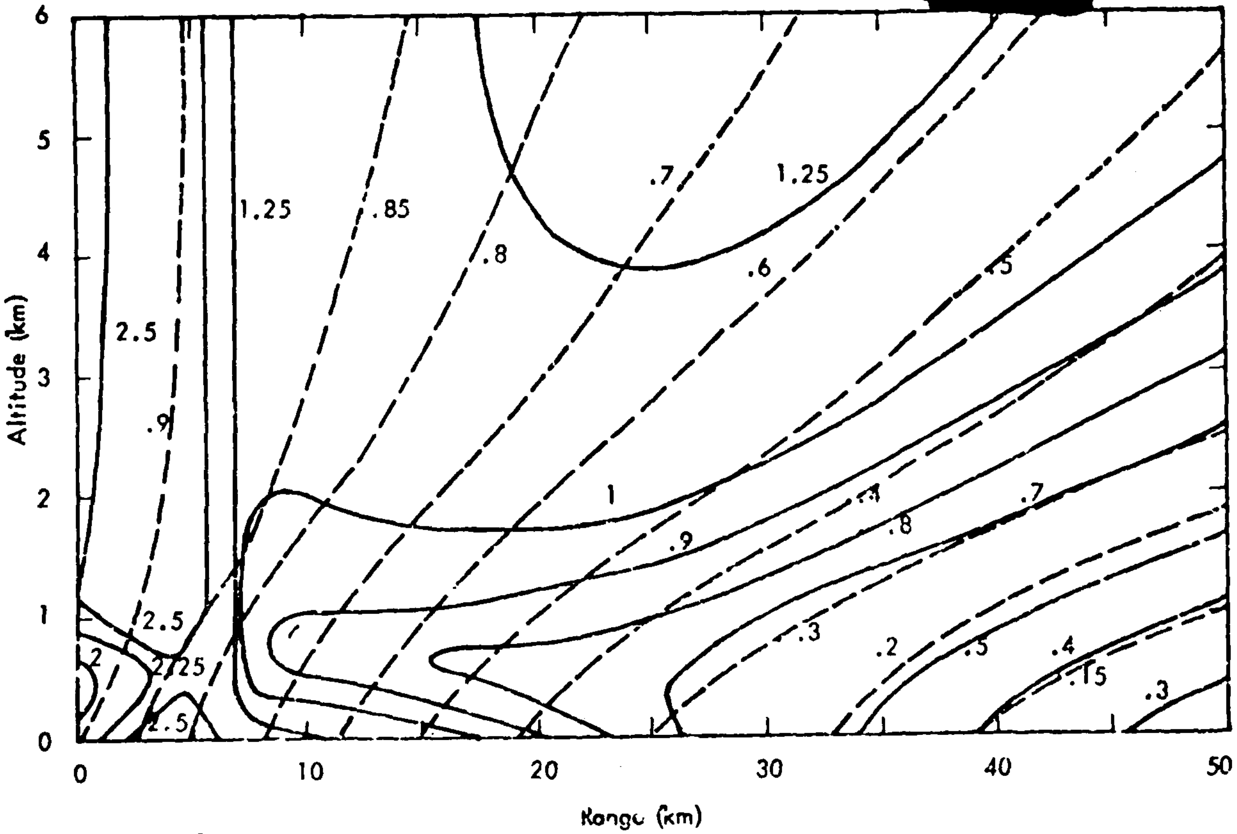

[redacted] FIGURE 4-11 TRANSMISSION WITH AND WITHOUT ALBEDO SURFACES

[redacted]

[redacted]

[redacted]

[redacted] are noted near the ground for these ranges. At higher altitudes ratios of 1.5 are obtained. These represent large differences in exposure levels and could represent the difference between sure-safe and sure-kill environments.

[redacted] Directly above the burst ratios of 2.5 are obtained. At larger ranges representing lower exposures ratios near 3 are experienced at the lower altitudes. In general thermal effects become more important as the yield is increased and as shown in the last three figures, the effects of the albedo surfaces are largest at the longer ranges.

4.5 [redacted] Thermal Effects of Underwater Bursts

[redacted] Thermal effects of underwater nuclear detonations are generally ignored. In Chapter 3 of DNA EM-1, only land surface and subsurface bursts are treated in any detail. It is stated that in the case of underwater bursts, thermal effects in the atmosphere are usually insignificant, and the fact that a 20 kt burst in 90 feet of water produced negligible thermal radiation is cited. (20 kt at 90 ft is a very shallow detonation -- $\sim 33W^{1/3}$.) The presence of ice in the Arctic would tend to reduce thermal effects in the atmosphere even more.

[redacted] Since the thermal energy of an underwater detonation is largely absorbed by the water, the question arises as to whether there will be left a body of heated water sufficient to create and maintain an ice-free pool in a region of otherwise total ice cover. Neither DNA EM-1 nor the Underwater Handbook addresses this question. A limited amount of experimental data has been collected on the temperature changes produced in water by underwater explosions. While most of the data have been acquired on experiments conducted with a steam-generating explosive (Lithanol), developed for the purpose of simulating the bubble behavior of underwater nuclear detonations, a few parallel

[redacted]

[redacted]

[redacted] tests were conducted with Pentolite, a conventional high explosive, and water temperature data were collected during Operation Wigwam. The high explosive tests were conducted in Chesapeake Bay, Puerto Rico, and Panama City during the period 1965 to 1969. Lithanol charges up to 13,000 pounds were used.

[redacted] None of these data has demonstrated any significant heating of the water. The results of the non-nuclear tests have been published in the open literature (Young, 1971 and 1973). Young and Scott, 1970, summarized the existing experimental and theoretical knowledge of the heating of water by underwater explosions and examined phenomena that had not been treated in earlier studies (e.g., Young, 1968 and Young and Scott, 1968).

[redacted] A simple calculation will show that it is not surprising that significant heating effects of underwater explosions have not been observed. Assume an explosion deep enough that the first bubble at its maximum radius does not penetrate the surface, say $d = 240W^{1/4}$. Assume that 100% of the available energy remains in the bubble and is used to heat the water in the cylinder less half sphere that is between the bubble and the surface. It can be shown that the temperature rise in that volume of water is about $2.4W^{1/4}$ °C, where W is in kt. A 10 kt detonation would heat this water less than 5°C and a 100 kt explosion less than 8°C.

[redacted] The conclusions of Young and Scott, 1970 provide the best summary of what has been found in the investigations of the heating effects of underwater explosions:

[redacted]

[redacted] Page 4-34 was deleted

[redacted]

[redacted]

4.6 [redacted] Thermal Damage Effects

[redacted] Thermal damage effects result from absorption of the thermal energy on the target accompanied by a surface temperature increase during the delivery time of the nuclear weapon pulse. The temperature reached in the target depends upon the thermal characteristics of the material, the thermal pulse amplitude and duration, the thickness of the material and the absorptivity of the surface. The range of magnitude of thermal effects ranges from personnel burns that can occur at levels as low as 2 cal/cm^2 to massive melting and ablation of metals in blast hardened structures requiring a thousand cal/cm^2 or more.

[redacted] Thermal burns on personnel in the Arctic will be reduced because of the amount of exposed skin will be much less than in temperate climates. The degree of incapacitation depends upon the fraction of the body burned as well as on the severity of the burn. First degree burns can result from exposures as low as 2 cal/cm^2 for low yield weapons, but a first degree burn must occur over most of the body to produce a casualty. Thus, one would not expect casualties from such burns in the arctic. A less extensive second degree burn may cause a casualty but this takes about twice the exposure for a first degree burn. A mitigating factor is that the parts of the body most likely to be exposed are the face and hands, and a burn on these portions of the body affects performance more than other parts.

[redacted]

[redacted]

[redacted] Flash blindness casualties may be affected in the artic. During the day, the casualties will probably be less than in temperate climates because the high level of light will generally require some eye protection which will reduce the thermal radiation received by the eye, even under the possibly higher arctic transmission. Even if no eye protection is worn, the pupil of the eye will be very small and will reduce the problem. During the long winter nights, however, the eye will be more sensitive to flash blindness.

[redacted] The type of clothing worn in the arctic will tend to reduce the effects of burns. In temperate climates only thin layers of material are usually worn, and if these ignite or melt as can happen with synthetic fabrics, an extensive burn can result. Dark materials will be affected at levels as low as 10 cal/cm^2 for low yield weapons while white materials may require twice as much exposure because of their smaller absorption. In the Arctic since one would probably be wearing several thickness of material, a burn would be much less likely to reach the skin.

[redacted] The effect of the frost covering surfaces in the arctic will be to reduce the absorption of the thermal energy because of its high reflectance. However, the thickness of the frost would be crucial because the fraction of the energy absorbed during the early part of the pulse could melt the frost and expose the underlying surface to the later portion of the pulse. No discussion of this effect was noted in the literature, but the magnitude of the effect can be estimated as follows.

[redacted] Consider the surface loading expressed as the equivalent g/cm [redacted] of water on the surface. Then with the assumed standard temperature of -24°C it will take about 24 cal/cm^2 to bring the frost to melt and another 81 cal/cm^2 to completely melt it for each g/cm^2 of water loading, for a total of 105 cal/cm^2 of absorbed

[redacted]

[redacted]

[redacted] energy. The albedo can be as large as .9 for fresh snow and frost. Therefore, about 1000 cal/cm^2 of incident energy is required to completely remove a frost equivalent to 1 g/cm^2 of water. The hoarfrost and snow buildup can be easily this large under arctic conditions; so that this would result in a very effective thermal shield even at high exposure levels. Note that a frost equivalent to a .01 cm rain would require about a 10 cal/cm^2 exposure to disperse and expose the underlying material. This could be of importance in considering the damage to combustible materials and other materials whose damage level is low such as canvas tents and truck tops.

[redacted] The ignition threshold for materials such as leaves, and newspapers is typically defined for conditions representing a nominal humidity of 30% - 40% in temperate climates. The relative humidity in the Arctic is generally much higher than this, but the absolute humidity or the moisture available in the air is low in the Arctic temperatures. This might result in an effective lower humidity for these materials and a lowering of their ignition threshold.

[redacted] During the warm weather months, one would expect the ignition of fires and their subsequent spread in inhabited areas or forest and dry tundra areas to progress much as in temperate areas. During the cold winters, however, the lower temperatures imply a larger heat input to raise materials to the ignition temperature and sustain burning. Thus, one would expect extensive fires to be a less significant damage mechanism than in temperate climates. Because of the extreme conditions existing in the arctic, however, loss of shelter becomes a very significant factor in survivability and in retaining the capability of performing a mission.

[redacted]

[redacted] The thermal damage threshold for hardened targets such as radars which have been designed to survive large blast overpressures would probably not change under arctic conditions. The amount of energy necessary to raise the temperature from the low arctic value would be negligible compared to that required to cause the relevent material damage. It is possible that for specific designs the high surface temperatures in conjunction with the lower overall structure temperature might result in larger thermo-mechanical loading and an increased warping force. If this occurred in materials that became more brittle at the lower temperatures, then there might be some chance for the structure to suffer damage at a lower exposure due to the lower temperatures. No studies of this applied to weapons effects were found.

4.7 [redacted] Conclusions and Recommendations

[redacted] The arctic is characterized in general as a region of relatively large surface visibilities with the high probability of high albedo surfaces in the form of snow or ice covered terrain and low cloud layers. This combination leads to a very high transmission of thermal radiation as compared to average conditions in temperate locations. At the same time arctic meteorological conditions result in the large probability of occurrence of water and ice fogs and blowing snow which tend to reduce the visibility to less than 1 mile when these conditions are existing. This is a much smaller visibility than will be found in heavily polluted temperate climates. Thus, an extreme variability in possible thermal damage ranges must be expected in the arctic depending upon the specific meteorological conditions at the burst point.

4.7.1 [redacted] Conclusions

[redacted] The low absolute humidity characteristic of the arctic does result in an increase in the transmission of infrared energy as compared with temperate cases with the same visibility. Because of the relatively small amount of infrared energy in the [redacted] output spectrum of nuclear weapons the increase in overall transmission is small. The uncertainties in the other meteorological parameters are larger than this effect.

[redacted] The experimental data showing the transmission of thermal radiation under various arctic conditions are very limited and can not be used independently as a prediction method for general transmission calculations in the arctic. The data do indicate a very pronounced ducting effect for cases in which a high albedo snow layer exists in conjunction with a cloud layer. Enhancements as large as a factor of 100 over the direct exposure were noted for low visibility cases. However, because the direct exposure may be low for these cases, the total exposure may be less than would be noted at the same position for a high visibility. Enhancements of a factor of two were noted in the high visibility cases.

[redacted] Two different Monte Carlo calculations have been made of thermal transmission including the presence of two reflecting surfaces as well as attempts at handling the problem analytically. The simple techniques result in significant over-estimates of the enhancement due to poor handling of the attenuation in the atmosphere even under high visibility conductions. The Monte Carlo calculations indicate possible enhancements of as much as 2.5 due to the ducting effect over the general region of interest for thermal damage.

[redacted] Reliable Monte Carlo calculations require careful specification of atmospheric parameters including detailed information on the suspended particulate matter. The current standard atmosphere profile tables include a 75° latitude model which is suggested for use at all higher latitudes. For the purpose of low altitude nuclear effects this is not a serious problem since [redacted] the available meteorological information gives a good description of the arctic atmospheric conditions near the surface which is of most importance.

[redacted] A few studies have been made of the particle distributions and concentrations for various conditions in the arctic. These have usually been oriented towards providing information on the visibility for aircraft operation. Recent measurements have indicated that layers of aerosols at altitudes of 1 km to 3 km exist often during the winter portion of the year leading to lower visibilities in these layers than observed on the surface. This could lead to predictions of a higher thermal fluence than actually exists for these conditions if the current techniques of using the surface visibility to specify the aerosol distributions are used. One calculation has compared the relative transmission of ice fog and super-cooled water fog. There has been no general study made of the transmission for various wavelengths for the observed particle size distributions and the effects expected in the transmission of nuclear weapon thermal energy.

[redacted] No studies were found relating to the change of thermal damage thresholds due to arctic conditions. The discussion in Section 4.6 reveals that one would expect the thermal damage threshold to be larger under arctic conditions except in particular cases where brittle materials conceivably would be subjected to a more damaging thermo-mechanically induced force than under temperate conditons.

4.7.2 [redacted] Recommendations

[redacted] Analyses of the meteorological information available [redacted] arctic sites should be made to define the relative occurrence of high and low visibility conditions on a seasonal basis.

[redacted]

[redacted] The parameters of interest include visibility, ground albedo, cloud layer definition, aerosol concentrations and distributions and ice and water fog concentrations and distributions.

[redacted] From these analyses reasonable model atmospheres could be defined for purposes of thermal transmission studies. Calculations should be made of the thermal transmission for these model atmospheres emphasizing those cases which result in an enhancement over that expected in temperate climates such as those involving the ducting effect in high visibility conditions.

[redacted] From these calculations, figures showing the predicted exposures under arctic conditions should be prepared. Comparisons should be made with blast HOB charts since in general blast and thermal are competing nuclear damage mechanisms. It may be that considering the reduction that occurs in blast effects over snow that thermal will be of more importance in the arctic even considering the low visibility conditions that can occur.

[redacted] 4.8 Bibliography

Cantor, Israel and Petriw, Andrew, Atmospheric Attenuation of Light Radiation From a Point Source in an Arctic Environment, Technical Report ECOM-2453, U. S. Army Electronics Command, Fort Monmouth, NH, October 1964, UNCLASSIFIED.

Defense Nuclear Agency, Capabilities of Nuclear Weapons, Part I-Phenomenology, Part II - Damage Criteria (U), DNA EM-1 (Change 1), Dolan, P. J., Ed., Defense Nuclear Agency, Washington, D. C. July 1978, SECRET RD.

Glasstone, Samuel and Dolan, P. J., Eds., The Effects of Nuclear Weapons, Third Edition, The U. S. Department of Defense and the U. S. Department of Energy, 1977, UNCLASSIFIED.

[redacted]

[redacted]

Keith, J. R., Nuclear Weapons Thermal Radiation Phenomena, Volume 1 - Analysis, Chapter 2 - Atmospheric Transmission, K-73-534(R), Kaman Sciences Corporation, Colorado Springs, CO., September 1973, UNCLASSIFIED.

Keith, J. R., and Sachs, D. C., Damage Assessment and Strike Burst Environments and Damage Descriptions, DNA 4639F, Kaman Sciences Corporation, Colorado Springs, CO, December 1977, SECRET FRD.

Keith, J. R. Analysis of Soviet Weather Data, K-79-10U(R) Kaman Sciences Corporation, Colorado Springs, CO, February 1979, UNCLASSIFIED.

Kumai, Motoi and Russell, J. D., The Attenuation and Backscattering of Infrared Radiation by Ice Fog and Water Fog, CRREL-RR 264, Cold Regions Research and Engineering Laboratory, U. S. Army Terrestrial Sciences Center, Hanover, NH, April 1969, UNCLASSIFIED. AD-689447.

Larson, P. and Orvig, Svenn, Albedo of Arctic Surfaces, Publication in Meteorology No. 54, Arctic Meterological Research Group, McGill University, Montreal, for Air Force Cambridge Research Laboratories, Bedford, MA, October 1962, UNCLASSIFIED.

Mitchell, J. M., Jr., Visual Range in the Polar Regions with Particular Reference to the Alaskan Arctic, From: Polar Atmosphere Symposium, Part 1. Meteorology Section, Symposium at Oslo, July 1956, Sutcliffe, R. C., Ed., Pergamon Press, Almsford, NY, 1958, UNCLASSIFIED.

Wells, M. B., Collins, D. G., and Cunningham, K., Light Transport in the Atmosphere - Volume I: Monte Carlo Studies, RRA-T63-1, ECOM-00240-1, Radiation Research Associates, Inc., Fort Worth, TX, for U. S. Army Electronics Command, Fort Monmouth, NJ, September 1966, UNCLASSIFIED.

[redacted]

[redacted]

Wells, M. B., Collins, D. G., and Marshall, J. D., Monte Carlo Calculations of the Transmission of Thermal Radiation From Nuclear Detonations in Model Atmospheres, RRA-T810, ECOM-00240-4, Radiation Research Associates, Inc., Fort Worth, TX, for U. S. Army Electronics Command, Fort Monmouth, NJ, March 1969, UNCLASSIFIED.

Young, George A., The Transport of the Products of Very Deep Underwater Explosions (U), NOLTR 67-179, U. S. Naval Ordnance Laboratory, White Oak, Silver Spring, MD, 1968, CONFIDENTIAL, FORMERLY RESTRICTED DATA, AD-388 179L.

Young, George A., The Physical Effects of Conventional Explosions on the Ocean Environment, NOLTR 71-120, Naval Ordnance Laboratory, White Oak, Silver Spring, MD, 3 August 1971, UNCLASSIFIED.

Young, George A., Guide-Lines for Evaluating the Environmental Effects of Underwater Explosion Tests, NOLTR 72-211, Naval Ordnance Laboratory, White Oak, Silver Spring, MD, 13 February 1973, UNCLASSIFIED, AD-758 641.

Young, George A. and Scott, B. W., Explosion Debris Distribution Following Large Lithanol Underwater Explosions (U), NOLTR 68-162, U. S Naval Ordnance Laboratory, White Oak, Silver Spring, MD, [illegible], CONFIDENTIAL, AD-395 126L.

Young, George A. and Scott, Bruce W., Temperature Changes Produced in Water by Underwater Explosions (U), NOLTR 70-29, Naval Ordnance Laboratory, White Oak, MD, 12 August 1970, CONFIDENTIAL, AD-511 453.

[redacted]

[redacted]

THIS PAGE IS INTENTIONALLY LEFT BLANK

[redacted]

[redacted]

SECTION 5
NUCLEAR RADIATION

[redacted] The nuclear radiations considered include the prompt gamma rays, the prompt neutrons, the secondary gamma rays from neutron interactions with air and ground, ground activation products, and the radiation from the fission products from the weapon. The last two components are typically treated together and considered in two time regimes. The initial radiation occurs within a minute or so following detonation while the residual radiation is that which is contained in the rising debris and subsequently is distributed over a wide area as fallout. For the underwater bursts the initial radiation is associated with the base surge, and there will also be some radioactivity remaining in the water which should be considered when considering possible ship or submarine contamination.

5.1 Arctic Environmental Differences

[redacted] The primary atmospheric parameter affecting the prompt radiation dose is the density. As shown in Section 1.2 the January 75° standard atmosphere has a density 16% greater than the midlatitude standard typically used for weapons effects studies. For the temperature extremes noted in Section 1.2 the density will be even larger. For these cases the radiation will tend to be decreased relative to temperate areas.

[redacted] The ground composition can have an effect on the neutron and gamma ray transport in the atmosphere primarily involving the secondary gamma rays. The amount of water in the ground is important.

[redacted] Under arctic conditions involving a snow or ice cover changes might be noted in the neutron and gamma ray dose.

[redacted]

[redacted] Fallout depends upon many parameters which are significantly different in the arctic. The particle size distribution and composition of the swept up debris cloud will be significantly different for the snow/ice situations. The atmosphere profiles of pressure, density and temperature may change cloud rise characteristics. The meteorological conditions in the arctic including wind and precipitation patterns could affect the fallout distributions.

[redacted] The freezing conditions that occur in the arctic area may be important in terms of retaining radioactivity from the base surge on ships near the area.

5.2 [redacted] Prompt Radiation Effects

[redacted] The characteristics of prompt nuclear radiation under arctic conditions will be discussed with regard to effects of the air density, the ground composition, and the depth of burst.

5.2.1 [redacted] Air Density Effects

[redacted] The vast majority of the predictions that are made of the effects of prompt radiation use scaling relationships applied to infinite uniform air transport results. The techniques can involve codes such as ATR (Harris, 1972) or graphical techniques as contained in EM-1. (DNA, 1978).

[redacted] The basic transport results are typically presented as a $4\pi R^2$ dose as a function $F(\rho R)$ of the amount of air between source and receiver (ρR). $F(\rho R)$ will depend upon the particular source spectrum of interest and the particular dose response function desired. The dose at a particular range R is then given by

$$D = \frac{F(\rho R)}{4\pi R^2}$$

where for a uniform density (ρ) case the amount of air is just the product of ρ and R. If the density varies over the path, an [redacted] integral of the density over the path is used in the above expression. At the same range in atmospheres of different densities the dose will be related by the expression

$$\frac{D_2}{D_1} = \frac{F(\rho_2 R)}{F(\rho_1 R)} \; .$$

The function $F(\rho R)$ typically shows a buildup from zero as contributions from multiple scattering increase the dose, then a decrease with increasing ρR as various extinction processes begin to dominate the transport.

[redacted] At ranges for typical environment levels of interest near sea level the $F(\rho R)$ is a decreasing function of ρR. Thus, if $\rho_2 > \rho_1$ then the dose D_2 is less than D_1. Thus, for the winter arctic conditions where the density is greater than in temperate climates a decrease in the radiation will be expected.

[redacted] Example curves are given for several different prompt radiation doses of interest in military systems. In all cases a 1 MT nominal thermonuclear weapon is assumed for the source function for the radiation. The neutron fission heating is used to assess the vulnerability of warheads. In Figure 5-1 the neutron fission heating is shown as a function of range for several different ratios of the density to the density of sea level standard midlatitude atmosphere. Ignoring surface effects, the top curve represents the neutron fluence versus range for the weapon chosen near sea level for temperate climates. The curve marked 1.157 represents the neutron fluence expected for the arctic winter standard case. Note that for a 10^{15} heating level a reduction of about 10% is noted in the range. The higher ratios refer to densities corresponding to more severe cold temperatures that might occur in the arctic. For the extreme case corresponding to a temperature of about -80° which occurs very rarely a reduction of about 21% is noted.

[redacted]

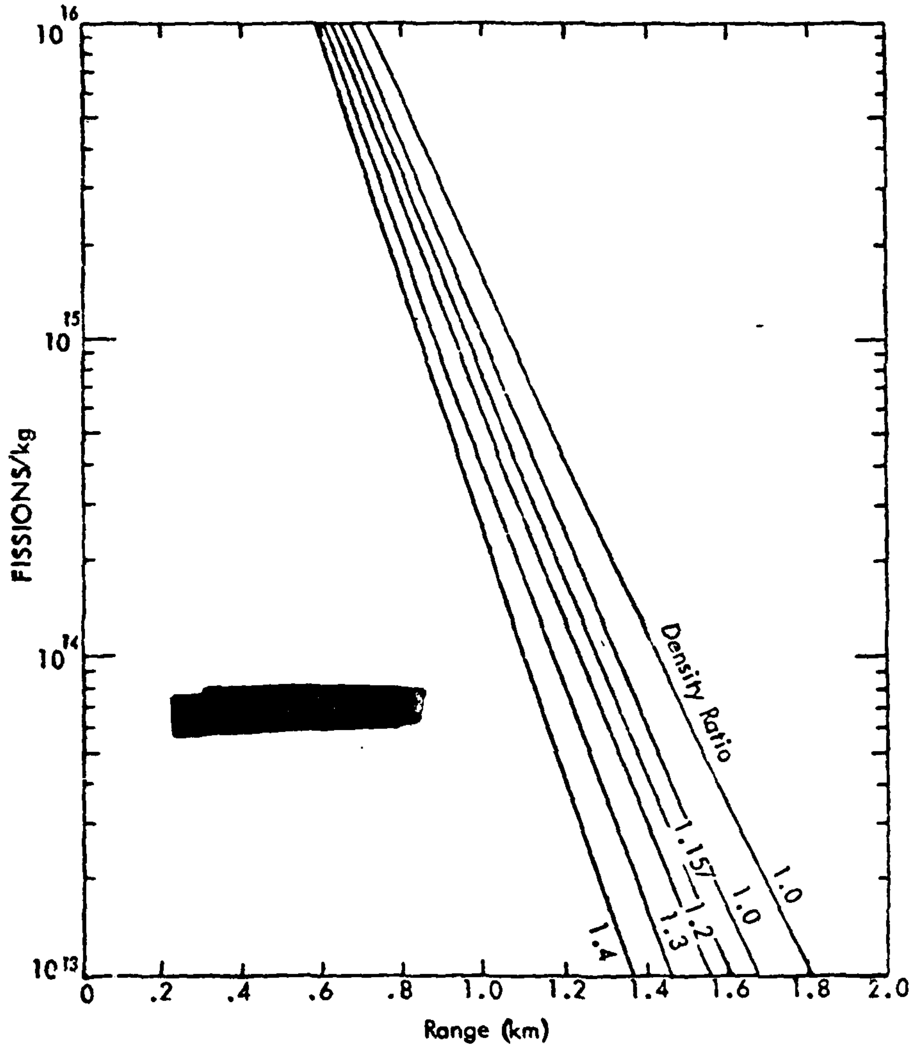

[redacted] FIGURE 5-1 FISSION HEATING AS A FUNCTION OF RANGE

[redacted]

[redacted]

[redacted] The neutron fluence expressed as the 1 MeV Silicon Equivalent fluence is more commonly used to assess the vulnerability of systems. Figure 5-2 shows the 1 MeV Si Eq fluence versus range for the density ratios considered. For a level of 10^{12} the nominal arctic reduction is about 12%. The extreme difference at 10^{12} is about 25%. At higher levels corresponding to vulnerability criteria for harder systems, the difference is slightly less. At 10^{14} the reductions in range are 10% and 22% respectively.

[redacted] The prompt gamma ray dose rate is a common damage mechanism for TREE. In Figure 5-3 gamma dose rates are shown for the range of densities considered previously and for yields of 10 KT and 1 MT. For the 1 MT case and for a level of 10^{10} rad (Si)/sec the reduction for the arctic winter case is 11% and for the extreme case the reduction is 23%. For the 10KT burst, the corresponding reductions are 10% and 20%.

[redacted] In Figure 5-4 the total dose from the prompt gamma rays is shown for a 1 MT source for the density ratios chosen. For the 10^5 level a reduction in range of about 9% is noted for the arctic winter case and a reduction of about 19% is noted for the extreme case.

[redacted] Note that all reductions found for the arctic winter case are about 10% and the reductions for the extreme case are between 20% and 25%. These correspond to area coverage reductions of 20% and 38% to 44% respectively, which might not be insignificant for specific system considerations. Note also that if one enters the curves at a certain range, for instance 1.2 km on Figure 5-2. the 1 MeV Si Equivalent fluence decreases from about 3.5×10^{13} for temperate climates to 1.5×10^{13} for normal arctic winter to 3.5×10^{12} for arctic extreme weather. These are very significant changes in the fluence levels and could easily span the range from sure kill to sure safe for a system.

[redacted]

[redacted]

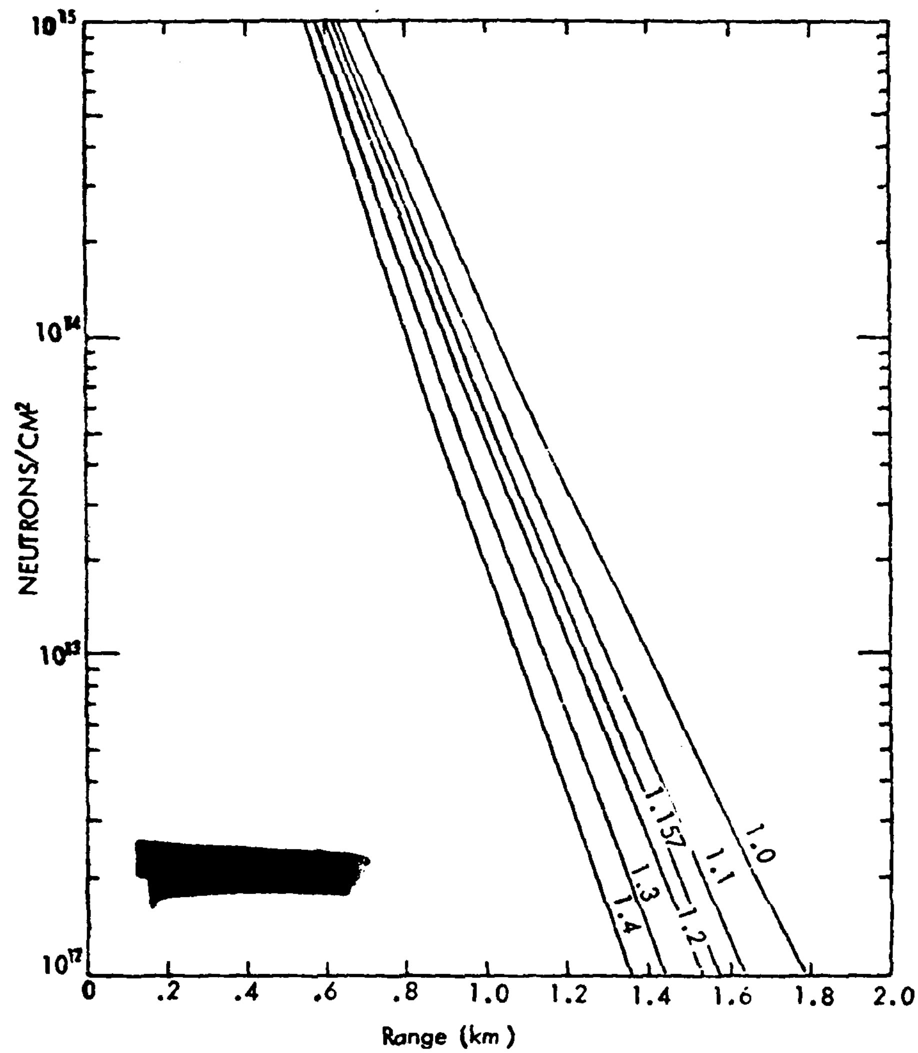

[redacted] FIGURE 5-2 SILICON EQUIVALENT NEUTRON FLUENCE AS A FUNCTION OF RANGE

[redacted]

[redacted]

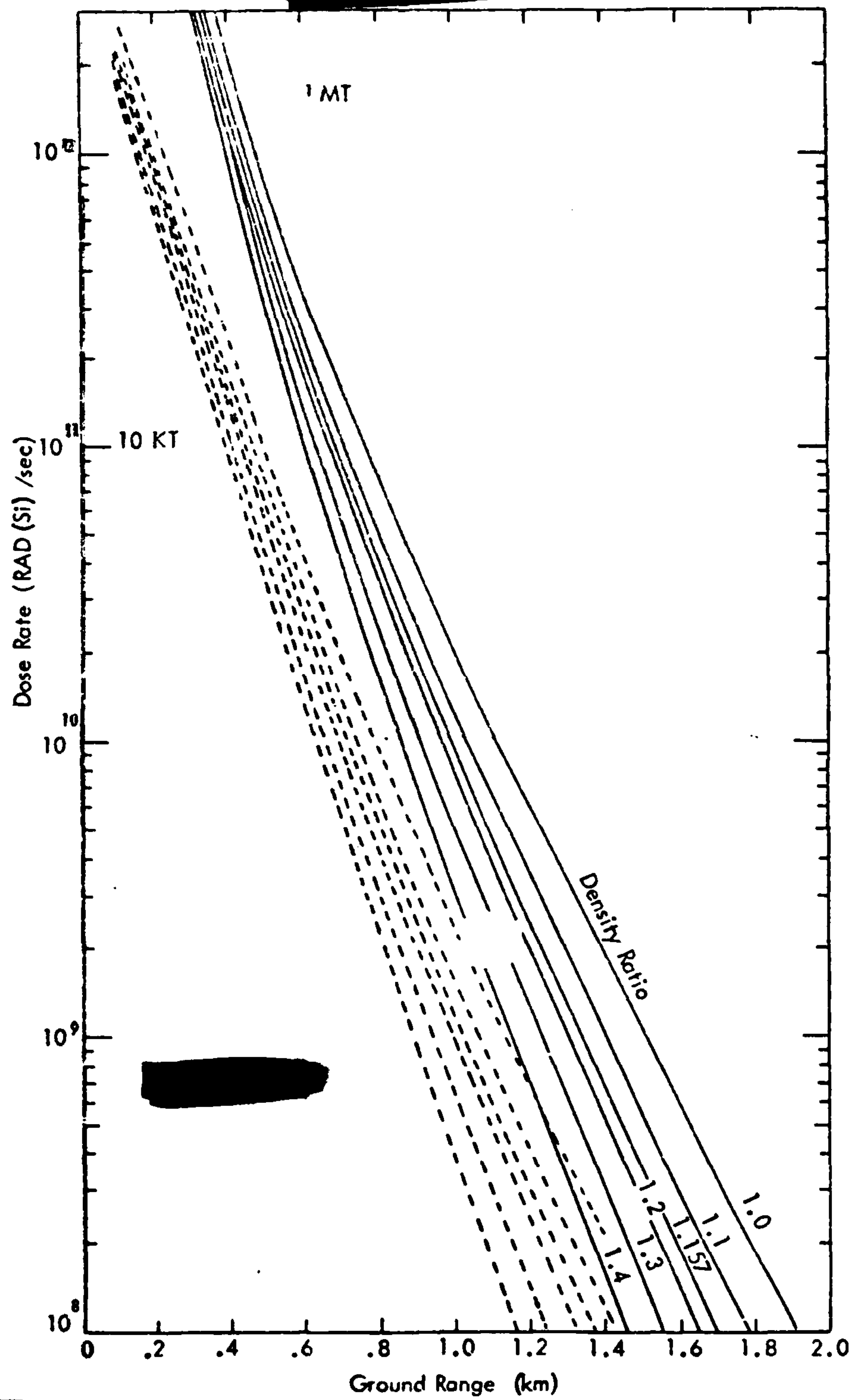

[redacted]

[redacted] FIGURE 5-3 PROMPT γ DOSE RATE AS A FUNCTION OF RANGE

[redacted]

[redacted]

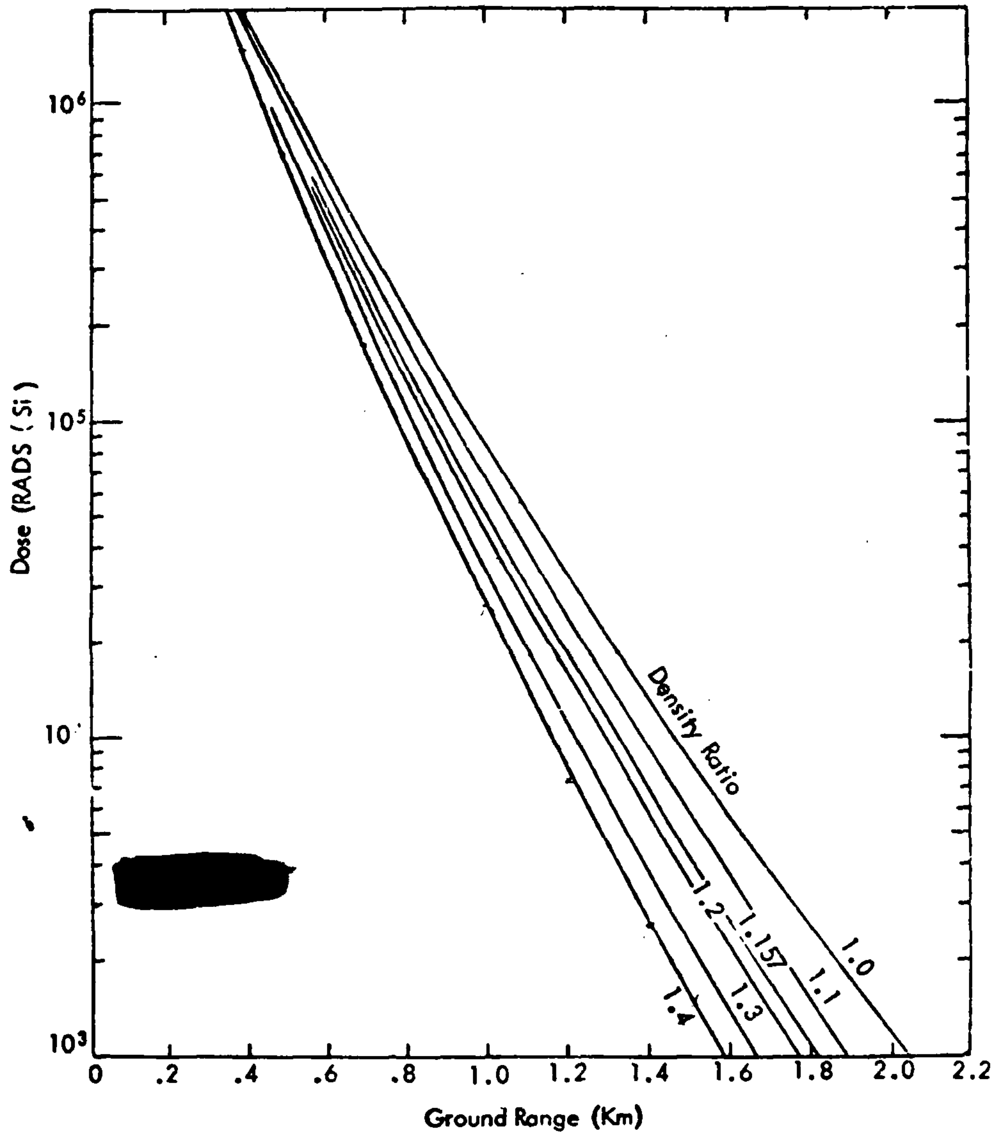

[redacted] FIGURE 5-4 PROMPT GAMMA DOSE AS A FUNCTION OF RANGE

[redacted]

[redacted]

[redacted]

[redacted] The initial fission product radiation depends upon the density in a more complicated fashion than does the prompt radiation. The time scale is such that the atmosphere is significantly perturbed by the weapon. The fireball within which the debris is contained is growing and rising. The shock wave is moving outwards through the air altering the integrated density. Several techniques have been derived to handle this component of the radiation dose as described in EM-1 and computed in ATR. Essentially, infinite air results are scaled to account for the fact that there is a hydrodynamic enhancement because of the low density

[redacted] Page 5-10 was deleted

[redacted]

[redacted] fireball region. If the initial dose is desired, scaling is a difficult task since the time dependence of the various effects must be considered and integrated. The above two techniques use a scaling method due to Mooney and French (1965) to include the ground effects on the dose.

[redacted] Another method developed (KSC, 1974) uses the density profile defined by the HULL code as a function of time and transports the gamma rays through the highly perturbed air by Monte Carlo methods. The HEAT code has been exercised several times to compute specific cases of interest for Ballistic Missile Defense systems. A sample calculation is shown in Figure 5-6 showing the tissue dose as a function of ground range for a 5 MT burst at an altitude of 3.4 ft. The HEAT results are seen to be considerably less than the RRA results which were thought to be compatible with EM-1. However, note that there is significant difference between the RRA model and EM-1. The 500-rad tissue dose level is a very severe personnel dose. At this level and below the difference between the HEAT and EM-1 results are less than 10% while the RRA results are much larger.

[redacted] In comparing HEAT cases run, it was found that the density scaling results using the integrated density from the fireball to field point agreed with HEAT results especially for scaling between comparable cases. For the higher density arctic cases, the fireball will be slightly smaller. Cube root scaling is used to define the fireball radii with increasing altitude (decreasing density). If we use the scaling for higher densities also then reductions of the fireball size of about 4% and 10% would be seen for the arctic and severe density cases. These are within the uncertainties of the fireball modeling itself.

[redacted]

[redacted]

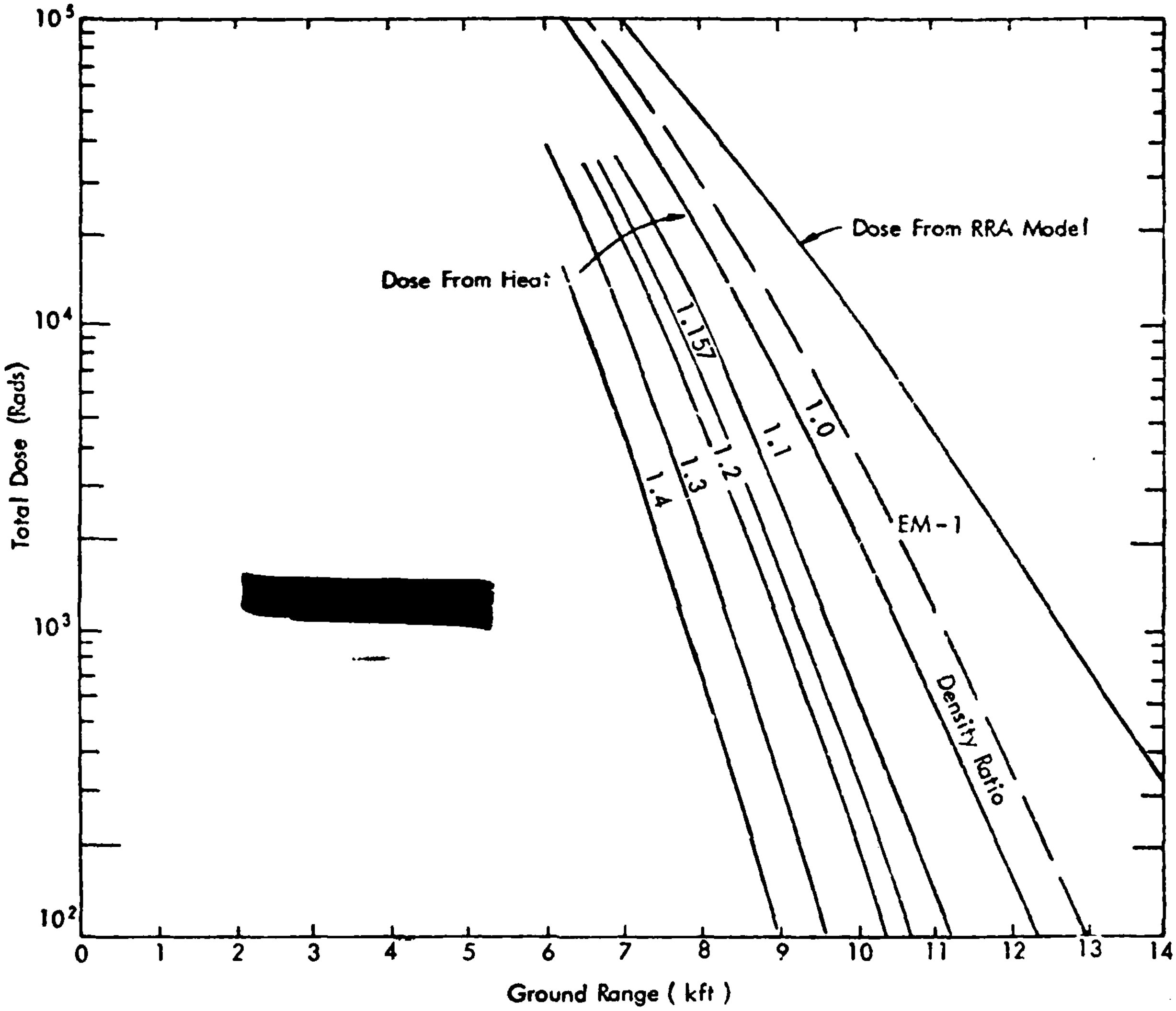

[redacted]

[redacted] FIGURE 5-6 TISSUE DOSE VS GROUND RANGE, 5 MT, 3.4 KFT HOB

[redacted]

[redacted]

[redacted] Therefore, the HEAT results have been scaled by the same scheme as before to show possible dose reductions in Figure 5-6. At the 500 rad tissue level, the reduction is about 13% for the arctic winter case and about 25% for the severe case. Again, these represent significant reductions in area coverage for the arctic cases.

5.2.2 [redacted] Effects of Ground Composition

[redacted] For sources and/or detectors near the ground surface, the radiation fluences are depressed below the infinite air results because there is absorption in the ground and loss of radiation from the atmosphere. The ground composition can affect the production of secondary gamma rays. A set of such calculations (Campbell and Sandmeier, 1973) has been made for several sources and several detector and receiver altitudes above the surface. Surface compositions of dry ground, wet ground and sea water were used to determine the effects of composition. Figure 5-7 shows the results as a function of slant range for a source at 5 m and a detector at 2.5 m above the surface. The results are presented as tissue dose, and the neutron and secondary gamma contributions are shown separately. The neutron dose is seen to be much less than in the free air case and to be essentially independent of surface composition. The secondary gamma doses for the surface cases are larger than for the free air case at the smaller ranges and drop lower at longer ranges. Note that there is some variation in the secondary gamma ray dose for the three compositions and that the difference becomes less with increasing range. The dry ground gives the highest secondary gamma dose and the larger the fraction of water in the ground the smaller the secondary gamma dose.

[redacted]

[redacted]

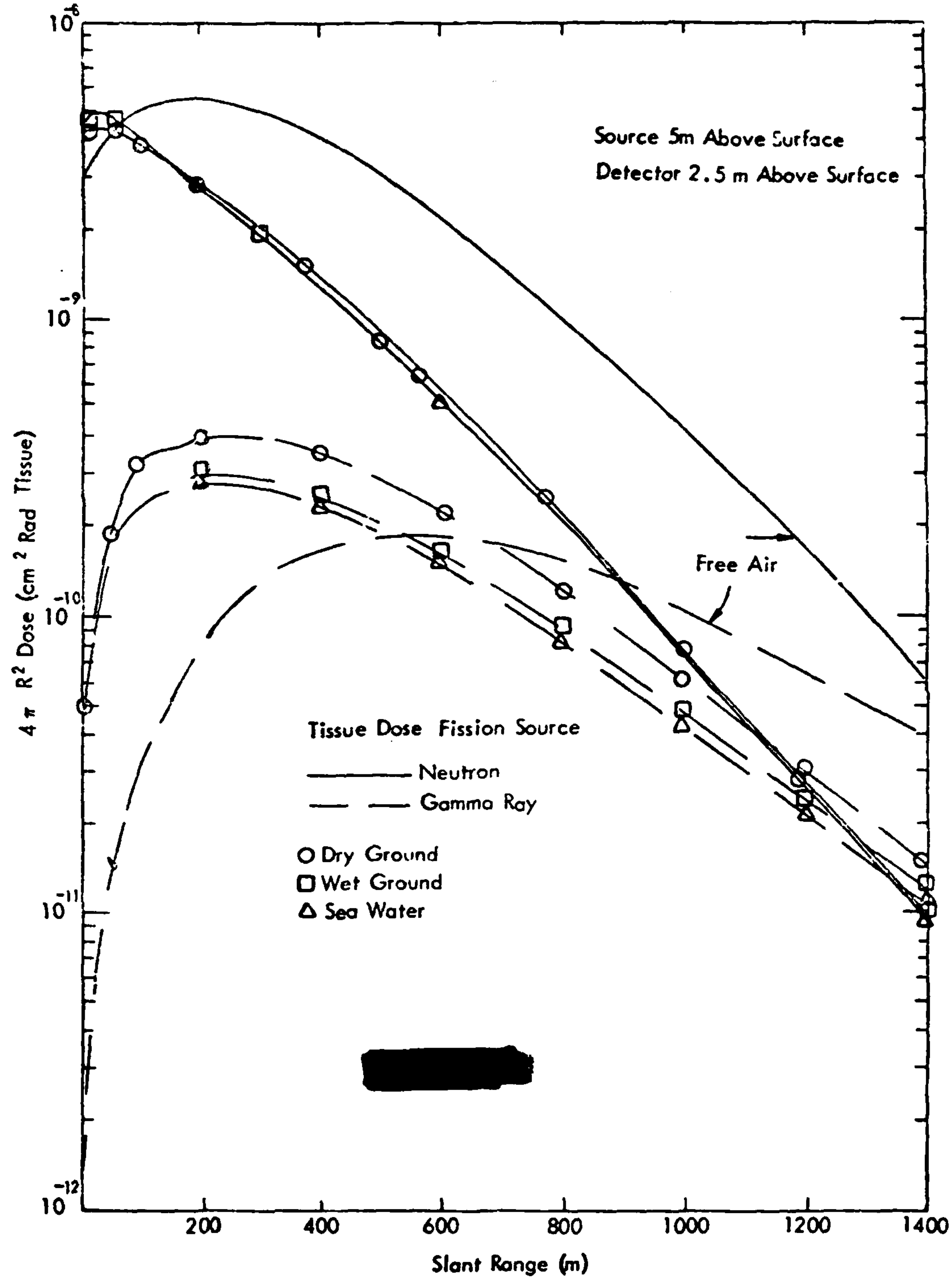

[redacted]IGURE 5-7 EFFECT OF SURFACE COMPOSITION ON NEUTRON AND SECONDARY GAMMA DOSES

[redacted]

[redacted]

[redacted]

[redacted]

[redacted] Arctic soils are said to represent the same general classes that are observed in temperate climates; so no marked departure in the radiation doses would be expected. In the tundra and muskeg areas, the water content is higher than in the temperate climates; so the wet ground curves would be more representative. In those areas with heavy snow or ice cover or over the open sea the sea water curve should be used. It is probable that the curves over fresh water would show some slight decrease below that shown for sea water because of the absence of the salt contribution to the secondary gamma rays.

[redacted]

[redacted] In conclusion, the effect of the ice or snow cover on the prompt radiation would not be expected to be large and would generally be represented by the values that were computed for sea water. The wet ground results should be used for prediction purposes rather than the dry ground as being more representative of arctic conditons.

5.2.3 [redacted] Depth of Burst Effects

[redacted] If the burst occurs below the surface of ground or water, the prompt radiation from the device is strongly affected by the surface material. Only a few feet of material is necessary to markedly reduce the amount of radiation reaching the atmosphere and being transported in the manner described above. No particular differences in this effect would be expected in the arctic as compared with other underground and underwater bursts. In the case of a burst beneath snow, the depth should be measured as the equivalent water depth since the density can be much less than water.

[redacted] The initial radiation from the early time fission products can be an important contributor to the radiation dose even for bursts under the surface. The fission products and activated materials are ejected above the surface and form a radiation source which may be highly anisotropic because of the surrounding surface material ejected into the atmosphere. Calculations of this effect have been made for shallow-buried munitions in the ground, and no major changes would be expected for arctic ground conditions. For those cases involving bursts in ice or snow, no comparable calculations have been made. An estimate of the effect could be made by measuring the snow/ice depth as equivalent soil mass. There is some evidence, however, that for equivalent conditions a larger amount of snow or ice could be ejected into the air resulting in a reduction in the radiation.

[redacted]

5.3 [redacted] Residual Radiation Effects

[redacted] Residual radiation is that radiation that is emitted later than one minute after the explosion. The sources and characteristics of this radiation vary depending on the extent to which fission and fusion reactions contribute to the energy of the weapon. Residual radiation from a fission weapon arises mainly from fission products and, to a lesser extent, from radioactive isotopes formed by neutron reactions in weapon materials and from uranium and plutonium that have escaped fission. Other sources of residual radiation hazard are the activity induced by neutrons that interact with various elements present in the earth, sea, air, or other substances in the explosion environment. The most important of these sources is the neutron-induced activity in soils. The radioactivity from a thermonuclear weapon will not contain the same quantity of fission products that are associated with a pure fission weapon of the same yield; however, the large number of high energy neutrons will produce larger quantities of neutron-induced activity in weapon components and the surroundings. The total radioactivity from such a weapon will, however, generally be less than from a pure fission weapon of the same yield.

[redacted] The residual radioactive contamination (fallout) that results from fission products that are distributed subsequently to a contact surface or subsurface burst is much greater than the radioactive contamination that results from the induced neutron activity. Thus, the neutron-induced activity may be neglected for contact, surface, and subsurface bursts.

[redacted] If a weapon is burst in the transition zone (burst height $<100W^{.35}$ feet) as far as fallout is concerned, the neutron-induced activity generally can also be neglected if the burst height is in the lower three-quarters of the fallout transition zone, i.e., if the burst is below about $75W^{0.35}$ feet. If the height of burst is in the upper quarter of the transition zone (between about $75W^{0.35}$ feet and $100W^{0.35}$ feet), the neutron-induced activity may not be negligible compared to fallout.

[redacted]

[redacted]

[redacted]

5.3.1 [redacted] Induced Activity

[redacted] The type, intensity, and energy distribution of the induced activity produced by the neutrons will depend on which isotopes are produced and in what quantity. These factors depend on the number and energy distribution of the incident neutrons and the chemical composition of the soil. Induced contamination contours are independent of wind, except for some wind redistribution of the surface contaminant. The contours can be expected to be roughly circular.

[redacted] Examination of several thousand analyses of the chemical composition of soils and the relative probabilities of neutron capture by the various elements present in the various samples has indicated that sodium, manganese, and aluminum generally will contribute most of the induced radioactivity. Small changes in the quantities of these materials can change the activity significantly. Other elements can also influence the radioactivity. Some elements have a relatively high probability for capturing neutrons (cross section), but the isotope that is formed after the capture either is not radioactive, does not emit gamma rays, or has such a long half life that the low activity does not produce a hazardous dose rate. The presence of such elements in the soil will tend to lower the hazard from neutron-induced activity.

[redacted] Calculations (Pugh and Galiano, 1959) have shown that the induced activity in sea water is about a factor of 1000 less than in Nevada Test Site soil for times after burst of 1 hour or greater. At early times the contribution of the very short half life ^{28}Al in the soil makes the ratio even larger. From the fact that sea ice has slightly less salt content of sea water and ice over land has a low salt or mineral content, one can assume that induced activity in an snow/ice layer will be less than in sea water.

[redacted]

[redacted]

[redacted] Less induced activation should occur in ice/snow/soil configurations compared to bare soil due to the shielding effect of the ice or snow layer. The magnitude of the effect depends upon the depth of ice or snow. In areas such as the Greenland ice cap, where ice is over 1000-feet thick, little or no neutron induced radiation should occur. The same result should prevail where snow packs of 30-50 feet may occur. Data to support quantitative conclusions with respect to ice and snow have not been discovered.

5.3.2 [redacted] Radioactive Fallout

[redacted] A yet unpublished report (Spencer, Chilton and Eisenhauer) contains an excellent discussion of fallout gamma rays from nuclear detonations with exhaustive literature references in all phases of the fallout problem. In these lists, there are no references to work involving the effects of the arctic environment on fallout.

[redacted] The source of fallout is a combination of the fission products, weapon activation products and activation products from surrounding materials such as soil. For low altitude or surface bursts much of the activated materials will be vaporized or fragmented by the strong shock interactions and swept up into the rising cloud and will contribute to the total fallout dose.

[redacted] At very early times, the fireball is nearly spherical or hemispherical for a surface burst and is beginning to rise as the blast wave begins to move outwards but there has been no significant movement of material. The mixing and entraining of the swept up soil materials is occurring. Calculational models of this development have been described (Huebsch and Olken, 1976) using the HULL hydrodynamics code to describe the flow field from the low altitude burst. Routines are added which describe the growth of water, ice, soluble salts or insoluble particles in the rising expanding cloud. It is possible to include the effect of different meteorological conditions in this model. No cases have been run for conditions approximating the Arctic.

[redacted]

[redacted]

[redacted] A toroidal circulation builds up with very large upward velocities and the gamma source is strongly radiating and moving upwards rapidly. While the movement is occurring the vaporized materials will be cooling and will condense into very small particles. If solid or liquid particles are present, the material will partly diffuse into the surfaces of the particles.

[redacted] For altitudes above which significant solid materials are drawn into the cloud only very small particles will be produced and there will be little localized fallout. In this case, the residual dose near the burst will be primarily due to the induced activity, if any. For lower altitudes of burst, large quantities of material will be entrained and there will be a wide range of particle sizes in the cloud. The larger sizes will precipitate out to form the local intense fallout field and the smaller sizes will remain in the cloud for a long time and may be dispersed over a wide region.

[redacted] The spectrum of debris particles tends to be representative of the soil composition and type. Thus, for bursts in the arctic over land no significant differences would be expected in the cloud loading except possibly a slightly smaller fraction of soil material as compared with water since the water content of the soils in the arctic is typically larger.

[redacted] A burst over snow or ice in the arctic would not contain any of these large solid particles and the average size of the cloud particles would be very small. This would lead to less intense local fallout patterns and a large amount of the radioactive material would be swept to high altitudes and widely dispersed. This case may be nearly the same as occurs with a burst over sea water where the cloud material consists of weapon debris, salt and water. The particles are extremely small but highly hygroscopic.

[redacted]

[redacted]

[redacted] Thus, their size buildup can be very sensitive to local meteorolcgical conditions. The fallout from water bursts is described in EM-1. A much less intense local fallout is expected unless rainout occurs.

[redacted] The salt swept into the atmosphere may have a seeding effect and result in a weapon induced rainout of local material. Because of the lower temperatures and the very high humidity in the arctic, these seeding effects may be enhanced. The moisture capacity of the atmosphere is much less and precipitation may be much more likely than in temperate climates. The particle growth in the cloud may also be affected by the atmospheric parameters. No work in this area was found in the literature.

[redacted] For low yield weapons, most of the moisture comes from air entrained by the developing cloud. In the arctic, the absolute humidity is very low because of the low temperatures so that the water available for producing the larger sized particles may be less. Thus, under these conditions there may be fewer large particles produced and a less intense local fallout.

[redacted] Models have been developed which describe the rising debris cloud and its dispersal by winds. The diffusion of the radioactive material and the influences of precipitation, converging and settling of the particles by gravitation and diffusion are considered. The meteorologic parameters including precipitation, wind patterns, and humidity have a strong effect on the late time fallout.

[redacted] Much of the Arctic region is quite arid. Annual precipitation over the Polar basin, i.e., the Arctic Sea, is less than six inches of water equivalent per year. Most of the precipitation

[redacted]

[redacted]

[redacted] falls as snow. There are local areas such as north of Hudson Bay and eastern Canada with moderately high snowfall (50-100 in.). Lowest snowfall is in the northern Canadian islands and in north Greenland, where total annual precipitation is frequently less than four inches of water.

[redacted] Contrary to some popular opinion, surface winds in the Arctic are on the average very light. Observations from Soviet drifting stations in the central Polar Ocean indicate that monthly mean speed at the surface is about 8-10 knots. However, in well developed storms wind observations show speeds on the order of 50 knots. The mean wind speed increases rapidly with altitude and just below the tropopause (7-8km) the <u>highest</u> monthly <u>mean</u> wind speed may reach 40-50 knots. Maximum wind speeds may be much higher. Wind variability is larger in the Arctic.

[redacted] The fallout prediction models range in complexity from empirical fits to fallout measurements made on the U.S. nuclear test series to very sophisticated numerical models which attempt to describe the development and dispersal of the cloud from first principles. WSEG is an example of the first type of code which has seen wide usage in system codes because of its fast running time and realistic results. The yield of the burst and the wind speed description are the major input parameters. There is no provision for adjusting to other meteorological parameters.

[redacted] NUCROM (Baum et al, 1974) is an example of a code with intermediate complexity. It is a simplified rainout model which allows some freedom in introducing meteorological parameters. A stabilized debris cloud model is used which is then separated into segments as a function of altitude. Diffusion and migration under the influence of wind are considered and scavenging by precipitation events is allowed. The scavenging efficiencies are handled in a gross manner and detailed particle distributions are not considered.

[redacted]

[redacted]

[redacted] DELFIC (Maloney and Klemm, 1975) is an example of a code which attempts to calculate nuclear fallout from basic physical principles without recourse to empirical modeling of the test results. Detailed calculations are made of the debris cloud rise and loading by particulate matter. Particle size distributions and their evolution with time are computed. A detailed atmospheric definition is used. The distribution of activity with particle size is considered. Precipitation clouds are defined and detailed descriptions of the in-cloud and below-cloud scavenging as a function of debris particle size are given. This code is a long running, expensive code to use but is capable of including the full range of Arctic meteorological parameters.

[redacted] Representative calculations were made (Normant, 1974) of the scavenging by rain and snow clouds for tactical nuclear conditions in Germany. In these cases the burst altitude is high enough to minimize the local strong fallout and the activity is contained in micron-sized particles which would disperse over a very wide area with a low intensity. Scavenging by precipitation can, however, under the right conditions produce a very intense local fallout field. The effect is most important for low yields because the stabilization altitude for large yields is higher than normal cloud altitudes.

[redacted] In Figure 5-8 the rain and snow washout coefficients are compared. The precipitation events were picked to fit European conditions with the rain precipitation rate being 20 mm/hr and the snow being 10 mm/hr. For the larger particle sizes the rain coefficient is seen to be almost an order of magnitude larger than the snow but may be comparable in the micron region.

[redacted]

[redacted]

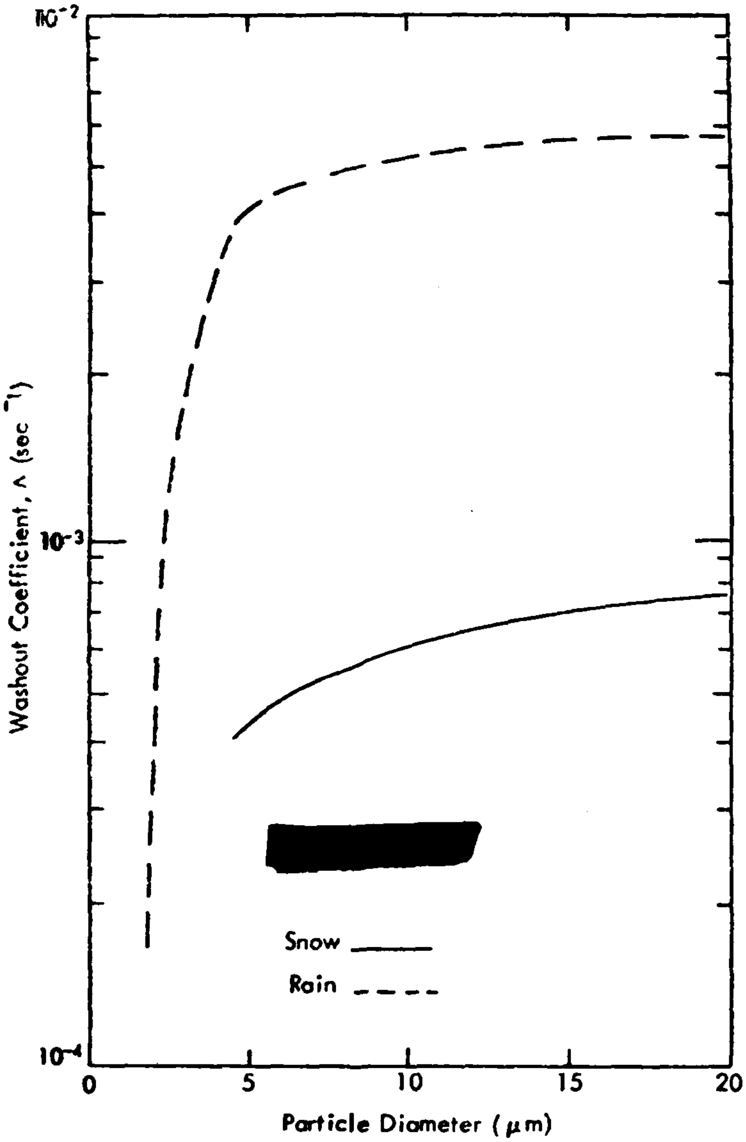

[redacted] FIGURE 5-8 COMPARISON OF RAIN AND SNOW WASHOUT COEFFICIENTS

[redacted]

[redacted]

[redacted] In Figure 5-9 the fraction of particles scavenged is noted for interactions of 10 minutes and 1 hour with rain and snow clouds. Note that for particle sizes above about .3 micron all of the particles are scavenged even in a 10 minute interaction with a rain cloud. The critical diameter is about .03 micron for snow, and a large proportion of the particles with sizes above this diameter are scavenged for a 10 minute interaction. Normant's calculations of the snow scavenging efficiencies do not agree with other calculations and experiments as will be described in Figure 5-11.

[redacted] The main point of these results is that a fairly short interaction of the debris cloud with a precipitation event can result in essentially complete removal of activity from the cloud and deposition on the ground with the precipitation. Calculations made with typical Arctic precipitation rates would be of interest. Considerations of induced precipitation events and the interaction with the debris cloud would be of great interest and may represent the major difference expected in the Arctic.

[redacted] In the previous figures the submicron particle size is seen to be a region where the scavenging efficiency shows a large dependence upon particle size. This is due to the detailed physical interactions that are occurring and their relative importance. For very small particles Brownian diffusion is very important, and for large particles inertial accretion of particles dominates. The interactions are very complex for micron size particles, and electrical forces may play a major role.

[redacted] An extensive study of scavenging was performed at Illinois Institute of Technology Research Institute (Knutson, 1974) with theoretical and experimental studies of the relative rain and snow scavenging efficiencies being considered. Representative results are shown in Figure 5-10 where the snow

[redacted]

[redacted]

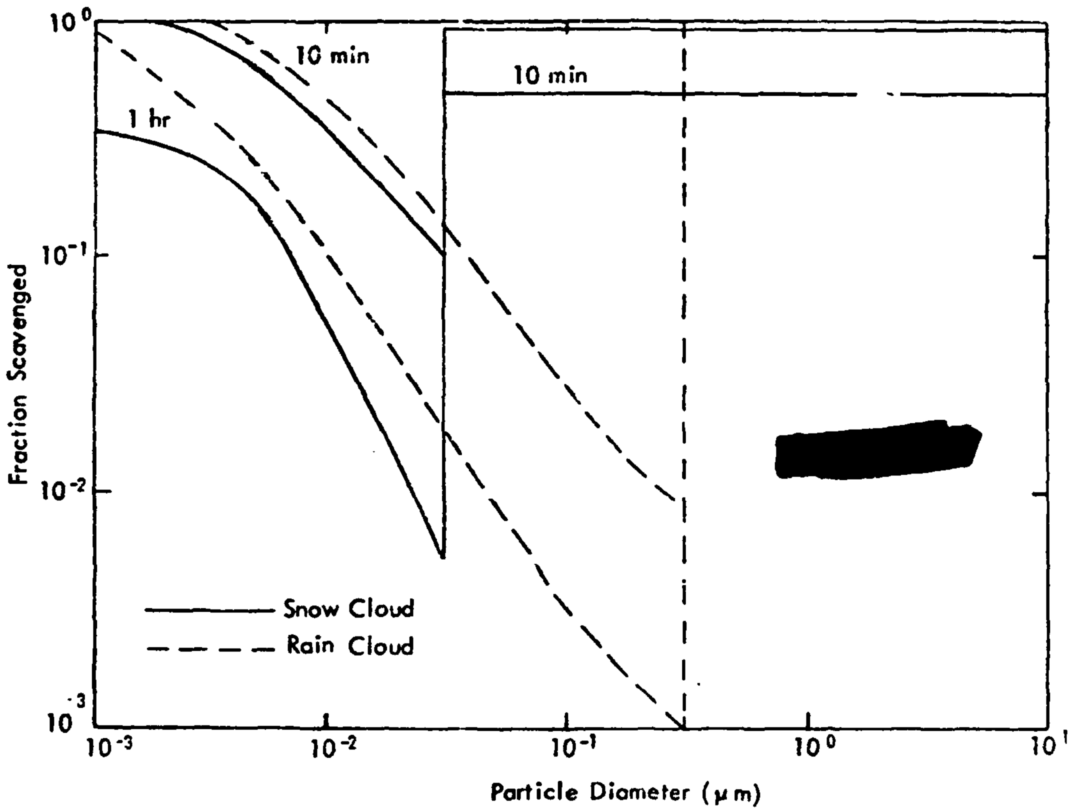

[redacted] FIGURE 5-9 COMPARISON OF CLOUD SCAVENGING FRACTION

[redacted]

[redacted]

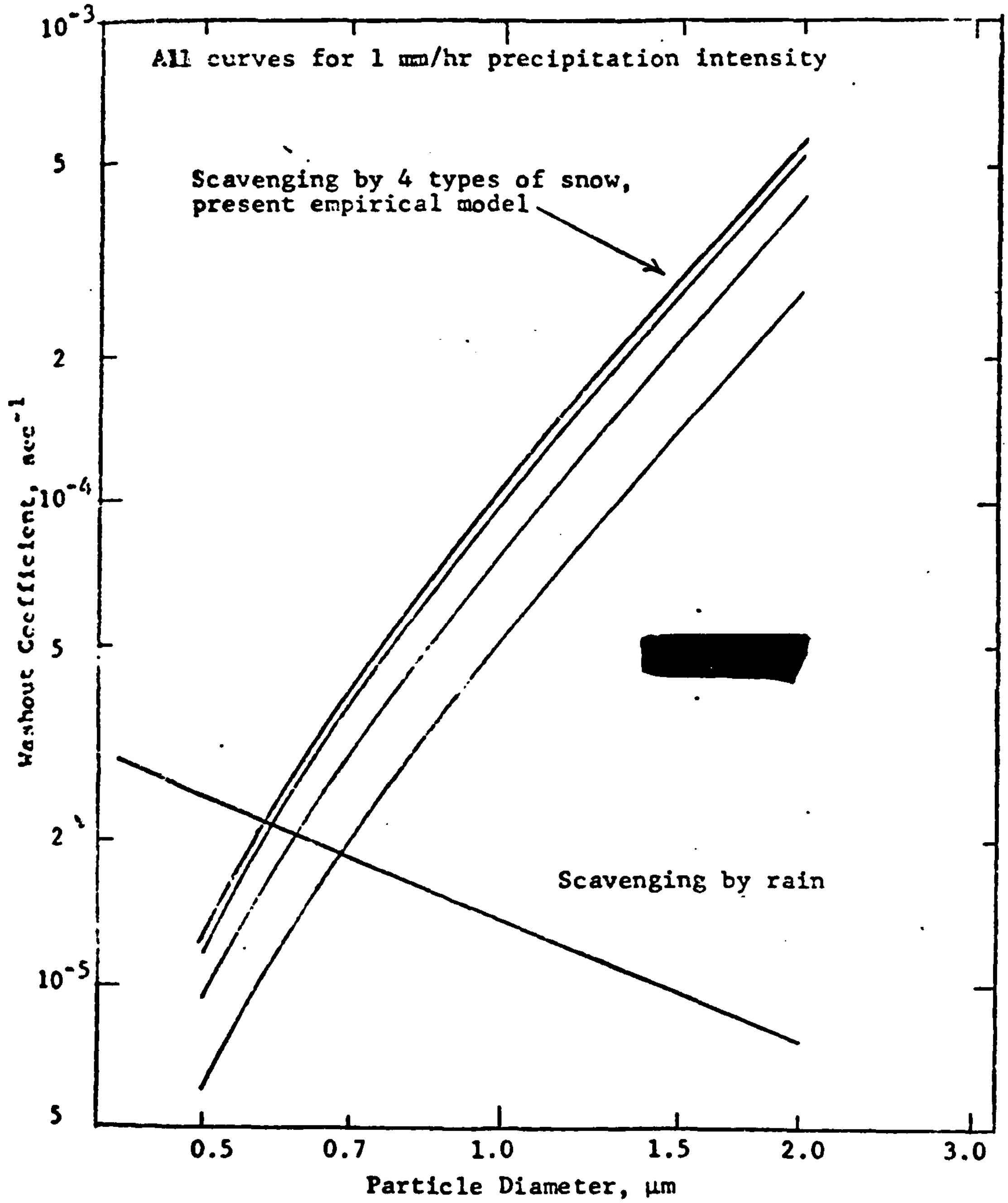

[redacted] FIGURE 5-10. EMPIRICAL MODELS FOR PARTICLE SCAVENGING BY SNOW AND RAIN (KNUTSON, 1974).

[redacted]

[redacted]

[redacted] scavenging is predicted to be much larger than rain for particle sizes above .5 micron. This contradicts the results given in Figures 5-8 and 5-9 and represents the current uncertainties in these types of data.

[redacted] A recent extensive review (Pitter, 1976) considers snow and ice scavenging and the detailed physical interactions that occur. In Figure 5-11 results from various investigations are compared for ice crystal scavenging. Very wide variations are noted for the submicron to micron size range. The left hand portion of Figure 5-11 summarizes theoretical and laboratory results for the snow scavenging coefficient. The Pitter (labeled present results), Starr and Mason, and Sood and Jackson results all show general agreement with the minimum in the scavenging efficiency occuring at about .5 micron. The Knutson results are considerably larger at the .5 to 2 micron size range but are decreasing rapidly at .2 micron with no indication of an increase at smaller sizes. The DELFIC-PSM results equivalent to the results given in Figure 5-9 are also shown and are seen to be drastically different above .05. An abrupt increase in the efficiency at .05 micron is noted then no variation with increase in particle size. The differences in the results are due to different ways of handling the physical processes between the particles and the snow flakes. Also noted on the right hand portion of the figure are the results of various field measurements of aerosol scavenging coefficients.

[redacted] The main point emphasized by this figure is the current extreme variation in values of the scavenging efficiency for snow. The micron particle size is interesting for airbursts and surface bursts over water, snow and ice. This is precisely where a large uncertainty exists, and the differences noted would cause a large difference in the local fallout from a burst when natural or induced precipitation was occurring.

[redacted]

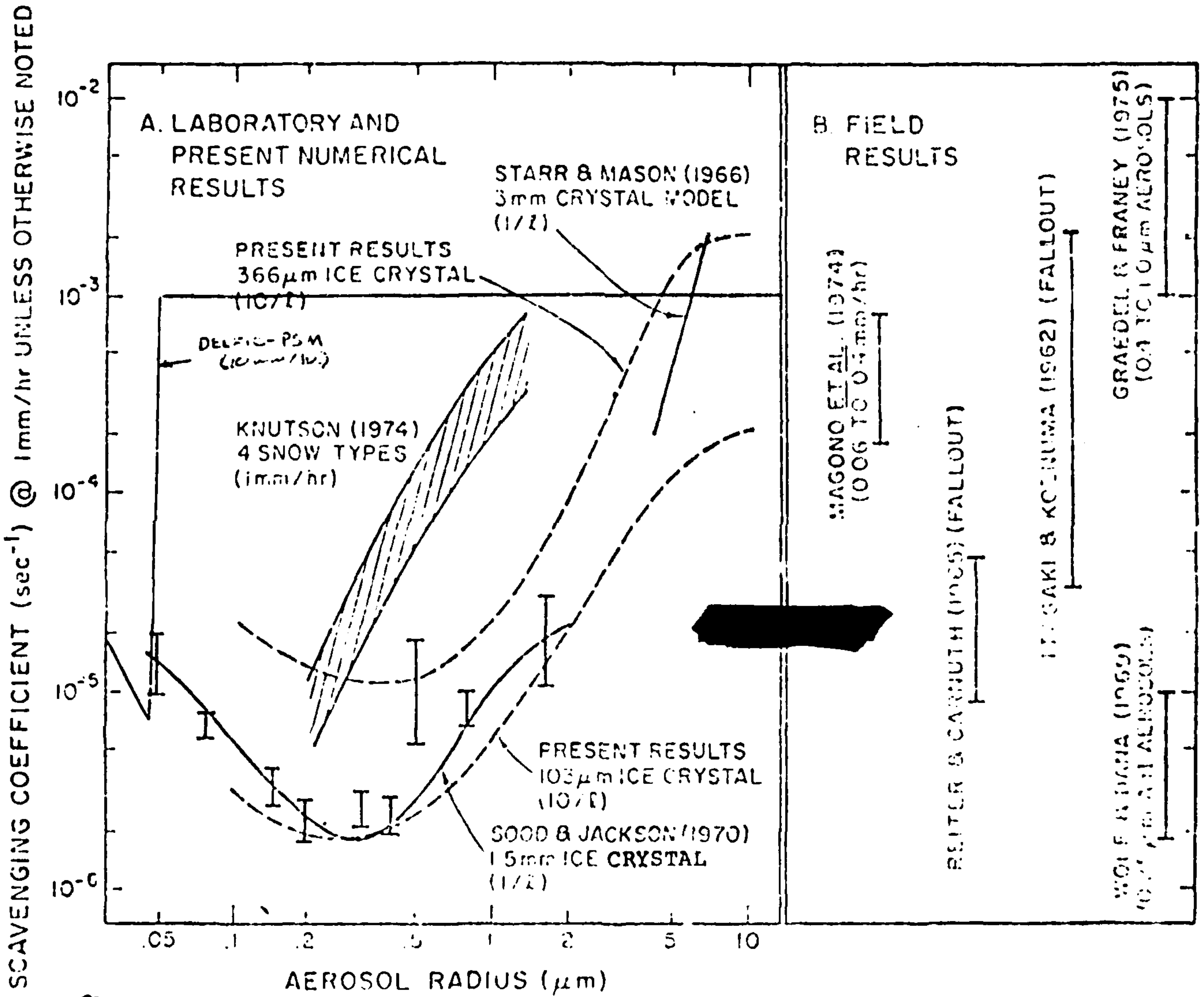

FIGURE 5-11. COMPARISON OF LABORATORY AND FIELD RESULTS FOR ICE CRYSTAL SCAVENGING COEFFICIENTS (Pitter, 1976).

[redacted]

[redacted]

5.3.3 [redacted] Underwater Bursts

5.3.3.1 [redacted] General

[redacted] The sources of radioactivity from an underwater nuclear explosion are (1) the fission product activity in the column and crown, or plumes, (2) the base surge, and (3) the residual radioactivity deposited in the ocean, or radioactive pool. These phenomena are described for a burst in temperate regions in Chapter 5 of DNA EM-1 and in Chapters 7, 9, and 10 of the Underwater Handbook, and methods for predicting the magnitude and duration of the effects are presented. Existing manuals, however, do not address the modifications to these effects that might result from an underwater detonation in Arctic regions.

[redacted] The Arctic environment can affect the sources of radioactivity from underwater nuclear explosions in several ways:

[redacted] • Ice cover may modify the characteristics of the surface phenomena and attendant radiation fields. These phenomena are variable at best, depending as they do on the state of the bubble as it reaches the surface. Part of the energy remaining in the bubble is expended in breaking through solid ice or imparting upward motion to blocks of ice.

[redacted] • Depending upon the depth of burst, an underwater explosion that vents may form a radioactive column, plumes, or base surge. The cold Arctic temperatures will cause freezing of some of these products, producing a local fallout field on the ice and the formation of radioactive ice on the weather decks of ships close to the detonation.

[redacted] • The presence of ice and the typical Arctic water density profile may affect the formation and migration of the radioactive pool, which normally rises to the surface and diffuses fairly rapidly. Heavy ice cover may contain the pool from a venting explosion to the area cleared by the explosion. In the case of a very deep, non-venting explosion, a solid ice cover may contain the pool below the ice so there is no above-surface evidence of its existence.

[redacted]

[redacted]

[redacted] Where the extent of the ice permits operations by surface ships, those operating in the vicinity o: an underwater burst may encounter a buildup of radioactive material on the superstructure and weather decks due to the freez'ng of the base surge and spray from the radioactive pool. Shirasawa and Bjerke, 1968 studied this problem in some detail, using the same computer model (DAEDALUS) used to compute dose rates and total dose for the various conditions presented in the examples of Figures 5-46 through 5-75 of DNA EM-1. The report of Shirasawa and Bjerke is the source of the material in the remainder of this section, including the figures.

[redacted] The factors considered in the study include the transit radiation exposure due to radiation emitted directly from the base surge or the contaminated pool, and the deposit

[redacted]

[redacted]

radiation exposure due to emission from fission products after they have settled on ship surfaces. The transit exposure estimates were based on the DAEDALUS model output (exposure rate) with the assumption that the Arctic environment does not alter the radiation characteristics of the base surge and radioactive pool. The deposit exposure estimates were based on the rate and extent of shipboard icing and the concentration of fission products. A number of previous studies were consulted to determine the rate of formation and distribution of ice and its associated fission products from the base surge and pool. A typical destroyer was selected as the representative ship for the calculations, a nominal 10 kt ASW weapon was chosen, four explosion depths were selected (65, 150, 500, 1000 ft in 5000 ft of water), three post-detonation entry times (10, 20, 30 min), and three ship transit speeds (10, 20, 30 kt).

[redacted] The rate of ice increase is a function of temperature and wind speed. Figure 5-12 is a semi-quantitative presentation of the relation of these parameters. The various regions surrounding the conditions for icing shown in Figure 5-1 indicate the following:

Region I	Wind force is not sufficient to blow spray over ship.
Region II	Temperature is not low enough to cause spray to freeze on surfaces.
Region III	Wind force is so high that green water covers decks and keeps melting ice (ice is possible on higher superstructure).
Region IV	Temperature is so low that spray freezes before striking ship.

[redacted] The central area of the diagram where a "heavy" icing rate is indicated corresponds to 2 tons per hour or greater. The "light" area denotes rates of 1 ton per hour or less. In

[redacted]

[redacted]

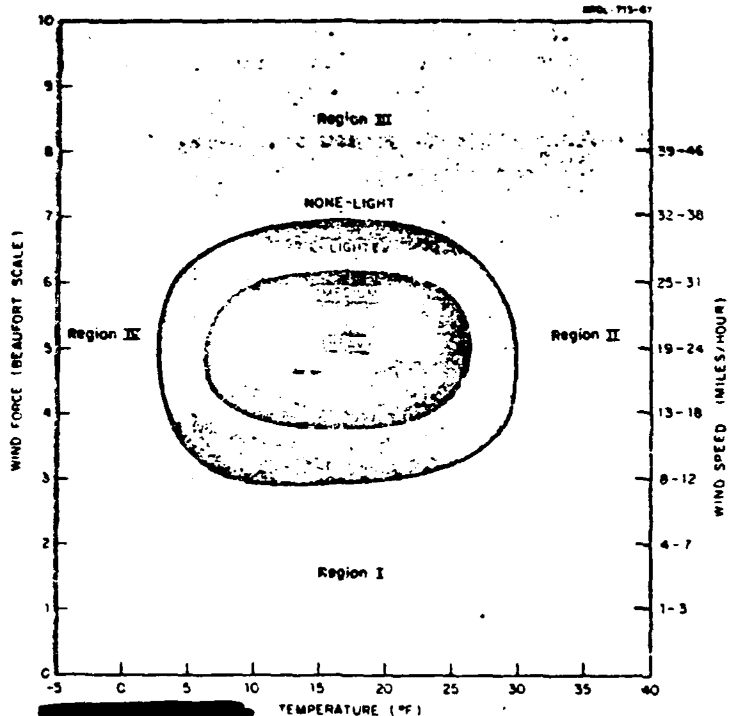

[redacted]

[redacted] Figure 5-12. Icing Rate as Related to Wind Force and Temperature

(Shirasawa and Bjerke, 1968)

[redacted]

[redacted]

this presentation, the situation described for Region I is the least clear. However, in the studies cited no icing was observed when the wind force was less than Beaufort Force 3 in spite of the low temperatures.

[redacted] Serious icing occurs where temperatures below 29°F (-1.5°C) are combined with flying spray, which forms only with winds of 17 kt or more (U.S. Navy Hydrographic Office Pub. No. 705). The areas within which these conditions occur are more restricted in latitude than is generally realized, owing to the modifying influence of water temperatures on surface air temperatures; however, a significant proportion of ocean operating areas may be subject to serious icing conditions. Figure 5-13 shows areas of probable superstructure icing for January-March, May, and November, based on a southern limit of 10% frequency of temperatures below 32°F (0°C).

[redacted] Shirasawa and Bjerke present the results of the computer calculations for a number of combinations of parameters, but in view of the conclusions of the study these will not be given in detail here. To provide for maximum ionizing radiation exposure, they assumed an early (10 min) entry time into the base surge followed by a traversal of the pool, under a no-wind no-drift condition and with concentric base surge and pool still undergoing dynamic expansion during the traversal. Figures 5-14 and 5-15 summarize the calculations and present a comparison between the deposited and transit contributions to the total exposure, for a 65 ft and a 500 ft depth of burst respectively. It is immediately apparent from the figures that the activity entrapped by ice accretions, regardless of source, is not a major contributor to the total radiological hazard. In each case, the exposure contribution made by base-surge deposit is only 8% or less, while the pool spray deposit is negligible.

[redacted]

[redacted]

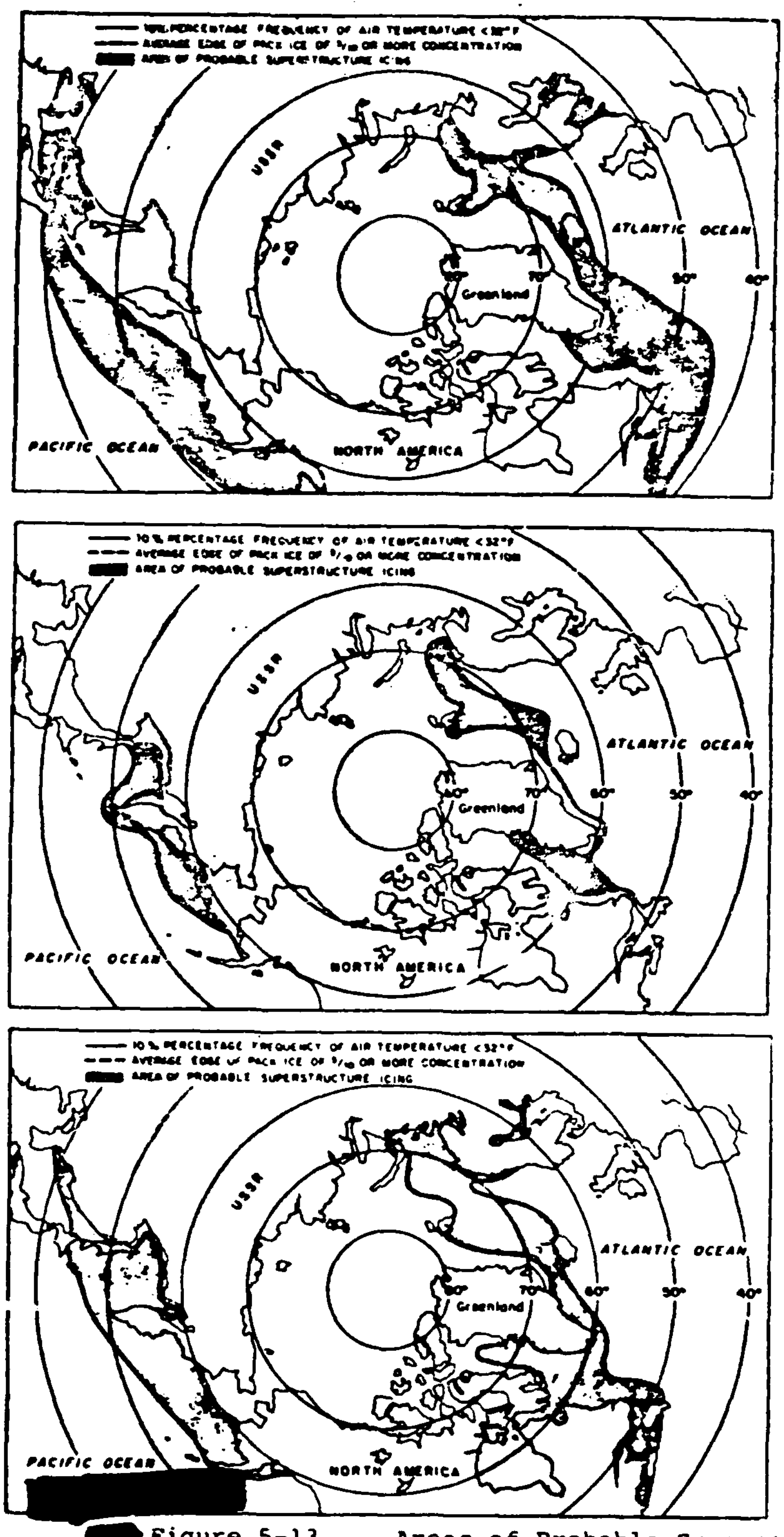

January-March

May

November

[redacted]

[redacted] Figure 5-13. Areas of Probable Superstructure Icing (Shirasawa and Bjerke, 1968)

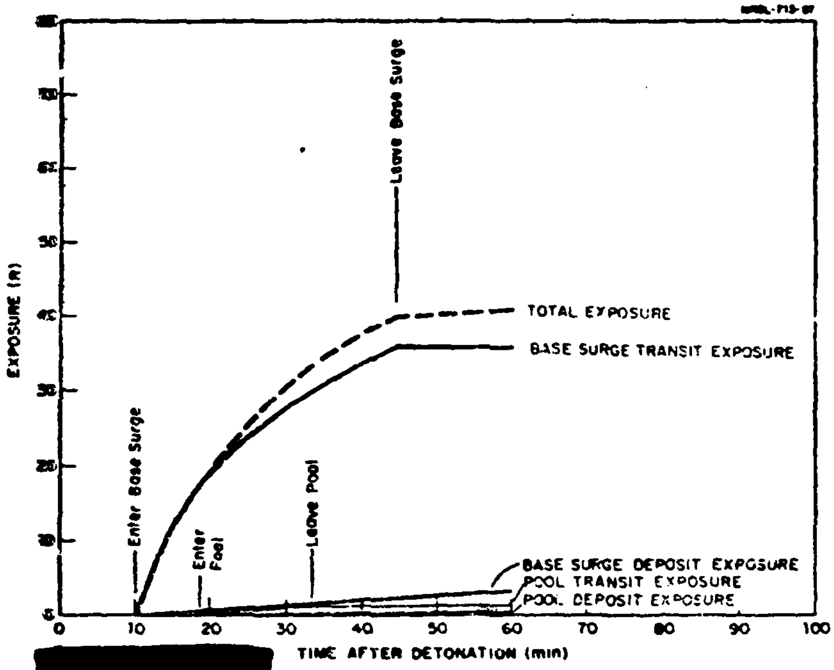

[redacted]

[redacted] Figure 5-14. Total Exposure From Transit and Deposit Radiation for 65 ft Depth of Burst and 10 min Post-Detonation Entry (10 knot ship speed)

(Shirasawa and Bjerke, 1968)

[redacted]

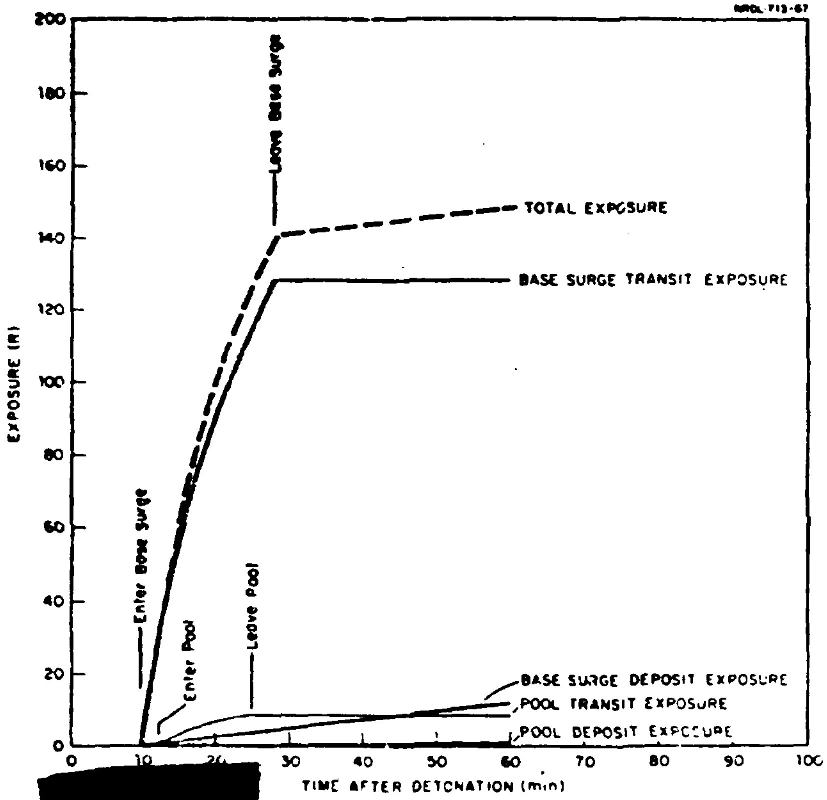

[redacted] Figure 5-15. Total Exposure From Transit and Deposit Radiation for 500 ft Depth of Burst and 10 min Post-Detonation Entry (10 knot ship speed)

(Shirasawa and Bjerke, 1968)

[redacted]

[redacted]

[redacted] The discussion and conclusions of the Shirasawa and Bjerke report are quoted:

[redacted] "In our preceding consideration of contamination by ice-entrapped fission products, the possibility of countermeasures has been wholly ignored. This was purposely done to permit a maximum hazard evaluation. However, it is obvious that several immediate possibilities exist for reducing degradation of personnel and ship capability following contamination of weather surfaces. Three immediate countermeasures which might be considered are:

1. Reduction of number of personnel in high exposure areas and rotation of personnel.
2. Use of ship washdown system.
3. Initiation of ice removal procedures.

The importance of countermeasures is borne out by consideration of the exposure rates existing on shipboard after traversal maneuvers, because of continued exposure from deposited activity, however small. Implementation of countermeasures will also prevent or minimize contamination ingress as well.

[redacted] "Operation of the washdown system aboard a destroyer was shown to be feasible in freezing weather.* Initiation of this countermeasure upon leaving the radioactive pool would contribute to a significant reduction in the ice deposited by pool spray and/or base surge contact. Though icing may continue during the use of the washdown system, the relatively warmer water from the sea would serve to melt and rinse away the contaminated ice accumulated during the pool and/or base surge traversal. It was estimated * that use of the system for 80 minutes or more under conditions of an air temperature of 10°F and a wind velocity of 21 knots would produce a maximum of 1-inch of ice. This of course would be "clean" ice. It has been estimated that 6 inches of ice, or an ice accumulation of 200 tons, on horizontal and vertical surfaces would interfere with the operation of a destroyer in an 80-knot beam wind.

[redacted] "Removal of slush ice after washdown cessation can, if ship mission and stability permits, be accomplished quite successfully by personnel with shovels, brooms, boards and buckets. These procedures would effect the most direct and efficient removal of

---

* Editor's Note: The reference is to a report by Perkins, W. W. and Railey, R. M., Operation of Shipboard Washdown in Freezing Weather, U.S. Naval Radiological Defense Laboratory USNRDL-TR-972, 31 December 1965, Unclassified

[redacted]

[redacted]

contaminated ice. However, these procedures may create the attendant problem of personnel exposure and the potential hazard of tracking activity inside the ship with subsequent danger of ingestion.

[redacted] "The following conclusions would appear to be justified within the general limits of this study.

1. The radiological consequences to naval ships of coming in contact with the post-detonation formations typical of underwater nuclear explosions are not significantly changed by an arctic environment.
2. Radiation exposure resulting from freezing spray of radioactive-pool derivation does not present itself as a problem insofar as interference with the tactical missions of ships is concerned.
3. Radiation exposure from the freezing spray of base surge aerosol exceeds that of pool spray deposit, but it is well below levels which would threaten degradation of ship's effort.
4. Initiation of ship washdown operation and/or manual removal of slush ice can reduce the amounts of deposited fission products to levels comparable to those existing in more moderate environments.
5. The limiting radiation hazard for involvement in post-detonation ship maneuvers will be the transit exposure as a result of encountering the base surge and the pool. There is no reason to believe that this exposure will be significantly changed by an arctic environment."

[redacted] It may be concluded, on the basis of the foregoing, that the estimates of Figures 5-46 through 5-75 of DNA EM-1, prepared for use in temperate climates, may also be used for Arctic environments.

5.3.3.4 [redacted] Radioactive Pool

[redacted] Chapter 10 of the Underwater Handbook contains a detailed technical review of the literature as of December 1966 on the distribution of the radioactive debris and associated

[redacted]

[redacted]

nuclear radiation from underwater nuclear explosions. It was concluded at that time that no adequate comprehensive radiological prediction system existed in the literature. With respect to the radioactive pool, a review of the literature since that time reveals little reason to alter that conclusion significantly. Rinnert, 1967 and 1968 has developed FORTRAN IV computer programs to estimate the exposure rate history and total exposure for surface and subsurface traversals of a radioactive pool, but these are based on the pool model of Ksanda, 1963 and the work of Pritchett, 1966, both of which were available when Chapter 10 was written and were referenced.

[redacted] The Rinnert reports are concerned mostly with the documentation of the programs and do not present results of calculations for ranges of input parameters. They each have an example, however, of information that can be derived from the programs. These examples are presented here, since neither DNA EM-1 nor the Underwater Handbook contains estimates of exposure for a submarine traversal of a radioactive pool. Figure 5-16 shows the calculated exposure rate history for a single set of parameters, and Table 5-1 shows the total exposure for traverses as calculated by the modified Ksanda model (Rinnert, 1967) and by the modified Pritchett model (Rinnert, 1968), for several sets of parameters. Both examples are for unshielded detectors. The submarine's hull and internal piping systems would reduce these exposures by varying amounts, which may be calculated from standard references (e.g., DASA 1892).

[redacted]

[redacted]

[redacted]

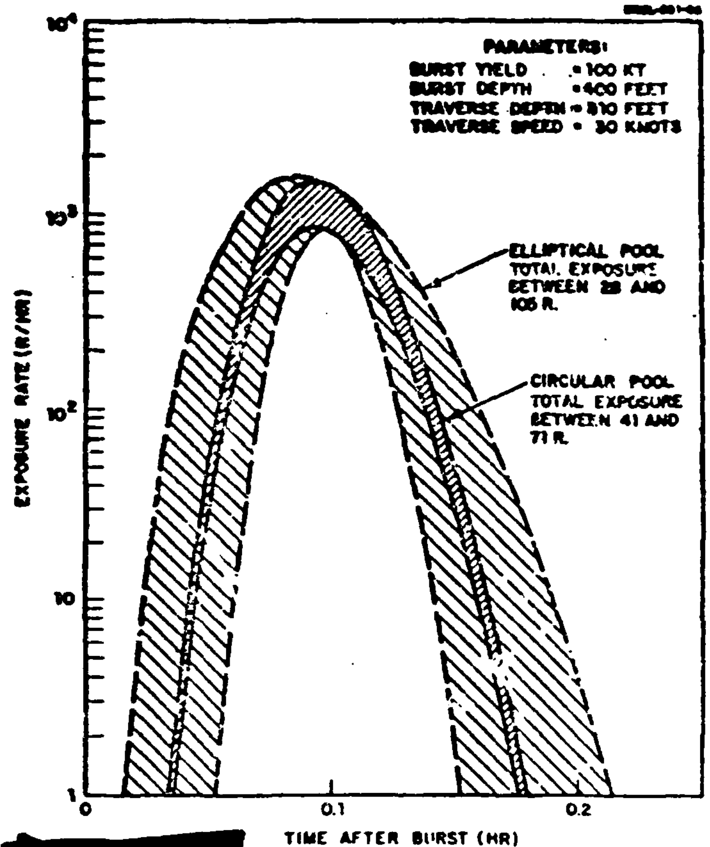

[redacted]

[redacted] Figure 5-16. Examples of Exposure Rate History of Unshielded Detector Traversing Radioactive Pool

Bands indicate range of estimates for circular pool and for elliptical pool whose minor axis is half the major axis.

[redacted]

[redacted]

[redacted] TABLE 5-1. TOTAL EXPOSURE FOR SUBMARINE TRAVERSE OF A RADIOACTIVE POOL

(Rinnert, 1968)

Speed of Traverse (Knots)	Total Exposure for Traverse (Roentgens)		Parameters*
	Modified Pritchett Model	Modified Ksanda Model	
5	4.19	5.09 - 7.30	W = 1
10	5.30	6.29 - 9.03	DOB = 300
15	6.22	7.13 - 10.2	SO = 4000
20	6.89	7.79 - 11.2	ZD = 50
30	8.28	8.82 - 12.7	
40	9.27	9.64 - 13.8	
5	0.48	0.89 - 1.26	W = 1
10	0.52	1.10 - 1.55	DOB = 300
15	0.59	1.20 - 1.70	SO = 4000
20	0.677	1.27 - 1.79	ZD = 300
30	0.12	1.37 - 1.92	
40	1.7×10^{-27}	1.43 - 2.01	
5	14.4	15.7 - 22.9	W = 100
10	17.7	19.3 - 28.3	DOB = 949
15	20.3	21.9 - 32.0	SO = 10,000
20	22.2	23.9 - 34.9	ZD = 50
30	26.2	27.0 - 39.5	
40	30.8	29.5 - 43.1	
5	1.68	2.81 - 4.07	W = 100
10	1.89	3.58 - 5.19	DOB = 949
15	1.97	3.89 - 5.63	SO = 10,000
20	2.11	4.09 - 5.92	ZD = 300
30	2.58	4.35 - 6.30	
40	3.12	4.53 - 6.56	

[redacted]

W Yield, kilotons
DOB Depth of burst, feet
SO Stand-off distance, yards (traverse begins at stand-off distance at time of burst and proceeds across pool, passing through surface zero)
ZD Depth of traverse, feet

[redacted]

[redacted]

[redacted] It should also be noted that the DAEDALUS calculations referred to in the previous section, presented by Shirasawa and Bjerke, 1968 and in Chapter 5 of DNA EM-1, provide predictions of the free field radiation 15 ft above the ocean surface, and therefore consider radiation coming from only a thin surface layer of the pool. There is little experimental evidence to confirm model predictions of the rate of growth and migration of a radioactive pool, of the fraction of its radioactive content left at various de ths as the bubble oscillates and migrates toward the surface the subsequent history of deep pools left behind, or the con ons under which a substantial amount of radioactivity may ne appear at the surface.

[redacted] In view of the uncertainties surrounding radioactive pool formation and behavior under non-Arctic conditions, and the total lack of experimental data of this nature under Arctic conditions, an assessment of the possible effects of the Arctic environment must be regarded as conjectural. Two characteristics of Arctic regions that might alter the behavior of the radioactive pool from what might be expected elsewhere are the presence of ice cover and the strong density gradient in the water column.

[redacted] An underwater explosion at a depth that vents will normally cause the development of a radioactive surface pool initially centered at surface zero. In the case of scattered or broken ice, which is usually only a few meters thick, it is expected that the pool would undergo its normal expansion and diffusion, and there would be little effect of the ice except to

[redacted]

provide a certain amount of shielding against that portion of the radioactivity that is below it. In the case of consolidated pack ice, with extensive pressure ridges and ice keels, the venting explosion will blast a hole in the ice and the radioactive pool will initially be centered in the ice-free water of the hole. Since a 10 m pressure ridge will be accompanied by about a 50 m ice keel, and in extreme cases ice keels may extend to 150 m (Bowditch, 1977, Chapter 36), the horizontal migration and diffusion of the pool may be impeded. If such should occur, the radioactivity in the exposed pool would be smaller in extent and more concentrated than might be expected from the DNA EM-1 examples in Chapter 5. However, since it appears that solid pack ice is necessary for this condition to arise, the effect would be apparent only to aerial observation, and of significance only to the determination of the location of an underwater burst sometime after the fact.

[redacted] As is discussed in Section 7, it is not known how much of the explosion energy is required to break through solid ice cover and vent However, for very small yields or very deep explosions, it may be that the bubble will have insufficient energy when it reaches the surface to fracture whatever thickness of ice is present. In this case a radioactive surface pool will not be formed and the pool will be trapped below the ice layer. This would prevent the detection of the explosion by aerial survey methods, although the radioactive pool would remain a hazard to submarine operations.

[redacted] In Section 1.2.7 it was noted that, in general, strong positive density gradients exist in the upper few hundred meters of the Arctic water column. This region (pycnocline) severely impedes the upward migration of heat and salt and effectively insulates the surface from the water masses below. This characteristic of the region leads to the speculation that much radioactive debris may often be trapped below the surface, whether or not an ice layer is present.

[redacted]

[redacted]

[redacted] Quoting from Chapter 10 of the Underwater Handbook:

> "For deep and very deep explosions, where the bubble experiences several oscillations as it migrates toward the surface, radioactivity may be ejected from the bubble at minima .... Measurements at Operation Wigwam ... indicate that there are both a radioactive surface pool and random lens-like pools of debris in the thermocline layer. These deep pools were measured some days after detonation and were found to be small and quite stable. Whether these deep deposits represent radioactivity that was left behind by the migrating bubble or material carried to the surface by hydrodynamic flow and returned to its original stability level, is not known."

[redacted] Except for the shallowest explosions that vent most of their fission products to the atmosphere with a water column or plumes, and then fall back to form a radioactive pool with surface waters, underwater nuclear detonations in the Arctic will cause a substantial amount of the highly saline, deeper water to mix with the radioactive material. It is conceivable that this water mass with its trapped fission products will sink to and remain in the pycnocline. In addition, any radioactive pools left at depth by the pulsating bubble would have their ascent stopped at the pycnocline. Thus the radioactive effects of the surface pool could be substantially less than those predicted by existing models. The pools would remain a submarine hazard, however.

[redacted]

Pages 5-47 and 5-48 were deleted

[redacted]

[redacted]

[redacted]

[redacted] On the basis of the work of Kaulum and Bennett, 1971, it may be concluded that there are combinations of yield and depth that give a high probability that the radioactive debris from an underwater nuclear explosion may be contained beneath the surface for periods of time long enough for the radioactivity to decay to undetectable levels. Figure 5-17, based on calculations for a wide range of density gradients, including typical Arctic gradients, provides a reasonable basis for estimating the conditions under which a radioactive surface pool would not be formed for yields of 100 kt or less, whether or not ice cover were present. Ice cover would prevent such formation for any detonation deep enough not to rupture the ice. The subsurface pools would, however, be a hazard to submarines.

5.4 [redacted] Radiation Damage Effectiveness

[redacted] There is no reason to expect any changes in the radiation damage vulnerability levels in Arctic conditions. The possible exception is some slight enhancement of effects on personnel. The severe winter Arctic environment imposes a heavy strain on personnel at best so that radiation effects might have a more deleterious reaction at lower levels.

[redacted] Bunkers or personnel shelters buried under snow or ice would provide slightly better protection than concrete on an overburden weight basis. Information on the protection factors is widely available such as given in EM-1.

[redacted]

5.5 [redacted] Conclusions and Recommendations

5.5.1 [redacted] Conclusions

[redacted] No studies considering the effect of arctic environment on prompt radiation environments were found except the Ft. Bliss study (OSWD, 1960). However, the techniques that have been developed to compute radiation environments in temperate environments can be used with no basic changes except using the proper model atmosphere. The density is the only important parameter of interest.

[redacted] Scaling the available infinite air transport results to the arctic winter ground level density indicates that the environment levels corresponding to typical damage criteria for hardened electronics occur at about a 15% smaller radius under arctic conditions than under temperate conditions. At a particular range the fluence or dose level can be 1/2 to 1/3 as large for arctic winter conditions as in temperate conditions. Thus, prompt radiation effects tend to be depressed in the arctic which is an advantage for considering damage to U.S. installations from Soviet bursts. However, the reduction in prompt radiation effects should be considered when considering the effectiveness of U.S. bursts against Soviet systems.

[redacted] The presence of the surface layer under the atmosphere tends to reduce the radiation environment in the air as compared with the free air values. No calculations of this effect have been made for arctic surfaces and conditions. Inspection of the available calculations indicates that there is essentially no difference in the neutron dose as measured close to the surface for wet or dry ground or sea water. The dose from the secondary gamma rays for wet ground is about 20% lower and for sea water is about 30% lower than for dry ground. The dose over fresh water or ice might be somewhat lower still. Since most of the

[redacted]

[redacted] Arctic is covered by wet tundra, fresh water ice or sea and sea ice, one would expect a small reduction in the dose resulting from neutrons from this effect.

[redacted] The dose from the early time fission products can be important in contributing to the total dose received by reentry vehicles, airplanes and ground installations as well as an important contributor to personnel casualties. In addition to the reduction due to the increased density there would be some effect due to the smaller fireball. No calculations of this effect have been made. Scaling estimates indicate that a reduction of about 15% in the range corresponding to a tissue dose of 500 rad can be expected in arctic conditions. This is about the same uncertainty that exists in current modeling of this radiation component.

[redacted] Differences in the fallout in arctic conditions could arise in several ways: differences in the induced activity, differences in the size of the particles the active particles are attached to, differences in the debris cloud development and dispersal due to the meteorological conditions, and for underwater bursts differences in the radioactive material ejection into the air due to the ice cover.

[redacted] The induced activity in bursts over arctic soils will probably be essentially the same as in temperate climates since there is in general the same range of soil types there. For bursts over sea water or sea ice the induced activity is much less than over ground and for bursts over fresh water, snow, or ice the induced activity is zero. Thus, in many situations in the arctic the residual radiation source is due only to the fission yield of the weapon and no induced activity from the thermonuclear component will exist.

[redacted]

[redacted]

[redacted] For bursts over arctic soil the particle sizes which result in the rising debris cloud would not be expected to be different than existing in more temperate climates since the basic soil types are comparable. For bursts on snow, ice or sea water, however, one would expect considerably different debris cloud characteristics. One probably would not expect the arctic case to be much different from a sea burst in temperate areas.

[redacted] Debris cloud development and dispersal has not been considered for arctic conditions. One might expect somewhat different development because of the different density and temperature profiles. Winds are not significantly different in the Arctic except perhaps being more variable; so no significant differences in fallout predictions would be expected except an increase in the uncertainties of such already uncertain predictions.

[redacted] Relative scavenging efficiencies of snow and water have been measured and analyzed with conflicting results. Some studies indicate a much larger scavenging efficiency for snow than water while other studies indicate no difference. The Arctic has a much lower precipitation rate than most temperate areas so that one might expect less of the activity to be scavenged and might expect therefore a more wide ranging and less intense fallout pattern that might occur in temporate areas if precipitation occurs. No studies have been made of induced precipitation by nuclear bursts in the Arctic.

[redacted] The major uncertainties in predicting the effects of nuclear radiation from an underwater burst result from a lack of knowledge of the amount of explosive energy that is required to break through an ice layer and that is therefore lost as far as the development of surface and above-surface phenomena are

[redacted]

[redacted] concerned. This in turn leads to uncertainty concerning the amount of radioactive material ejected to the atmosphere, the extent of its initial dispersion, and, in the cases of very small yields or great depths of burst, whether the ice will contain the effects of the detonation so that there will be no atmospheric phenomena. It is considered that available studies, though unverified experimentally, are adequate to the understanding of the effects of radioactive products freezing on exposed surfaces and the probable effects of the arctic environment on evolution of the radioactive pool.

[redacted] Studies have been made of the accumulation of activity on ships in icing conditions. This does not seem to be a very important mechanism of damage.

5.5.2 [redacted] Recommendations

[redacted] The effects noted in the prompt radiation environments were not very large but could be of significance for specific systems. It is recommended that currently available air transport results be scaled to provide isofluence and isodose profiles for neutrons, gamma rays and x-rays from selected weapon classes as a function of burst altitude. This could be done for the standard arctic conditions as well as for other extreme conditions which can exist as indicated in Section 1.2.

[redacted] These predictions should be incorporated into the appropriate chapters of EM-1 and perhaps could be a part of a more general section relating to the effects of atmospheric departures from standard on radiation transport.

[redacted] The effects on the early fission product dose should be determined for a few selected cases including possible fireball and cloud development changes. These calculations should be used to indicate scaling procedures so that inexpensive predictions can be prepared for a range of practical cases.

[redacted] Fallout prediction is at best very uncertain. The additional complications introduced by arctic conditions for which the U.S. will never have empirical data make the predictions even more untrustworthy. Since fallout is usually treated as a collateral damage mechanism in military situations, there may be no need to have accurate prediction techniques in the Arctic.

[redacted] Basic studies are required to specify the size distribution of the debris particles in the Arctic. Resolution of the discrepancies that exist in the analyses of the relative scavenging efficiencies of snow and water is necessary before predictions of the fallout under arctic conditions can be made.

[redacted] Computer models exist that could be used to compare the fallout from arctic and temperate climates. These models require as inputs such information as the debris cloud development, loading and particle size distributions, wind patterns as a function of altitude, precipitation patterns and rates, scavenging efficiencies, and particle diffusion characteristics. It is recommended that preliminary studies in these various areas be performed to identify the maximum differences that might exist in these parameters between the arctic and temperate climates. Predictions of the fallout using the minimum parameter differences should be made. If militarily significant differences occur between the arctic and temperate conditions, then additional research may be required in specific areas.

[redacted] Fallout predictions from underwater bursts are very uncertain. The ultimate destiny of the radioactive materials for various DOB is very uncertain and specifically the fraction that appears above the surface to contribute to fallout is unknown. It has been conjectured that the forces associated with the range of yields and depths of burst that are likely [redacted] to be of interest for underwater bursts are so great that the energy loss in breaking through ice would have minimal effect on the development of surface and above-surface phenomena. Since the fallout is in general less than that expected over land, there may be some question about its importance except in very specific cases involving nearby surface ships. If hydrodynamic calculations are made of the bubble development and shock interactions with the water and ice layers, tracer particles should be introduced in an attempt to determine the distribution of the radioactive particles for various DOB conditions.

5.6 BIBLIOGRAPHY

Baum, Sanford, Wong, Paul W., and Dolan, Phillip J., NUCROM: A Model of Rainout from Nuclear Clouds, DNA 3389F, EGU 72-204, Stanford Research Institute, Menlo Park, California, 27 August 1974, UNCLASSIFIED.

Bowditch, Nathaniel, American Practical Navigator, Defense Mapping Agency Hydrographic Center, Pub. No. 9, 1977 Edition.

Campbell, J. E., and Sandmeier, H. A., Radiation Transport in Air Over Seawater for Application to Low-Altitude, Low-Yield Tactical Nuclear Detonations, NWEF Report 1102, Naval Weapons Evaluation Facility, Albuquerque, New Mexico, 10 April 1973, UNCLASSIFIED.

Caudle, K. F. and Farley, T. E., Nuclear Weapons Effects in Arctic ASW (U), NOLTR 68-86, Naval Ordnance Laboratory, White Oak, MD, 22 May 1968, CONFIDENTIAL, AD-391458L.

DASA, Department of Defense Land Fallout Prediction System, Multi-Volume Series, DASA-1800, now Defense Nuclear Agency, Washington D. C., various dates, Secret RD.

[redacted]

Defense Nuclear Agency, Capabilities of Nuclear Weapons, Part I - Phenomenology. Part II - Damage Criteria, (U), DNA EM-1 (Change 1), Dolan, P. J., Ed., Defense Nuclear Agency, Washington, DC, July 1976, Secret RD.

Defense Nuclear Agency, Handbook of Underwater Nuclear Explosions (U), Three Volumes, each consisting of Parts 1 and 2, DNA 1240H, Defense Nuclear Agency, Washington, DC, Secret RD.

Greede, T. E. and Franey, J. P., Field Measurements of Submicron Aerosol Washout by Snow, Geophysics Research Letters, 2, pp 325-328, 1975, UNCLASSIFIED.

Harris, P. J., et al, Models of Radiation in Air - The ATR Code, DNA 2803I, Science Applications, Inc., LaJolla, CA, May 1972, UNCLASSIFIED.

Huebsch, J. O. and Olken, F., An Analytical Model of the Formation of Multimaterial Particles in Nuclear Explosion Clouds, DNA 3988F, Euclid Research Group, Berkeley, CA, March 1976, CONFIDENTIAL, ADC 009993.

Itagoki, K. and Koenuma, S., Altitude Distribution of Fallout Contained in Rain and Snow, Journal of Geophysical Research, 68, pp. 3927-3933, 1962, UNCLASSIFIED.

Jordano, R. J., et al, Sensitivity of HF Blackout Predictions to Atmospheric Parameters (U), ARBRL-CR-00357, General Electric Company - TEMPO, 816 State Street, Santa Barbara, CA, January 1978, CONFIDENTIAL.

Kaman Sciences, Summary of Ballistic Missile Defense System Vulnerability, Lethality, and Threat Analysis (U), Annual Report, K-74-444(R), Kaman Sciences Corporation, Colo. Springs, CO, 4 December 1974, SECRET RD CNWDI.

[redacted]

[redacted]

Kaulum, Keith W., The Location of Clandestine Underwater Nuclear Explosions, Phase II, Radioactive Plume Detection (U), ESA-TR-70-04, Environmental Science Associates, Burlingame, CA, October 1970, CONFIDENTIAL, AD-512526L.

Kaulum, K. W. and Bennett, C. B., The Location of Clandestine Underwater Nuclear Explosions, Phase I, The Contained Pool Search (U), ESA-TR-71-02, Environmental Science Associates, Burlingame, CA, August 1971, CONFIDENTIAL, AD-516872L.

Knutson, E. O., Scavenging Study of Snow and Ice Crystals, IITRI Report No. C6105-28, IIT Research Institute, Chicago, Il, August 1974, UNCLASSIFIED.

Ksanda, C. F., Analysis and Prediction of the Properties of Diffusing Radioactive Pools from Nuclear Explosions in the Ocean (U), USNRDL-TR-725, U. S. Naval Radiological Defense Laboratory, San Francisco, CA, 19 December 1963, CONFIDENTIAL, AD-350547.

Magono, C., et al, A Measurement of Scavenging Effect of Falling Snow Crystals on the Aerosol Concentration, Journal of Meteorological Society of Japan, 52, pp. 407-416, 1974, UNCLASSIFIED.

Maloney, J. C. and Klemm, W. J., Department of Defense Land Fallout Prediction System - An Updated User-Oriented Documentation for DELFIC Mark V, BRL-1783, Ballistic Research Laboratories, Aberdeen Proving Ground, MD, May 1975, UNCLASSIFIED.

Mooney, L. G. and French P. L., Improved Models for Predicting Nuclear Weapon Initial Radiation Environments (U), RRA-T93, DASA 2615, Radiation Research Associates, Fort Worth, Texas, 31 December 1969, SECRET RD CNWDI.

Normant, H. G., A Precipitation Scavenging Model for Studies of Tactical Nuclear Operations, DNA 3661F, Mt. Auburn Research Associates, Inc., Newton, Mass, 18 June 1975, UNCLASSIFIED.

[redacted]

[redacted]

Office of Special Weapons Development, Nuclear Weapons Effects in an Arctic Environment, OSWD 59-2, United States Continental Army Command, Office of Special Weapons Development, Fort Bliss, TX, June 1960, UNCLASSIFIED, AD-344936.

Pitter, R. L., Snow and Ice Scavenging, UCRL 13759, Lawrence Livermore Laboratory, Livermore, CA, August 1977, UNCLASSIFIED.

Pritchett, J. W., Explosion Product Redistribution Mechanisms for Scaled Migrating Underwater Explosion Bubbles, USNRDL-TR-1044, U. S. Naval Radiological Defense Laboratory, San Francisco, CA 94135, 23 May 1966, Unclassified, AD-657 939.

Pritchett, John W., The Containment of Underwater Nuclear Explosions - Theoretical Calculations of Deep Burst Hydrodynamics (U), IRA-TR-1-71, Information Research Associates, Inc., Berkeley, California 94704, 15 February 1971, CONFIDENTIAL, AD-514 861.

Pugh, G. E. and Galiano, R. J., An Analytical Model of Close-In Deposition of Fallout for Use in Operational-Type Studies, Research Memo No. 10, Weapons System Evaluation Group, 1959, UNCLASSIFIED.

Recter, R. and Carnuth, W., Washout Balance Between 700 and 300 Above Sea Level, Proceedings of Conference on Cloud Physics, Tokyo and Sapporo, Japan, pp 390-394, 1965, UNCLASSIFIED.

Rinnert, H. R., Exposure Rate History and Total Exposure for a Surface or Subsurface Traversal of a Radioactive Pool, USNRDL-TR-67-51, U.S. Naval Radiological Defense Laboratory, San Francisco, California 94135, 12 May 1967, UNCLASSIFIED, AD-817 959L.

Rinnert, H. R., Maximum Exposure Rate and Total Exposure for an Early-Time Subsurface Traversal of a Radioactive Pool, USNRDL-TR-68-31, U.S. Naval Radiological Defense Laboratory, San Francisco, CA 94135, 12 February 1968, UNCLASSIFIED, AD-831 244L.

[redacted]

[redacted]

Shirasawa, T. H. and Bjerke, R. A., Nuclear ASW in Arctic Waters: Influence of the Environment on the Radiological Hazard During a Ship Maneuver Following an Underwater Nuclear Explosion, USNDPL-TR-68-46, U.S. Naval Radiological Defense Laboratory, San Francisco, California 94135, 12 March 1968, UNCLASSIFIED, AD-834 435L.

Sood, S. K. and Jackson, M. P., Scavenging by Snow and Ice Crystals, from "Precipitation Scavenging (1970)", 121-136, conf-700601 from NTIS, 1970, UNCLASSIFIED.

Spencer, L. V., Chilton, A. B., and Eisenhaur, C. M., Structure Shielding Against Fallout Gamma Rays From Nuclear Detonations, National Bureau of Standards, in press.

Starr, J. R. and Mason, B. J., The Capture of Airborne Particles by Water Drops and Simulated Snow Crystals, Quarterly Journal of the Royal Meteorological Society, 92, pp 490-499, 1966, UNCLASSIFIED.

U. S. Navy Hydrographic Office, Oceanographic Atlas of the North Atlantic Ocean; Part II - Arctic, H.O. Publication No. 705, U. S. Navy Hydrographic Office, Washington, DC, 1958 (Reprinted 1968), UNCLASSIFIED.

Wolf, M. A. and Dana, M. T., Experimental Studies in Precipitation Scavenging, BNWL-1051, Battelle-Northwest, 1969 UNCLASSIFIED.

[redacted]

[redacted]

THIS PAGE IS INTENTIONALLY LEFT BLANK

[redacted]

[redacted]

SECTION 6
COMMUNICATIONS AND EMP

[redacted] This study was nominally limited to low altitude bursts and effects, and no large effort was to be expended on high altitude effects. During the literature searches one study (Jordano, et al, 1976) was found which specifically addressed the latitude dependence on HF absorption and the effects of model atmosphere differences on debris cloud development. This report was reviewed and a summary of the results is included.

[redacted] Some changes are expected in the EMP on the surface due to the differences in the magnetic field intensities and direction. The variation in EMP SMILE diagrams for various latitudes and various longitudes in the polar region are given.

6.1 [redacted] Arctic Environmental Differences

[redacted] The different profiles for the atmospheric parameters (density, pressure and temperature) for the arctic region can effect the debris cloud development and stabilization altitude. The delayed gamma-ray source function may then be different, which can cause differences in the ionization levels and attenuation properties of the atmosphere for electromagnetic wave propagation. The reaction rate constant. that determine the sustained ionization levels are a function of the temperature and particle concentrations. The concentration of minor species can be important in determining deionization rates and may be altered at high latitudes due to the differences in energetic particle effects noted in this region at high altitudes.

[redacted]

[redacted] The greater intensity of the magnetic field in the polar areas will increase the magnitude of EMP in the region. The direction is more vertical than at lower latitudes which will affect the relative magnitudes of the horizontal and vertical components of the EMP and may affect the coupling of the EMP into targets.

[redacted] The coupling of energy into structures and cables buried under the ice and snow may be affected because of the differences between the conductivity, capacitivity and permeability of ice and snow and of more typical soil materials.

6.2 [redacted] Attenuation of HF Communication

[redacted] The changes in HF absorption from a near surface burst due to the different profiles of density, pressure and temperatures has been considered by Jordano et al (1978). The calculations were done by defining high latitude atmospheric models, incorporating the models in existing communication codes, and comparing the effect on HF communication links passing through the D region. The effect of the atmospheric differences on the debris dynamics was also considered. The influence of the atmospheric parameters on the deionization kinetics was considered, but the effect of differing concentrations of the minor species was not included.

[redacted]

[redacted]

[redacted] for the July and January 60° N models are shown in Figure 6-1. The July and January extreme profiles were defined by adding to or subtracting from the 60°N profiles a component representing the diurnal variation plus a two-sigma random variation in such a manner as to increase the variation from the mean standard profile. The circles plotted for altitudes below 30 km represent the 75°N January temperature profile described in Section 1.2 and are seen to agree with the defined January extreme model. The WEPH VI/ROSCOE system defines the pressure and density profiles from the temperature profile using hydrostatic equilibrium and the perfect gas law. Above 80 km atomic oxygen is included to match measured mean molecular weights.

[redacted]

[redacted]

[redacted]

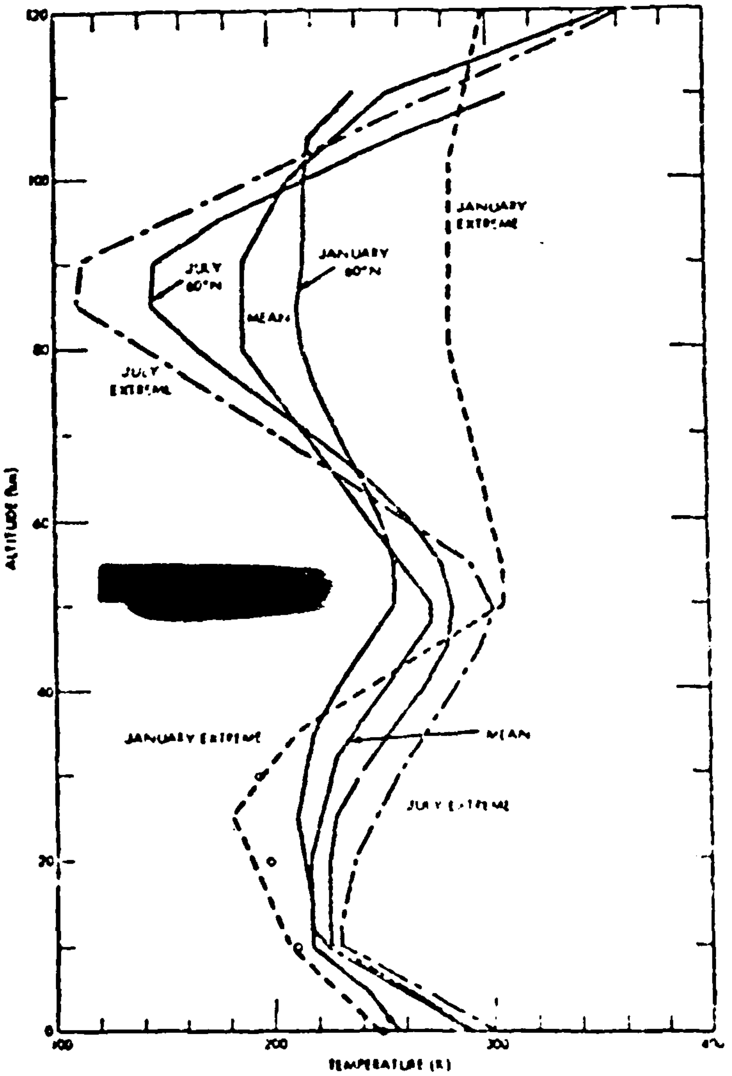

[redacted]igure 6-1 Temperature profiles for alternate atmospheres. (Jordano, et al, 1979)

[redacted]

[redacted]

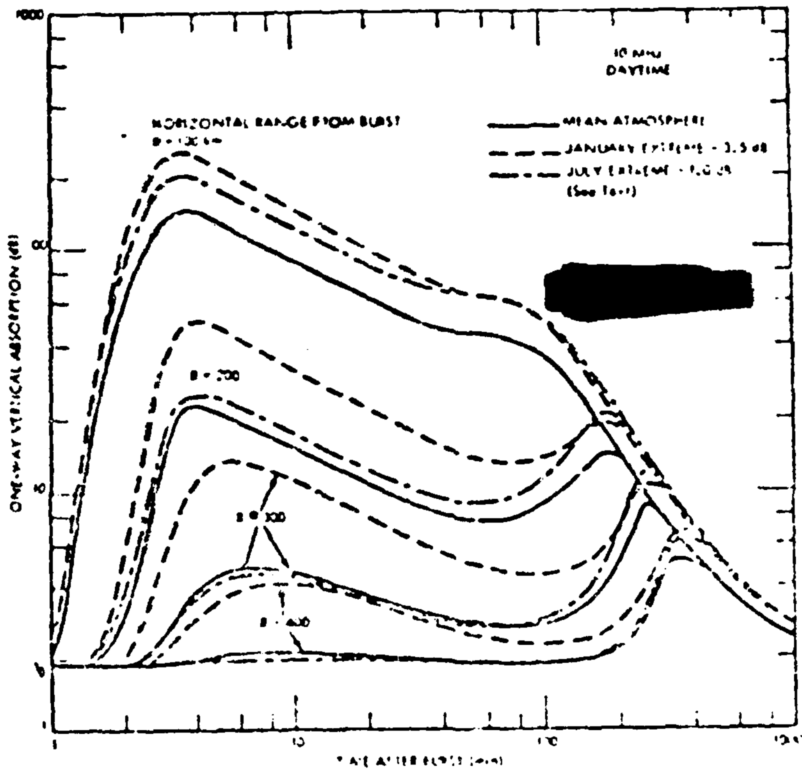

[redacted] Figure 6-2 Absorption caused by nuclear burst in alternate atmospheres in the daytime (fixed debris dynamics).

(Jordano, et al, 1978)

[redacted]

[redacted]

[redacted]

[redacted]

[redacted]

[redacted] The fireball model is discussed in detail by Jordano, et al, and the trends observed are explained by consideration of the starting conditions which determine the initial fireball volume and density, the mass entrainment and mixing phase with dominates the cooling phase until low temperatures are reached. The expansion against the ambient pressure which dominates the

[redacted] Page 6-7 was deleted

[redacted]

[redacted] final temperature decrease and the ambient temperature in the stabilization region which determines the final temperature the fireball must reach for equilibrium and stabilization.

[redacted]

[redacted] Page 6-9 was deleted

[redacted]

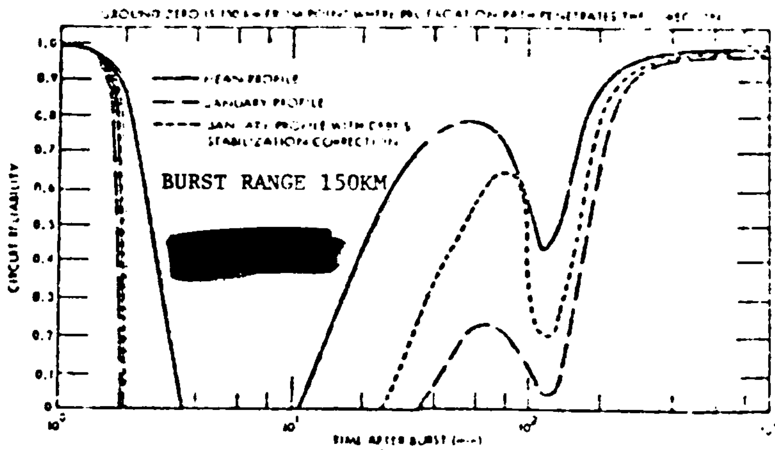

(a)

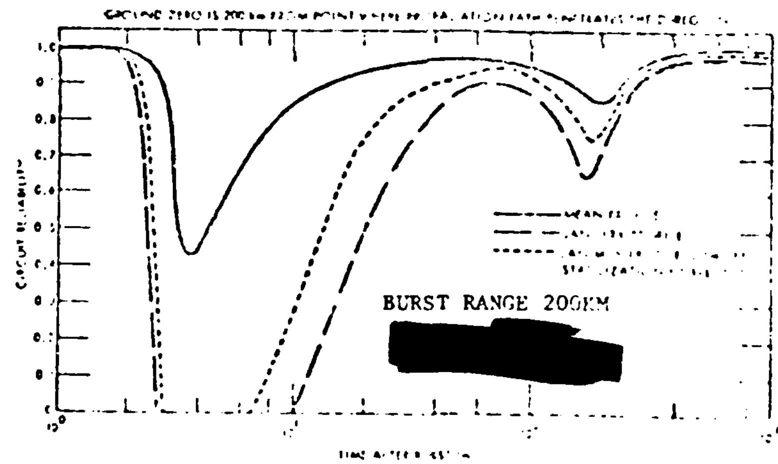

(b)

[redacted] FIGURE 6-5. CIRCUIT RELIABILITY, OLNEY, MARYLAND TO MAYNARD, MASSACHUSETTS (Jordano, et al, 1978).

[redacted]

[redacted]

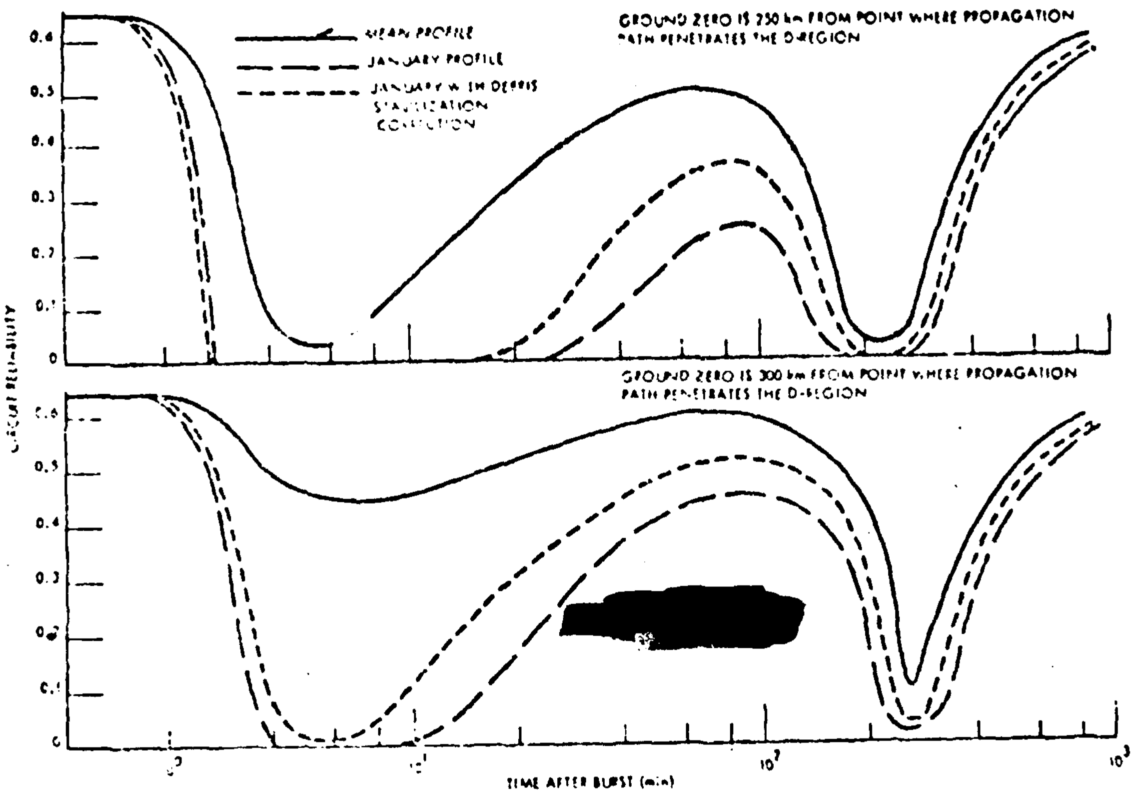

[redacted] FIGURE 6-6. CIRCUIT RELIABILITY, FORT HUACHUCA, ARIZONA TO WESTERN EUROPE; BURST RANGES = 250 km, 300 km (Jordano et al, 1978).

[redacted] Pages 6-12 through 6-19 were deleted

[redacted]

[redacted] It is recommended that additional studies be made on the debris dynamics for Arctic atmospheres. The results of these studies have implications in the determination of fallout under Arctic conditions as well as in the effect on communication blackout.

[redacted] The concentration of minor species in the high altitudes should be considered and their effect on the deionization kinetics should be determined. Prediction of the communication blackout expected by bursts in the Arctic including all of these effects should be made for a wide range of frequencies.

[redacted]

[redacted]

[redacted] The horizontal and vertical components of EMP should be determined for the polar region. Changes in coupling to surface based systems should be considered. Predictions should be made of the coupling of the EMP to cables and facilities buried in frozen ground or covered with snow.

[redacted] 6.5 Bibliography

Ammer, H., et al, The Electromagnetic Pulse from High Altitude Nuclear Bursts (U), K-78-103(R), Kaman Sciences Corporation, Colorado Springs, CO, 1978, SECRET RESTRICTED DATA.

COSPAR, COSPAR International Reference Atmosphere, 1965, North Holland Publishing Company, Amsterdam, 1965, UNCLASSIFIED.

COSPAR, COSPAR International Reference Atmosphere, 1972, Compiled by COSPAR Working Group A, Akademie-Verlag, Berlin, 1972, UNCLASSIFIED

Defense Nuclear Agency, Capabilities of Nuclear Weapons (U), DNA EM-1, Defense Nuclear Agency Effects Manual Number 1, Headquarters, Defense Nuclear Agency, Washington, D. C., 1 July 1972 (Change 1, 1 July 1978), SECRET RESTRICTED DATA. Two volumes, Part I - Phenomenology, Part II - Damage Criteria.

ESSA, U. S. Standard Atmosphere Supplements, 1966, U. S. Government Printing Office, Washington, D. C., 1966, UNCLASSIFIED.

General Research Company, Physical Custodian for Development of ROSCOE: A Radar and Optical Systems Code for Nuclear Effects DNA 3385, General Research Company, Santa Barbara, CA, March 1974, UNCLASSIFIED.

Jordano, R. J. et al, Sensitivity of HF Blackout Predictions to Atmospheric Parameters (U), ARBRL-CR-00357, General Electric Company - TEMPO, 816 State Street, Santa Barbara, CA, 1978, CONFIDENTIAL.

[redacted]

[redacted]

Knapp, W. S., WEPH VI, A Fortran Code for the Calculation of Ionization and Electromagnetic Propagation Effects Due to Nuclear Detonations (U), DNA 3766T-2, GE75TMP-53, General Electric Company - TEMPO, Santa Barbara, CA, October 1976 CONFIDENTIAL.

Kumer, J. B., et al, Low Altitude Phenomenology for Optical Systems, Volume II, RADIR Code Documentation (U), DNA [illegible], LMSC B340290, Lockheed Palo Alto Research Laboratory, CA September 1975, SECRET

NASA, U. S. Standard Atmosphere, 1962, U. S. Government Printing Office, Washington, D. C., 1962, UNCLASSIFIED.

[redacted]

[redacted]

[redacted] SECTION 7
[redacted] UNDERWATER SHOCK

7.1 [redacted] Arctic Environmental Differences

7.1.1 [redacted] Sound Velocity Profile

[redacted] As discussed in Section 1, the deep sound channel axis is located at the water/ice interface for typical Arctic sound velocity profiles when ice cover is present. In the absence of ice cover the deep sound channel is near the surface, usually within 200 meters. This contrasts with conditions at more southerly latitudes for which the deep sound channel is generally located at a depth of the order of 1000 meters. The effect of this difference is to modify propagation of shock and acoustic waves. The principal mode in the Arctic is by refracted surface-reflected paths (RSR) and the caustics and convergence zones prominent in deep water refracted path (RRR) propagation at moderate latitudes in the Atlantic and Pacific Oceans are not present. Because of their absence, underwater damage associated with convergence zones will not occur.

7.1.2 [redacted] Ice Cover

[redacted] Ice cover modifies the interaction of the blast wave with the sea surface. The principal effects are the modification of the reflectivity at the surface, increasing damage to submerged structures at short range, reducing the size of the spray dome, and reducing the blast wave transmitted to the atmosphere.

7.2 [redacted] Underwater Blast Generation

[redacted] Upon detonation of an underwater nuclear device a shock wave is generated and a steam bubble is formed. The steam bubble oscillates and emits an energy pulse at each minimum. A maximum of three bubble pulse emissions can occur

[redacted]

before the steam condenses. The bubble also migrates toward the surface and, if the detonation is not sufficiently deep, it can vent the surface prior to emission of a bubble pulse.

[redacted] The Arctic environment does not affect the generation and coupling of the shock wave to the ocean medium, nor does it affect the formation of the steam bubble for deep detonations. The ice cover may have a second-order effect on upward migration of the bubble and therefore the yield-detonation depth relationship for venting prior to emision of the first bubble pulse. If the detonation occurs close enough to the surface so that ice melt is involved in the initial generation of the bubble, the ice cover can introduce a small modifying effect.

7.3 [redacted] Sea Surface Effects

7.3.1 [redacted] Underwater Blast Wave

7.3.1.1 [redacted] Surface Reflection

[redacted] Since air provides a pressure-release surface, the reflection of an underwater signal from an air/water interface is essentially unity, but the phase undergoes a shift of 180°. Because of the very high signal levels, the negative pressure of the reflected signal cannot be sustained in the water. As a result cavitation occurs and the reflected signal is clipped. It is this cavitation that produces the spray dome.

[redacted] The reflection of a shock wave from ice cover has been treated by Barash, 1966a. In place of a single reflection from the ice/air interface, the energy reflected from the ice cover is partitioned among various paths as shown in Figure 7-1a for compressional wave paths in the ice, and Figure 7-1b for shear wave paths. Figure 7-2 shows the shape of the direct shock wave for the configuration indicated. When ice is not present, the reflected signal is simply a phase-inverted replica of

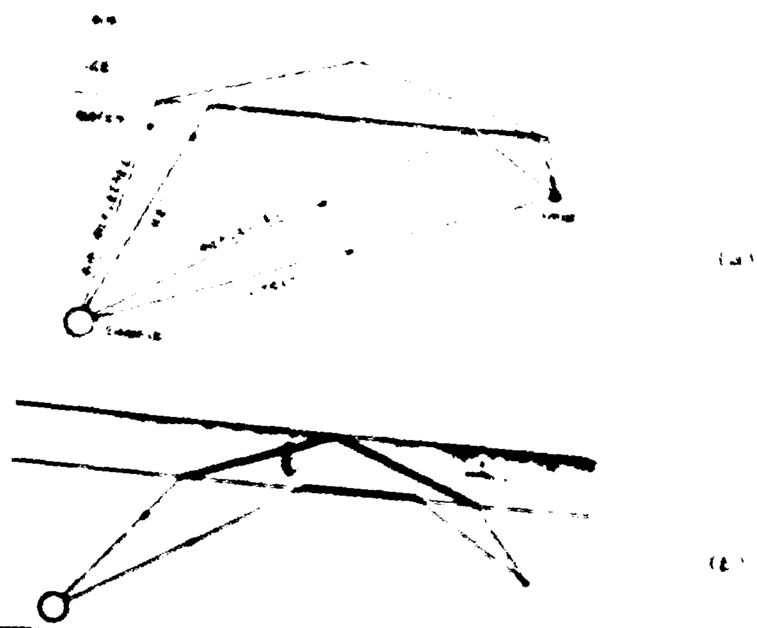

[redacted]

[redacted] Figure 7-1. Under-Ice Explosion Propagation Paths
(a) Compression Waves
(b) Shear Waves
(Barash, 1966a)

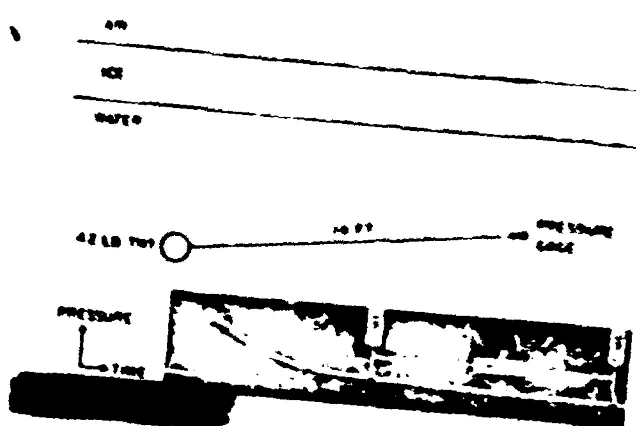

[redacted]

[redacted] Figure 7-2. Direct Shock Wave (Barash, 1966a)

[redacted]

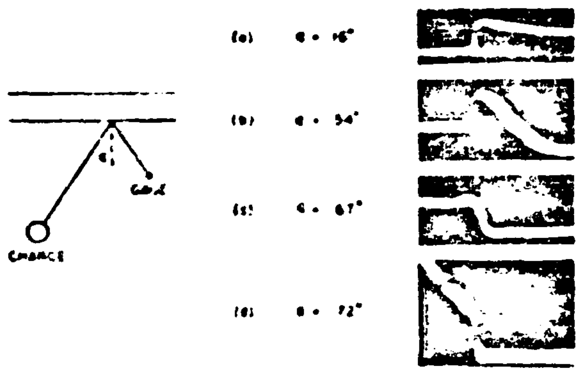

[redacted]

[redacted] Figure 7-3. Reflected Wave Form for Various Angles of Incidence. (Barash, 1966a)

the direct signal with the same peak pressure (neglecting cavitation effects). When ice is present, Figure 7-3 shows the shape of the reflected signal as a function of incident angle. At angles near normal incidence, the shape of the reflected signal is comparable to that of the direct, but with reduced amplitude. Most important is to note that the phase is positive. As the incident angle increases, the reflected signal decays more rapidly than the direct, and goes negative.

[redacted]

[redacted]

[redacted] Figure 7-4 (Barash 1966a) describes empirically the reflection factor as a function of incident angle for five different values of incident pressure. Barash defines the reflection factor as the ratio of the peak pressure contribution of the reflected wave, measured at a particular gage location, to the pressure that would be expected there if the pulse underwent no loss in peak pressure upon reflection. The dependence of the reflection factor on incident pressure is due to nonlinearity for high pressure levels. Also shown on the figure are the negative pressure contributions of the reflected pulses.

[redacted] Figure 7-5 shows the complete pressure-time history for four different geometries. In record (a) the reflected wave is a positive pulse superposed on the tail of the direct wave, and both are cut off by the negative air-reflected wave. In record (b) the ice wave and air-reflected wave arrive before the direct shock wave. The reflected pulse, which arrives later, consists of a small positive peak followed immediately by a large negative signal. The resultant absolute pressure at that time goes no lower than about zero, because natural water is unable to sustain appreciable tensions. The final arrival is the shear-propagated wave. In record (c) both the reflected wave and the ice wave are superposed on a portion of the direct wave, and all three are cut off by the air-reflected wave. In record (d) the peak pressure in the reflected wave is great enough and arrives early enough that the resultant peak pressure is greater than that due to the direct wave alone.

[redacted] The effect of the increase in the positive phase will be to increase the damage to submerged structures at short range. As range increases, the incident angle increases and the contribution of the reflected signal to the positive phase is reduced substantially. In all cases the positive phase is

[redacted]

[redacted]

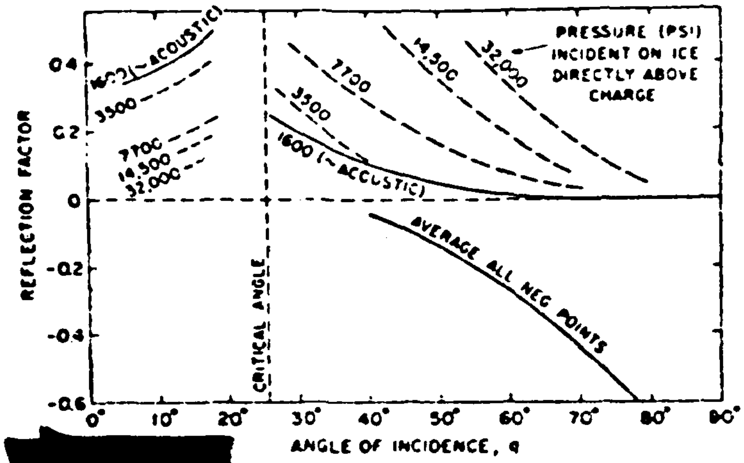

[redacted]

[redacted] Figure 7-4. Reflection Factor as a Function of Angle of Incidence for Various Values of Incident Pressure. (Barash, 1966a)

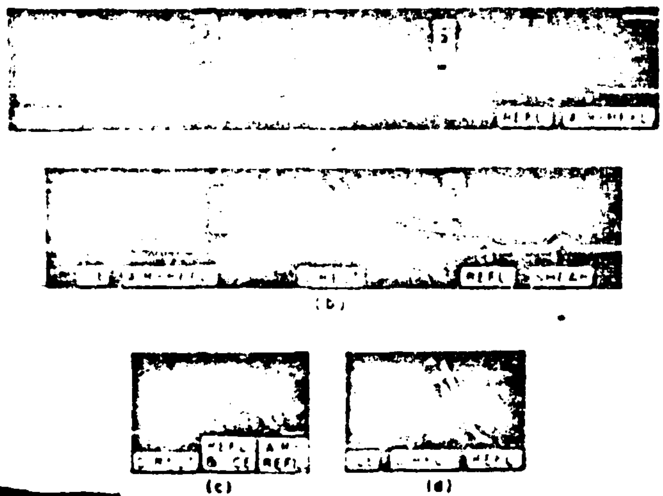

[redacted]

[redacted] Figure 7-5. Examples of Pressure-Time Records for Under-Ice Explosions. (Barash, 1966a)

[redacted]

cut off by the reflection from the ice/air interface and the total signal goes negative. However, the peak negative amplitude is reduced, so that cavitation effects will be reduced, resulting in a reduction of the spray dome.

7.3.1.2 [redacted] Coupling to the Atmosphere (see Section 2.4)

[redacted] For deep detonations, the blast wave generated in the air by an underwater detonation is discussed by Rudlin and Silva, 1960, and in DASA 1200-III for an ice-free sea surface. We are concerned here only with the modification of the results described therein by the presence of ice.

[redacted] For deep detonations, the atmospheric blast wave is caused by two phenomena - first, the transmission of the underwater shock through the sea surface to the atmosphere, and second, the cavitation process, which imparts a supersonic velocity to the sea surface, causing the development of the spray dome and radiating a shock wave. Analytic models for predicting these effects are poorly developed and current conclusions in the ice-free case are based principally on experimental data. Linear acoustic theory predicts that the portion of the atmospheric blast wave due to the first of these phenomena, the transmission of the underwater shock pressure wave through the sea surface, will be reduced by about 1/3 directly over the detonation when ice cover is present. Although linear acoustic theory is in poor repute as a prediction technique for atmospheric blast waves due to an underwater detonation (Rudlin and Silva, 1960), it appears reasonable to conclude that some reduction will occur when ice is present. As discussed in Section 7.3.1.1, the presence of the ice cover alters the sea surface reflection to reduce cavitation and the spray dome. The reduction of cavitation can be expected to reduce the velocity imparted to the sea surface, thereby reducing the air

[redacted]

blast associated with the second phenomenon. There is no data base or analytic procedure available for estimating the magnitude of this reduction, which may be significant.

[redacted] For intermediate and shallower detonations, the plume becomes the dominant mechanism for producing the atmospheric blast wave. This is caused by the bubble venting the surface. Nothing is known about the effect of ice cover on this phenomenon, but, as noted in Section 7.2, it is estimated to be of secondary importance. In any event, the rigidity of the ice and the extraction of energy by ice breakup and melt is estimated to reduce the magnitude of the atmospheric blast caused by the plume, although the effect may be quite small.

7.3.2 [redacted] Atmospheric Burst

7.3.2.1 [redacted] Effect of Atmosphere

[redacted] Atmospheric effects increase the duration and impulse of the blast wave generated by all atmospheric detonations. (See Section 2.2 for a discussion of these effects.)

7.3.2.2 [redacted] Coupling to the Ocean (see Section 2.5.2)

[redacted] Coupling to the ocean, or transmission of the air blast wave through the sea surface interface, is discussed by Sakurai and Pinkston, 1967. A theoretical analytic procedure for prediction is compared to experimental data obtained with 21-lb spherical charges for the case of no ice cover. Except for detonation altitudes quite close to the surface, a modified acoustic theory is found to be reasonably accurate. As the charge approaches the surface, finite amplitude theory becomes necessary.

[redacted] The existing theory is too complex to permit an assessment of the effect of ice cover. However, on the basis of fundamental acoustic concepts, the introduction of an ice layer, which has an acoustic impedance higher than that of

[redacted]

[redacted]

water, can only reduce the transmission of energy through the interface. In addition, the increased rigidity of the ice sheet will reduce the deformation of the surface when finite amplitude theory is necessary, making acoustic theory more applicable. Thus, all that can be said at this time is that atmospheric effects would tend to increase the transfer of energy to the water, while ice cover would tend to decrease it. No estimate can be made as to whether the total effect is one of increase or decrease.

7.3.3 [redacted] Ice Fracturing

[redacted] An underwater explosion that would vent in the absence of ice cover would be expected, in most cases, to cause fracturing of any ice cover present. The extent of the fracturing would be a function of a set of parameters defining the size and location of the explosion and a set of parameters defining the physical nature of the ice. The significance of ice fracturing rests mainly on two possible effects - increase in underwater ambient noise, which will be treated in Section 9 on Acoustic Effects, and the production of ice missiles that could be a hazard to low-flying aircraft or anything else in the vicinity of the explosion. The present discussion concerns the current ability to estimate the degree of this hazard.

[redacted] It was shown in Section 1 that the strength of sea ice varies widely, from almost no strength under some conditions, possibly 2/3 the strength of fresh water ice under others, comparable to fresh water ice under still other conditions, to two or three times the strength of fresh water ice for very cold perennial sea ice. It is in this context that one must view the results of the very few field tests that have been performed using explosives under ice.

[redacted]

[redacted]

[redacted] Of the tests of explosives in conjunction with ice, the ones that are pertinent to the present discussion have generally been conducted in connection with the development of devices to provide means for nuclear submarines to surface through the ice pack in an emergency. For this reason, the goal has been to use the minimum possible size of charge, and to explode it at the optimum depth for fracturing the ice. This optimum depth is relatively close to the bottom surface of the ice.

[redacted] Barash, 1962 and 1966b, has reported on a test series at Moonshine Lake, a fresh water lake in Minnesota. The tests were conducted during January through March, 1960. Charges used were 1 lb, 8 lb, and 42 lb, mostly TNT spheres, detonated at positions from 2 ft above to 20 ft below the ice sheet, which was of the order of 2-2½ ft thick. The water depth at the detonation site varied from about 15 to 66 ft.

[redacted] Figure 7-6, from Barash 1962, shows there is an optimum charge depth for ice fracturing for a given size charge. For these tests the optimum depth varied from about $1.0W^{1/3}$ for the 1 lb charge to $2.3W^{1/3}$ for the 42 lb charge. The radius of the maximum broken ice area in the three cases varied between 7.7 and $8.5W^{1/3}$, and was about twice the maximum bubble radius. Barash suggests that the shapes of the radius vs charge depth curves are related to the size and dynamic state of the bubble at the time it vents, and further suggests that the bubble plays a more important role than the shock wave in determining the size of the hole. To test this proposition, he reports on a laboratory experiment in which one gram charges of various compositions were fired at the optimum depth beneath a sheet of material simulating ice. Figure 7-7, also from Barash 1962, shows the results of these tests, and

[redacted]

[redacted]

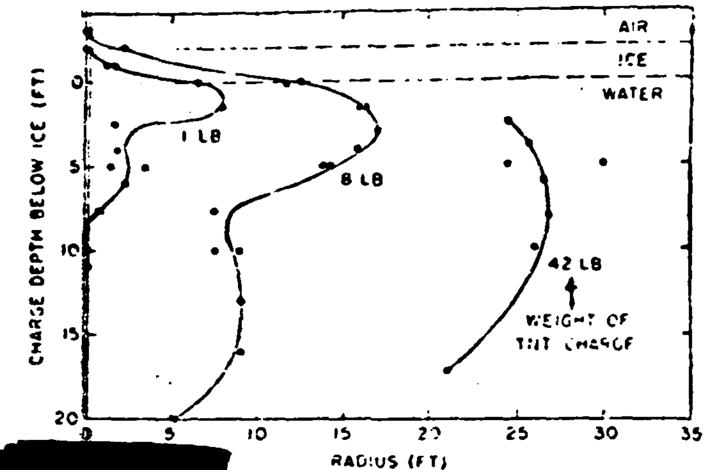

[redacted]

[redacted] Figure 7-6. Radius of Broken Ice Area for Different Charge Weights and Charge Depths Below Ice. (Barash, 1962)

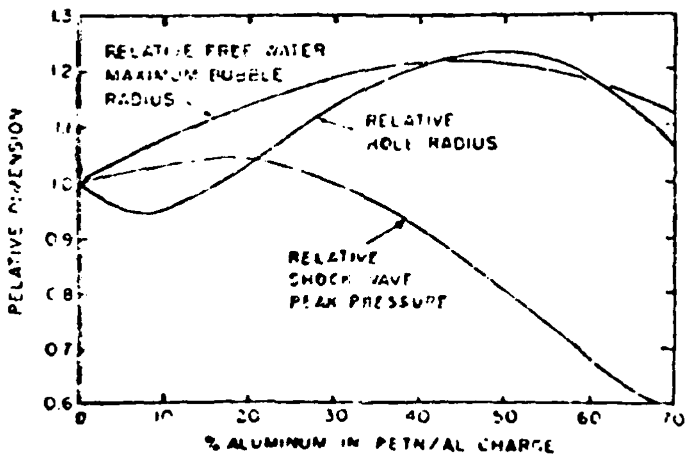

[redacted]

[redacted] Figure 7-7. Hole Radius for Various Explosive Mixtures, (Barash, 1962)

[redacted]

[redacted]

demonstrates that for this case at least, the hole radius is approximately proportional to the bubble radius, rather than to the shock wave characteristics.

[redacted] Leslie and Nelson, 1961, reported on a test series of three shots conducted in late August, 1961, in which charges of 20, 35 and 60 lb of HBX-3 were detonated beneath a large floe of what was determined to be old polar ice. The floe was located some 200 nm north of Pt. Barrow in about 950 fathoms of water. Its thickness at the test sites varied from about 8 to 16 ft. All detonations were $1.0W^{1/3}$ ft below the bottom of the ice, the implication being that this was considered to be optimum depth. Since the charge placement method required the detonations to be relatively near the ice edge, large portions of the floe cracked off and began to drift away immediately after each shot, complicating estimates of the size of pulverized or cracked areas. However, the radius of the cracked areas in terms of the maximum bubble radius was larger than in the Moonshine Lake tests.

[redacted] In the tests reported by Leslie and Nelson, core samples were taken of ice in the vicinity of the detonations and the strength and salinity of the ice were measured. The ice was of very low salinity, about $1.2^{o}/oo$ maximum,* indicating that it was quite old. Its tensile strength, measured by the standard ring test, averaged about 15 kg/cm^2 throughout most of its thickness, being a little less near the relatively warmer surface and a little greater near the bottom. The sample temperatures were all about $30^{o}F$ ($-1^{o}C$).

[redacted] Another sea ice test, referred to by Barash, 1962, but for which very little data were given, was a charge of 600 lb of HBX-3 detonated under thin (about 2.5 ft) seasonal ice in the Bering Sea. According to Barash, the broken area radius

* $^{o}/oo$ - Parts per thousand

[redacted]

was only about 1.5 times the maximum bubble radius. The water depth and the detonation depth below the ice were not given. Figure 7-8, from Barash 1962, summarizes the results of the three test series reported by Barash.

[redacted] Caudle and Farley, 1968, reviewed the available data on ice missiles and ejecta. They used some earlier work by Kurtz, 1966, in drawing their conclusions. In the experiments reported by Kurtz, data were obtained from several shots of 136 lb of C4 (equivalent to about 148 lb of TNT). It was observed that the radius of ejected ice that completely covered the preshot areas was about twice the radius of the hole; the size of the ice in this region ranged from 25-ft blocks to fine chips. The maximum height to which surface material (fine ice and snow) was thrown was about 130 ft. The average extreme range of missiles weighing 1 lb or more was about nine times the radius of the hole.

[redacted] Kurtz scaled the results of these experiments by cube-root scaling to approximate the 1-kt nuclear situation. Figure 7-9, from Caudle and Farley after Kurtz, shows the scaled radius of the hole in the ice as a function of the scaled depth of burst for several scaled bottom depths and one scaled ice thickness. Kurtz concluded that such cube-root scaling holds over a limited range of explosive yields as long as the ice thickness and water depth are also scaled. This conclusion was verified for charges up to 1000 lb, but when a 940-lb explosive was tested with an ice thickness and water depth less than the scaled values, the hole radius was some 25% greater than would otherwise have been predicted for the proper scaled values. It is impossible to say whether the result was influenced by the ice thickness, the water depth, or both. Nor can it be said how much the discrepancy might increase with increasing yields. Certainly any predictions based on

[redacted]

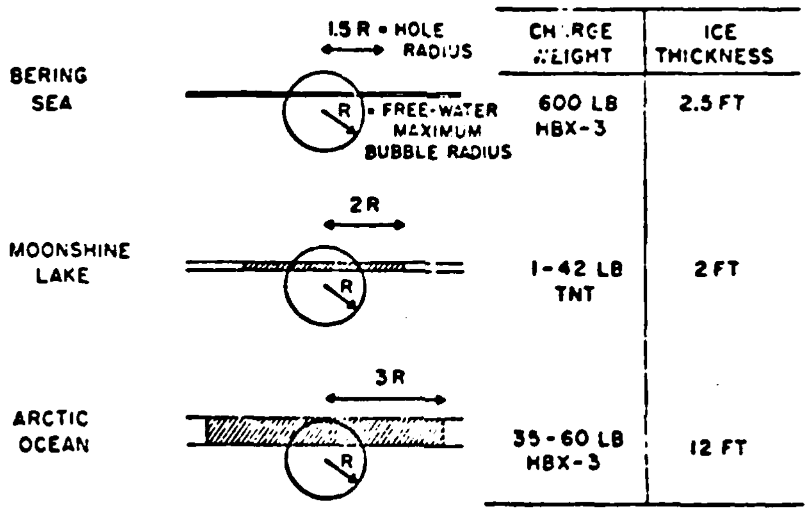

[redacted]

[redacted] Figure 7-8. Comparison of Three Test Series. (Barash, 1962)

[redacted]

[redacted]

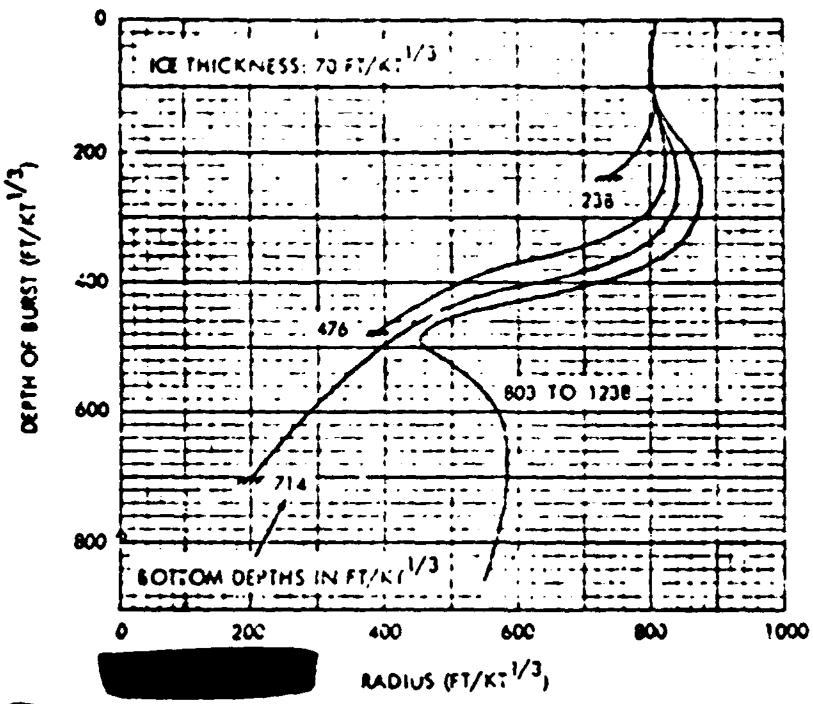

[redacted]

[redacted] Figure 7-9. Hole Radius as a Function of Depth of Burst for Several Water Depths. Depths Are Measured From the Bottom of the Ice Layer. (Caudle and Farley, 1968)

Figure 7-9 must be considered only rough approximations. For one thing, the scaled ice thickness and water depths shown would probably never be realized in actual situations.

[redacted] Caudle and Farley, 1968, summarized the questions that need answering before it can be determined how rough approximations based on Figure 7-9 may be:

- Over what range of yields can cube-root scaling be expected to hold? If it fails, what type of scaling is applicable?
- How does ice thickness affect the hole formation quantitatively?
- What role does the water depth play?
- How do the hole-producing phenomena differ for nuclear and chemical explosions?

[redacted]

[redacted]

At the present state of knowledge, it is perhaps sufficient to note that the effect dimensions of ice fracturing and missile ejection are of the same order of magnitude as those of hazard from the airblast from underwater nuclear explosions. The hazard is confined to a relatively small area around the explosion in which comparable hazards from other causes exist.

[redacted]

[redacted]

[redacted]

[redacted]

[redacted]

[redacted]

[redacted] In Arctic regions, the sound velocity generally increases with increasing depth. For these conditions, energy is always refracted upward; convergence zones and caustics do not occur. Thus, submarine damage at long ranges associated with the convergence zones is not anticipated.

7.4.2 [redacted] Atmospheric Burst (see Section 2.5.2)

[redacted] No assessment of the effect of ice cover on underwater blast damage due to an atmospheric burst can be made at the current state of knowledge.

7.5 [redacted] Conclusions and Recommendations (See Section 2.7 for related material.)

7.5.1 [redacted] Conclusions

[redacted] Ice cover does not affect the generation of the shock wave from underwater detonations or the generation of the steam bubble and bubble pulse emission for deep detonations. For

[redacted]

[redacted]

shallow detonations, ice cover may affect migration of the steam bubble and venting, and may extract some energy from the steam generated if ice melt occurs.

[redacted]

[redacted] The effect of ice cover on the coupling of the air blast from an atmospheric detonation to the ocean cannot be estimated.

[redacted] It is not known how to estimate the hazard from ice missiles resulting from an underwater detonation under ice. The effects of ice thickness, detonation depth, and water depth on the size of the hole and amount of ejecta produced are unclear.

[redacted]

[redacted]

Neither is it known over what range cube-root scaling may apply, if at all, when these parameters are varied. The few tests that have been conducted have not encompassed a wide variety of ice types.

7.5.2 [redacted] Recommendations

[redacted] The most important need is the development of analytic procedures to accurately predict the reflection of the underwater blast wave for an ice-covered sea surface. This would permit the prediction of the total pressure field at any underwater point. Knowledge of the total pressure field would permit a more accurate prediction of submarine damage and of the cavitation processes that affect the spray dome and the atmospheric blast effects. The theoretical development should also include the prediction of the shock transmitted to the atmosphere.

[redacted] To complete the prediction of the atmospheric blast waves resulting from an underwater detonation, the effect of ice cover on the plume should also be investigated.

[redacted] The development of an analytic procedure for predicting the effect of ice cover on the underwater blast wave generated by an atmospheric burst should also be undertaken.

[redacted] Sufficient under-ice testing of explosives should be conducted to permit a better assessment of the extent of hazard from ice missiles.

7.6 [redacted] Bibliography

Barash, Robert M., Underwater Explosions Beneath Ice, NOLTR 62-96, United States Naval Ordnance Laboratory, White Oak, Silver Spring, MD, 1 June 1962, Unclassified, AD-332 122.

[redacted]

[redacted]

Barash, Robert M., Measurements of Underwater Explosion Pulses Reflected from an Ice Layer, U.S. Navy Journal of Underwater Acoustics, Volume 16, No. 2, pp. 279-288, April 1966a, Confidential. Reprinted as AD-484 936, Unclassified.

Barash, Robert M., Ice-Breaking by Explosives, NOLTR 66-229, United States Naval Ordnance Laboratory, White Oak, Silver Spring, MD, 6 December 1966b, Unclassified, AD-807 900.

Caudle, K. F. and Farley, T. E., Nuclear Weapons Effects in Arctic ASW(U), NOLTR 68-86, Naval Ordnance Laboratory, White Oak, Silver Spring, MD, 22 May 1968, Confidential, AD-391 458L.

Defense Nuclear Agency, Capabilities of Nuclear Weapons(U), DNA EM-1, Defense Nuclear Agency Effects Manual Number 1, Headquarters, Defense Nuclear Agency, Washington, D.C., 1 July 1972 (Change 1, 1 July 1978), Secret, Restricted Data. Two volumes, Part I - Phenomenology, Part II - Damage Criteria.

Defense Nuclear Agency, Handbook of Underwater Nuclear Explosions(U), DNA 1240 H, Defense Nuclear Agency, Washington, D.C., November 1971, Secret, Restricted Data. Three volumes, each consisting of Parts 1 and 2, some Confidential, Formerly Restricted Data.

[redacted]

[redacted]

Defense Nuclear Agency, Nuclear Weapons Blast Phenomena, Volume III, Air and Subsurface Explosions(U), DASA 1200-III, Defense Nuclear Agency, Washington, D.C., Revised 15 June 1972, Secret, Formerly Restricted Data, AD-51: 266L.

Feit, David and Thompson, William, Jr., Analytical Study of Certain Aspects of Underwater Shockwave Propagation: Sloping Bottom, Icecap, Sedimentary Bottom, U-246-174, Cambridge Acoustical Associates, Inc., 129 Mount Auburn St., Cambridge, MA 02138, October 1966, Unclassified, AD-644 197.

Gaspin, J. B. and Price, R. S., The Underpressure Field from Explosions in Water as Modified by Cavitation, NOLTR 72-103, Naval Ordnance Laboratory, White Oak, Silver Spring, MD, 9 May 1972, Unclassified.

Holland, Norma O., Airblast from Underwater Nuclear Bursts(U), NOLTR 70-115, U.S. Naval Ordnance Laboratory, White Oak, MD 20910, 21 July 1970, Confidential, AD-511 025.

Kaltwasser, M., Hydra Program - Theoretical and Experimental Determination of Energy Partition of Selected Underwater Explosives, USNRDL-TR-702, U.S. Naval Radiological Defense Laboratory, San Francisco, CA 94135, 28 October 1963, Unclassified, AD-426 763.

Kurtz, Maurice K., Jr., Ice Cratering Experiments, Technical Memorandum 56-7, Lawrence Radiation Laboratory, Livermore, CA, November 1966, Unclassified.

[redacted]

[redacted]

Kutschale, Henry, Ice Vibrations in the Central Arctic Ocean Induced by Air Waves from Russian Nuclear Blasts(U), Technical Report No. 1, CU-1-62, Lamont Geological Observatory, Columbia University, Palisades, New York, 12 November 1962, Confidential.

Leslie, Donald M. and Nelson, Carl A., Explosion Tests Under Thick Polar Ice, NOLTR 61-146, United States Naval Ordnance Laboratory, White Oak, MD, 1 November 1961, Unclassified, AD-327 953.

Malme, Charles I., Carbonell, Jaime R., and Dyer, Ira, Mechanisms in the Generation of Airblasts by Underwater Explosions, NOLTR 66-88, United States Naval Ordnance Laboratory, White Oak, MD, 23 September 1966, Unclassified, AD-654 175.

Rudlin, L. and Silva, John C., Airblast from Underwater Nuclear Explosions(U), NAV ORD Report 6714, U.S. Naval Ordnance Laboratory, White Oak, MD, 1 February 1960, Confidential, Formerly Restricted Data, AD-319 260.

Sakurai, Akira and Pinkston, J. M., Water Shock Waves Resulting from Explosions Above an Air-Water Interface, Report 1, Results of a Theoretical Investigation, Technical Report No. 1-771, U.S. Army Engineer Waterways Experiment Station, Vicksburg, MS, April 1967, Unclassified.

[redacted]

[redacted]

[redacted] SECTION 8
WATER WAVES

8.1 [redacted] Arctic Environmental Differences

8.1.1 [redacted] Ice Cover

[redacted] Ice cover is by far the most important environmental difference of the Arctic region in its effect upon explosion-generated, gravity water waves. Ice cover, whether solid or in ice fields of loose or packed floes, will affect the generation, propagation, and damage potential of explosion-generated waves in ways that may be unpredictable within present knowledge. Not only the degree but even the directions of the effects on generation and damage potential are unavailable. The possible effects of ice cover on explosion-generated waves have received neither experimental nor theoretical attention. Observations on the effects of ice fields on storm waves and swell may be indicative of the effects on propagation of explosion waves, but even here it must be kept in mind that explosion waves are characteristically different from the normal sinusoidal ocean waves.

8.1.2 [redacted] Bathymetry

[redacted] The bathymetry of the Arctic Ocean is characteristically different from other ocean areas in that the continental shelves are very extensive and thus there is no deep water near any shoreline. Also, the slopes of the continental shelves are very gentle. Water depth is a primary parameter in the generation of explosion-produced water waves, and water depth and bottom slope affect both the propagation of the water waves and their damage potential on the continental shelf and on the shore. Estimates of the effects of the bathymetry can be made within the present knowledge of explosion-generated waves.

[redacted]

[redacted]

8.2 [redacted] Wave Generation Parameters

8.2.1 [redacted] Effect of Water Depth

[redacted] The existence of large areas of shallow water in the Arctic makes the water-depth factor in explosion-generated wave production more important than it is in the usual open ocean area. The amplitude predictions for explosion-generated waves are empirical, and the shallow water predictions are not as well founded as the deep water predictions.

[redacted] [redacted] The wave generating mechanism is the gravitational restoration of the cavity produced in the water by the explosion. The wave amplitude of the maximum wave for a deep water explosion may be predicted by an empirical relationship (Van Dorn et al., 1968). If η_m is the amplitude (in feet) of the maximum wave, r the range (in feet), Y the yield of the explosion (in pounds, TNT), and Z the height of burst above the free surface (in feet), then:

$$\eta_m\, r/Y^{0.54} = 18 \quad \text{for} \quad 0.25 > Z/Y^{0.3} > -0.25$$

for surface explosions, and

$$\eta_m\, r/Y^{0.54} = 10 \quad \text{for} \quad Z/Y^{0.3} < -0.25$$

for subsurface explosions.

[redacted] In shallow water, where the water cavity is intercepted by the bottom, the wave height is diminished by approximately one-half the deep water height but the wave length, which is determined by the cavity radius which in turn is relatively independent of water depth, remains the same (Van Dorn et al.). Therefore the wave characteristics are changed in that the wave is less steep and less apt to break and dissipate energy on gentle slopes. Thus for the same wave height, there is a greater potential for runup on shore or for creating a surf-zone condition nearer shore than would be expected for a deep water wave.

[redacted]

[redacted]

8.2.2 [redacted] Effect of Ice Cover on Deep Explosions

[redacted] Neither experimental results nor theoretical treatments of the effect of ice cover on explosion-generated water wave production are available.

[redacted] Experiments on breaking lake ice (Barash, 1962 and 1966) and thick sea ice (Leslie and Nelson, 1961) by explosives demonstrated that at optimum standoff distance below the ice, an explosive would shatter ice on the surface in an area defined by 1½ to 3 bubble radii. It would appear that the only effect of ice cover on the water cavity created by a deep explosion would be a reduction in the cavity size by the energy required to break the ice. However, most of the shock energy that goes into ice breaking has already departed the volume of the incipient explosion bubble and is lost to it whether used for ice breaking or ejecting water in a spray dome or plume. The effect of the ice cover may be quite small. In any case, it is difficult to imagine any increase in wave production due to ice cover.

[redacted] The explosion-generated wave is formed by the collapse of the water cavity, and near the origin, before the transition to the wave form, the amplitude of the disturbance is large and the water very turbulent. If the surrounding area were ice covered, it is possible that the close-in high waves might overspill the surrounding ice cover. This overspill could dissipate wave energy and interfere with the formation of the outgoing wave train.

[redacted] In summary, for deep explosions there are no experimental and no theoretical results available on the effects of ice cover on wave generation. The conjecture is that the worst case (maximum wave amplitude) occurs for no ice cover.

[redacted]

[redacted]

8.2.3 [redacted] Effect of Ice Cover on Shallow Bursts

[redacted] If it were not for the Upper Critical Depth phenomenon, the effect of ice cover on shallow bursts would be similar to the effect of ice cover on deep bursts, and the worst case (largest waves) could be assumed to exist for the no-ice case.

[redacted] Examination of Figure 8-1 (Van Dorn et al., 1968) reveals two maxima in wave amplitude versus depth. The smaller maximum occurs at a depth called the Lower Critical Depth, which is the depth at which the explosion bubble emerges at the surface in a contracted phase following its first expansion. Explosions near the surface exhibit a very large scatter in wave amplitudes, with the maxima a factor of two or three times that of the maxima of the wave amplitudes from the explosions at the Lower Critical Depth. The depth at which the larger maximum occurs is called the Upper Critical Depth.

[redacted] No satisfactory explanation for the existence of the Upper Critical Depth is available. To quote one source (Bjork and Gittings, 1972): "It arises, of course, from the strong interaction of the explosion with the surface concomitant with shallow explosions."

[redacted] The existence of an Upper Critical Depth for nuclear explosions has not been established. There are sufficient differences in the nature of the explosion bubble from conventional to nuclear to make it possible that the phenomenon does not exist for the nuclear case. Research to attempt to explain the Upper Critical Depth has been conducted with the idea in mind that if the causes were known, the existence (or non-existence) for the nuclear burst might be established. A computer simulation of a 5 Mt burst at the suspected Upper Critical Depth failed to exhibit the enhanced wave amplitude, but only one depth was tried and the authors (Bjork and

[redacted]

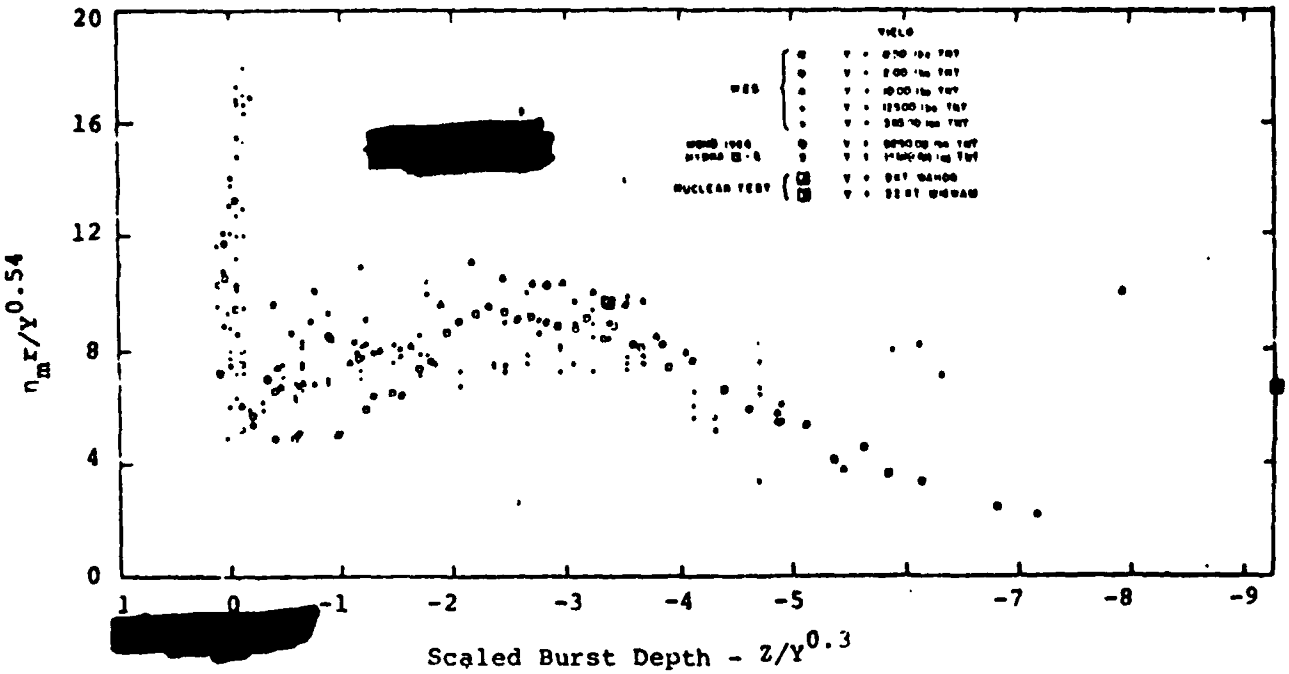

Figure 8-1. An Empirical Curve for the Relationship Between Values of $\eta_m r$, Charge Depth and Explosion Yield (Van Dorn et al., 1968).

[redacted]

Gittings) speculated that the Upper Critical Depth was probably slightly deeper than the depth used in the computer run. A mathematical model of a point-source explosion (Falade and Holt, 1978) does show evidence of the Upper Critical Depth.

[redacted] Experiments with conventional explosives, Figure 8-1, have shown considerable scatter for near-surface explosions. To quote one study (Van Dorn et al.): "However, since the entire region interior to this maximum is filled with data, it would appear to be a precarious stability condition that results in maximum effects, and one that is not readily reproducible. Nevertheless, the possibility that a near-surface explosion might produce waves of this magnitude cannot be ignored when making wave predictions."

[redacted] If the Upper Critical Depth exists for nuclear explosions and is a result of some interaction with the water surface, then until the nature of that interaction can be identified it is impossible to conclude what the effect of ice cover might be. Since the ice cover could increase or decrease the interaction, it is not even possible to predict whether the ice cover would increase or decrease the amplitude of the waves.

[redacted] As in the deep-explosion case, the surrounding ice cover could interfere with the transition from the water cavity collapse to the formation of the smooth wave form by the overspilling onto the ice of the turbulent water. The result of this interference could only be a decrease in the amplitude of the outgoing water wave.

8.3 [redacted] Wave Propagation

8.3.1 [redacted] Effect of Water Depth on Propagation

[redacted] The prevalence of large areas of shallow water and broad continental slopes in the Arctic poses problems in the calculation of the propagation of explosion-generated water waves.

[redacted]

[redacted]

[redacted] When the water depth is non-uniform and becomes of the order of a quarter wave length of the maximum amplitude water wave, there is no single theory for predicting the evolution of the wave and a piece-wise, continuous computation scheme must be used (Van Dorn et al., 1968). The procedure is available, but the fact that it is site-dependent and must be carried out piece-wise for each wave considered adds practical difficulties in estimating the propagation of explosion waves in the Arctic Ocean.

8.3.2 [redacted] Effect of Ice Cover on Propagation

[redacted] It has long been observed that ice floes and ice packs have an attenuating effect on ocean waves (Robin, 1963a & b). Waves entering an ice field are damped by two processes (Shapiro and Simpson, 1953): (1) the pressure cushioning effect of the structural differences between ice and water and therefore the masses that are affected by the wave motion, and (2) the multiple reflections that take place between the ice/water boundaries. An ice field acts as a filter that limits the period of wave energy that can be transmitted into and through the field. The longer the wave length of the incident wave, the deeper the wave energy can penetrate into the field. Waves of sufficiently small periods cannot exist in an ice field.

[redacted] The best available record of observations of ocean swell penetration into loose fields of large ice floes (Robin, 1963b) shows there is a wave length (and period) for ocean swell for which little attenuation takes place in an ice field. Table 8-1 (Robin, 1963b) presents these periods as a function of ice thickness.

[redacted]

[redacted]

[redacted] TABLE 8-1. Conditions for Little Attenuation by Ice Fields of Incident Water Waves (Robin, 1963b).

Ice Thickness (m)	Wave Length (m)	Period (sec)
0.5	450	17
1.0	760	22
2.0	1280	27.5
3.0	1730	33
5.0	2540	40

UNCLASSIFIED

[redacted] Since explosion-generated waves of interest are in the range of 20 sec to 100 sec in period, with 10 sec as the most likely minimum period, the conclusion would seem to be that propagation of explosion-generated waves would be little affected by ice fields.

[redacted] Some caution must be used since the observations on which the table is based are on periodic waves. Explosion waves are not periodic and the sine wave is not a good approximation of their shape. It is not clear whether mathematical filter models could be applied to the explosion-generated wave forms to calculate the filter effects of ice fields on these aperiodic waves, and no information is available to estimate the difference, if any, that these departures from the characteristics of swell-like waves might make. There seems to be little possibility that an ice field could increase the amplitude of explosion-generated waves. The worst-case estimate (highest waves) would be for the no-ice condition.

8.4 [redacted] Wave Damage Potential

8.4.1 [redacted] Effect of Ice Cover in the Deep Ocean

[redacted] The damage potential of explosion-generated water waves in the deep ocean (depths greater than 100 fathoms) is a function of the maximum amplitude and the wave length of the maximum amplitude wave. Damage potential against surface ships

[redacted]

is probably not affected by ice cover. Against a stationary object such as an oil rig, the ice set in motion by the wave might increase the hazard to the installation. No quantitative estimate can be given.

8.4.2 [redacted] Effect of the Bottom Slope of the Continental Shelf

[redacted] The gentle slopes of the continental shelf in the Arctic will produce shoaling waves far from the shore. The shoaling begins when the water depth is about one-quarter of the wave length of a given wave of the explosion wave train. Over a sloping bottom of decreasing depth the wave amplitude increases until the wave amplitude is about 78% of the water depth, at which point the wave breaks, dissipating much of its energy and turning the area into a surf zone. For a given wave height the more gentle the slope of the bottom the farther from shore the wave will break.

[redacted] Site-dependent calculation schemes can be applied (Van Dorn et al., 1968) to estimate wave heights and delineate the areas in which the surf-zone effect takes place. Estimates of the hazards of the surf-zone areas can be made for conventional ships (Wang, 1973), surface-effect vehicles (Wang et al., 1977), submarines, and fixed installations. The estimates referred to are for open water. Ice cover has not been considered.

8.4.3 [redacted] Effect of Ice Cover on the Continental Shelf

[redacted] It appears likely that ice cover would have a major effect on the waves over the continental shelf but no information is available. Clearly the encounter between steep-fronted shoaling waves and fixed ice or loose ice floes must interfere with the normal amplitude growth and breaking phenomena.

[redacted]

[redacted] Observations on wave energy penetrating into ice fields (Robin 1963a&b, Hunkins, 1962) are for low amplitude, smooth, swell-like waves and yield no information on the effects of ice cover on breaking or near-breaking waves.

[redacted] Any installation on the bottom on the continental shelf could be subjected to scour from the wave action on floating ice. Installations on the bottom, to be secure from this hazard, would have to be at a depth greater than the sum of the depth of the ice keels and the depth of the wave trough. Since the trough of an explosion-generated wave on the shelf could be of the order of 50-60 ft deep and ice keels may be of the order of 100 ft, scouring might take place on the bottom in water depths of the order of 200 ft.

8.4.4 [redacted] Effect of Ice Cover on Runup

[redacted] The effect of ice cover - solid, packed, or loose ice - on the surf-zone phenomena created in the absence of ice cover by the breaking of shoaling, explosion-generated waves is unknown. Thus the effect on runup of such ice cover is unknown, even assuming the absence of shore-fast or near-shore ice. Shore-ice might decrease runup on shore by causing the high amplitude waves to overspill the ice and in effect dissipating the wave energy before it reaches the actual shore line or shore-line installations.

[redacted] The damage potential of shore runup, if runup does occur, must be significantly increased by the presence of near-shore ice cover. The scouring action on the shore line and on shore installations of wave-driven ice would seem to have even greater damage potential than runup without ice.

[redacted]

[redacted]

8.5 [redacted] Conclusions and Recommendations

8.5.1 [redacted] Conclusions

[redacted] Ice Cover

[redacted] The major uncertainties concerning explosion-generated waves in the Arctic result directly from ice cover, the outstanding difference in the Arctic environment compared with other ocean areas.

[redacted] No observations, no experimental data, nor any theory have dealt with explosion wave generation from deep or shallow explosions under ice cover. It is conjectured that for deep explosions, the waves generated are no greater in amplitude than for the no-ice environment. For shallow depths of burst, even the direction of the effect of ice cover is unascertainable because the effect, if any, of the ice cover on the unknown surface interaction that produces the Upper Critical Depth phenomenon is unknown. The possibility that ice cover increases the coupling of the explosion energy to the water cannot be dismissed. Wave energy normally represents only about 2% to 5% of the explosion energy; therefore small increases in coupling could substantially affect the wave energy.

[redacted] The effect of ice cover on the formation of the close-in wave formed from the water cavity collapse is unknown. Ice cover surrounding the explosion cavity could interfere with the wave train formation by dissipating energy in waves over-spilling the ice.

[redacted] The effect of ice cover on the propagation of explosion-generated waves is unknown. All observations of the effects of ice fields on ocean waves deal with relatively low amplitude waves. The observed penetration of ocean swell through ice fields shows that for swell-like waves little attenuation of wave energy would occur at the wave periods of interest, 20 sec to 100 sec.

[redacted]

[redacted] The effect of ice cover on the shoaling waves and creation of the surf-zone environment on continental shelves is unknown. It seems almost certain that ice cover, whether solid or loose ice, would interfere with the orderly growth in amplitude of the shoaling waves and in the breaking of these waves. The conjecture would be that the surf-zone conditions are less severe than for open water conditions.

[redacted] The effects of ice cover on runup are unknown. It can be conjectured that loose ice would be carried ashore by the runup, thus adding to its damage potential. Shore-fast ice, on the other hand, might well dissipate the wave energy by runup on the ice well away from shore.

[redacted] It must be noted that waves of the explosion-generated type are not observed in nature. The periods of interest, 20 sec to 100 sec, fall between storm waves and tsunamis; therefore the effects of ice cover on propagation, breaking, bottom scouring, and runup cannot be extrapolated with any confidence from observations on waves generated by natural sources.

[redacted] Bathymetry

[redacted] Explosion wave characteristics such as amplitude and wave length are much more reliably predictable in deep water than in shallow; therefore the estimated damage potential in deep water is more reliable than in shallow water. The Arctic environment by virtue of the prevalence of shallow water areas simply increases the uncertainty of the details of wave characteristics. Methods of estimation do exist (Van Dorn et al.), but they must be applied to the specific site and thus do not permit generalized predictions. The broad continental shelves will have the effect of producing surf-zone environments at great distances from shore, thus limiting runup to, probably, inconsequential levels. But the characteristics of the surf-zone environment and the area affected cannot be generalized; they must be estimated for the yield, detonation location, and the bottom profile for the area into which the waves propagate.

8.5.2 [redacted] Recommendations

[redacted] Effect of Ice Cover on Wave Generation

[redacted] Research is needed to determine the effect of ice cover on the generation of explosion waves for both deep and shallow depths of burst. Wave predictions are now based on empirically-derived equations, and the effects of ice cover would have to be similarly obtained. Field testing using small (kilogram size) conventional explosives under real ice cover offers a plausible way to obtain the required information. Laboratory tests in pressure vessels using gram-size charges and lucite or some similar material to simulate ice might be used to investigate a wide range of conditions.

[redacted] The two questions that require answers are: (1) what is the effect of ice cover on the size and shape of the water cavity formed as a result of the explosion, and (2) what is the effect of ice cover (solid, closely packed, or loose ice) on the formation of the out-going wave train.

[redacted] It seems doubtful that either of these questions can be answered by theory or mathematical modeling, but small field tests and laboratory tests with conventional explosives might yield the needed information. It should be noted that no scaling to larger yields is involved in these experiments. The conclusion would be that if ice cover has a large effect on the Upper Critical Depth for small explosions, it would have the same qualitative effect on the Upper Critical Depth for large explosions. Similarly, the effect of surrounding ice cover on the formation of the out-going wave train should be qualitatively the same regardless of the yield of the explosion.

[redacted]

[redacted] Existence of the Upper Critical Depth

[redacted] Because of the great variation in wave height resulting from conventional explosions at depths of burst at or near the Upper Critical Depth, accurate prediction of wave heights from nuclear explosions in the Arctic (and, for that matter, in any area) depends markedly on whether the Upper Critical Depth phenomenon occurs for nuclear explosions. Prediction of the importance and even the possible direction of the effect of some variation from normal such as ice cover cannot be determined in the absence of an understanding of the Upper Critical Depth interaction.

[redacted] Research needs to be conducted to determine the cause of the Upper Critical Depth and whether the Upper Critical Depth exists for nuclear explosions. In the absence of underwater nuclear bursts, the approach is limited to theoretical studies or small-charge testing in the field or in the laboratory. A considerable amount of research has been done both in theory and field testing, but the physical cause of the Upper Critical Depth remains obscure. Mathematical models of point charges (to simulate nuclear bursts) by Holt and others at the University of California (Falade and Holt, 1978) yield Upper Critical Depth wave heights as the shot depth is varied, but the transfer from mathematical initial conditions to a nuclear event remains uncertain. The computer model (Bjork and Gittings, 1972) seems to offer the best available approach to investigating the Upper Critical Depth for nuclear explosions. The only run attempted failed to exhibit the enhanced wave heights of the Upper Critical Depth, and it is not clear how many runs might be needed to locate the proper depth. If the Upper Critical Depth exists for this computer model, it would be reasonable to conclude that the probability is high that it also exists for nuclear explosions. It might also be feasible to introduce ice cover into this computer model.

[redacted]

[redacted]

[redacted] So much effort has been expended on the Upper Critical Depth that, in spite of its importance to wave prediction, it is not clear that further effort is warranted unless some novel method with high probability of success is proposed.

[redacted] Effect of Ice Cover on Wave Propagation

[redacted] Research is needed to determine the effect of ice cover on the propagation of explosion-generated waves. Conclusions drawn from observation and from theoretical studies of the penetration of swell and storm waves into ice fields may be misleading because of the differences in the characteristics of the wave types and because of the large amplitudes that explosion waves must have and maintain to have a damage potential. Present mathematical models perhaps could be extended from the currently used sinusoidal waves to the explosion-generated wave forms and the ice field treated as a filter for these waves. It is not clear whether wave theory can handle this research, but probably simulated ice cover in a laboratory wave tank would be an effective research tool to obtain the required information. Probably both a theoretical and experimental approach will be necessary for confidence in the results. The scaling required has to do with ice floe size and thickness in relation to the wave length of the explosion-generated wave and does not involve scaling up conventional explosion effects to nuclear explosion effects.

[redacted] Effects of Ice Cover on Damage Potential in Shallow Water and on Runup

[redacted] The damage potential of explosion-generated water waves arises from (1) large amplitude waves in deep water, (2) shoaling waves leading to creation of a surf-zone environment in shallow water, and (3) runup of waves on the shore.

[redacted]

[redacted]

[redacted] Research on the effect of ice cover on propagation would yield information on the deep water case.

[redacted] Information is also needed on the effect of ice cover on the surf-zone environment and on runup, but it is not evident that research tools are capable, at present, of investigating these situations. The surf-zone environment and the runup for areas without ice cover are only grossly estimated using available theory and empirical information, and extension to the more complicated case with ice cover seems impractical with the present state of the art.

8.6 [redacted] Bibliography

Barash, Robert M., Underwater Explosions Beneath Ice, NOLTR 62-96, United States Naval Ordnance Laboratory, White Oak, Silver Spring, MD, 1 June 1962, Unclassified, D-332 122.

Barash, Robert M., Ice-Breaking by Explosives, NOLTR 66-229, U.S. Naval Ordnance Laboratory, White Oak, MD, 6 December 1966, Unclassified, AD-807 900.

Bjork, R. L. and Gittings, M. L., Wave Generation by Shallow Underwater Explosions, DNA 2949Z, Systems, Science and Software, P.O. Box 1620, La Jolla, CA 92037, December 1972, Unclassified, AD-907 595.

Defense Nuclear Agency, Capabilities of Nuclear Weapons(U), DNA EM-1, Defense Nuclear Agency Effects Manual Number 1, Headquarters, Defense Nuclear Agency, Washington, D.C., 1 July 1972 (Change 1, 1 July 1978), Secret, Restricted Data. Two volumes, Part I - Phenomenology, Part II - Damage Criteria.

[redacted]

[redacted]

Defense Nuclear Agency, Handbook of Underwater Nuclear Explosions(U), DNA 1240 H, Defense Nuclear Agency, Washington, D.C., November 1971, Secret, Restricted Data. Three volumes, each consisting of Parts 1 and 2, some Confidential, Formerly Restricted Data.

Evans, D. V. and Davies, T. V., Wave-Ice Interaction, Report No. 1313, Davidson Laboratory, Stevens Institute of Technology, Castle Point Station, Hoboken, New Jersey, August 1968, Unclassified, AD-674 895.

Falade, Adebowale and Holt, Maurice, Surface Waves Generated by Shallow Underwater Explosions, Physics of Fluids, Vol. 21, No. 10, October 1978, pp 1709-1716.

Hendrickson, James A. and Webb, Lois M., Theoretical Investigation of Semi-Infinite Ice Floes in Water of Finite Depth, P-457/SN-113, National Engineering Science Company, 711 South Fair Oaks Avenue, Pasadena, CA, June 1963, Unclassified, AD-414 532.

Henry, Charles A., Wave-Ice Interaction Model Experiments, Report No. 1314, Davidson Laboratory, Stevens Institute of Technology, Castle Point Station, Hoboken, New Jersey, December 1968, Unclassified, AD-680 449.

Hunkins, Kenneth, Waves on the Arctic Ocean, J. Geophys. Res., Volume 67, No. 6, June 1962, Lamont Geological Observatory, Columbia University, Palisades, New York.

[redacted]

[redacted]

Keller, Joseph B. and Goldstein, Edward, Water Wave Reflection Due to Surface Tension and Floating Ice, Trans. Am. Geophys. Un., Volume 34, No. 1, February 1953, Institute for Mathematics and Mechanics, New York University, New York, New York.

Leslie, Donald M. and Nelson, Carl A., Explosion Tests Under Thick Polar Ice, NOLTR 61-146, U.S. Naval Ordnance Laboratory, White Oak, MD, 1 November 1961, Unclassified, AD-327 953.

Malme, Charles I., Carbonell, Jaime R., and Dyer, Ira, Mechanisms in the Generation of Airblasts by Underwater Explosions, NOLTR 66-88, United States Naval Ordnance Laboratory, White Oak, MD, 23 September 1966, Unclassified, AD-654 175.

Pace, C. E., et al., Surface Waves Resulting from Explosions in Deep Water, Report 4 - Effect of Charge Depth of Submergence on Wave Height and Energy Coupling, Technical Report No. 1-647, U.S. Army Engineer Waterways Experiment Station, Vicksburg, MS, 1969, Unclassified.

Robin, G. de Q., Ocean Waves and Pack Ice, The Polar Record, Volume 11, No. 73, January 1963, Scott Polar Institute, Cambridge University, Cambridge, England.

Robin, G. de Q., Wave Propagation Through Fields of Pack Ice, Phil. Trans. of Royal Soc. of London, Series A, Volume 255, No. 1057, 21 February 1963, Scott Polar Institute, Cambridge University, Cambridge, England.

[redacted]

[redacted]

Shapiro, A. and Simpson, L. S., The Effect of a Broken Ice Field on Water Waves, Trans. Am. Geophys. Un., Volume 34, No. 1, February 1953, Division of Oceanography, U.S. Navy Hydrographic Office, Washington, D.C.

Van Dorn, W. G., LeMehaute, B., and Hwang, Li-San, Handbook of Explosion-Generated Water Waves, Volume 1--State of the Art, TC-130, Tetra Tech, Incorporated, 630 North Rosemead Boulevard, Pasadena, CA 91107, October 1968, Unclassified, AD-845 485.

Wang, S., Explosion-Generated Wave Effects on Naval Operations in Selected Locations(U). TC-265, Tetra Tech, Incorporated, 630 North Rosemead Boulevard, Pasadena, CA 91107, February 1973, Secret, AD-525 446.

Wang, S., Wade, R., and Wier, W., Vulnerability of Surface Effect Vehicles to Explosion Generated Water Waves, TC-645, Tetra Tech, Incorporated, 630 North Rosemead Boulevard, Pasadena, CA 91107, December 1977, Unclassified.

[redacted]

[redacted]

THIS PAGE IS INTENTIONALLY LEFT BLANK

[redacted]

[redacted]

[redacted] SECTION 9
[redacted] ACOUSTIC EFFECTS

9.1 [redacted] Arctic Environmental Differences

[redacted] The Arctic oceanic environment has two distinctive features whose impact on hydroacoustics in that region is such as to set Arctic waters apart, acoustically, from ocean areas in more temperate latitudes; viz., the ice canopy and the Arctic water mass structure. These features are discussed in Sections 1.2.5 and 1.2.7. The ice cover affects the acoustic characteristics of the polar regions in several ways. First, the canopy presents an undersurface whose reflective and scattering characteristics are quite different from those of the air-water interface in open water. Second, as a result of gross ice movement, thermal effects, and turbulent wind flow at the ice surface, the ice cover itself is the dominant source of underwater ambient noise in the Arctic. The virtual absence of surface shipping in Arctic waters assures the dominance of ice-generated noise even at the lower frequencies. Third, the ice cover is an impediment to solar heating of the surface water, maintains near-freezing temperatures at the top of the water column, and thus has a profound influence on the near-surface sound speed structure. The overall temperature and salinity characteristics of the Arctic water column result in a distinctive sound speed profile characterized by a monotonic increase in sound speed from the surface to the bottom (see Figure 1-28 in Section 1.2.7). Acousticians refer to this structure as an acoustic half-channel. This condition contrasts sharply with sound speed structures encountered in other environments, where the sound speed minimum typically occurs well below the surface and, at equatorial latitudes, can occur as deep as 1200 meters. Within the half-channel acoustic energy propagates to long

[redacted]

range principally via RSR (refracted, surface-reflected) paths. RRR (pure refracted) propagation does not occur under half-channel conditions, thus precluding the formation of convergence zones. Convergence zone formation is typical of all deep-water regions where thermoclinal conditions persist.

9.2 [redacted] Nuclear Source Levels

[redacted] The equivalent acoustic source level of an underwater nuclear detonation is a function of weapon yield. Figure 9-1 shows source level spectra as calculated for five weapon yields ranging from 10 tons to 100 kilotons (Blatstein, 1977). It is noted that only the shock wave was considered in the computations. However, since the bulk of the blast energy is contained in the shock wave for that portion of the frequency domain represented, these levels may be applied in cases where a bubble pulse is generated as well as in those cases where no bubble pulse is present. No special considerations arise with respect to the equivalent acoustic source levels of underwater nuclear detonations by virtue of their supposed occurrence within the Arctic environment.

9.3 [redacted] Propagation Loss

[redacted] As previously noted, in Arctic waters acoustic energy is propagated to long range via paths involving repeated cycles of upward refraction to the surface followed by reflection back down into the water column. A ray diagram computed for typical Arctic half-channel conditions is shown in Figure 9-2 (Urick, 1975). Since, as Figure 9-2 indicates, Arctic propagation typically involves numerous surface interactions, it is appropriate at this point to address the reflectivity of the undersurface of the ice canopy. In the absence of bottomside roughness theory predicts that, for all grazing angles of practical interest to the underwater acoustician, reflections from the bottom of the ice cover will be lossless. However,

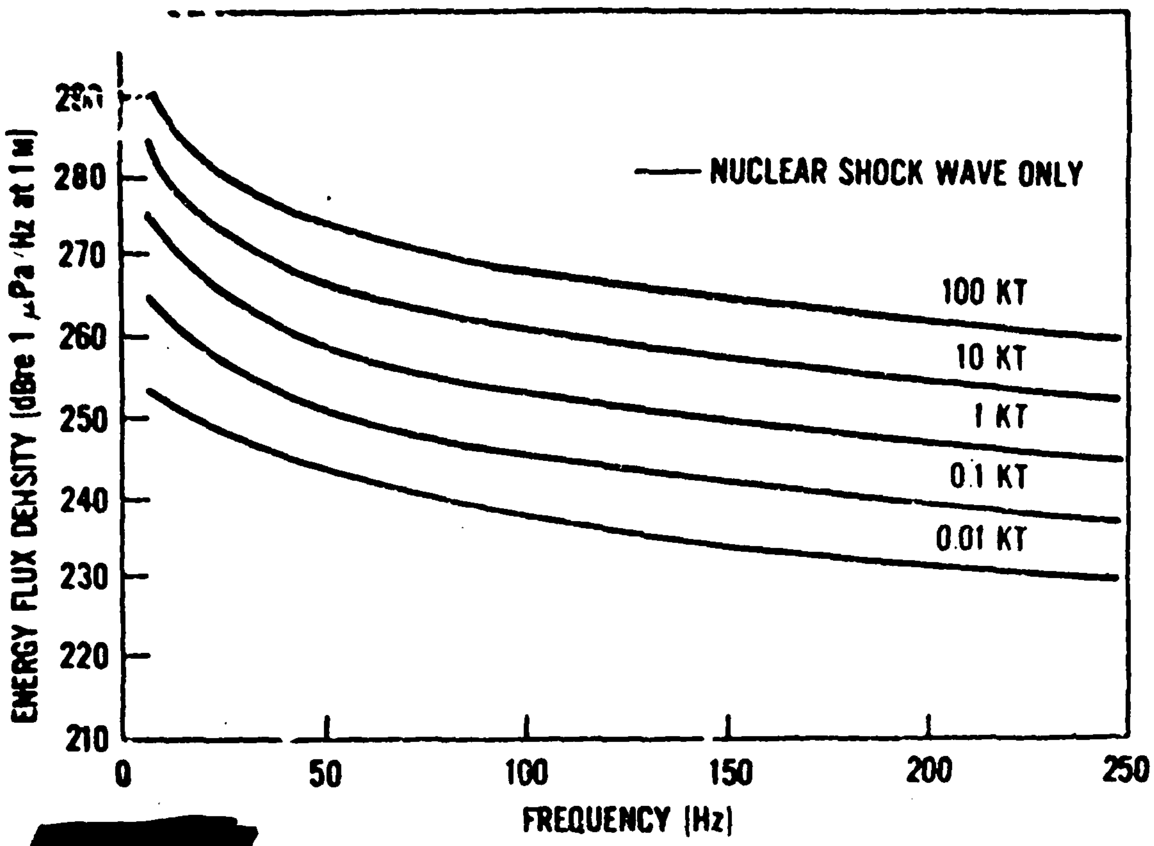

Figure 9-1. Equivalent Acoustic Source Levels (Blatstein, 1977)

[redacted]

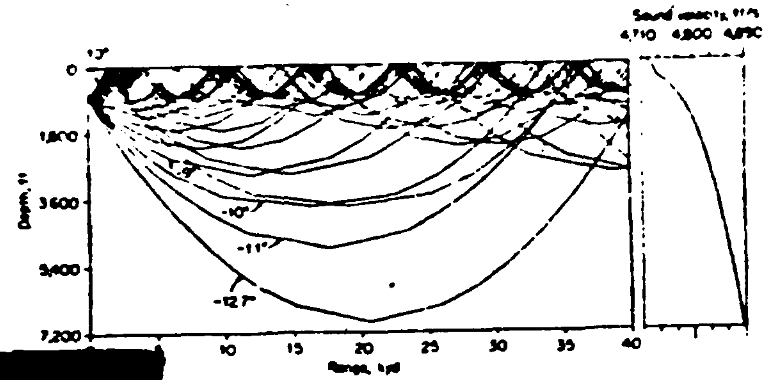

[redacted]

Figure 9-2. Ray Diagram for Transmission in the Arctic.

Ray interval 1°, with 12.7° added. The velocity profile is shown at the right. (Urick, 1975).

the underside of the Arctic ice cover is not smooth and, in practice, experimentally-determined reflection losses are normally substantial. It has been determined that under-ice reflection losses result principally from scattering from the sea ice ridges distributed in random fashion about the ice canopy. In addition, reflection losses have been determined, both theoretically and empirically, to be strongly dependent upon both the linear density (number per unit distance) and draft (depth) of the ridges (Diachok, 1974). At low frequencies (i.e. frequencies for which the acoustic wavelength is significantly larger than the average ridge depth), reflection losses increase with increasing frequency, typically ranging between 0.5 and 3 dB per bounce. At high frequencies (i.e., frequencies for which the acoustic wavelength is very much shorter than the average ridge depth), reflection losses are essentially independent of frequency and vary, typically, between 2 and 8 dB per bounce. Due to the high scattering strength of the underside of the ice cover, propagation losses increase much more rapidly with range than would be expected

[redacted]

[redacted]

under similar refraction conditions in the absence of an ice cover. Figure 9-3 shows smoothed Arctic transmission loss-vs-range curves for discrete frequencies ranging from 20 to 3200 Hz (Buck, 1968). A curve representing spherical spreading (free field, no absorption) is shown for reference. As the figure illustrates, losses are characteristically less than the free-field prediction out to some range, and greater thereafter, reflecting the effect of ice interaction losses and absorption. Also, the crossover range is observed to decrease with increasing frequency, reflecting the increased reflection and absorption losses at the higher frequencies.

[redacted] A discussion of scattering at the ice undersurface in the context of its expected impact on reverberation in Arctic waters is presented in Section 9.5.

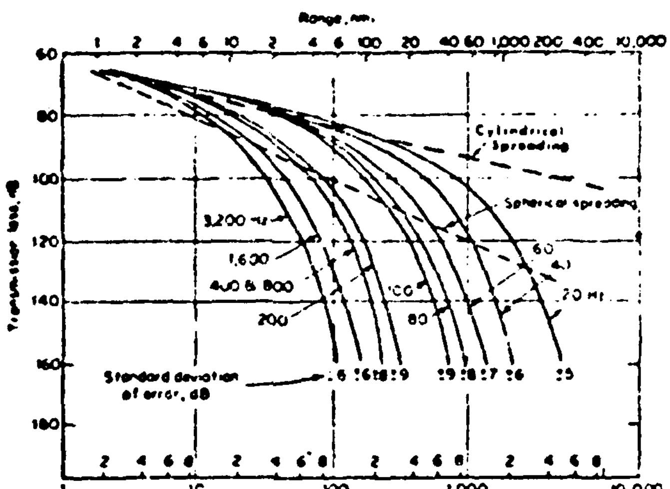

[redacted]

[redacted] Figure 9-3. Average Transmission Loss in the Arctic. (After Buck, 1968)

[redacted]

[redacted]

9.4 [redacted] Localized Ambient Noise

[redacted] One of the principal noise generating mechanisms at play in the under-ice ocean environment is the interaction of ice floes caused by winds, currents and/or tidal forces. In the event of an underwater nuclear detonation beneath a continuous ice sheet (shorefast), it is reasonable to expect that the interaction of the ice fragments formed as a result of the extensive fracturing action of the blast would appreciably increase noise levels locally until the refreezing process in the open water areas surrounding the fragments eventually returned the cover to its previous unbroken state. The energy deposited in the water by the underwater explosion would not have a noticeable effect on the refreezing rate. See the discussion in Section 4. At present, there is no experimental blast data to indicate the magnitude of the noise level increase that might be anticipated or the period of time during which noise levels would be significantly elevated. However, the data shown in Figure 9-4 (Diachok, 1976) demonstrate a naturally-occurring localized effect, and hence give some indication of after-blast levels that might be encountered. The data show, for frequencies of 100, 315 and 1000 Hz, the spatial variability of ambient noise across an ice-water boundary region at the edge of the Marginal Ice Zone. The data were taken along a line running transverse to the ice edge and extending from about 80 km away from the boundary on the open water side to a point nearly 200 km distant from the edge on the ice side. The levels are observed to peak at the edge, falling off gradually with distance on both sides. The levels at the fringe result principally from the gross movement of ice floes in that region. The peaking effect is indicative of the higher levels experienced in regions of free ice movement when

[redacted]

[redacted]

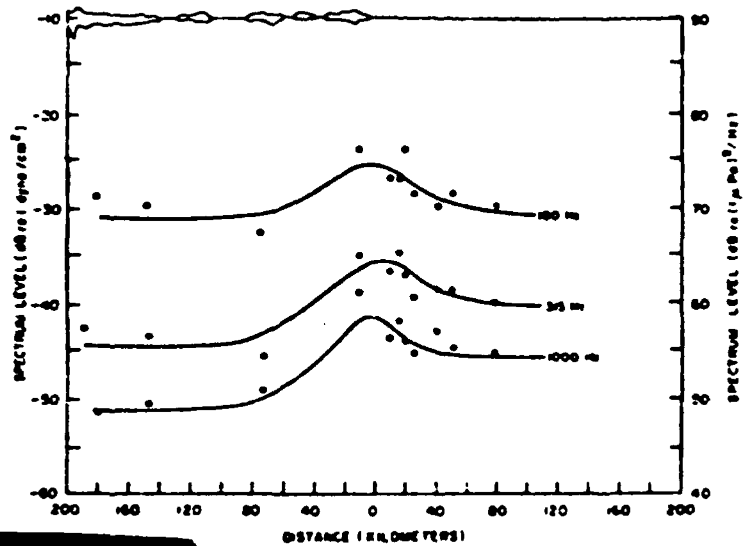

[redacted]

Figure 9-4. Variations of Median Ambient Noise Sound Pressure Spectrum Levels with Distance from a Diffuse Ice-Water Boundary for Frequencies of 100, 315 and 1000 Hz. Sea Stace: 1 (Diachok, 1976).

compared with those in open water or in areas where there is either a continuous or very close ice cover. It is significant to note here that, for all three frequencies, the differences between the peak levels and the under-ice levels obtained well within the ice pack are substantial. At 100 Hz a difference of 5 or 6 dB is indicated, while at 315 and 1000 Hz the differences are on the order of 10 dB. In this case the areal concentration of ice changed from 1/8 at the fringe to 7/8 over a distance of approximately 10 km. In instances for which the ice edge is more compact - that is, where a similar change in areal concentration occurs over a much shorter distance (say 1 km) - noise levels beneath the fringe tend to be much higher

[redacted]

than those obtained beneath a diffuse boundary, resulting in much greater differences between edge- and under-ice levels than shown in the figure.

[redacted] It is possible that local noise enhancement resulting from a nuclear blast would also occur in environments for which the ice cover was not continuous. However, it is probable that the effect would be observed only when areal ice concentrations are quite high.

9.5 [redacted] Reverberation

[redacted] Acoustic reverberation in the ocean environment occurs as a result of reradiation, or scattering, of acoustic energy incident upon the ocean surface, ocean bottom and other inhomogeneities within its volume. Steep bottom slopes such as are encountered at basin edges, seamounts, and island chains have been shown, in the case of large yield detonations, to be particularly strong reverberation sources.

[redacted]

[redacted]

[redacted]

[redacted] An example of the character of basin reverberation is shown in Figure 9-5 (Plona, et al., 1976). Presented are reverberation levels at 50 Hz vs time for a 10-ton chemical explosion in the Artemis IV test series conducted in the Atlantic Ocean several years ago. The dark trace is the experimental data and the light trace is the prediction obtained with the USI reverberation model. The time scale is referenced to the time of reception of the direct signal. The peaks in the time series correspond to reflections from basin boundary segments located near Cape Hatteras and the Bahama Islands. For this example reverberant returns exceed the local ambient level (≈75 dB//μPa/Hz) by as much as 26 or 27 dB.

[redacted] In the ice-covered Arctic oceanic areas it is expected that the character of basin reverberation will be considerably different from that of reverberation observed in open water regions elsewhere. This expectation arises as a result of the refractive properties of the Arctic water column and the acoustic characteristics of the ice canopy.

[redacted] The undersurface of the ice is, characteristically, a strong scatterer of acoustic energy. Figure 9-6 shows examples of under-ice scattering strengths for spring pack ice and summer polar ice, compared with surface scattering strengths obtained in open water under Sea State 5 conditions (Urick, 1975). The scattering strengths for the spring ice cover are observed to be on the order of 25 dB higher than the corresponding open water strengths. By contrast the summer polar ice cover is observed to be a much weaker scatterer than the spring canopy, indicative of a more gently contoured undersurface in the former case.

[redacted]

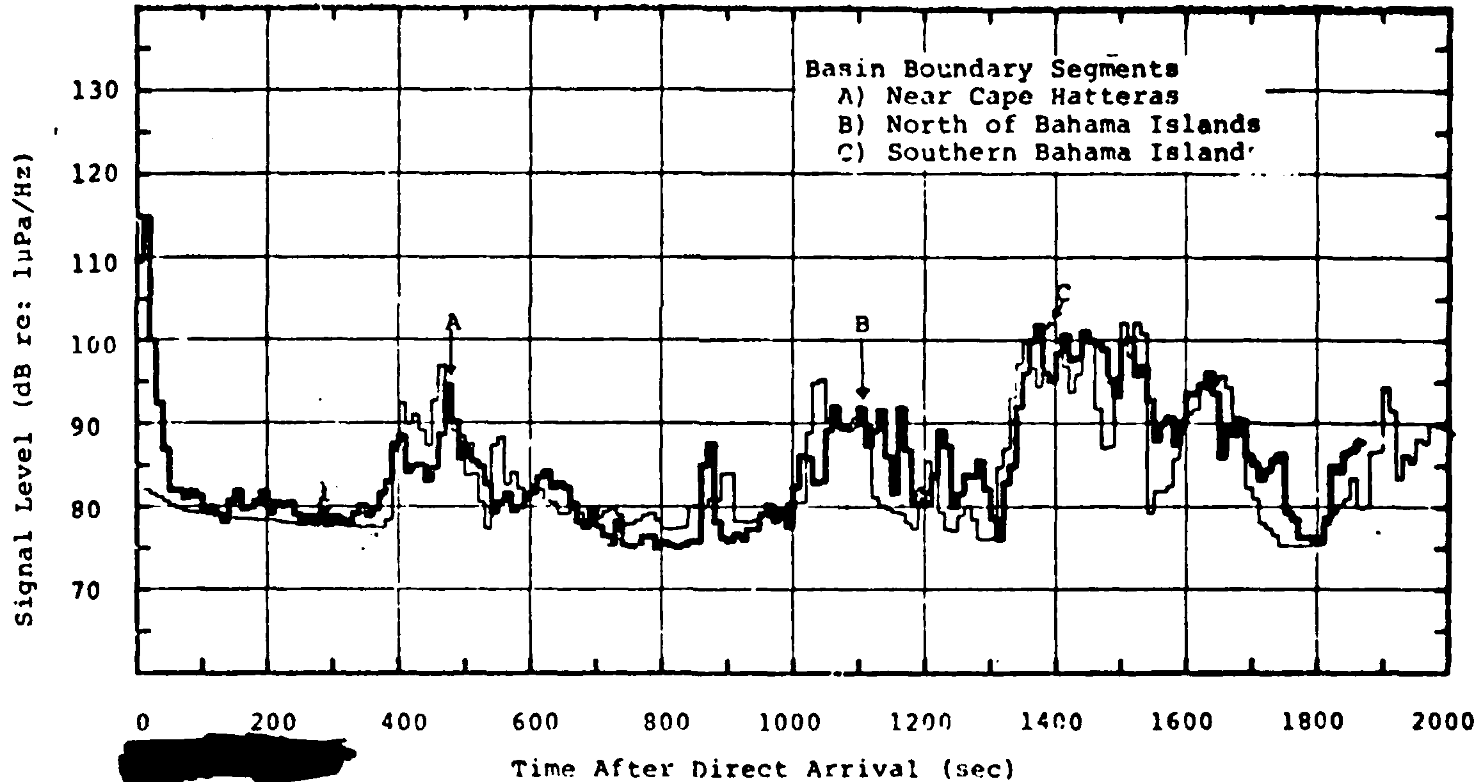

Figure 9-5. Comparison of Model Computation (fine trace) with Experimental Data (heavy trace) for Artemis Shot #9(1-1) at 50 Hz. Source-to-receiver separation distance is 411 nm.

(Plona et al., 1976)

[redacted]

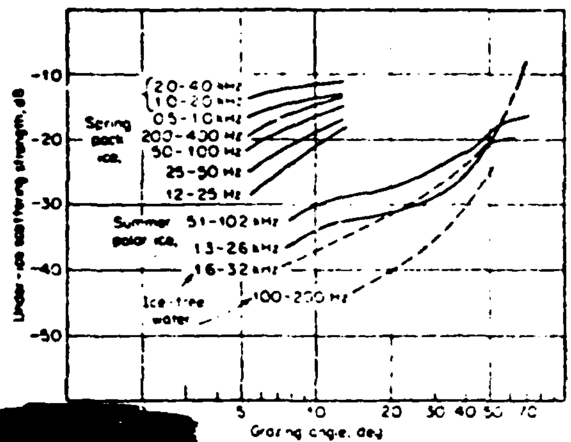

[redacted]

[redacted] Figure 9-6. Ice Cover Scattering Strengths. (Urick, 1975).

[redacted] The combination of high surface scattering strength and upward refracting sound speed structure should result, initially, in surface reverberation levels as much as 25 dB higher than would be expected in open water. As a result of the relatively rapid increase in propagation loss with range due to the high reflection loss at the ice undersurface, the reverberation from distant boundaries (coastlines, island chains and seamounts) is expected to be greatly reduced.

[redacted] Reverberation measurements made in the Arctic (Zittel, 1979) substantiate these expectations. Figure 9-7 shows received reverberation spectral levels observed on a single hydrophone for a 440 lb charge detonated at a depth of 800 ft. At 300 seconds following the direct arrival, the received levels are well above the ambient noise over the entire

[redacted]

[redacted]

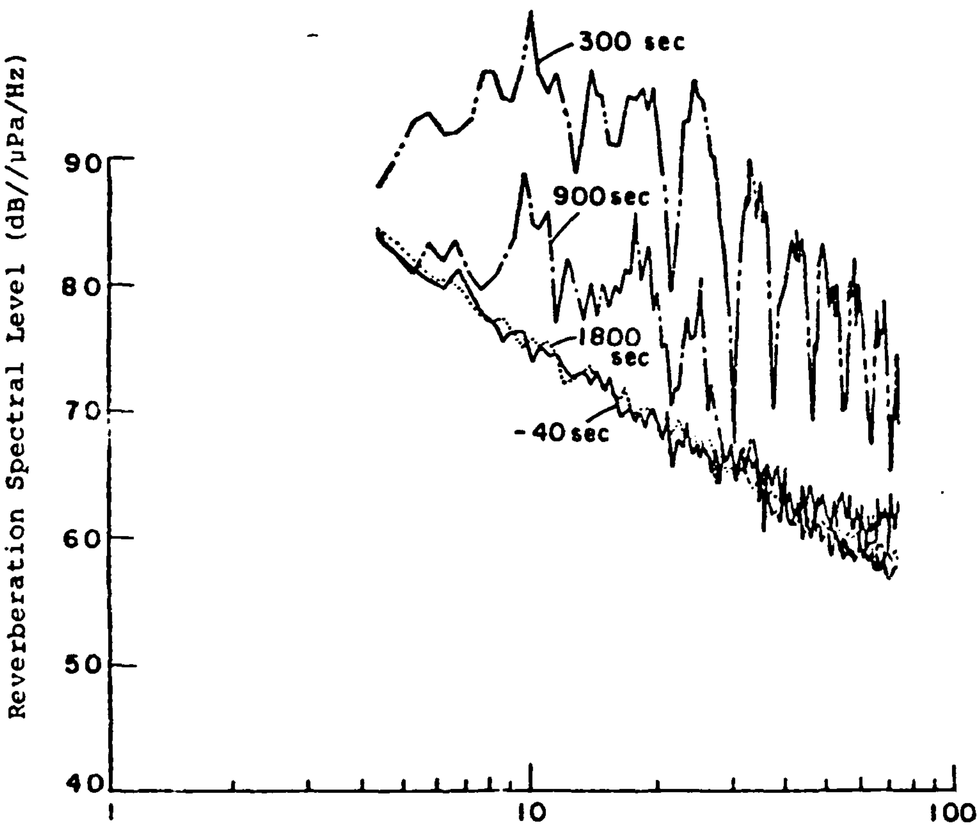

[redacted]

Frequency (Hz)

[redacted] Figure 9-7. Reverberation Spectral Level as a Function of Frequency at Various Times Relative to Shot Instant. (Zittel, 1979)

[redacted]

frequency range of about 5 to 70 Hz. At 900 seconds the levels below about 20 Hz are 10 to 15 dB lower due to the increased range and a different set of scattering surfaces, but the spectral shape is quite similar to that observed at 300 seconds. At about 25 to 30 Hz the reverberation levels abruptly drop, disappearing into the background noise. Since the charge was detonated near the receiver, we assume a monostatic case for interpretive purposes. At 300 seconds the scattering surfaces are at a range somewhat less than 200 km. From Figure 9-3 it can be seen that propagation loss does not depart significantly from cylindrical spreading until the frequency exceeds 80 Hz. By contrast, at 900 seconds, comparable to a range somewhat less than 600 km, propagation loss significantly departs from cylindrical spreading for frequencies greater than about 20 Hz, resulting in the sudden drop in reverberation levels at about 25 Hz.

[redacted] Figure 9-8, (Zittel, 1979) shows a typical reverberation versus time curve observed on a horizontal array with a beam pattern of about 8°. Although the details of the curve are dependent upon the basin characteristics, the general characteristics are about what we would expect in the absence of ice cover.

[redacted] In summary, long term reverberation resulting from scattering from the basin boundaries will not be affected by ice cover at frequencies below the order of 25 Hz. Above 25 Hz, long time reverberation will be very significantly reduced. Thus, from the standpoint of reverberation, only those systems that operate below 25 Hz can be considered to be low frequency systems whose performance will be degraded for periods of time that correspond to basin dimensions. This is in contrast to the division between low and high frequency systems of 300 Hz in ice-free regions. For high frequency

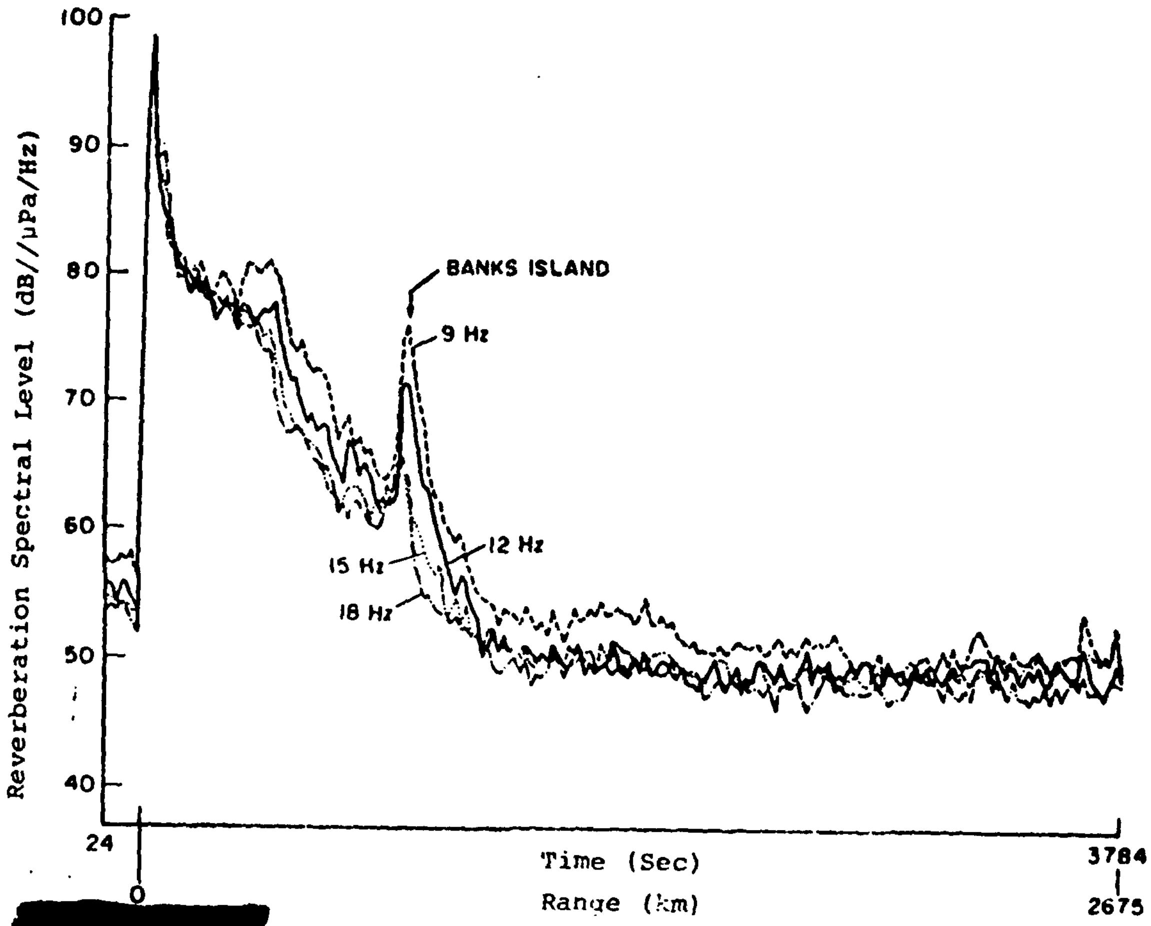

[redacted]

[redacted]igure 9-8. Reverberation Spectral Level as a Func[illegible]n of Time and Range at Various Frequencies. (Zittel, 19[illegible]9)

[redacted]

systems, degradation will be limited to less than 15 minutes, decreasing with increasing frequency, but may be much more severe when present due to the much higher surface scattering strengths.

9.6 [redacted] Conclusions and Recommendations

[redacted] The current state-of-the-art of hydroacoustics theory in general, and of Arctic hydroacoustics theory in particular, is generally adequate for the proper understanding of the various acoustic mechanisms and phenomena of interest in the study of nuclear weapons effects in the cold regions. This understanding, however, is based on a limited amount of available data. At present, acoustic modeling capabilities may be limited by the paucity of critical environmental data. Perhaps the most pressing need is better definition of the Arctic ice pack in terms of its spatial and temporal characteristics, particularly those relating to under-ice roughness and areal ice concentrations.

[redacted] H. W. Kutschale of the Lamont-Doherty Geological Observatory, Columbia University has been making acoustic measurements and collecting environmental data in annual field expeditions for the last few years. The work is being supported by ONR Code 461. The most recent work has been in the Eurasian Basin, where little previous information was available. However, the environmental data collected have concentrated on the properties of the bottom and the water column. Laser-equipped aircraft have not been available to make measurements of the ice profile. Kutschale reports that comparisons of measured acoustic data with predictions made with the PE and FFP models have given fairly good results, but that the ice roughness factor is the greatest unknown. (Private communication June 1960. Reports of the work have not been given formal distribution.)

[redacted]

[redacted] It is recommended that Arctic environmental data continue to be collected, with special attention being given to measurements of under-ice roughness and to the concentrations of ice expected to occur in various areas as a function of season.

9.7 [redacted] Bibliography

Birch, William B., Reverberation Under Ice - An ASW Problem(U), U.S. Navy Journal of Underwater Acoustics, Volume 21, No. 1, pp. 57-68, January 1971, Confidential.

Blatstein, I. M., The Effect of Reverberation from Underwater Nuclear Explosions on Acoustic Detection Systems, Interim Report(U), NSWC/WOL/TR 76-82, Naval Surface Weapons Center, White Oak Laboratory, Silver Spring, MD, February 2, 1977, Secret, Formerly Restricted Data.

Blatstein, Ira M., et al., The Effect of Ocean Basin Reverberation on ASW Protection of a Convoy, Volume 1 - Effect on TACTAS(U), NSWC TR 79-105, Naval Surface Weapons Center, White Oak Laboratory, Silver Spring, MD, 10 May 1979, SECRET.

Brown, J. R., Reverberation Under Arctic Ice, J. Acoust. Soc. Am., Volume 36, No. 3, pp. 601-603, March 1964.

Brown, J. R. and Brown, D. W., Reverberation Under Arctic Sea-Ice, J. Acoust. Soc. Am., Volume 40, No. 2, pp. 399-404, August 1966, Reprint available as AD-648 209.

Buck, Beaumont, M., Arctic Acoustic Transmission Loss and Ambient Noise, in Arctic Drifting Stations, Arctic Institute of North America, November 1968, AD-692 263.

[redacted]

Buck, B. M., Low-Frequency Underwater Acoustic Measurements in the Arctic Ocean, 1965-1968(U), Report No. TR69-10, AC Electronics-Defense Research Laboratories, General Motors Corporation, February 1969, Confidential, AD-502 211.

Buck, Beaumont M., Recent Measurements of Underwater Acoustic Data at Three Manned Ice Stations in the Central Arctic(U), Proceedings of the Fourteenth Conference on the Naval Minefield, Volume 1, pp. 101-140, NOLTR 71-71, Naval Ordnance Laboratory, White Oak, Silver Spring, MD, 30 April 1971, Secret (Buck paper is Confidential).

Buck, Beaumont M. and Greene, Charles R., Arctic Deep-Water Propagation Measurements, J. Acoust. Soc. Am., Volume 36, No. 8, pp. 1526-1533, August 1964.

Chapman, R. P. and Scott, H. D., Backscattering Strength of Young Sea Ice, J. Acoust. Soc. Am., Volume 36, No. 12, pp. 2417-2418, December 1964.

Chapman, R. P. and Scott, H. D., Backscattering Strengths of Sea Ice, J. Acoust. Soc. Am., Volume 39, No. 6, pp. 1191-1193, June 1966.

Diachok, O. I., Effects of Sea Ice Ridge Characteristics on Under-Ice Reflection Loss in Arctic/Subarctic Waters, NAVOCEANO Technical Note No. 6130-4-74, U.S. Naval Oceanographic Office, Washington, D.C., August 1974, Unclassified.

Diachok, O. I., Recent Advances in Arctic Hydroacoustics, Naval Research Reviews (published by the Office of Naval Research), May 1976, pp. 48-63, Unclassified.

[redacted]

[redacted]

Frankenstein, G. E. and Smith, North, The Use of Explosives for Ice Cratering, Proceedings of the Fourteenth Conference on the Naval Minefield, Volume 1, pp. 203-214, NOLTR 71-71, Naval Ordnance Laboratory, White Oak, Silver Spring, MD, 30 April 1971, Secret (Frankenstein and Smith paper is Unclassified).

Ganton, J. H. and Milne, A. R., Ambient Underwater Noise in Arctic Waters: A Synopsis of Time-Series in the Canadian Archipelago(U), Report 72-3, Defence Research Establishment Pacific, Victoria, B.C., June 1972, Confidential, AD-523 218.

Mellen, R. H., Underwater Sound in the Arctic Ocean, U.S. Navy Journal of Underwater Acoustics, Volume 16, No. 2, pp. 247-259, April 1966, Confidential (Mellen paper is Unclassified). Reprint available as AD-484 962.

Mellen, R. H. and Marsh, H. W., Underwater Sound Reverberation in the Arctic Ocean, J. Acoust. Soc. Am., Volume 35, No. 10, pp. 1645-1648, October 1963.

Milne, A. R., Underwater Backscattering Strengths of Arctic Pack Ice, J. Acoust. Soc. Am., Volume 36, No. 8, pp. 1551-1556, August 1964.

Milne, A. R., Sound Propagation and Ambient Noise Under Sea Ice, Chapter 7 of Underwater Acoustics, Volume 2, V. M. Albers (ed.), Plenum Press, New York, 1967, Reprint available as AD-666 546.

[redacted]

[redacted]

Plona, T. J., Mole, L. A. and Weinstein, M. S., Hydroacoustic Reverberation from Large Underwater Detonations(U), Underwater Systems, Inc., 30 June 1976, Confidential.

Urick, Robert J., Principles of Underwater Sound, 2nd Edition, McGraw-Hill Book Company, New York NY, 1975.

Verral, R., Ambient Noise Measurements in Jones Sound(U), Technical Memorandum No. 77-12, Defence Research Establishment Pacific, November 1977, Confidential.

Weinstein, M. S., Woolston, D. D., Young D. F. and Mole, L. A., Arctic Underwater Surveillance(U), Underwater Systems, Inc., Silver Spring, MD, May 1972, Confidential, AD-523 276.

Wenz, G. M., Acoustic Ambient Noise in the Ocean: Spectra and Sources, J. Acoust. Soc. Am., Volume 34, No. 12, pp. 1936-1956, December 1962.

Zittel, John David, Ocean Basin Reverberation, Thesis submitted in partial fulfillment of the requirements for the degree of Ocean Engineer, Massachusetts Institute of Technology and Woods Hole Oceanographic Institution Joint Program in Oceanographic Engineering, M.I.T., 1979.

[redacted]

[redacted]

THIS PAGE IS INTENTIONALLY LEFT BLANK

[redacted]

[redacted]

DISTRIBUTION

	No. of Copies
Director, Defense Advanced Research Projects Agency 1400 Wilson Boulevard Arlington, VA 22209	2
Director, Defense Nuclear Agency	
ATTN: STSP	2
TITL	1
M. Rubenstein	1
C.P. Kowles	1
Washington, D.C. 20305	
Director, Defense Technical Information Center ATTN: DD Cameron Station Alexandria, VA 22314	2
Commander, Naval Surface Weapons Center/White Oak ATTN: F31 (Mr. Downs) Silver Spring, MD 20910	2
Commander, Naval Research Laboratory ATTN: Technical Information Div. 4555 Overlook Ave., S.W. Washington, D.C. 20375	3
Director, Arctic Submarine Laboratory ATTN: W.K. Lyon (Code 54) Naval Ocean Systems Center San Diego, CA 92132	1
Naval Underwater Systems Center ATTN: Technical Director (Mr. Van Winkle) New London, CT 06320	2
Director, NORDA ATTN: Technical Director (R. Goodman) NSTL Station Bay St. Louis, MS 39529	2
Director, U.S. Naval Oceanographic Office ATTN: Technical Director Washington, D.C. 20390	2
Commander, Naval Arctic Research Laboratory Point Barrow, AK 99723	2

[redacted]

[redacted]

DISTRIBUTION

	No. of Copies
Department of the Army Cold Regions Research and Engineering Lab ATTN: Dr. Wilford F. Weeks Hanover, NH 03755	2
Department of the Navy Office of Naval Research ATTN: R.G. Joiner (Code 464)	2
M. Odegard (Code 480)	2
R. McGregor (Code 461) 800 N. Quincy Street Arlington, VA 22217	1
Office of Naval Research Branch Office Room 286, 536 South Clark Street Chicago, IL 60605	1
Director, Naval Research Laboratory ATTN: Code 2627 Washington, D.C. 20375	1
Director Joint Strategic Target Planning Staff Offutt AFB, NB 68113	1
Studies Analysis and Gaming Agency Joint Chiefs of Staff ATTN: Strategic Forces Div. Washington, D.C. 20301	1
Chief U.S. Army Nuclear and Chemical Agency ATTN: Dr. C. Davidson North Area - Bg 2073 Fort Belvoir, VA 22060	1
Commander-in-Chief Strategic Air Command ATTN: LTC B. Stephan Offutt AFB, NB 68113	1
Energy Systems, Inc. ATTN: Dr. Bill Ogle P.O. Box 3075 Anchorage, AK 99510	1

[redacted]

[redacted]

DISTRIBUTION

	No. of Copies
Kaman Sciences Corporation ATTN: J. Keith 1500 Garden of the Gods Road Colorado Springs, CO 80907	1
Mission Research Corporation ATTN: W.E. Ware P.O. Box 6238 Colorado Springs, CO 80934	1
R&D Associates ATTN: Mr. R. Port P.O. Box 9695 Marina Del Rey, CA 90291	1
Underwater Systems, Inc. ATTN: W.E. Wallace 1776 East Jefferson St. Rockville, MD 20852	1

[redacted]